CONF 790236

Time Dependent Fracture of Materials at Elevated Temperature

Proceedings of a Workshop
- — Assessing the State-of-the-Art
- — Recommending Basic Research Relevant to Energy Technologies
- — Held on February 15 - 16, 1979

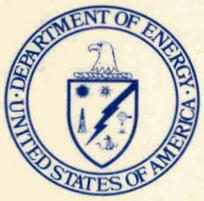

U.S. Department of Energy
Office of Basic Energy Sciences
Division of Materials Sciences

June 1979

DISCLAIMER

CONF 790236
UC-25

Time Dependent Fracture of Materials at Elevated Temperature

Proceedings of a Workshop
- — Assessing the State-of-the-Art
- — Recommending Basic Research Relevant to Energy Technologies
- — Held on February 15 - 16, 1979

Editor
Stanley M. Wolf

U.S. Department of Energy
Office of Basic Energy Sciences
Division of Materials Sciences
Washington, D.C. 20545

June 1979

Available from:

National Technical Information Service (NTIS)
U.S. Department of Commerce
5285 Port Royal Road
Springfield, Virginia 22161

Price: Printed Copy: $ 9.25
Microfiche: $ 3.00

TABLE OF CONTENTS

WORKSHOP OVERVIEW

by
Stanley M. Wolf
Division of Materials Sciences, DOE

Over half of the United States' energy utilization, primarily in the sectors of electricity production and transportation and to a lesser extent of industrial usage, is based on systems designed to convert the heat from fossil fuel combustion or nuclear fission to work. Thus our use of energy involves operation of materials at elevated temperature. Yet, even with the gains made in the past thirty years, system thermal efficiencies are restricted to modest values because of limitations of commercial structural alloys and the necessarily conservative design practices. For example, new electricity power generating stations operate at thermal efficiencies of only ∿40% (if using fossil fuel, ∿32% if nuclear). The conventional internal combustion engine converts less of the available energy to propulsion than it dissipates in either its cooling system or exhaust.[1]

As fuel becomes more scarce and expensive, more efficient systems will become increasingly cost effective, and more severe operating temperatures and corrosive environments will be encountered. Trends are already apparent --- advanced energy technologies such as topping cycles for electric utilities and turbine engines for automobiles are considering ceramic components and time-dependent deformation in design.

The importance of time-dependent structural stability of high temperature alloys is recognized by several DOE programs which support materials research and development totalling ~$16 millions annually (Table 1) on: component structural design and testing methodology, nuclear fuel cladding and duct and piping alloys for nuclear breeder and advanced gas reactors, refractory bricks for the firewall in open-cycle MHD air preheaters, ceramic blades and vanes for vehicular and auxilliary power turbines, receivers for solar thermal converters, as well as fundamental studies of constitutive equations, creep rupture, fatigue, and radiation enhanced creep.

Given the interest of DOE technologies in time dependent fracture and the recent progress in the development of constitutive equations for creep deformation and of diffusion-controlled void growth models for creep rupture of metals, a workshop on this subject was felt timely. Its purpose was to assess directions for basic materials research, viz., for extending our current understanding of creep deformation and rupture of metals and ceramics to more complex alloys, loading conditions, and environments relevant to energy systems. A group of thirty five materials engineers and scientists representing aspects of the component design, materials engineering and materials research communities were invited to participate in this assessment (Table II).

The workshop was organized in three sessions. The first consisted of formal presentations on:

- design considerations identifying ranges of stress, temperature, lifetime, and environments anticipated in solar thermal, nuclear breeder, and fusion energy concepts, and metal turbines and ceramic heat engines;

- materials engineering reviews of data and life prediction methods, and discrepancies and assumptions therein, for creep rupture and creep-fatigue of metals and ceramics; and

- materials science outlines of models and experiments on monotonic creep, cyclic creep and constitutive equations for metals, diffusion or plasticity-modified diffusion controlled crack growth, and pertinent grain boundary structure and properties.

Significant insights were made in the above presentations. It was clear that time-dependent fracture in energy systems derives from transients and cycles in loading and temperature, multiaxial stresses, and environment-enhanced deformation and failure. These topics pose meaningful challenges to researchers attempting to elucidate mechanisms controlling materials behavior or to formulate quantitatively their effects for later extension into an engineering framework.

In the second session, the participitants separated into four smaller "subgroups" to discuss unresolved or new issues warranting fundamental study in the areas of:

Deformation Aspects --- to emphasize deformation aspects of failure, including strain localization at boundaries or inclusions, monotonic and cyclic creep mechanisms, their correlation with constitutive equations, damage characterization, multiaxial stress, aging, and impurity and environmental effects.

High Temperature Rupture --- to focus on cavitation and cracking under diffusion and diffusion-plus-plasticity controlled conditions caused by steady state, transient, and cyclic loading.

Grain Boundary Structure and Properties --- to evaluate aspects of boundaries and interfaces important to creep rupture and creep fatigue, such as boundary structure, chemistry, diffusion, impurity effects, and near-boundary deformation.

Engineering Needs --- to suggest the contribution of materials science to designer needs, such as code requirements, accelerated test methods, non-destructive evaluation, among others.

Each subgroup report represents a concensus of its members on high priority research areas. These reports are substantive and worthy of careful review. A few of their points are noted below as an introduction to the types of issues discussed, including controversial ones. Some of these statements incorporate the views of more than one subgroup.

1. General test conditions and alloys: Information should be compiled giving representative alloys and service conditions encountered in energy plants to assist the selection of relevant time-dependent fracture research. It appears now that such research should emphasize transient and cyclic effects in metals and steady state for ceramics; it should take into account that in most high temperature applications, alloys are used at about one-third to one-half their melting temperatures. Materials having microstructures representative of those of engineering alloys warrant study to "map out" controlling features. Idealized model systems should be investigated to determine specific mechanisms and environmental effects thereon.

2. Cumulative damage: It is imperative to characterize quantitatively various types of damage, i.e., voids, cracks, changes in composition and microstructure in order to assess the role of each in deformation and fracture.

3. Heterogeneous deformation: The details of this, principally grain boundary sliding at elevated temperature but also other modes such as shear localization, must be established. Careful measurements of the inelastic strain components are needed to validate the kinetics and energetics of various creep models; new measurement techniques will likely be required. The effects on grain boundary sliding of its structure, impurity segregation, and second phase distribution remain largely undocumented; these should be related, as appropriate, to environment- and radiation-induced changes in deformation.

4. Transient and multiaxial deformation: Experimental data on these is required to assist evaluation of physical mechanisms and development of service life models.

5. Constitutive equations: An improved mechanistic basis of these is needed so that their range of applicability can be defined both at the macrocontinuum level (for structural component behavior) and microcontinuum level (at crack tips). At this time equations should be aimed towards a specific (rather than general) class of materials and applications, and have a form compatible with efficient numerical computations. Corroborating accelerated test methods and bench mark tests should be devised.

6. Cavitation: Theoretical analysis of cavity nucleation and growth should incorporate effects of stress or strain concentrations caused by grain boundary sliding and by coarse slip bands. Parallel measurements should be conducted to delineate where cavitation is controlled by diffusional flow, or power law creep, or both and to allow statistical correlation with geometric and strength variability in microstructures. In ceramics with glassy phases at the boundaries, viscous hole growth should be considered. Mechanisms accelerating (or retarding) nucleation and growth of cavities under cyclic loads or irradiation should be discerned, with particular attention given to cavitation ahead of the crack tip.

7. Macro-crack growth: Both theory and experiment are required to determine: the mechanisms of creep crack growth, especially intergranular cracking, the stress and temperature ranges of growth; effects of statistical aspects of microstructure (particularly in ceramics); the roles of stress wave shape and hold times in cyclic loading; and the effects of environments and irradiation.

8. Boundary diffusion: Given the several references above to grain boundary sliding, it is especially important to obtain reliable data on self and impurity diffusion along grain and interphase boundaries and to understand the seemingly anomolous diffusion along contaminated boundaries in ceramics. Diffusion should be correlated with boundary type and structure and degree of segregation.

9. Boundary structure and cohesive strength: High resolution experimental probes and computer simulation techniques should be used to investigate boundary structure, particularly of non-special grain and interphase boundaries, with solute segregation, and in complex materials. The structure of defects --- vacancies, interstitials, dislocations --- their dissociation at boundaries, and the effects of solute segregation warrant study. Measurement of grain and interphase boundary cohesion is needed, especially as a function of solute segregation; however, techniques must be developed.

10. Design methodology and service life prediction: Approaches are being evaluated based on crack initiation and growth. These should incorporate probabilistic evaluation of properties rather than deterministic as now used by the ASME codes. Accelerated tests should be validated with respect to physical mechanisms expected during the longer-term material service, and service life models formulated based on these mechanisms.

In the third session of the workshop, the chairman of each subgroup presented its findings to all workshop participants in order to gain their perspectives and to increase interaction among the design, engineering, and science representatives. This proceedings is being published in the hope that it will be of value to the materials community interested in high temperature behavior of structural materials.

This Division thanks the workshop attendees for their active participation. Each speaker's further effort in preparing his presentation and manuscript is gratefully acknowledged, as is that of each subgroup chair- and cochairperson in synthesizing a concise report from the various discussions. Ms. Robin Spahr's assistance with the correspondence and this proceedings is appreciated.

Reference

1. O. Pinkus and D. C.Wilcox, Strategy for Energy Conservation Through Tribology, Report from a workshop held in Washington D.C., February 7-9, 1977, American Society of Mechanical Engineers, New York, 1977.

TABLE I: DOE RESEARCH & DEVELOPMENT ON ELEVATED TEMPERATURE DEFORMATION AND FRACTURE OF STRUCTURAL MATERIALS

DOE DIVISION/OFFICE*	FY 79 Estimate** (10^6)
Reactor Research & Technology (ET)	
Component Materials & Structural Support	4.4
Materials & Chemistry	3.2
Fuel Systems	1.4
Nuclear Power Development (ET)	2.3
Advanced Nuclear Systems & Projects (ET)	.2
Magnetic Fusion Energy (ET)	.5
Magnetohydrodynamics (ET)	.3
Fossil Fuel Utilization (ET)	.9
Solar Energy Technology (ET)	.6
Transportation (C/S)	.5
Materials Sciences (ER)	2.0

* ET: under the Assistant Secretary for Energy Technology
C/S: under the Assistant Secretary for Conservation and Solar Applications
ER: under the Director, Office of Energy Research

** Portion of total office/division funds directed towards high temperature mechanical behavior of materials.

TABLE II: WORKSHOP PARTICIPANTS

Name	Organization
Ali Argon	Massachusetts Institute of Technology
Robert Balluffi	Massachusetts Institute of Technology
Joseph Blass	Oak Ridge National Laboratory
Rowland Cannon	Massachusetts Institute of Technology
David Clarke	Rockwell International
Louis Coffin	General Electric Company
Bruce Cramer	McDonald Douglas Astronautics East
Dwight Diercks	Southwest Research Institute
Anthony Evans	University of California/Berkeley
Gopal Gupta	Foster Wheeler Development Corporation
Edward Hart	Cornell University
Art Heuer	Case Western Reserve University
Paul Ho	T. J. Watson Research Center, IBM
Bernard Kear	United Technologies Research Center
Campbell Laird	University of Pennsylvania
Terence Langdon	University of Southern California
Fred Lange	Rockwell International
Che-Yu Li	Cornell University
Saurindra Majumdar	Argonne National Laboratory
Frank McClintock	Massachusetts Institute of Technology
David Moon	Westinghouse R&D Center
William Nix	Stanford University
Rishi Raj	Cornell University
James Rice	Brown University
David Richerson	AiResearch Manufacturing Company
Robert Swindeman	Oak Ridge National Laboratory
David Taplin	University of Houston
Arthur Turner	Argonne National Laboratory
Vaclav Vitek	University of Pennsylvania
Julia Weertman	Northwestern University
Calvin White	Oak Ridge National Laboratory
Sheldon Wiederhorn	National Bureau of Standards
Gary Wire	Westinghouse-Hanford
William Wolfer	University of Wisconsin
David Woodford	General Electric Company

TIME-DEPENDENT FRACTURE OF MATERIALS AT ELEVATED TEMPERATURE

FOR

SOLAR THERMAL POWER SYSTEMS

By

G. D. Gupta

Foster Wheeler Development Corporation
12 Peach Tree Hill Road
Livingston, New Jersey 07039

SUMMARY

Various Solar Thermal Power Systems are briefly described. The components of solar power systems in which time-dependent fracture problems become important are identified. Typical materials of interest, temperature ranges, and stress states are developed; and the number of cycles during the design life of these systems are indicated. The ASME Code procedures used by designers to predict the life of these components are briefly described. Some of the major problems assoicated with the use of these ASME procedures in the design of solar components are indicated. Finally, a number of test and development needs are identified which would enable the designers to predict the life of the solar power system components with a reasonable degree of confidence.

INTRODUCTION

The Central Receiver Solar Thermal Power System (CRSTPS) is one of the systems which are currently being studied for the development of solar energy as an alternate to the nonrenewable fossil energy resources. A central receiver solar power system contains a large number of mirrors which concentrate the solar radiation on to a receiver placed on the top of a tower. The concentrated solar radiation provides the energy source for a heat engine which generates the electrical power.

The objective of this presentation is to discuss the following questions:

- How do the time-dependent fracture problems arise in solar thermal power systems?
- What tools does the industry presently have to treat these problems?
- What are the problems in using these tools?
- What are the general areas in which further tests and developments are needed?

In order to understand the first question, a further look into various components of the receiver is needed. The receiver, located on the tower, absorbs the concentrated solar radiation and raises the temperature of a working fluid. In general, depending on the heat engine, the working fluid could be all liquid, all gaseous, or a two-phase mixture. The system which is in the most advanced state of development uses a Rankine thermodynamic cycle with steam/water as working fluids. A typical system is shown in Figure 1 in which a "once-through" receiver is depicted.

The feedwater from the condenser is pumped to the receiver tubes. A "once-through" receiver is divided into three main sections, namely: preheater, in which the feedwater is heated to saturation temperature at the operating pressure; boiler, in which water is boiled to saturated steam; and superheater, in which the steam is superheated to the desired temperature. The superheater steam is sent down to a steam turbine which runs an electric generator. A thermal storage system can also be interfaced with this system in order to maintain the steam turbine operation without diurnal interruption. Typical temperature and pressure conditions occurring in this system are listed in Table 1. Clearly, the superheater section of the receiver, parts of the thermal storage subsystem, and the superheater outlet pipe are the components in which time-dependent fracture is an important consideration.

A variation of this system uses two fluid loops for steam generation. Liquid sodium or molten salt is heated in the primary loop at the receiver. The heat is transferred to water in the secondary loop in a steam generator. The major advantages of this system are:

- Lower operating pressure in the receiver
- Smaller receiver
- Higher heat fluxes.

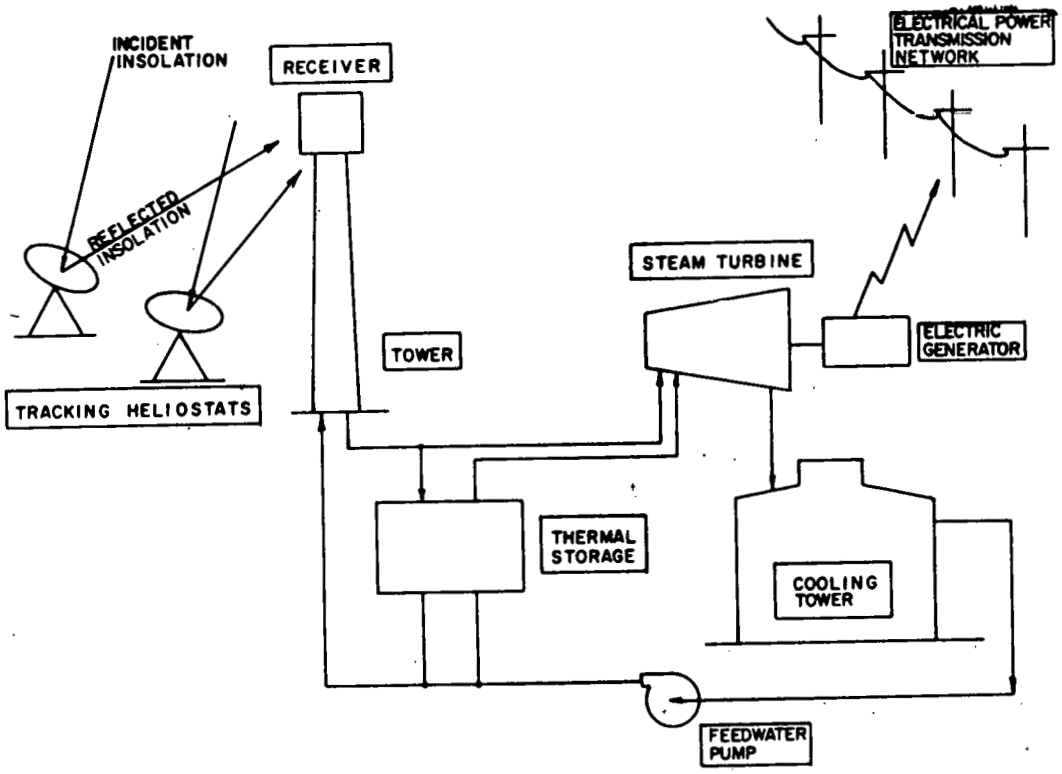

Figure 1 Schematic--Solar Rankine Cycle System (Water/Steam)

Table 1 Maximum Temperatures and Pressures in Various Systems

SYSTEMS WITH STEAM TURBINE		SYSTEMS WITH GAS TURBINE
WATER/STEAM COOLED	LIQUID METAL COOLED	
STEAM OUTLET: ~950 - 1000°F ~1300-3000psi	STEAM OUTLET: ~950 - 1000°F ~1300-3000psi	GAS OUTLET: ~1400-1600°F ~100-200psi
BOILER METAL: <800°F ~1700-3300psi	STEAM GENERATOR METAL: ~1100 - 1300°F ~1300-3000 psi	RECEIVER METAL: ~1500 - 1800°F ~100-200 psi
SUPERHEATER METAL: ~1200°F ~1500-3200psi	LIQUID METAL OUTLET: ~1100-1300°F ~100-300psi	
	RECEIVER METAL. ~1200-1400°F ~100-300psi	

However, the receiver must now operate at higher temperatures. There are two major components (namely, receiver and steam generator) where time-dependent fracture becomes important. The relevant temperatures and pressures are listed in Table 1.

Another system which is now being studied uses a Brayton thermodynamic cycle. A typical example of such a system is shown in Figure 2. The ambient air is pressurized in a compressor and via a regenerator is sent to the solar receiver. The air passing through the receiver gets heated to approximately 1500°F and is directed to a gas turbine which in turn runs an electrical generator as well as the air compressor. The hot exhaust from the gas turbine is utilized to preheat the incoming air in the regenerator. Typical temperatures and pressures are also listed in Table 1.

TIME-DEPENDENT FRACTURE PROBLEM

What makes solar power systems different from the fossil and nuclear power plants is their severe elevated temperature cyclic duty. Over a 30-year design life of a solar receiver, the diurnal variations produce 10,950 cycles. Flux variation due to cloud covers further increase the cyclic duty required of the solar receiver. Assuming an 8-hour per day operation, the total hold-time during a 30-year service life would be 87,600 hours. It is this elevated temperature operation coupled with the cyclic nature of loading which activates the creep rupture, creep ratcheting, and creep-fatigue interaction mechanisms of time-dependent fracture.

A wide spectrum of materials are of interest in these systems. A typical set of temperature ranges and the corresponding materials are listed in Table 2.

The solar heat flux falls only on one side of the receiver tubes. A nonsymmetrical temperature distribution on the cross-section of the receiver tubes is, therefore, generated. A typical temperature distribution is shown in Figure 3. In addition to through-the-thickness temperature gradient, a large front-to-back temperature gradient also occurs. A predominantly biaxial state of stress exists at the maximum temperature region and may vary from all compressive at the outer wall to tensile-compressive at the inner wall as shown in Figure 4. The tensile stresses develop in the hoop direction due to pressure; however, thermal stresses, in both hoop and longitudinal directions, are compressive at the hot surface and tensile at the colder surface of the receiver tube.

CREEP-FATIGUE EVALUATION

A designer has to demonstrate that various components of the solar system would retain their structural integrity under the operating loads for a design life of 30 years. A creep-fatigue evaluation must be performed according to some cumulative damage procedure. One procedure used in industry today is described in the ASME Boiler and Pressure Vessel Code in Code Case N-47.[1] The procedure calls for evaluating creep damage and fatigue damage separately and

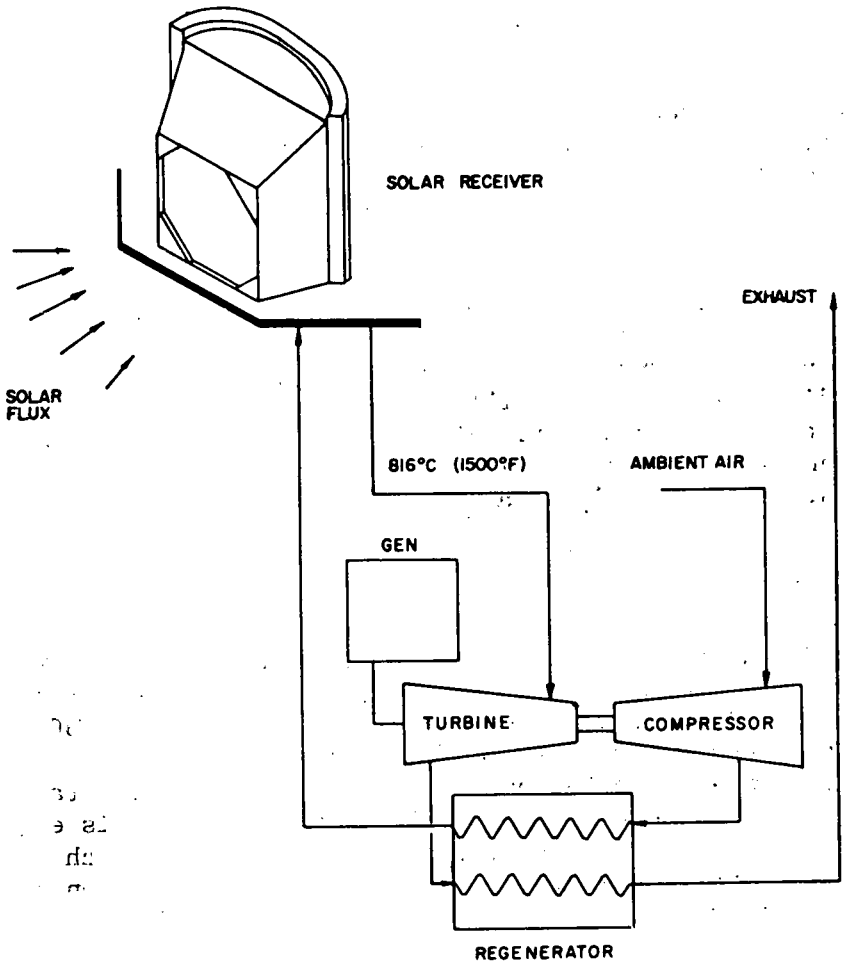

Figure 2 Schematic--Solar Brayton Cycle System

Table 2 Temperature Ranges and Materials in the Solar Power Systems

TEMPERATURE RANGE (°F)	MATERIALS OF INTEREST
800 - 1000	$1\frac{1}{4}$Cr $\frac{1}{2}$Mo; $2\frac{1}{4}$Cr 1Mo; 304SS
1000 - 1200	304SS; 316SS; I-800H
1200 - 1400	I-800H; INCONELS (Ni-Cr-Fe)
1400 - 1600	INCONELS; HAYNES 188 (Co-Cr-Ni)
1600 - 1800	HAYNES 188; SUPERALLOYS
1800 - UP	STRUCTURAL CERAMICS (Si_3N_4, SiC); REFRACTORY BASED ALLOYS (Ta; Mo; Cb; W)

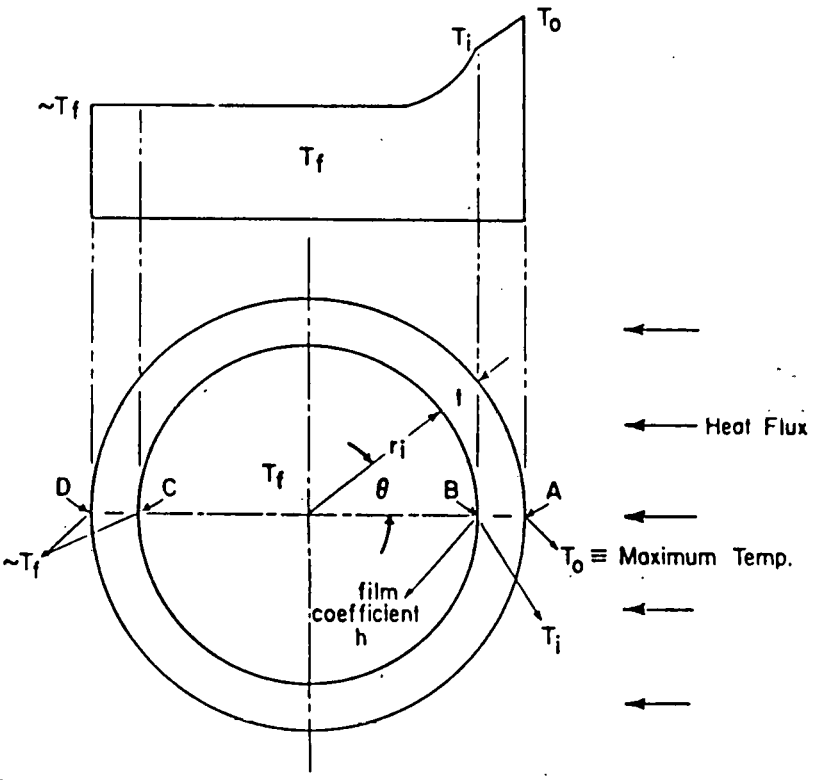

Figure 3 Typical Temperature Distribution in a Solar Receiver Tube

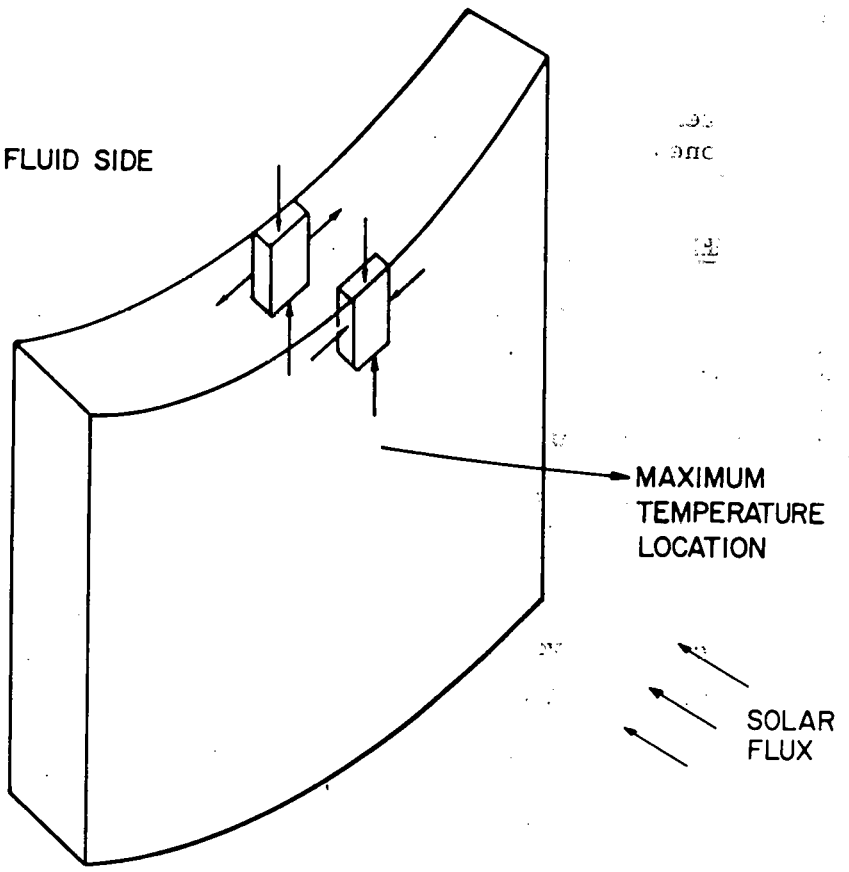

Figure 4 Stress State at the Maximum Temperature Location in a Receiver Tube

use a linear (or bilinear) cumulative damage equation:

$$\Sigma \frac{t}{T_d} + \Sigma \frac{n}{N_d} \leq D \qquad (1)$$

The first term represents the cumulative creep damage in which T_d is the creep rupture time related to the effective stress during a hold time, t, between any two consecutive cycles. The second term represents the cumulative fatigue damage in which N_d is the fatigue life related to the effective strain range value corresponding to n number of cycles. D is the material dependent damage parameter.

PROBLEMS WITH ASME CODE ANALYSIS

There are a number of serious problems associated with the use of the ASME Code Case N-47 for the design of solar components. Some of the major problems are listed below:

- Highly conservative - will result in excessive economic penalties
- Treat tensile and compressive hold identically
- Data available for only limited number of materials
- Most data based on uniaxial tests; multiaxial effects not well characterized.

Because of these problems, an ASME Solar Energy Standards Committee has been formed which is attempting to develop appropriate code rules for use in the design of solar components.

TESTS AND DEVELOPMENT NEEDS

Under a contract from the U.S. Department of Energy, Foster Wheeler Development Corporation has recently completed a study in which the design problems of solar thermal power systems were examined in relation to the currently available Structural Design Code rules. As a result of this study, an interim structural design standard was prepared, and a number of test and development programs needed to generate new design data and to update the interim design standard were identified.[2] Some of the major test and development needs are listed below:

- Validity of accelerated tests to long-time service
- Effect of compressive hold-time (healing?)
- Effect of multiaxial stresses on creep and fatigue damage
- Material variability studies
- Creep and thermal ratcheting

- Creep-fatigue damage criteria
- Development of simplified methods for creep-fatigue evaluation.

REFERENCES

1. ASME Boiler and Pressure Vessel Code, Case Interpretations, N-47 (earlier Code Case 1592), New York, 1977.

2. I. Berman, A. C. Gangadharan, G. D. Cupta, and T. V. Narayanan, "Final Report - Phases 1 and 2: An Interim Structural Design Standard for Solar Energy Applications," prepared for Sandia Laboratories, Livermore, California, January 1979.

DESIGN CONSIDERATIONS: GAS TURBINES FOR ELECTRIC POWER GENERATION

David M. Moon
Westinghouse Research & Development Center

ABSTRACT

Of all of the present day power generating equipment the gas turbine represents one of the most sophisticated designs from the standpoint of time dependent deformation behavior. The large size of the equipment, which limits the amount of full scale testing, together with the demanding performance requirements and high level of reliability desired places a high degree of emphasis on the high temperature deformation design process.

As an example of the various design considerations used in this equipment, a brief overview of the turbine will be given, highlighting the materials, stress, temperatures and load history experienced by the major components. Particular attention will then be focused on the vane segment design considerations. This component is not only structurally complicated, but experiences steep temperature gradients imposed by internal cooling and large temperature transients during cyclic duty operation which have to be addressed in the design procedure. Based on this discussion the limitations of the current design procedures will be highlighted and the areas requiring additional research inputs will be discussed.

CERAMIC DESIGN REQUIREMENTS FOR LONG-LIFE HEAT ENGINES

David W. Richerson

AiResearch Manufacturing Company of Arizona

1.0 INTRODUCTION

Heat engines have continually evolved to higher temperature designs to provide improved cycle performance. In the past this has been achieved by development of improved alloys and cooled component designs. Metal alloys are approaching peak operating temperature capabilities with little further temperature increase likely without incorporation of complex and/or expensive cooling schemes. Advanced ceramic materials have the potential for uncooled operation at temperatures significantly higher than metal alloys and are currently being developed for heat engine applications.

During the past 15 years, over 300 ceramic materials have been evaluated as candidates for heat engine (especially gas turbine) applications. Most ceramic materials evaluated had inadequate strength, poor oxidation resistance or could not withstand high thermal stresses. The best materials defined in these studies were silicon nitride (Si_3N_4) and silicon carbide (SiC). Both materials have high strength, low thermal expansion, high thermal conductivity and good oxidation resistance. Recent studies indicate aluminum nitride (AlN) and Sialons (Si_3N_4 - Al_2O_3 solid solution alloys) may also be good candidates for some heat engine components.

Ceramic material technology is evolving rapidly with new materials being introduced and existing materials being significantly improved. However, ceramics for heat engine applications are still at a relatively early stage of development compared to metals. Mechanisms of material densification and of resulting properties such as creep, slow crack growth and stress corrosion are not adequately understood to allow component design or life prediction. Basic research is necessary to define the mechanisms and provide the necessary data base.

The following sections will briefly describe the potential application of ceramic materials to high temperature power generation gas turbine engines with emphasis on the conditions to which the ceramic components will be exposed.

2.0 TYPES OF GAS TURBINE APPLICATIONS

Three categories will be discussed:

- o Open Cycle Gas Turbines
- o Closed Cycle Gas Turbines
- o Waste Heat Recovery

2.1 Open Cycle Gas Turbines

In an open cycle gas turbine the hot combustion gases pass through the turbine. Interaction of these gases (and any included particulate matter) with the turbine rotor and stator components typically limits the operating temperature of the turbine and the life of the components. This is currently true for metals and is likely to be a factor for ceramics, although very little data are available. Impurities in the combustion gases such as sulfur, sodium and vanadium are particularly deleterious to metals. Studies are required to determine the effects of these and other impurities on candidate ceramic materials at temperatures between 2000 and 3000°F.

Much interest is presently focused on coal and coal-derived fuels. Three approaches have been or are being evaluated:

- o Direct coal burning
- o Coal-derived liquid fuels
- o Coal gasification

Direct coal burning in an open-cycle gas turbine does not appear feasible. Coal contains a significant percentage of non-combustible material that would pass through the turbine as slag or ash. Ash content and composition vary according to the coal source. Illinois No. 6 coal contains 11.6 weight percent ash compared to Wyoming coal with 5.7 weight percent. Table I compares the chemical analysis of the slag of these and other coals sources.

TABLE I COMPOSITION OF VARIOUS COAL SLAGS

Rank Location	Lignite Zap, N.D.	M.V.B. Ehrenfield, Pennsylvania	H.V.C. Victoria, Illinois	Sub.bit Hanna, Wyoming
Seam	Zap	L.Freeport	Illinois 6	80
Ash Composition %				
SiO_2	20-23	37	50	29
Al_2O_3	9-14	23	22	19
Fe_2O_3	6-7	34	11	10
TiO_2	0.5	0.8	0.9	0.8
CaO	18-20	0.8	9.0	18.7
MgO	6-7	0.4	1.1	2.9
Na_2O	8-11	0.2	0.35	0.2
K_2O	0.3	1.3	2.2	0.7
SO_3	21	1.6	1.6	17.78
%ash	7-11	15.1	14.3	6.6
%sulfur	0.6-0.8	4.04	2.6	1.2

All contain significant amounts of sodium compounds, sulfur and other chemical species that could interact with turbine components.

Previous studies have demonstrated that coal slag adheres to open cycle turbine components resulting in a rapid decrease in gas flow and a loss in aerodynamic efficiency. This slag fouling has prevented direct coal burning in open cycle gas turbine engines.

Coal-derived liquid fuels produce cleaner combustion products than direct coal burning, but some ash or slag is still present. As with direct coal burning, slag fouling limits the application of coal-derived liquid fuels.

Coal gasification produces still cleaner fuels, especially if procedures are added to remove particulates and sulfur. Coal gasification fuels appear viable for use in open cycle gas turbines. However, energy is required to gasify the coal, cool the resulting gas prior to cleaning and remove the particulates and sulfur. This wasted energy limits the overall plant efficiency and demands other systems in the plant be operated as efficiently as possible. Therefore, the gas turbine must be operated at very high inlet temperatures and bottomed by a conventional steam turbine.

A current DOE study entitled "Ceramic Technology Readiness Program" is evaluating material requirements for a turbine with an average inlet temperature of 2600°F. Considering typical temperature distribution in a turbine, some first stage stator vanes will be exposed to 2900 - 3000°F. Ceramic materials are being considered for these and other uncooled components exposed to temperatures above 2000°F. The Ceramic Technology Readiness Program has defined the following basic technology needs for ceramics for this type application:

- Measurement of strength, creep, static fatigue, cyclic fatigue and other properties in the 2000 - 3000°F range
- Determination of the mechanisms of slow crack growth and incorporation into a life prediction methodology
- Determination of the effects of long term exposure to the gas turbine combustion environment and incorporation into a life prediction methodology
- Material development to resolve any deficiencies defined by the above basic property studies

2.2 Closed Cycle Gas Turbine

In a closed cycle gas turbine the combustion gases do not pass through the turbine, but are instead passed over a heat exchanger which transfers the heat to an enclosed working fluid. Thus, the heat exchanger is subjected to higher temperatures than the turbine and is the only component exposed to the combustion gases. Figure 1 shows a simple schematic of a combined closed cycle/steam power system.

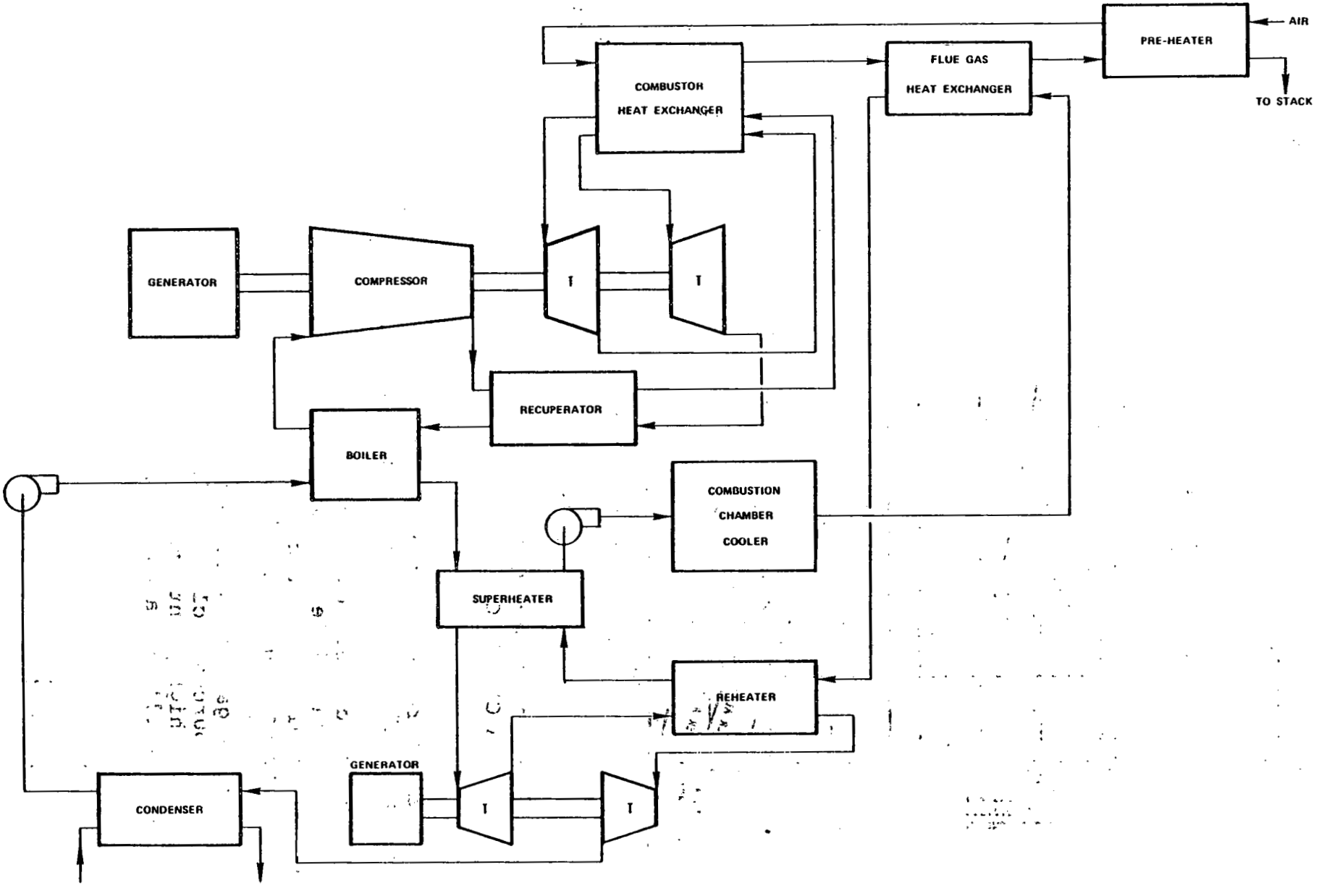

FIGURE 1

SCHEMATIC OF COMBINED CLOSED-CYCLE/STEAM POWER SYSTEM

Figure 2 shows the component temperature and cycle efficiency as a function of turbine inlet temperature.

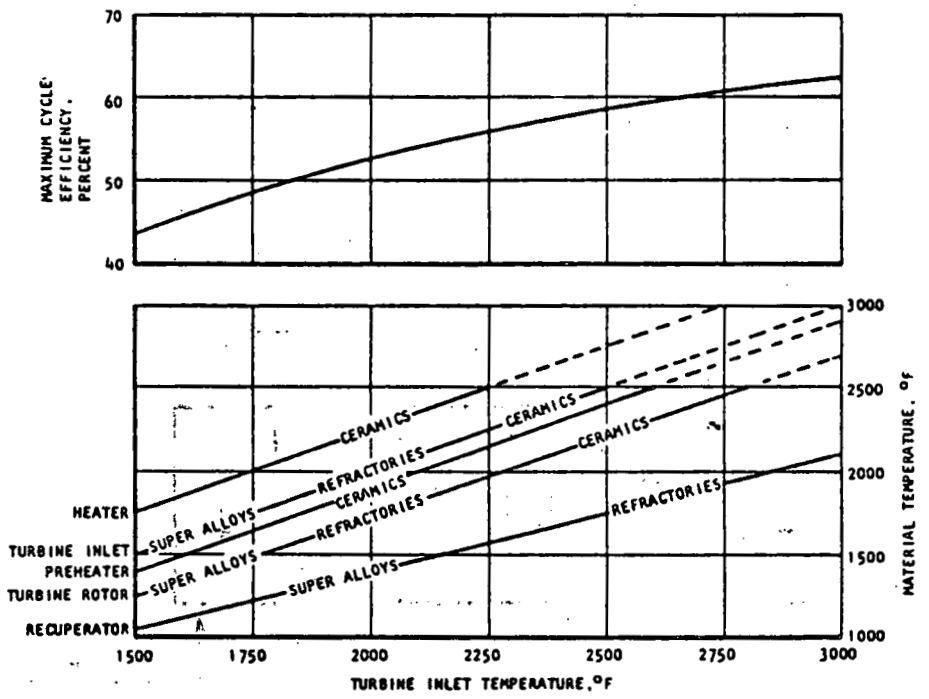

FIGURE 2

COMPONENT TEMPERATURE AND CYCLE EFFICIENCY
FOR A CLOSED CYCLE GAS TURBINE ENGINE

The term "heater" refers to the heat source heat exchanger and the term "refractories" refers to refractory metals.

The heat source heat exchanger is operated at higher temperatures than the turbine inlet. Based on current metal properties and economics, a ceramic heat source heat exchanger is required for any turbine inlet temperature over 1500°F.

Closed cycle gas turbines have the advantage of using a wide variety of heat sources including direct coal burning. With the use of ceramics, very high plant efficiencies can be achieved. Figure 3 summarizes the results of a DOE study conducted by AiResearch.

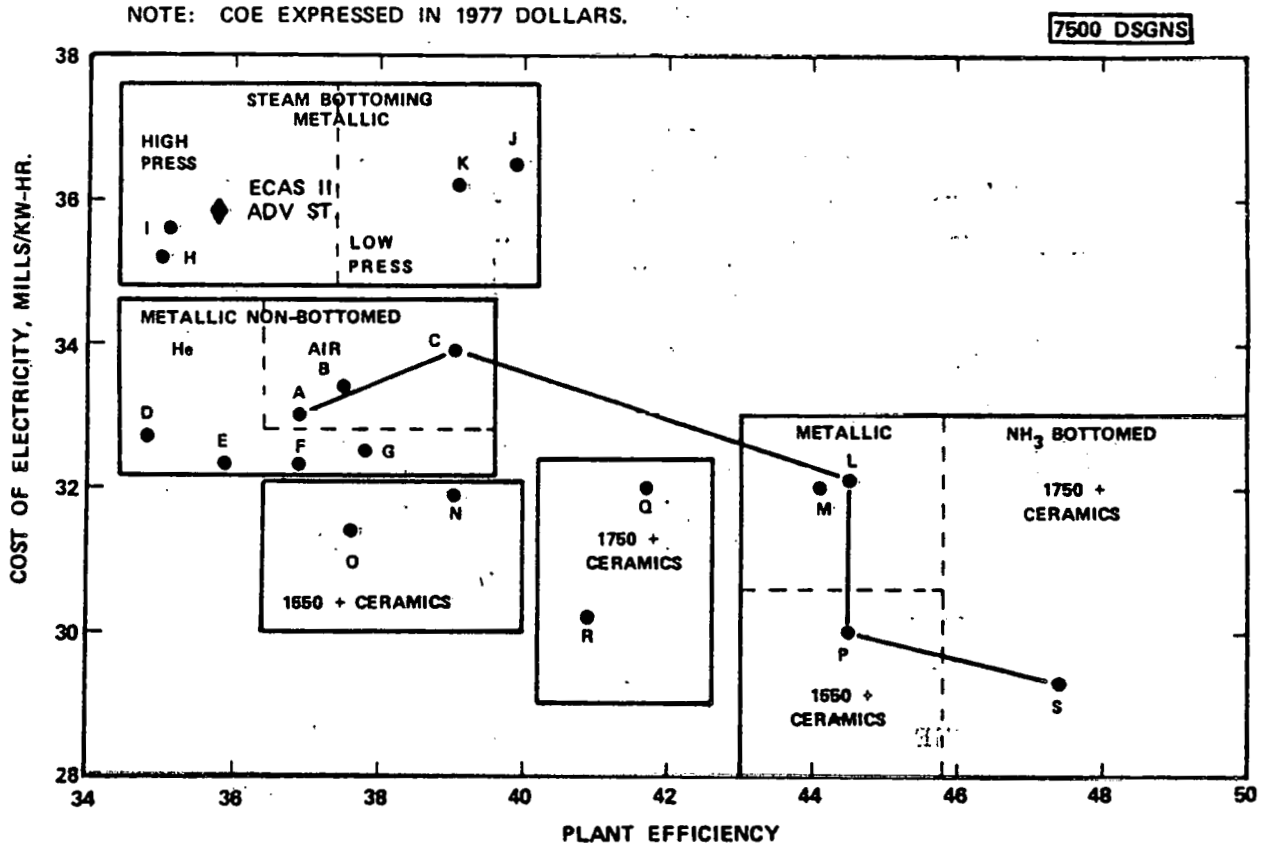

FIGURE 3

DOE/AIRESEARCH CLOSED CYCLE GAS TURBINE HEATER PROGRAM - TASK 1 SUMMARY

Use of ceramics in a closed cycle gas turbine can achieve high efficiency operation and low cost electricity at much lower temperatures than required for a coal gasification/open cycle system.

2.3 Waste Heat Recovery

Many industrial processes release large amounts of hot gases. Significant energy could be produced by using the waste heat from these processes to operate a turbine. In most cases the key component is a ceramic heat exchanger. Examples of two systems are shown in Figures 4 and 5.

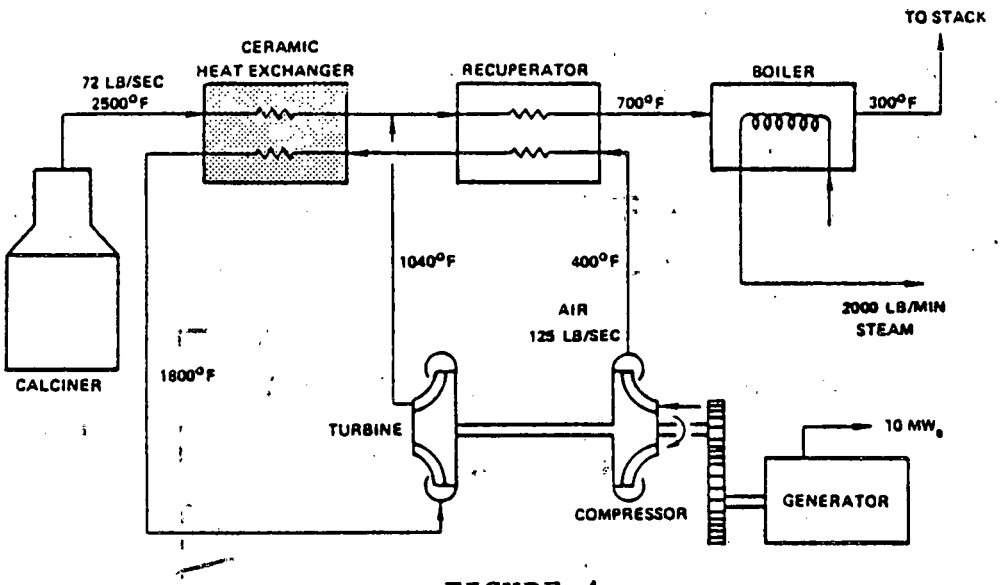

FIGURE 4

ENERGY CONSERVATION - COKE CALCINER

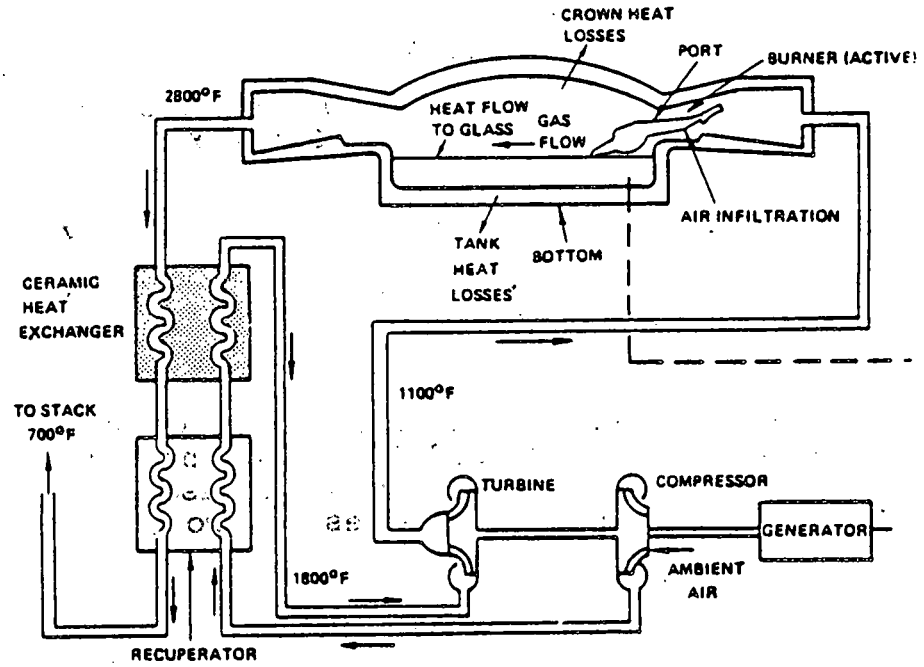

FIGURE 5

ENERGY CONSERVATION - GLASS FURNACE

3.0 CONCLUSIONS

Ceramic materials provide the potential for large increases in the efficiency of power generation. However, candidate ceramic materials are still in the development stage and much basic technology regarding properties as a function of temperature, slow crack growth under static and cyclic loading and environmental effects must be obtained by basic and applied research.

Energy applications are currently materials-limited and significant progress will not occur until a major, long-range commitment is made to material development and characterization.

DESIGN CONSIDERATIONS FOR HIGH TEMPERATURE COMPONENTS IN FUSION ENERGY SYSTEMS *

Bruce A. Cramer

McDonnell Douglas Astronautics Company - St. Louis

First wall and blanket structures present one of the most critical design challenges of fusion reactors. The response and resulting life of these components, operating in high temperature and radiation environments, will have a significant influence on the economy of fusion power. First wall structures form the vacuum wall of the reactor plasma chamber and contain a circulating coolant. Even a very small leak of air or coolant into the chamber will be cause for shutdown of the reactor.

Structural analysis studies* have been directed at developing an understanding of the response of first wall structures to fusion reactor environments so that direction can be provided to future research efforts. These studies have shown the importance of fatigue crack growth and brittle fracture mechanisms. The growth of flaws to a coolant leak condition have been identified as a critical life determining failure mode. Neutron wall loading has a major effect on wall life due to both the increased rate of radiation damage and higher structural temperatures associated with higher neutron wall loadings.

Inelastic analyses have provided an indication of the very complex nature of the stress histories in a first wall structure. These studies have included effects of irradiation swelling, thermal creep, irradiation creep, and plasticity on structural response. Results show that residual tensile stresses have a significant impact on first wall life. These residual stresses result from creep relaxation of stresses during the plasma burn.

Primary materials needs for the design of fusion reactor first wall and blanket structures include fatigue crack growth rate data, fracture toughness data, swelling and creep interaction effects, and radiation surface and bulk damage interaction effects. These must be obtained based on in situ testing in the appropriate coolant environments for a variety of candidate structural materials. The wide range of loading conditions and operating environments suggest the importance of understanding the complete range of effects including cyclic frequency, hold times and strain rates.

Presented in the following pages are expanded discussions of the vugraphs used at the workshop. These address some of the key issues in fusion reactors as they relate to the subject of this workshop-time dependent fracture at elevated temperature.

* Work reported has largely been conducted under contract with the Electric Power Research Institute and DOE contract with General Atomic Company.

FUSION REACTOR CONCEPTS PROVIDE A WIDE RANGE OF ENVIRONMENTAL CONDITIONS

13-2271A

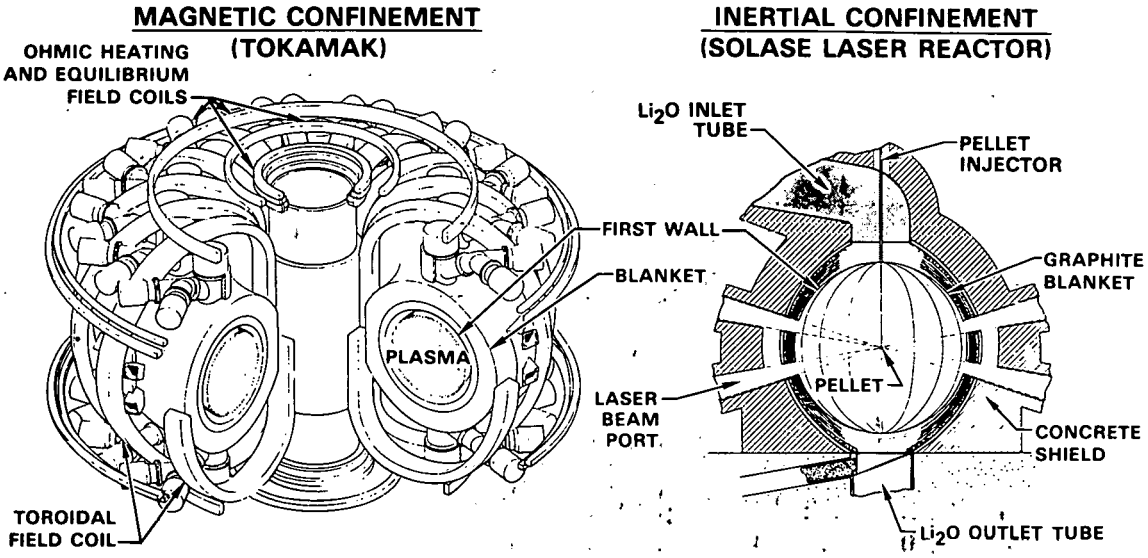

- CYCLIC BURNS (TOKAMAKS)
- STEADY STATE (MIRRORS)
- MAGNETIC FIELDS
- PLASMA DISRUPTIONS
- PULSED PELLET EXPLOSIONS
- BUFFER GAS BLAST WAVE
- X-RAY ABSORPTION
- REFLECTED LASER LIGHT
- COOLANTS (HELIUM, LIQUID LITHIUM, MOLTEN SALTS, WATER)

Several concepts for producing fusion power are presently being studied. These include magnetic confinement concepts such as a tokamak reactor and inertial confinement concepts such as the SOLASE laser reactor. The first wall and blanket structures of these reactors are subjected to a wide range of loading and environmental conditions at elevated temperature. Therefore, it is difficult, at the present time, to establish specific material requirements for fusion reactor first wall and blanket structures.

Shown in the above figure are the major features of conceptual tokamaks and laser fusion reactors. In the case of a tokamak reactor, conditions include cyclic thermal loads resulting from the cyclic plasma burns. Additionally, plasma disruptions result in a dynamic pulse load in the first wall. An alternate magnetic confinement fusion reactor concept, the mirror machine, operates in essentially a steady state mode. The first wall of a laser reactor is subjected to rapid pulsed loads due to x-rays, reflected laser light, buffer gas blast wave, and charged particles.

Operating environments will affect structural performance. Materials in fusion reactor first wall and blanket structures will be subjected to irradiation at elevated temperatures. Operating structural temperatures will be a function of the capability of the material. In typical stainless steel first walls for conceptual tokamak reactors, operating temperatures have been over 550°C. In addition to exposure to the plasma or pellet debris on one side of the first wall, these structures will be in contact with coolants which may affect properties such as fatigue crack growth. Leading candidate coolants for fusion reactor first wall and blanket structures include helium, liquid lithium, molten salts, and water.

RADIATION ENVIRONMENTS RESULT IN MATERIAL BULK AND SURFACE DAMAGE

13-2273A

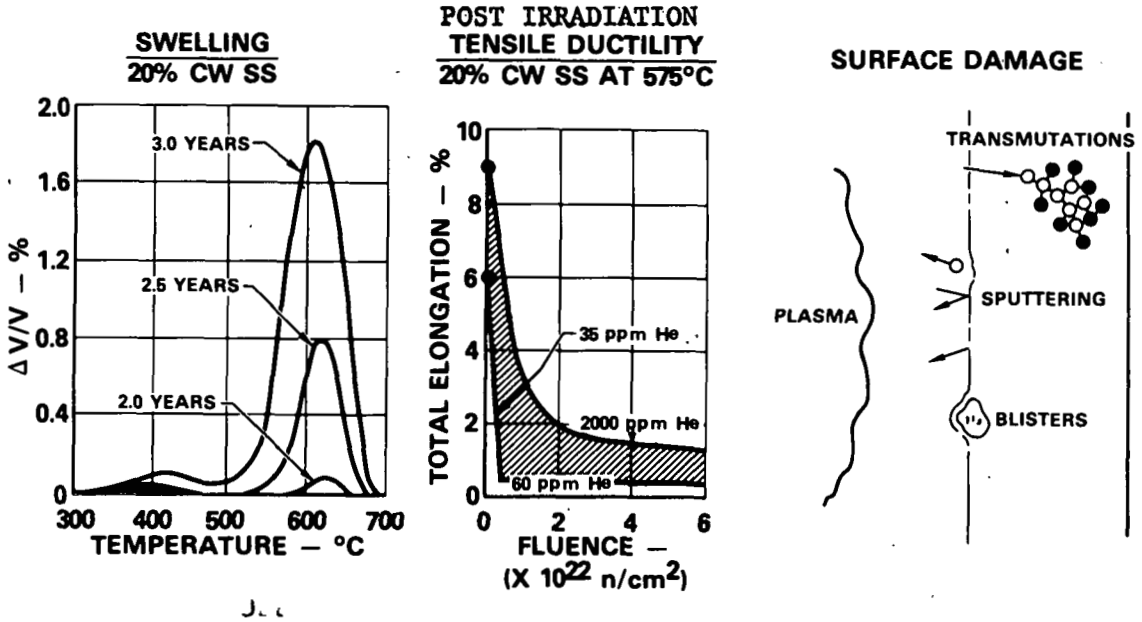

Radiation environments and complex loading conditions in a fusion reactor result in a variety of material phenomena at elevated temperature which will tend to degrade structural performance. These phenomena include bulk effects such as irradiation swelling and creep, strength changes due to matrix hardening, helium embrittlement, and surface effects such as sputtering and blistering. These effects, together with high temperature material effects, must be included in the analysis of fusion reactor first wall and blanket structures.

Shown in the above figure are examples of some of the radiation effects. Swelling of 20% cold worked 316 stainless steel is sensitive to temperature and is time dependent. This phenomena has been shown to increase in the presence of applied stresses. Perhaps the greatest concern in first wall and blanket structures are loss of uniform strain to failure and increases in ductile-brittle transition temperatures. Losses in elongation to less than 0.5% have been shown to result from irradiation as indicated in the figure. In addition to the bulk damage effects caused by high energy neutrons, the first wall surface is subjected to damage from charged particles, neutrons, neutral atoms, and electromagnetic radiation. These cause sputtering of atoms from the free surface, blistering by implantation, and transmutations as indicated schematically in the figure.

In situ testing will be needed to adequately assess the response of first wall structures. This testing will include representative first wall stress conditions and environmental conditions and include coolants such as helium, liquid lithium, and molten salts. Also, interactions between surface and bulk damage will need to be assessed.

FIRST WALL STRESSES ARE TIME DEPENDENT

13-2272

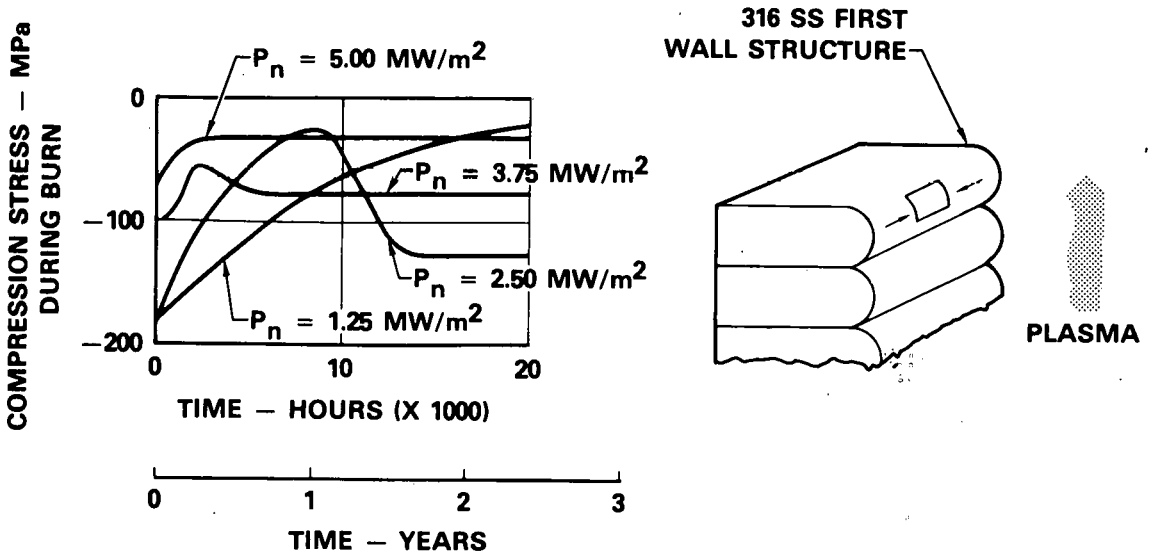

First wall structures in commercial fusion reactors will be subjected to combined effects of high temperature, stresses due to temperature gradients and internal constraints, stresses due to applied loads, thermal creep, irradiation creep, and irradiation swelling. All of these will be time dependent. The complex nature of the resulting stress histories in a fusion reactor first wall are demonstrated in the figure.

These results, shown at various levels of neutron wall loading, are based on inelastic analysis and include effects of thermal creep, irradiation swelling and irradiation creep. The compressive stresses, which occur during a plasma burn, result from high temperatures at the first wall surface adjacent to the plasma. The compressive stresses relax to relatively low levels with time and increase again as swelling is initiated. Further increases in the compressive stresses are prevented as irradiation creep and swelling offset each other. As a result of relaxation, significant residual stresses, both tensile and compressive, occur upon reactor shutdown.

Present computer codes provide capability for analyzing complex structures, including the nonlinear effects of creep and plasticity. However, the resulting stress and strain histories are functions of the constitutive equations used and the assumed relationships describing material behavior. This capability is limited even without the additional complications of irradiation effects. Constitutive equations, which adequately represent material response, must be developed so that the response of first wall structures to reactor environments can be better understood. This will provide a basis for development of structural materials and first wall design concepts to provide long first wall life.

ELASTIC STRESS DUE TO SWELLING IN 316 STAINLESS STEEL CANISTER MODULE

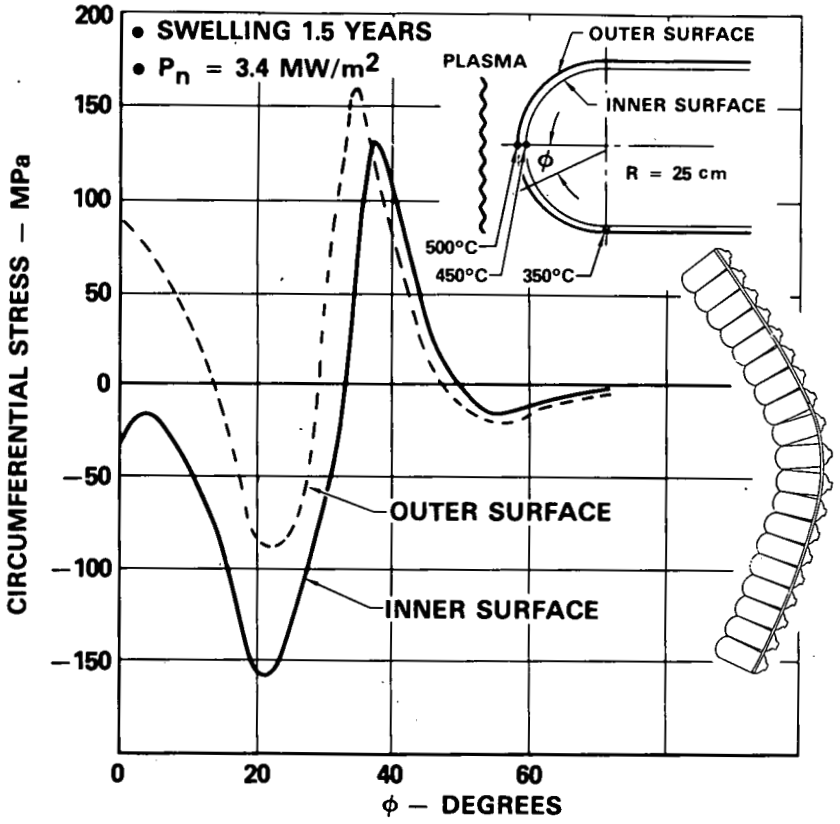

Stresses in fusion reactor first wall and blanket structures will vary significantly throughout a module. Additionally, the response of these structures will vary with location in the reactor because the neutron wall loading generally varies, particularly in the poloidal direction. Because of this it is very difficult to attain what might be called an optimum geometry for a first wall design.

Shown in the figure are stress distributions in a 316 stainless steel canister first wall configuration. Temperatures in this example vary from approximately 500°C at the tip of the canister to 350°C at the interface between the hemispherical dome and the cylinder. The peak temperature gradient through the 0.2 cm wall thickness is 50°C. This occurs at the tip of the dome (ϕ = 0). It can be noted that the major stresses in this case are essentially limited to the hemispherical dome. Both tensile and compressive stresses occur. The effects of change in stress state due to relaxation have not been included in this analysis. Additional sources of stress such as those due to coolant pressure and temperature variations, which also have not been included here, must be included in the final analysis.

CYCLIC LOADING SPECTRUM IN POWER GENERATING TOKAMAK REACTOR PLASMA CHAMBER

13-17238

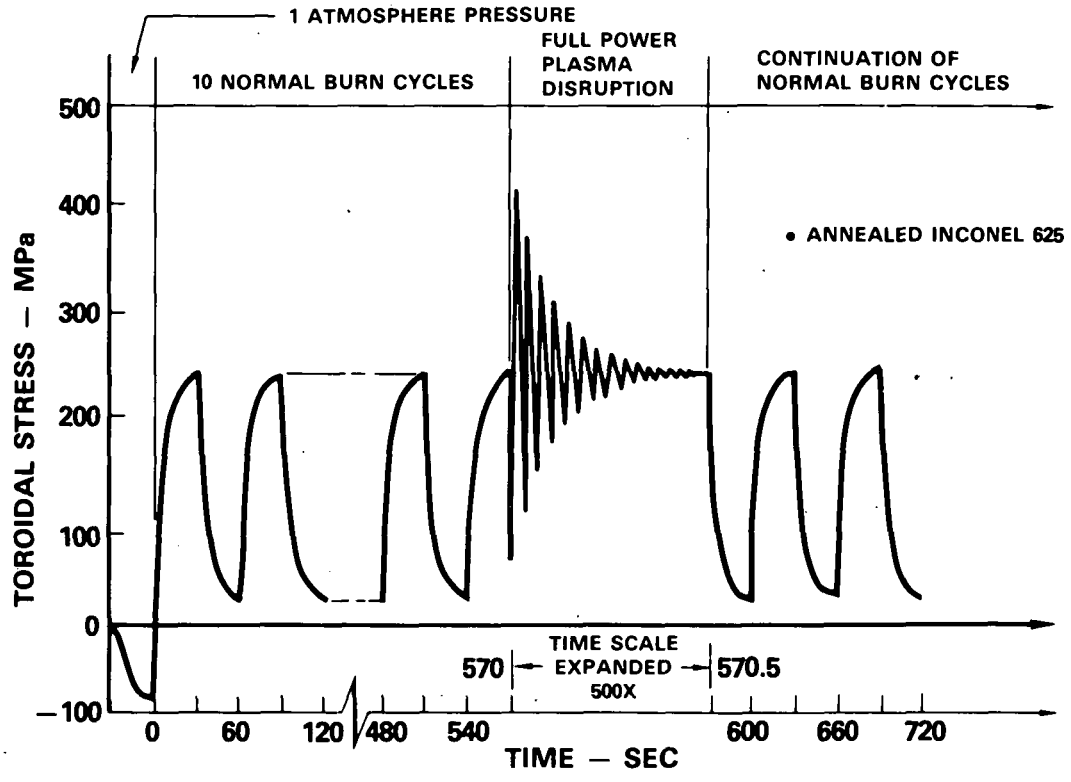

Stresses in fusion reactor first wall and blanket structures will generally be cyclic. In a tokamak reactor, cyclic stresses result from changes in temperatures and temperature distributions between plasma burn and nonburn portions of the cycle. In laser reactors, pellet micro-explosions cause rapid cyclic temperature and shock waves. Even in the case of a steady state mirror reactor, periodic shutdowns will be required. In all of these reactors local coolant pressure fluctuations can be expected and time dependent variations in the neutron wall loading may occur.

Shown in the figure is a cyclic stress history for an Inconel 625 plasma chamber for the Power Generating Tokamak Fusion Reactor concept of an Engineering Test Facility (ETF). The structural configuration is a sandwich with ribs between inside and outside skins forming channels for the coolant. The overall wall depth is 4.8 cm. The stress spectrum shown is for the outside skin where the thermal stresses are tension. The initial stress is compression due to the one atmosphere external pressure. Temperature variations between burn and nonburn (30 seconds each) cause cyclic tensile thermal stresses in the outside skin. In the study, it was assumed that a full power plasma disruption occurred each ten burn cycles. The disruption pulse causes a cyclic dynamic response of the structure. Due to the relatively short operating time required (approximately 0.2 years) for this test reactor and the relatively low temperature ($\sim$ 130°C) at the outside skin, creep and radiation effects such as swelling were not included. Results will be further complicated in a commercial reactor where stress levels will be time dependent.

FIRST WALL LIFE BASED ON FLAW GROWTH TO COOLANT LEAKAGE

13-13348

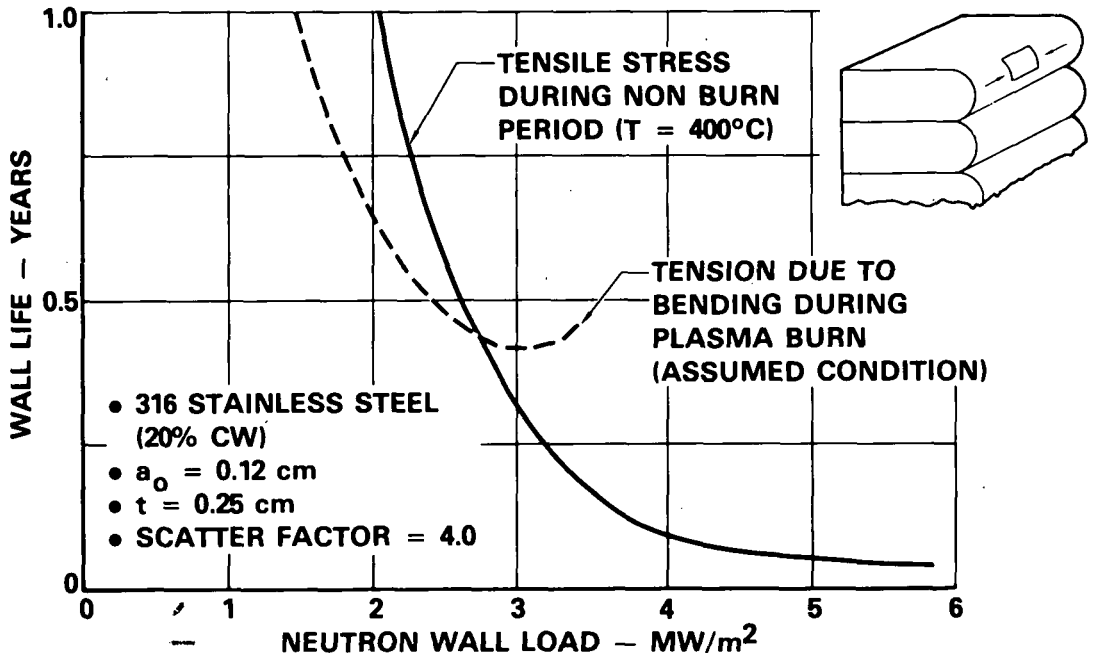

Flaw growth to a coolant leak is a critical life determining failure mode in tokamak first wall structures. Shown in the figure are resulting life predictions for a stainless steel first wall in a tokamak reactor having a plasma burn period of ninety minutes and a non burn period of six minutes. These results are based on linear elastic fracture mechanics analyses using the time dependent stress histories shown previously.

The reduction in life with increasing neutron wall load is due to both the increasing structural temperatures and increasing radiation damage. Life at low wall loadings tends to be controlled by stresses during the plasma burn. At higher wall loadings the structural life tends to be controlled by residual tensile stresses present during the non burn period. Brittle fracture due to high residual stresses will be particularly likely at high neutron wall loads. These studies resulted in an indication that wall life using 316 stainless steel as the structural material may be very short. However, this is based on a design that results in constraints. Predictions for less constrained structural configurations have resulted in longer predicted lives.

The interacting mechanisms associated with the fusion environment and the variety of system operating parameters are very complex. Therefore, it is difficult, at the present time, to place quantitative scatter bands on the resulting life predictions based on even the most complex of structural analyses. It is important to develop cumulative damage concepts, including effects of creep, crack initiation, and crack growth, applicable to fusion reactor environments, to provide a basis for adequately assessing first wall and blanket life.

Dup

LIQUID-METAL FAST BREEDER REACTOR STRUCTURAL MATERIALS DESIGN CONSIDERATIONS*,†

R. L. Huddleston[a]

Oak Ridge National Laboratory
Oak Ridge, Tennessee 37830

Introduction

The purpose of this paper is to provide DOE workshop participants with a brief overview of key structural materials design considerations for fission reactors and in particular for the "liquid-metal fast breeder reactor (LMFBR)" planned for construction on the Clinch River in Oak Ridge, Tennessee. Although there are some 72 operating power reactors in the United States, the Clinch River LMFBR, if completed, will be the first large-scale breeder reactor in this country. The light-water reactor (LWR) is the basic power reactor utilized throughout the United States today. This review will cover fission reactor operating temperatures and pressures to show the trend towards significantly higher temperature levels, and for the LMFBR, will also cover basic components, key design problems, high-temperature materials and environments, and approximate materials performance bounds.

Temperature and Pressure Levels

Some of the key design parameters for the LMFBR and LWR are compared in Table 1. Thermal design conditions for the CRBRP[b] and FFTF[c] are significantly more severe than for a typical LWR with the coolant temperature leaving the core of the LMFBR at approximately 593°C (1100°F) as compared to 343°C (650°F) in a typical LWR. Two other important thermal design parameters which play a key role in our materials problems are the coolant temperature rise during passage through the reactor core and the thermal transient magnitudes which can be introduced by operational events. The design thermal

---

*Research sponsored by the Division of Reactor Research and Technology, U.S. Department of Energy under contract W-7405-eng-26 with the Union Carbide Corporation.

†Work performed under DOE/RRT 189a OH048, High-Temperature Structural Design.

[a]J. J. Blass, ORNL, presented the paper in the absence of the author.

[b]CRBRP denotes the 375 megawatt Clinch River Breeder Reactor Plant to be constructed in Oak Ridge, Tennessee.

[c]FFTF denotes the Fast Flux Test Facility under construction at the Hanford Engineering Development Laboratory. This facility is very similar to the CRBRP except that the power generating components are omitted.

increase in coolant temperature in passing through the core of the breeder [i.e., 156°C (280°F) in the CRBRP] is approximately 3.5 times that in the LWR. Furthermore, at the core outlet, coolant stream-to-stream thermal variations are expected to approach the full thermal increase through the core. This can result in cyclic thermal variations of 156°C (280°F) in the CRBRP as compared to 44°C (80°F) in the LWR. Due to operational or duty cycle events, design thermal transient rates (thermal shocks) of 17 to 19°C/sec (30 to 35°F/sec) are required in the breeder as compared to rates of about 3°C/sec (5°F/sec) for the LWR.

Water serves as the primary coolant in the LWR with design pressures of 15.5 MPa (2250 psi) being about ten times that necessary for the liquid-sodium-cooled breeder.

Design life for both the CRBRP and the LWR is shown as 30 years in Table 1 although design life for the CRBRP is actually 40 years with 75% availability.

Looking further into the future, other advanced reactor systems are under study such as the HTGR (high-temperature gas-cooled reactor) and the VHTR (very high-temperature reactor for generating both process steam and power). Both have higher proposed core outlet temperatures than the LMFBR. A temperature of 850°C (1562°F) is under study for the HTGR gas turbine cycle and a temperature of 950°C (1742°F) under consideration for the VHTR.

Basic LMFBR Design

A conceptual drawing of the CRBRP is given in Fig. 1 with a simplified flow schematic shown in Fig. 2. The basic CRBRP design includes three heat transport loops consisting of a low pressure primary loop passing sodium coolant through the "reactor" and the "intermediate heat exchanger (IHX)," a slightly higher pressure secondary loop passing sodium coolant through the "IHX" and the "steam generator," and a steam-water loop passing through the "steam generator" and the "turbine-condenser system." Temperatures shown in Fig. 2 represent operating targets as opposed to the design temperatures given in Table 1. For safety reasons the sodium pressure in the secondary loop is higher than in the primary loop to ensure that any leakage will be toward the primary side.

Key structural components in the LMFBR include (1) a reactor vessel and associated internal components, (2) an intermediate heat exchanger for transport of heat between the primary and secondary sodium, (3) two evaporators and a superheater which utilize heat in the secondary sodium to generate steam, (4) a steam turbine and condenser system to drive power generation equipment, and (5) large pumps for circulation of the heat transport fluids.

LMFBR Environments

LMFBR components operate in four main environments which are summarized in Table 2. These include sodium (with the impurities noted), steam, air,

and irradiation. The neutron radiation fluence shown represents that for non-replaceable components. Replaceable components in the reactor core area such as cladding and ducts will see much higher fluences ranging up to 3×10^{23} n/cm^2.

Key Design Problems

LMFBR components are designed to withstand a range of in-service loadings, including such loadings as internal pressure, thermal heat-up, thermal transients, fluid momentum, vibration, and seismic. Design experience with FFTF and CRBRP components has shown that the most critical design problems arise from the thermal transient loadings. As a result of the relatively severe thermal transient events included in the design of the LMFBR, materials are expected to undergo cyclic stress-strain ranges with significant levels of both short-time plastic and time-dependent creep strain. It has been necessary for LMFBR designers to resort to rather complex and costly inelastic finite-element analysis methods to solve many of these thermal transient problems in order to show component compliance with ASME nuclear code rules (Code Case N-47-13).[1]

It is impossible in this short paper to cover all the LMFBR components and structural problems in any detail; what will be done in the balance of this paper is to review two thermal transient problems arising in two selected components. These can serve to illustrate the type of high-temperature materials problems that typically arise. Then, taking a broader view encompassing most of the key structural problems, an attempt has been made to place "bounds" on required material behavior to meet the range of problems anticipated in the LMFBR.

The first problem which will be described occurs in the "upper internals structure" of the reactor as a result of what is termed "thermal striping transients." A schematic of the CRBRP reactor vessel and internals is given in Fig. 3 for reference. During steady reactor operation as the sodium coolant flows upward through the many coolant passages in the reactor core, each sodium stream exits at the top of the core with a different temperature. As noted earlier in Table 1, the bulk temperature in the exit plenum is approximately 593°C (1100°F); however, stream-to-stream temperature differences as they exit from the core can run as high as 156°C (280°F) in the CRBRP. As these streams mix, a complex, fluctuating temperature condition is generated. Transient frequency is estimated to be of the order of 1 cps with the temperature anticipated to fluctuate through the full 156°C stream-to-stream difference. Some thermal lag will exist between the cyclic fluid and component temperatures depending on several factors including component thickness and surface heat-transfer coefficient. However, over a 30-yr lifetime, materials of construction can be expected to undergo up to 10^9 to 10^{10} cycles at strain ranges up to 0.5% and possibly higher in some areas. These thermal striping transients are expected to generate significant levels of high-cycle fatigue damage in critical areas. The current material solution to this problem will be described subsequently in this paper. Additional information can be obtained from a recently completed DOE-sponsored study of the thermal striping problem with recommendations for needed research and development.[2]

The second thermal transient problem selected for review arises at the "primary inlet nozzle" attachment to the intermediate heat exchanger in the FFTF. This attachment nozzle is similar to the one shown in Fig. 3 and attaches the hot-leg piping to the IHX vessel. Transient events which occur in a reactor are categorized as arising from Normal, Upset, and Emergency conditions in accordance with Section III of the ASME Boiler and Pressure Vessel Code.[3] Specific events result in severe changes in temperature, pressure, and flow rate. In critical areas such as nozzle attachments, these events lead to both cyclic, short-time plastic deformation and time-dependent creep deformation. In general, most of the major events of this type are expected to occur <200 times over a 30-yr life span and result in strain ranges generally <0.5%. There are, however, some transient events such as small load fluctuations which are expected to occur as many as 40,000 to 50,000 times, but obviously with much lower strain ranges.

Design specifications for the FFTF IHX primary inlet nozzle include more than ten different kinds of transient events during its design lifetime. These events vary in both intensity and frequency. There may be as many as 725 Upset and Emergency transient events and 118 Normal heat-ups and cooldowns. These events occur in random sequences and at unpredictable intervals. The analyst must therefore make certain assumptions in order to make the analysis feasible. A technique known as transient replacement or "umbrellaing" is generally used in solving these types of design problems. Basically this entails a review of the anticipated transients by the designer, and on the basis of their frequencies and intensities it is assumed that these transients can be safely lumped together into only one, two, or at most a few transients for analysis purposes. Care must be exercised, however, to avoid overconservatism and also that all failure modes which may be affected by the umbrellaing process are considered.

The umbrellaing technique was utilized by Gangadharan, Pai, and Berman[4] in their analysis of the effects of thermal transients on the primary inlet nozzle to the IHX. Preliminary work led them to the selection of a sequence of two upset transient events for analysis. The first of these denoted as "U2" represents a safety or control rod drop accident, while the second denoted as "U1" represents a reactor scram. Thermal and pressure histograms representing these two transient events are summarized in Fig. 4. To demonstrate Code compliance it was necessary to do an inelastic finite-element analysis. The resulting circumferential stress-strain loops for the most critical finite element are summarized in Fig. 4.

Significant plastic straining results during the severe U2 thermal downshock [points 20-40, downshock of −5.6°C/sec (−10°F/sec)] whereas much less plastic strain occurs during the less severe U1 downshock [points 63-73, downshock of −2.2°C/sec (−4°F/sec)]. A total inelastic strain range of 0.289% results. Maximum straining was found to occur in the first U2/U1 load cycle; hence, no strain ratchetting is anticipated and the 0.289% strain range obtained represents the maximum range for the component design life. The component was found to sustain negligible creep damage due to the 156-hr holds at 566°C (1050°F). Strain levels, creep damage, and fatigue damage all fall within ASME Code requirements.

High-Temperature Materials

There are only a limited number of materials currently approved by the ASME Code for application at temperatures above 427°C (800°F) in nuclear reactor components. These materials are summarized in Table 3. The temperature associated with an allowable stress of 41.4 MPa (6 ksi) was extracted from ASME Code Case N-47-13 to provide a general indication of the relative useful maximum temperature for each material. These numbers are summarized in Table 3 along with operating temperatures for each of the four materials in the CRBRP components shown. These comparative numbers provide a general indication of the degree to which the thermal capability of each material is utilized in the CRBRP.

Inconel 718 also noted in Table 3 is the current choice for solution of the thermal striping problems in the reactor upper internals. For use in components undergoing 1 cps thermal cycling transients for 30 years, the computed maximum coolant temperature fluctuation for use with 316 stainless steel and Inconel 718 components is compared in Fig. 5. For this type of service analysis indicates that Inconel 718 can operate at a cyclic ΔT of 238°C (429°F) as compared to only 31°C (56°F) for 316 stainless steel. As previously mentioned, cyclic ΔT's of 156°C (280°F) are expected to exist in the CRBRP reactor upper internals. Inconel 718 is not without its problems, however, as it has poor weld integrity, and components must be mechanically fastened to meet ASME Code rules. Both creep and fatigue data for Inconel 718 also need to be added to ASME Code Case N-47-13. These data are currently being generated.

Materials Performance Bounds

The two problems described should give some perspective on typical design problems, how they are solved, and the associated material performance needed. Although the two problems reviewed resulted primarily in fatigue damage, it should be pointed out that creep damage is the dominant damage component in many of the critical design problems. You as material scientists are interested in the range of conditions a material must encounter in a design such as the CRBRP encompassing all high-temperature components and loadings. Such bounds are difficult to generate; however, a review of available information led to the approximate bounds summarized in Table 4.

Summary

In summary, this paper has attempted to give a brief overview of the LMFBR, to describe its key components, to address two key structural problems, to review high-temperature materials utilized, and finally attempt to place bounds on expected operating conditions. The current status of materials utilization in the LMFBR might be summarized as follows:

- With the exception of the reactor upper internals, design needs for the LMFBR can be met with currently approved Code materials.

- Inconel 718 can potentially solve the thermal striping problems in the reactor upper internals.

- Temperature, stress-strain levels, and design lifetime of the LMFBR push currently approved Code materials toward their limits of usefulness.

References

1. Code Case N-47-13 (1592-13), *Cases of ASME Boiler and Pressure Vessel Code*, American Society of Mechanical Engineers, New York, May 1978.

2. Paul R. Huebotter, editor, *Report of the Thermal National Task Force on Thermal Striping in LMFBRs*, ANL-CT-78-46, Argonne National Laboratory (September 1978).

3. *ASME Boiler and Pressure Vessel Code*, Section III, Division 1, American Society of Mechanical Engineers, New York, July 1, 1974.

4. A. C. Gangadharan, D. H. Pai, and I. Berman, "Non-Linear Creep Fatigue Analysis of a Sodium Heat Exchanger Component for the Fast Flux Test Facility," *International Conference on Creep and Fatigue in Elevated Temperature Applications, Philadelphia, September 1973, and Sheffield, U.K., April 1974*, pp. 215.1–215.8.

Table 1. Comparison of design conditions for the liquid-metal fast breeder reactor (FFTF and CRBRP) and the light-water reactor

DESIGN CONDITIONS			
PARAMETER	LWR[a]	FFTF[b]	CRBRP[c]
TEMPERATURE (°F)			
CORE OUTLET	650	1100	1080
REACTOR OUTLET	650	1050	1015
PRESSURE (PSIA)			
REACTOR OUTLET	2250	15	15
PUMP DISCHARGE	2370	190	200
TRANSIENTS			
CORE OUTLET ΔT (°F)	80	350	280
RATE (°F/SEC)	5	35	30
COOLANT	WATER	SODIUM	SODIUM
DESIGN LIFE	30	20	30

[a] LIGHT WATER REACTOR
[b] FAST FLUX TEST FACILITY
[c] CLINCH RIVER BREEDER REACTOR PLANT

Table 2. Liquid-metal fast breeder reactor environments

- SODIUM (995°F, 175 PSI)

$O_2 < 1$ PPM	Cl < 30
C < 30	Li < 5
B < 25	K < 1000
Ca < 10	S < 10
	U < 0.01

- STEAM (905°F, 1450 PSI)
- AIR (900–995°F, 1 ATM)
- IRRADIATION –
  FLUENCES OF $< 10^{20}$ NEUTRONS/CM^2
  (E < 0.1 MeV OVER COMPONENT LIFETIME)

Table 3. ASME Code approved materials for nuclear reactor components operating above 427°C (800°F)

MATERIALS	TEMPERATURE FOR ASME ALLOWABLE STRESS (S_{MT}) OF 6 KSI (°F)	LMFBR OPERATING TEMPERATURE		
		REACTOR VESSEL	IHX	STEAM GENERATOR
2 1/4 Cr-1 Mo STL	~ 950	—	—	936
304 SS	~1050	995	995	—
316 SS	~1100	—	995	—
ALLOY 800H	~1175	—	—	936

INCONEL 718 – NEEDED FOR THERMAL STRIPING IN REACTOR UPPER INTERNALS

Table 4. Summary of approximate thermal loadings and material stress and strain response in CRBRP components

- THERMAL TRANSIENT LOADINGS
  - MOST < 1000 CYCLES IN 30 YEARS
  - USUALLY 20–30 CYCLES IN 30 YEARS WITH SHOCKS OF -10^{o}F/SEC AND ΔT OF < 280^{o}F
  - BALANCE OF TRANSIENTS ABOUT -4^{o}F/SEC OR LESS WITH $\Delta T < 280^{o}$F
- THERMAL STRIPING TRANSIENTS
  - -500 TO -600^{o}F/SEC, 1 CPS, < 10^{9} CYCLES, $\Delta T < 280^{o}$F
- MATERIAL STRAIN RANGE RESPONSE
  - USUALLY < 0.2 TO 0.3%
  - SELDOM > 0.5%
- MATERIAL STRESS RESPONSE
  - SHORT TERM STRESSES USUALLY < 2 X YIELD
  - (LONG TERM STRESSES DUE TO PRIMARY LOADINGS USUALLY < 0.5 X YIELD)

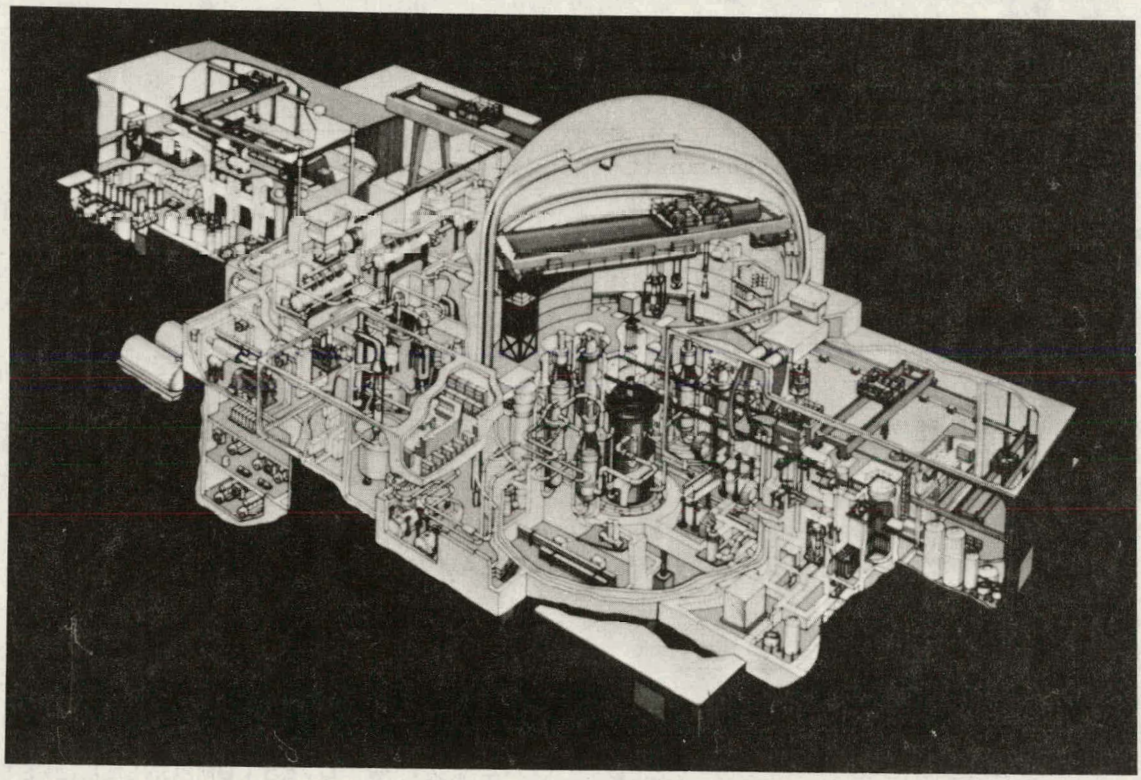

Fig. 1. Clinch River Breeder Reactor Plant

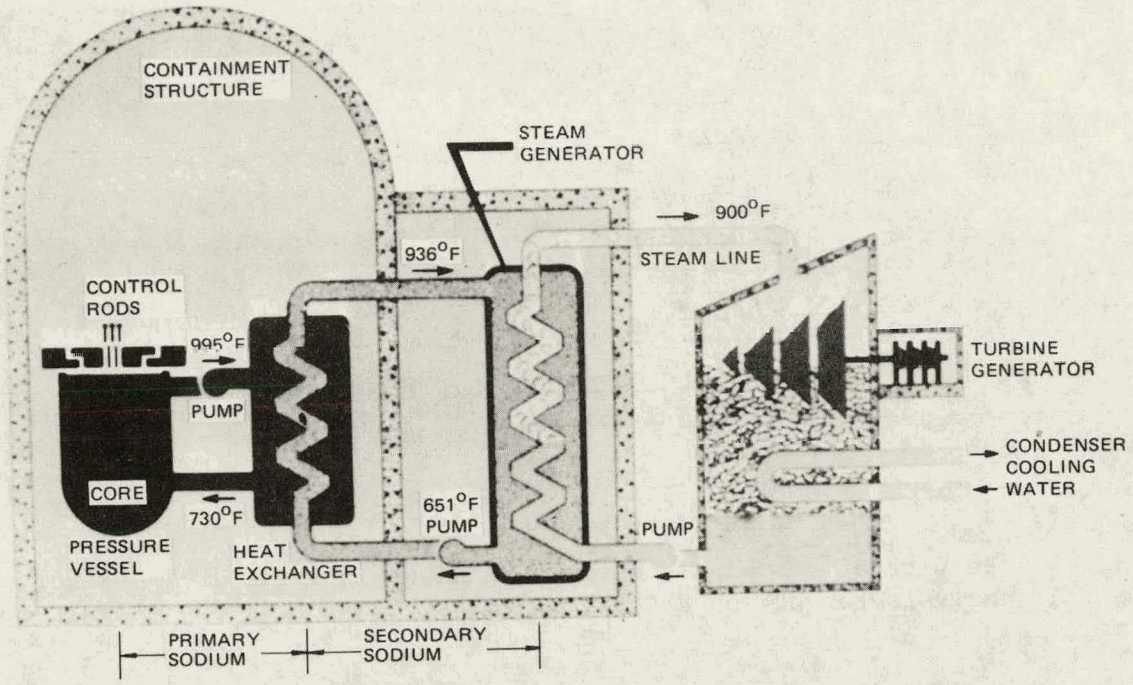

Fig. 2. CRBRP schematic showing the three basic heat transport loops

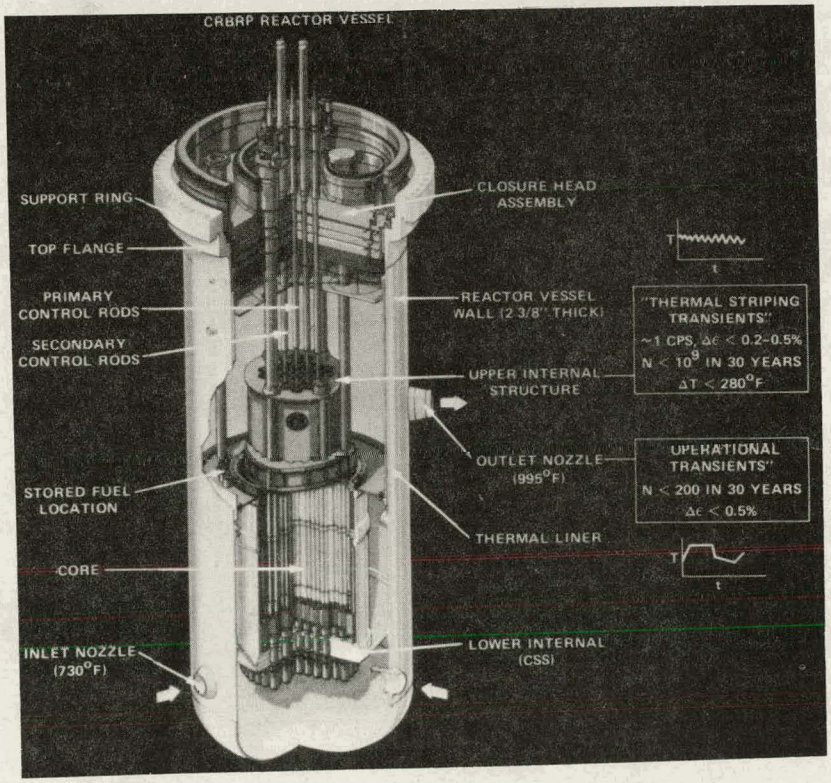

Fig. 3. CRBRP reactor vessel and internals with two key structural problems identified.

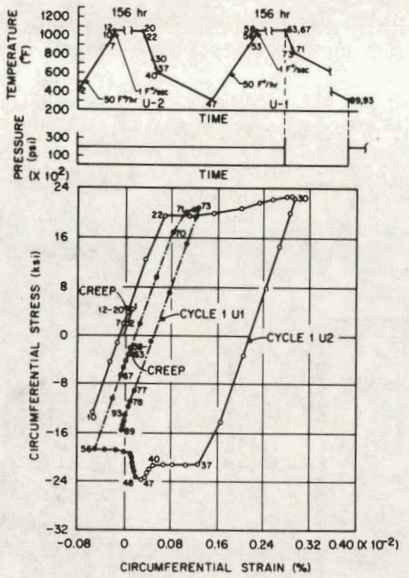

Fig. 4. Results of a typical thermal transient analysis (FFTF primary inlet nozzle analysis for U2 and U1 thermal transient events; 304 stainless steel material)

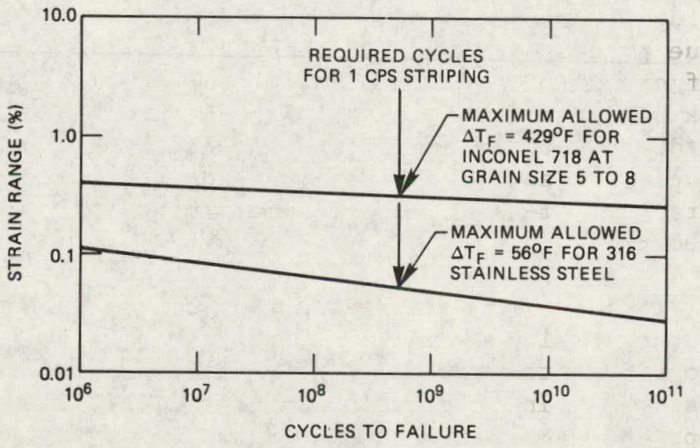

Fig. 5. A comparison of the relative resistance of Inconel 718 and 316 stainless steel to 1 cps thermal striping transients.

TIME DEPENDENT FATIGUE-PHENOMENOLOGY AND LIFE PREDICTION

L. F. Coffin
Corporate Research and Development
General Electric Co.
Schenectady, NY

I. INTRODUCTION

Fatigue at elevated temperatures, also called time-dependent fatigue, may have different meanings to each person who encounters the problem, depending on their previous training, current interests, and professional responsibilities. His work may involve him in a narrow part of the problem for which he seeks highly specific answers, whether it be the understanding of fatigue crack initiation, or the determination of the design life of a pressure vessel. To encourage a broader appreciation of the problem and to attempt to lower the communication barriers, it is appropriate to consider the several physical aspects of the problem, and to examine the many disciplines that are brought to bear either to understand the problem, to prevent it from occurring, to design around its complexities, or to live with it. Referring to Fig. 1, we imagine an engineering structure containing a notch. The structure might be a turbine rotor, or a pressure vessel, loaded centrifugally, or by internal pressure, and it presumably has some temperature gradient acting in the notch region. The centrifugal, pressure, or thermal stresses are cycled, most commonly from zero to tension by start-stop or load-unload operation of the equipment. We then envisage the fatigue process to occur in three stages: first, nucleation and early growth of cracks within the plastic zone developed at the notch root; second, crack propagation of a stable crack through the plastic zone; third, propagation of the crack through the elastic zone, the crack generating its own plastic zone, until fracture of the structure results, either by sudden fracture, leakage, or by excess vibration or deformation. These stages are shown in Fig. 1.

Also in Fig. 1 we identify some of the many disciplines which must be brought to bear on the problem. Consider first the plastic zone. Identification of the appropriate stresses and strains are required through analytical tools, such as finite element analyses. This requires the selection of appropriate material information and constitutive equations, heat transfer analysis, etc. With the aid of appropriate failure criteria, the conditions for the occurrence of microcracks or for nucleation and early growth can be specified. Elastoplastic analysis further aids in the specification of conditions for crack growth through the plastic zone, again coupled with an appropriate fracture criterion. Finally, elastic stress analysis and fracture mechanics concepts allow the determination of crack growth in the elastic regime.

Along the way we can identify several additional disciplines. Included are environmental effects on nucleation and growth, manufacturing techniques for surface preparation in the critical area, choice of material, testing

methods for developing failure criteria, low-cycle fatigue studies, development of high- and low-strain crack growth rules, time dependency, fractography, etc. Groups of these and other disciplines are lumped together into such activities as life prediction, design, code development, etc. There is also a whole structure of disciplines directed towards other aspects of the problem such as metal physics, corrosion and electrochemistry, physical and process metallurgy, statistics, and others.

To obtain some semblance of order among this confusion of disciplines, it is necessary to keep the physical picture of the problem in mind. Too often, in the interest of obtaining answers, we forget that fatigue failure is progressive, starting from a single grain or microscopic flaw, gradually growing to a size where it compromises the integrity of the structure. Our models or criteria should be continually examined to be sure that, indeed, the physical aspects of the phenomenon have not been lost sight of, or better yet, are the building blocks for the model or criterion.

The concept described in Fig. 1 where a test specimen, be it a smooth uniaxial low cycle fatigue specimen for determining fatigue initiation and early growth or a compact tension specimen for determining crack growth, is used to simulate the fatigue processes in the component under consideration, provides the important connecting link between life prediction for the component on one hand and the material's performance on the other. In the present discussion we shall consider only the question of initiation and early growth since this is the basis of most of the codes and design procedures in use today. In this case the concept is referred to as "smooth specimen simulation"[15] or the "local strain approach."[2]

The local strain concept is an attractive one in that it permits the massive body of smooth, uniaxially loaded fatigue data to be transferred to the design of the structure, but it is not without its problems. The assumption is made that laboratory specimen failure data are equated to crack initiation in the actual structure. This may be valid when the plastic zone is large relative to the specimen size, or when the strain gradient in the notch is small. Also such factors as biaxiality of stress (plane strain), or surface roughness represent sources of difficulty with the concept. A recent paper by Dowling,[2] however, interprets test results from an SAE round-robin test program with service-simulated loading applied to a notched compact-tension specimen, using the local strain approach and finds satisfactory predictive capability. At high temperature the method has been employed by Mowbray and McConnelee[3] and by Coffin.[4]

The local strain approach when applied to design assumes that fatigue life is determined by crack initiation. As indicated above, many engineering structures are designed in this way. An alternative approach which is finding increasing support with the advent of fracture mechanics concepts in design is to assume the presence of a pre-existing flaw, which negates any contribution from crack initiation and assumes that life is a result of the plastic or elastic crack growth cyclic life. Such procedures are warranted when the probability of defects is high in critically strained regions. Welded structures represent this situation. However, when the number of

similar parts being manufactured is high, when material quality is carefully controlled and when appropriate NDT techniques are employed to reduce the probability of defect initiated fatigue to low levels, then crack initiation concepts are valid.

An intermediate approach is to combine both of the above philosophies. Every effort is taken to ensure that defects are absent from critically-stressed regions and the structure is basically designed by crack initiation. However, to avoid the chance situation of a defect slipping through the inspection process a characteristic defect is assumed and the life so calculated. This quantity serves as the basis for determining the inspection frequency for crack detection of the component.

The point of this discussion relative to the more general thesis of the paper is that we must be concerned with all three of the elements shown in Figure 1 if we are to develop a technical background from which sound predictive procedures can be derived for the reliable performance of real structures subjected to complex loadings and environments.

II. PHENOMENOLOGY

In this section the rather extensive observations, obtained mostly from elevated temperature low-cycle fatigue tests, will be reviewed as background for treating the question of life prediction in the time dependent regime.

A. Strain Rate and Frequency

The effect of frequency and of strain rate on the low-cycle fatigue behavior of metals at high temperatures has been extensively investigated using tests with balanced loading (equal ramp rates in tensile going and compressive going). The earliest work of interest was that by Eckel on lead[5] who correlated his results with frequency of cycle and failure time.

Berling and Slot[6] studied the effect of temperature (703, 923, and 1133 K) and strain rate (4×10^{-3}, 4×10^{-4}, and $4 \times 10^{-5} s^{-1}$) on AISI 304, 316, and 348 stainless steel, showing the progressive decrease in cyclic-strain fatigue resistance with increasing temperature and decreasing strain rate. Coffin has reported on the frequency effect of Nickel A,[7] A286[8] Udimet 500,[9] and Rene 80[10] at elevated temperatures on smooth and notched[11] bars. From these results and those of Berling and Slot,[6] Coffin developed phenomenological representations for the frequency effect,[7] by combining the Coffin-Manson equation with the results of Eckel.[9,10,12]

Weeks et al[13] give results of extensive testing of AISI 304 and 316 over a wide range of strain rates and metallurgical conditions. The general conclusion from these test results and many others not cited here is that progressively decreasing frequency degrades the fatigue resistance of structural alloys at elevated temperatures under fully reversed cyclic-strain conditions in air environments. Accompanying this decrease in life is a change in appearance of the fracture surface from that of transgranular fracture to intergranular as the frequency of cycling decreases.[8,11] An important but unanswered question is whether eventual saturation in loss of life occurs at even lower frequencies.

To give an example of the effect of cyclic frequency, notched bar fatigue tests of A-286 were investigated with three specific aging heat treatments designed to alter the γ' size and the homogeneity of deformation. These heat treatments are identified elsewhere.[11]

The results of notched fatigue tests at 593°C on specimens with $K_t = 3$ testing at $\Delta\sigma/2 = 414$ MN/M^2 (60,000 psi) at three frequencies are shown in Figure 2. The dashed line for the standard treatment represents a regression analysis of results of tests under a variety of notches and stress levels. A strong frequency dependence of life is apparent below about 5 cpm for all heat treatments. However, the lives are substantially different at a given frequency for the different heat treatments. A double aging treatment (#3) in particular shows much less frequency sensitivity than the single lower temperature treatments.

Since for A286 failure at low frequencies was intergranular, elimination of transverse grain boundaries might be expected to increase the life in the low-cycle regime. Accordingly, two notched specimens with $K_t = 3.0$ were prepared from remelted stock which had been directionally solidified. Clearly a substantial improvement was obtained as seen in Figure 2.

If the transverse grain boundaries are retained but the environment is eliminated in A286, the high vacuum test point shown on Figure 2 at $\nu = 1.6 \times 10^{-3}$ Hz indicates a further improvement. This confirms that most of the frequency dependence observed in air tests is related to the influence of oxidation processes at the crack tip. The failure of the directionally solidified specimens tested in air to last as long as the vacuum test may be attributed in part to the cast structure in which transverse dendrite boundaries become preferred crack propagation sites.

Tests were also performed at higher frequencies (up to 30cpm). From the view that, at high frequencies, there would be little time for environmental attack, curves were constructed to indicate a common convergence point at 1000 cpm. Above this frequency the material can be expected to be environmentally insensitive and independent of frequency. For frequencies approaching this convergence point the fracture surfaces would be expected to be largely transgranular. Fractographs of the 30 cpm test supported this view.

B. Environment

Recognition of the important role of environment on fatigue damage is evidenced by the early work of Achter et al.[14] and of White.[15] McMahon and Coffin,[16] in examining the fatigue results of Udimet 500 in air, found strong evidence that localized oxidation was critically important to the failure process and concluded that life degradation was more a result of "oxidation" fatigue (analogous to corrosion fatigue) than of creep damage processes. This work was followed by investigations of comparative effects[8,17] in air and in vacuum [1.33 Pa(10^{-8} torr)] in which testing was conducted under fully reversed strains and equal ramp rates on a variety of materials. From these experiments it was concluded that the degradation processes were mostly environmental, since room temperature (time-independent) behavior could be produced by testing in vacuum rather than

in air at elevated temperature. Evidence for this conclusion was seen by the occurrence of transgranular fracture, and by fatigue lives comparable to those found at room temperature (based on plastic strain considerations), and independent of frequency and temperature. Figure 3 is an example of this behavior for A286. Further work was done on the effect of low frequencies on AISI 304 stainless steel[17] to show that in high vacuum lives were unaffected by decreasing frequencies and fracture was still transgranular at 923 K at frequencies of 166 Hz (0.01 cpm). Other investigators have reported that inert environments significantly improve the fatigue life over that in air, as reported, for example, by Andrews and Kirschler on 2 1/4 Cr - 1 Mo steel in sodium.[18]

C. Waveshapes

Laboratory tests can be carried out using a variety of waveshapes and the findings from these experiments are extremely important to the present discussion. Some typical waveshapes are shown in Figs. 4 and 5 and include tensile strain hold [Fig. 4(b)]; stress-hold and strain limit, the so-called CP cycle [Fig. 4(e)]; equal-equal slow-fast and fast-slow (Fig. 5). Over the years, a large amount of testing experience has shown that decreasing frequency of the cycle degraded the life,[19,20] and that waveshape had an important influence on life. Strain-hold time studies on austenitic stainless steels[21] and materials of similar strength and ductility reveal that tensile strain holds are the most damaging mode for equivalent periods. On the other hand, for the cast nickel-based superalloys, compressive strain-hold tests are most damaging.[22-23] Tests on carbon and low-alloy steels show that frequency, but not waveshape, influences the life.[24] A discussion of these waveshape effects is given elsewhere.[12,25]

In tensile strain-hold time tests on AISI 304 stainless steel,[21,26] significant differences in fracture morphology and in life are found when compared to combined tensile and compressive holds. Fractures for the former were largely intergranular while additions of compression hold times of shorter duration cause largely transgranular fracture and increased life. Similar findings have been reported recently for AISI 304 stainless steel.[27] Internal cavities have also been noted in 20Cr/25Ni/0.7Nb stainless steel at 1023 K[28] and on a 1 CrMoV steel at 838 K.[29]

Other types of unbalanced loop tests reveal similar degradation on life and changes in fracture morphology. These include fully reversed creep at constant stress[30,31] of AISI 316 stainless steel at 977 K, strain range partitioning waveshapes such as CP loops,[25] thermal mechanical tests on A286 [32] at 868 K. The common feature of all of the above tests was the significant decrease in life and the appearance of intergranular cracking and interior cracking and cavity formation when the time for which tensile stresses were applied exceeded the time spent under compressive stress in a given cycle.

D. Waveshape - Environment Interactions

An uncertainty would appear to exist between the degrading effects found for unbalanced loop tests conducted in air and the insensitivity to time-dependent damage when balanced loop tests are conducted in high vacuum. For this reason, unequal strain-rate tests were carried out both

on A286 and AISI 304 stainless steel in high vacuum. Results, shown in Fig. 8 for A286, reveal a pronounced waveshape effect on life in this environment. Sheffler[32] also noted this behavior, but his results were somewhat obscured by the thermomechanical nature of his tests. Looking particularly at the stainless steel results at 923°K in Table I, note that the slow-fast test carried out in vacuum is nearly as damaging as the corresponding air test, while for balanced loops (equal times in tensile and compressive going) the vacuum environment produces a nearly sevenfold increase in life over that in air. Fractography reveals that both the air and vacuum slow-fast tests failed by intergranular fracture, and, in addition, extensive interior grain boundary cracking is observed. This indicates that interior damage processes are unaffected by the external environment, but appear to be strongly influenced by the waveshape. Support of this position is found in the results of the air vs vacuum equal strain-rate tests where no interior damage was observed. On the other hand, fatigue cracks originated at the surface and were transgranular in vacuum but intergranular in air, showing environmental involvement. Of particular interest were the fast-slow test results on AISI 304 stainless steel at both 923 and 1083°K. Failures occurred away from the diametral control position from a ratchetting-instability process. Details of this behavior are discussed elsewhere.[33]

Unequal strain rate testing has also been performed on two copper-based alloys at 811°K.[34] Alloys were examined, identified as 1/2 hard AMZIRC and NARloy Z. Rates considered were $10^{-2}/4 \times 10^{-4}s^{-1}$ (tensile going/compressive going) $4 \times 10^{-4}/1 \times 10^{-2}s^{-1}$ for the AMZIRC copper, and $10^{-2}/4 \times 10^{-4}s^{-1}$, $4 \times 10^{-4}/1 \times 10^{-2}s^{-1}$, $4 \times 10^{-5}/1 \times 10^{-2}$, and $7 \times 10^{-6}/1 \times 10^{-2}s^{-1}$ for the NARloy Z alloy. Results obtained for this alloy are reproduced in Fig. 9 and reveal the striking degradation in fatigue life with increasing strain rate unbalance in slow-fast testing. Mean stresses were noted in the hysteresis loop, a behavior commonly found in unbalanced loop tests.[25,33]

III. PREDICTIVE METHODOLOGY

A wide variety of predictive approaches have been developed over the years, for application to designs for high temperature service. Many of these have been reviewed from time to time.[1,25] Because of the evolving physical understanding and phenomenology, the state of predictive methodology is one of change and improvement. Here we will discuss the current procedure and five of the newer methods currently under active study and evaluation.

A. Present ASME Creep-Fatigue Rules and Procedures

The present Code rules established in Case 1592 of the ASME Boiler and Pressure Vessel are predicated on a linear damage summation between fatigue damage and creep. In the case of creep, time for stress to rupture is used. The procedures are outlined in more detail in Figures 10 and 11. The predictive criterion used here, namely the linear summation of damage introduced by fatigue and by monotonic creep, is far removed from the actual damage processes encountered in time-dependent fatigue, as discussed above. For this reason, other life prediction approaches have been developed. Some of

them are described below.

B. Frequency Modified Fatigue Equations and Their Applications

It is difficult in the space allotted to this topic to adequately describe the complex phenomenology developed for the cyclic stress-strain and fatigue processes at elevated temperatures. One attempt was to formalize this complex behavior through the use of the so-called frequency-modified fatigue equations, which represent the material behavior through the use of the plastic (inelastic) strain range and the frequency of the cycle. These equations are:

$$\Delta\varepsilon_p = C_2(N_f\nu^{k-1})^{-\beta} \tag{1}$$

$$\Delta\varepsilon_e = \frac{\Delta\sigma}{E} = A\,\Delta\varepsilon_p^{n'}\nu^{k_1} \tag{2}$$

$$\Delta\varepsilon_e = \frac{\Delta\sigma}{E} = A'N_f^{-\beta'}\nu^{k_1'} \tag{3}$$

The coefficients for these equations are determined from regression analysis procedures utilizing available test data from smooth, uniaxially loaded specimens tested at specific temperatures, strain ranges and frequencies. Specific features and applicability of these equations are described elsewhere.[1,4] Examples of material behavior, described in more detail in reference [1], can be cited, including the cyclic stress-strain behavior as a function of temperature for AISI 304 stainless steel, Figure 12. Note that the frequency is accounted for by transferring it to the left hand side of equation (2) and plotting this parameter as the ordinate in Figure 12. Of interest is the decrease in stress range and cyclic strain hardening exponent with increasing temperature, and the increasing influence of the frequency of cycling on the resistance to cyclic deformation. Equation (2) can also be expressed in terms of the strain rate for cases of equal and constant ramp rates for each leg of the loop. Here

$$\Delta\varepsilon_e = \frac{\Delta\sigma}{E} = B\Delta\varepsilon_p^{n_1'}\dot{\varepsilon}_p^{m} \tag{4}$$

where $B = A/2k_1$, $n_1' = n'-k_1$ and $m = k_1$. Equation (2) or (4) may be useful in analytical procedures for elasto-plastic cyclic stress-strain solutions.

The frequency-modified Coffin-Manson equation, equation (1) is useful in characterizing high temperature low-cycle fatigue behavior. It has been found convenient again to transfer the frequency term to the left side in equation (1) and define this parameter as the frequency-modified plastic strain range. Equation (3), called the frequency-modified Basquin equation, can be similarly treated. Application of equation (1) and (3) are

shown in Figure 13 for test data on AISI 304 stainless steel continuously cycled at three strain rates and at three temperatures.[6]

Several features arising from the effect of increasing temperature on fatigue phenomenology are observed in this figure. We see the increasingly negative slope and the decreasing life of the plastic strain-cycles to failure representation. Increasing temperature and concomitant softening causes a progressive decrease in the elastic strain (or stress range/elastic modulus). With increasing temperature the transition fatigue life N_t (the life where the elastic and plastic strain ranges are equal) shifts to lower values of life. The role of the transition fatigue life in distinguishing between low-cycle and high-cycle fatigue is treated elsewhere.[4] Also note that increasing temperature has a small effect on the exponent β' which defines the slope of the elastic strain-cycle life line. From an engineering design viewpoint the total strain range $\Delta\varepsilon$ is a more commonly used quantity since from it is derived the pseudo-stress $E\Delta\varepsilon$. This can be found by combining equation (1) and (3). Combining the elastic and plastic lines of Figure 13 for two specific frequencies, 0.16 and 0.16×10^{-3} Hz (10 and 10^{-3}CPM), and the three temperatures Figure 14 results. Note the increasingly strong frequency effects as the temperature is raised and the large differences in life as the total strain range is decreased. For example, at a strain range of 0.003, the life at 0.16 Hz decreases from 5×10^5 cycles to 7×10^3 a 70 fold decrease for a change in temperature from 450 to 816°C. At 0.16×10^{-3}Hz on the other hand the lives are 5×10^5 cycles and 260, a 1900 fold decrease. At this same strain range, changing the frequency by a factor of a 1000 causes a 27 fold decrease in life. It should be pointed out that these comparisons are based on an extrapolation of the test data to lower frequencies on the assumption that the frequency exponents of equations (1-3) are independent of frequency.

The frequency-modified fatigue equation can be used to predict hold times. It has been suggested,[20] that holdtime behavior could be predicted from Eq. 1-3 by assuming that

$$v = \frac{1}{t_c' + t_h} \tag{5}$$

where t_c' is the time for strain reversal and t_h is the hold period for each cycle. Using the appropriate coefficients given in Ref. 1 good agreement with a format proposed by Conway et al[21] representation of which is shown in Fig. 15.

C. Strain range partitioning

This approach[25,31] is built around a series of experiments to establish inelastic strain-cycle life relationships for a given material and temperature. Four sets of cyclic life experiments are required identified as PP, CC, CP and PC tests (Fig. 16) where P symbolizes plasticity and implies a rapid, constant ramp rate tests, while C symbolizes creep and implies testing at constant load. Thus a PP test is one which is fast, balanced and continuously cycled, while a CC test is conducted

under reversed creep conditions at fixed tensile and compressive loads. It too, is balanced. The CP and PC tests are mixed, consisting of one leg (C) of a hysteresis loop at constant load, the reversed leg (P) at a rapid constant ramp rate. These two loops bring in the element of loop unbalance.

A procedure is involved whereby a given complex hysteresis loop is broken down into components of the four basic loops. Then using an approximate linear damage rule, called the interaction damage rule, a prediction of the life for the complex loop is made from the lives of the component loops. The procedure is shown in Fig. 17. The method is assumed to have broader applicability than to isothermal conditions, based on tests performed at various temperatures in which the CC, CP and PC baseline failure data show an insensitivity to temperature. The assumption is then made that the baseline data are temperature independent, such that thermo-mechanical loading conditions can be included in the predictive scheme. The method has been used for life prediction in a large number of cases.

D. Method of Ostergren.

Ostergren (35) has recently proposed that hold time and frequency effects at elevated temperature can be accounted for by a damage function based on the net tensile hysteresis energy. This damage measure is approximated by the quantity $\sigma_t \Delta\varepsilon_p$ where σ_t is the maximum stress in the cycle and $\Delta\varepsilon_p$ is the inelastic strain range. The tensile hysteresis energy is employed to account for the fact that low cycle fatigue is essentially a crack growth process, and that crack growth and damage occurs only during the tensile part of the cycle. The use of the tensile stress quantity in conjunction with the plastic strain range provides a means for accounting for loop unbalance, since, for the same inelastic strain, a positive mean stress gives a greater tensile hysteresis energy than a compressive mean stress.

In order to determine fatigue life, the method requires the substitution of $\sigma_t \Delta\varepsilon_p$ in equation (1). Additionally, two cases are treated, one where time-dependent damage is independent of wave shape, the other where damage is dependent on wave shape. The cast nickel base superalloys are considered to be in the former class since in general k = 1 for this class of materials (48), indicating no frequency effect in equation (1). For most other materials the criterion becomes

$$\sigma_t \Delta\varepsilon_p N_f^{\beta} \nu^{\beta(k-1)} = C \tag{6}$$

where

$$\nu = 1/(\tau_o + \tau_t - \tau_c) \text{ for } \tau_t > \tau_c \tag{7}$$

and

$$\nu = 1/\tau_o \text{ for } \tau_t < \tau_c \tag{8}$$

where τ_o is the time per cycle of continuous cycling, τ_t is the tension hold time and τ_c is the compression hold time. Figure 18 shows the correlation of equation (6) with test data on AISI 304 stainless steel.

The method is quite new and untested for wave shapes such as those produced by CP or PC procedures or by fast-slow or slow-fast testing.

E. Frequency separation

Frequency separation is another recently developed approach for predicting high temperature fatigue (36,37). It is an extension of the frequency-modified fatigue approach described earlier. The frequency-modified fatigue equations have been used as a basis for life prediction (1) by assuming that the period of the cycle but not the wave shape influences fatigue life. Sufficient evidence has been presented here and elsewhere to show that the assumption of wave shape independence on fatigue behavior is unsatisfactory. Accordingly two procedures have been introduced to correct for this inadequacy. Each are built around the concept expressed above that fatigue damage arises from the tension going (i.e. where $\dot{\varepsilon}_p > 0$) part of the hysteresis loop, and hence separation of each leg of the hysteresis loop into tension going and compression going was required.

The first of these procedures is very simple, requiring only that the frequency term in equation (1) is replaced by that associated with damage, i.e. the tension-going frequency. Actually, it is more straightforward to deal with time quantities rather than frequencies. Thus in equation (1), $\tau = 1/\nu = \tau_t + \tau_c$ where τ_t and τ_c are the tension and compression going times. Since the coefficients in equations (1-3) have been determined for balanced loop conditions, then $\tau_t = \tau_c$. By definition $\tau_t = 1/\nu_t$, $\tau_c = 1/\nu_c$. Thus for balanced loop conditions $1/\nu = 2/\nu_t$ or, equation (1), $\nu = \nu_t/2$. For any other loop, the tension going time τ_t is found, such that $\nu = 1/(2\tau_t)$ and this is used in equation (1).

The second procedure is more involved since the first procedure does not adequately predict severely unbalanced loop shapes. Reference is made to the loops and nomenclature show in Figure 5. It is assumed that the actual stress range for loops of unequal but constant ramp rates can be determined from the mean of the stress range for each leg of the loop. Thus $\Delta\sigma_{SF} = \Delta\sigma_{FS} = (\Delta\sigma_S + \Delta\sigma_F)/2$, where the subscript refers to slow and fast. Applying equation (2) of the frequency-modified fatigue equations to obtain the stress range for each frequency, one gets

$$\Delta\sigma_{SF} = \Delta\sigma_{FS} = \frac{A}{2}\left[\left(\frac{\nu_c}{2}\right)^{k_1} + \left(\frac{\nu_t}{2}\right)^{k_1}\right] \Delta\varepsilon_p^{n'} \quad . \tag{9}$$

It is next assumed that, if the stress range is known, the life can be determined, using equation (3). Substituting equation (9) into equation (3) to determine the fatigue life, one finds

$$N_f = \left(\frac{A'}{\Delta\sigma_{SF}}\right)^{1/\beta'} \left(\frac{\nu_t}{2}\right)^{k_1'/\beta'} \tag{10}$$

Note that the coefficients A', k_1' and β' are obtained from smooth bar, equal ramp rate tests as indicated earlier.

The applicability of the method to a variety of experiments on wave shape effects at high temperature is reported elsewhere (36). Shown in Figure 19 is a comparison of the method with hold time data of Jaske et al.

F. Damage rate equation

Another very recent addition to the growing family of high temperature fatigue prediction approaches is that of Majumdar and Maiya (39). The basis for the approach is crack growth and the separation of the growth processes into two distinct relations, depending on whether the externally applied stress is tension or compression. These relations are:

$$\frac{da}{dt} = \begin{cases} a_T \left|\varepsilon_p\right|^m \left|\dot{\varepsilon}_p\right|^k & \text{for tensile stress} \\ a_C \left|\varepsilon_p\right|^m \left|\dot{\varepsilon}_p\right|^k & \text{for compression stress} \end{cases} \qquad (11)$$

For continuous cycling, equation (11) is integrated over a given plastic strain range. When ε_p is constant, equation (11) and equation (1) are found to be identical. The method has been used to predict fatigue lives for Type 304 stainless steel under various monotonic and cyclic loading conditions. A refinement of the method has recently been introduced to include the additional effects of bulk cavity damage under unbalanced hysteresis loop cycling.

IV. SUMMARY

In this paper the time-dependent fatigue behavior of materials used or considered for use in present and advanced systems for power generation is outlined. A picture is first presented to show how basic mechanisms and phenomenological information relate to the performance of the component under consideration through the so-called local strain approach. By this means life prediction criteria and design rules can be formulated utilizing laboratory test information which is directly translated to predicting the performance of a component. The body of phenomenological information relative to time-dependent fatigue is reviewed. Included are effects of strain range, strain rate and frequency, environment and wave shape, all of which are shown to be important in developing both an understanding of and design base for time dependent fatigue. Using this body of information, some of the current methods being considered for the life prediction of components are review. These include the current ASME code case, frequency-modified fatigue equations, strain range partitioning, the damage function method, frequency separation and damage rate equations. From this review, it is hoped that a better

perspective on future directions for basic material science at high temperature can be achieved.

REFERENCES

1. Coffin, L. F., Symp. on Fatigue at Elevated Temperature, ASTM STP 520, 1972, 5-34.

2. Dowling, N. E., Brose, W. R. and Wilson, W. K., Fatigue Design, Analysis Procedures and Test Data, Advances in Engineering Series, Society of Automative Engineers, to be published.

3. Mowbray, D. F. and McConnelee, J. E., in Cyclic Stress-Strain Behavior Analysis, Experimentation, and FAilure Prediction, ASTM STP 519, American Society for Testing and Materials, 1973.

4. Coffin, L. F., James Clayton Memorial Lecture, Proc. Inst. Mech. Eng., London, 188, 1974, 109.

5. J. F. Eckel, Proc. ASTM 51, 745 (1951).

6. J. T. Berling and T. Slot, Fatigue at High Temperature, STP-465, pp. 3-30, ASTM (1968).

7. L. F. Coffin, Jr., Fracture, Proc. of Second Int. Conf. on Fracture, Brighton, England, pp. 643-54 (April 1969).

8. L. F. Coffin, Jr., Proc. Int. Conf. on Fatigue: Chemistry, Mechanics and Microstructure, pp. 590-600 (1972).

9. L. F. Coffin, Jr., Metall. Trans. 2, 3105 (1971).

10. L. F. Coffin, Jr., Metall. Trans. 5, 1053 (1974).

11. D. A. Woodford and L. F. Coffin, Jr., 4th Bolton Landing Conf., Claitors Pub. Division, Baton Rouge, p. 421 (1974).

12. L. F. Coffin, Jr., Fatigue at High Temperature, Fracture 1977; I. Intern. Conf. Fracture 4, Waterloo, Ontario, June 1977, pp. 263-292.

13. R. W. Weeks, D. R. Diercks, and C. F. Cheng, ANL Low Cycle Fatigue Studies - Program, Results and Analysis, ANL-8009 (November 1973).

14. M. R. Achter, G. J. Danek, Jr., and H. H. Smith, Trans. Metall. Soc. AIME 227, 1296 (1963).

15. D. J. White, Proc. Inst. Mech. Eng., Appl. Mech. Group 184, 223 (1969-1970).

16. C. J. McMahon and L. F. Coffin, Jr., Metall. Trans. 1, 3443 (1970).

17. L. F. Coffin, Jr., Metall. Trans. 3, 1777-88 (1972).

18. R. C. Andrews and L. H. Kirschler, MSA Research Corporation Report MSAR-66-174 (1966).

19. A. Coles et al., Inter. Conf. on Thermal and High Strain Fatigue, Monograph and Report Series 32, pp. 270-94, The Metals and Metallurgy Trust, London (1967).

20. L. F. Coffin, Jr., Proc. Air Force Conf. on Fatigue and Fracture of Aircraft Structures and Materials, AFFDL-TR70-144, pp. 301-309 (1969).

21. J. T. Berling and J. B. Conway, Proc. 1st Int. Conf. on Pressure Vessel Technology, Delft, Holland, Part 2, pp. 1233-46 (September 29 - October 2, 1969).

22. D. C. Lord and L. F. Coffin, Jr., Metall. Trans. 4, 1657 (1973).

23. W. Ostergren, J. Test. Eval. 4, 327-339 (1976).

24. M. M. Leven, Exp. Mech. 13, 353 (1973).

25. L. F. Coffin, Jr., et al, Time-Dependent Fatigue of Structural Alloys, Oak Ridge National Laboratory, ORNL 5073 (June 1977).

26. C. F. Cheng, et al., Fatigue at Elevated Temperatures, STP-520, pp. 355-364, ASTM (1973).

27. S. Majumdar and P. S. Maiya, submitted for presentation, ASME/CSME Pressure Vessel and Piping Conf., Montreal (June 1978).

28. B. Tomkins and J. Wareing, Materials, Met. Sci. J. 11, 414 (1977).

29. E. G. Ellison and A. J. F. Paterson, Inst. Mech. Eng. 190, 333 (1976).

30. G. R. Halford, Cyclic Creep-Rupture Behavior of Three High Temperature Alloys, NASA-TN-D-6039 (May 1971).

31. S. S. Manson, Fatigue at Elevated Temperatures, STP-520, pp. 744-82, ASTM (1973).

32. K. D. Sheffler, Vacuum Thermal-Mechanical Fatigue Testing of Two Iron Base High Temperature Alloys, NASA-CR-134524 (1974).

33. L. F. Coffin, Thermal Fatigue of Materials and Components, Am. Soc. Test. Mater. STP-612, 227, ASTM (1976).

34. J. B. Conway et al., "High Temperature Low-Cycle Fatigue of Copper-Base Alloys for Rocket Nozzles; Part II," Nat. Aero. and Space Admin. Report CR-135073 (August 1976).

35. Ostergren, W., Journal of Testing and Evaluation, ASTM, 4, 1976, 327.

36. Coffin, L. F., Symposium on Creep-Fatigue Interaction, Winter Annual Meeting American Society of Mechanical Engineers, New York, December 1976.

37. Coffin, L. F., Proc. International Conference on Materials, II, Boston, 1976, 866.

38. C. E. Jaske, H. Mindlin, and J. S. Perrin, presented at International Conference on Creep and Fatigue in Elevated Temperature Applications, Sheffield, England, Apr. 1-5, 1974.

39. Majumdar, S. and Maiya, P. S., Proc. International Conference on Materials-II, Boston, 1946, 924.

TABLE I

Frequency-separation tests (A286 at 595°C)

$\Delta\epsilon_p$	ν_t (cpm)	ν_c (cpm)	N_f	Type
		Air		
0.01	10	0.101	500	Fast-slow
0.01	0.2	0.2	280	Equal
0.01	0.101	10	192	Slow-fast
0.005	10	0.101	940	Fast-slow
0.005	0.2	0.2	683	Equal
0.005	0.101	10	320	Slow-fast
		Vacuum		
0.01	0.2	0.2	849	Equal
0.01	0.1	10	296	Slow-fast
0.01	0.1	10	284	Slow-fast
0.01	10	0.1	1129	Fast-slow

Frequency-separation tests (AISI 304 stainless steel)

t_t (min)	t_c (min)	N_f	Type
Air, $\Delta\epsilon_p = 0.02$, $T = 810°C$, $\nu = 0.132$ cpm			
0.075	7.5	>374[a]	Fast-slow
3.75	3.75	162	Equal
7.5	0.075	52	Slow-fast
Air, $\Delta\epsilon_p = 0.02$, $T = 650°C$, $\nu = 0.1$ cpm			
0.1	9.9	>198[a]	Fast-slow
5.0	5.0	215	Equal
9.9	0.1	106	Slow-fast
Vacuum, $\Delta\epsilon_p = 0.02$, $T = 650°C$			
10	0.1	148	Slow-fast
10	10	1407	Equal

[a]Failed off center.

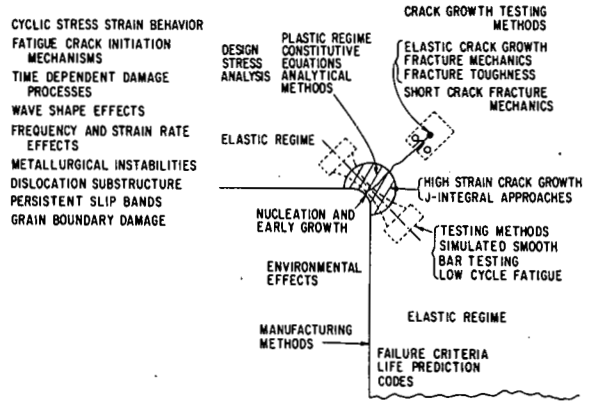

Fig. 1 - Schematic view of high-temperature fatigue problem showing physical stages in failure process and relevant disciplines.

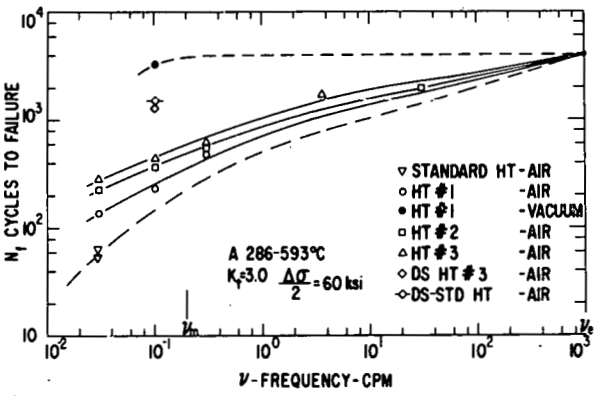

Fig. 2 - Effectof frequency on life of notched fatigue bars of A286 at 593°C in air and vacuum.(11)

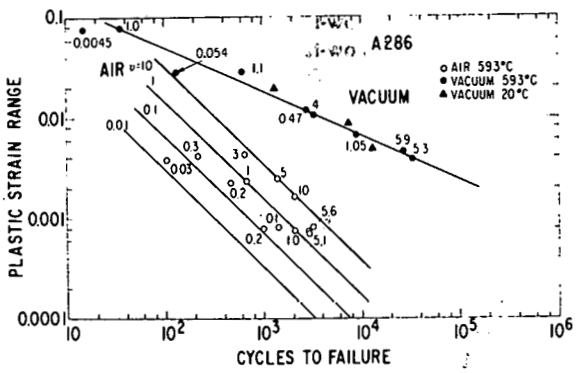

Fig. 3 - Plastic strain range vs fatigue life for A286 in air and vacuum at 866°K; equal strain rates; numbers adjacent to test points indicate frequency (cpm).(8)

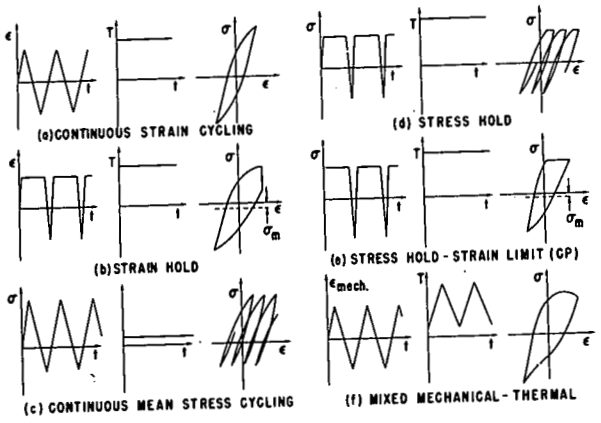

Fig. 4 - Waveshapes produced in closed loop testing for life prediction.(4)

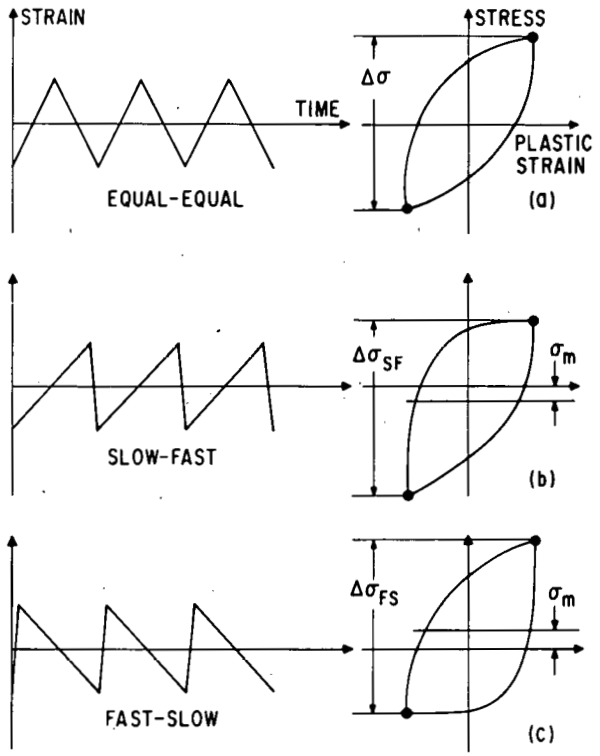

Fig. 5 - Waveshapes and resulting hysteresis loops for equal and unequal forward and reverse strain rates.(25)

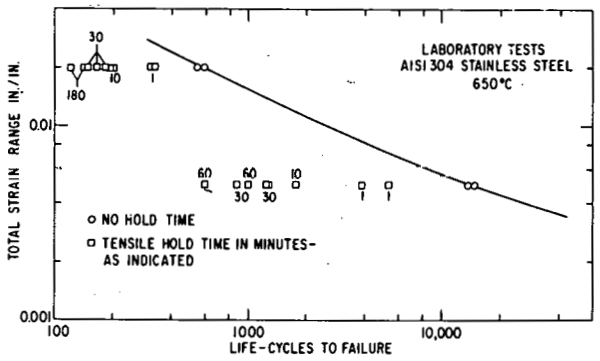

Fig. 6 - Effect of hold time on life of 304 stainless steel at 650°C. After Berling and Conway.(21)

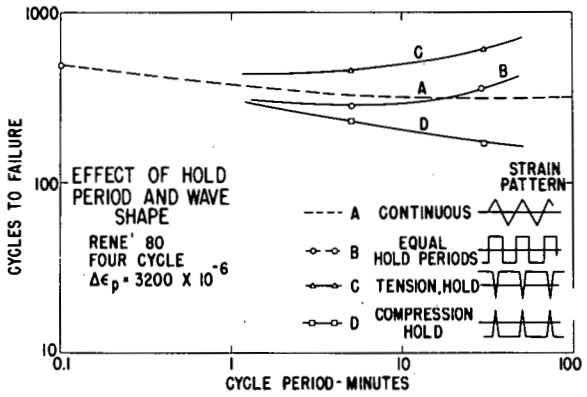

Fig. 7 - Effect of hold period and wave shape on fatigue life of cast Rene 80 at 1600°F, $\Delta\varepsilon^P$ = 3200 x 10^{-6}.(22)

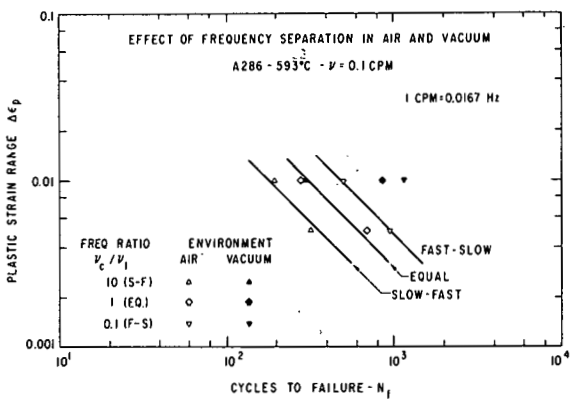

Fig. 8 - Effect of equal and unequal forward and reverse strain rates on A286 at 866°K in air and vacuum at constant frequency.(12)

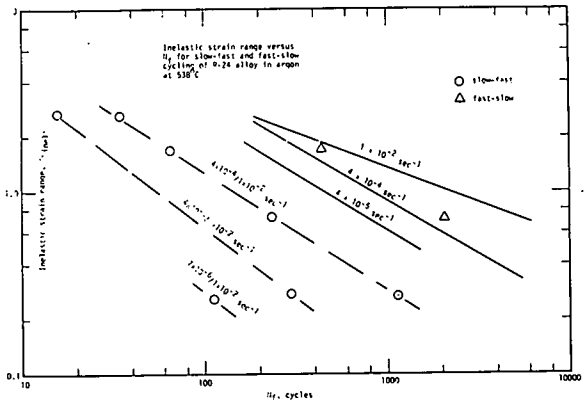

Fig. 9 - Slow-fast and fast-slow strain-rate rests on copper alloy NARloy Z at 811°K, after Conway et al.(34)

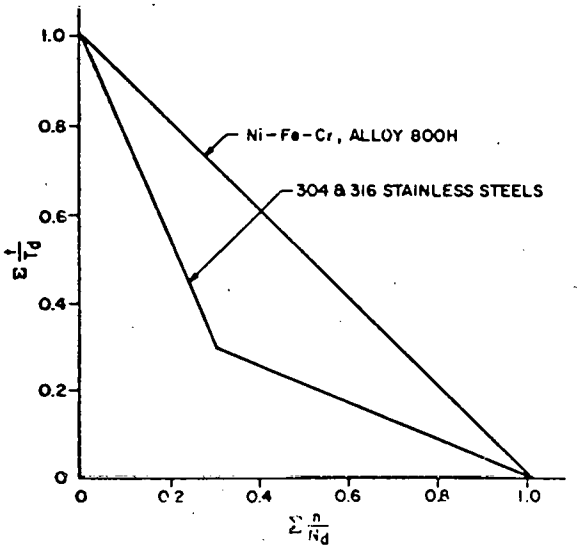

Fig. T-1420-2 Creep-fatigue damage envelope

Fig. 10 - Creep-fatigue damage envelope specified by ASME pressure vessel code for use in linear damage creep-fatigue analysis.

$$\sum_{j=1}^{p}\left(\frac{n}{N_d}\right)_j + \sum_{k=1}^{q}\left(\frac{t}{T_d}\right)_k \leq D$$

Code Case 1592 equation (5)

where

D = total creep-fatigue damage (see Fig. T-1420-2.)

n = number of applied cycles of loading condition, J

N_d = number of design allowable cycles of loading condition, j, from the fatigue curves corresponding to the maximum metal temperature during the cycles for the equivalent strain range.

t = time duration of the load condition, k

T_d = allowable time at a given stress intensity (for elastic analysis) or at a given effective stress (for inelastic analysis) from load, k. T_d values are obtained by entering the stress-to-rupture curve at a stress value equal to the calculated stress (from load k) divided by the factor K^1 = 0.9.

Fig. 11 - Linear cumulative creep and fatigue damage relation used in Code Case 1592, ASME Boiler and Pressure Vessel Code.

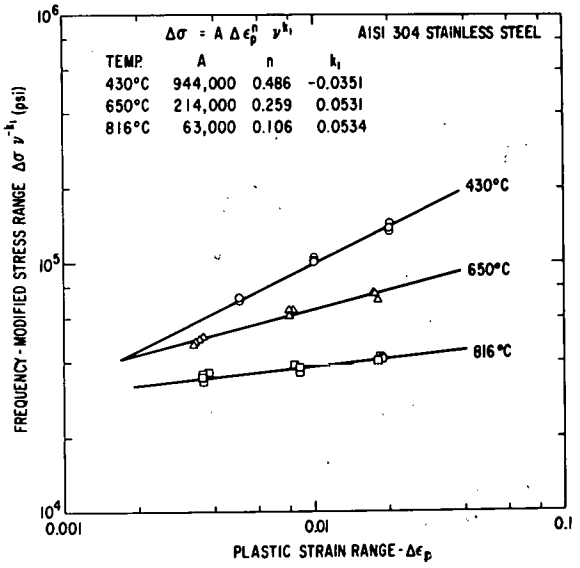

Fig. 12 - Representation of data of Berling and Slot(21) for 304 stainless steel by equation (2) showing interaction of frequency and stress range in plastic strain range for several temperatures.(1)

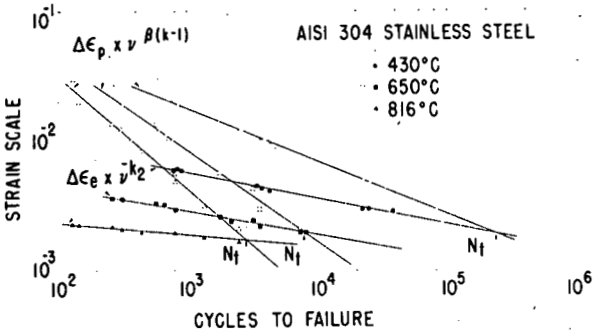

Fig. 13 - Representation of data of Berling and Slot[21] for 304 stainless steel by equations (1) and (3), showing frequency-modified elastic and plastic strain range at several temperatures in air. N_t is transition fatigue life.[1]

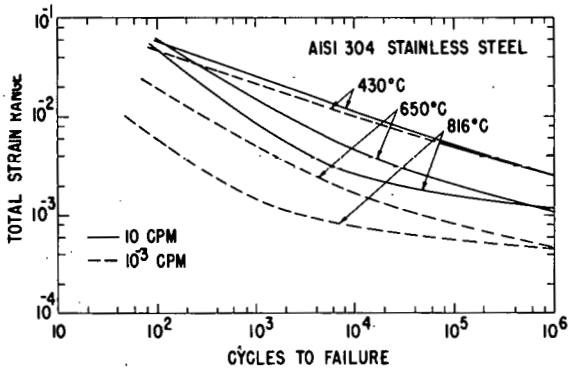

Fig. 14 - Representation of data of Berling and Slot[21] for 304 stainless steel showing total strain range vs. cycles to failure for two frequencies at several temperatures in air.

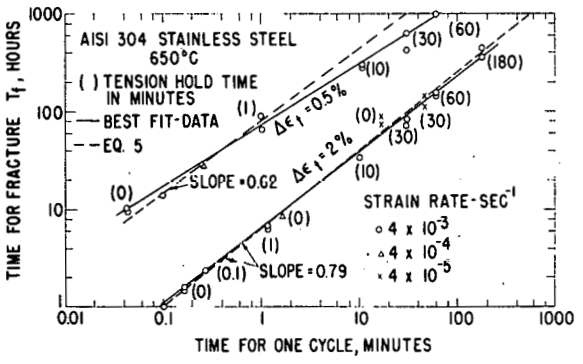

Fig. 15 - Comparison of period of cycle versus time to failure for holdtime tests with analytical results derived from Eq. 5.[1]

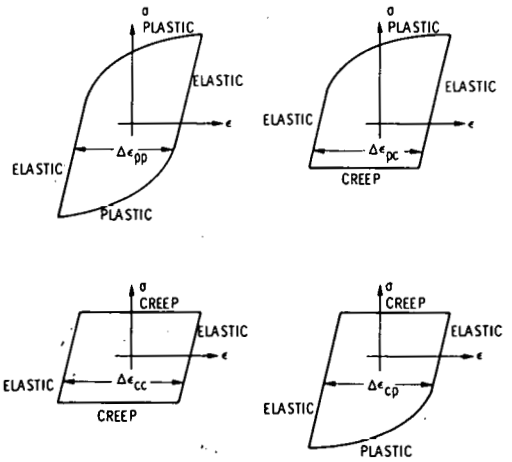

Fig. 16 - Idealized hysteresis loops for the four basic types of inelastic strainrange.[25]

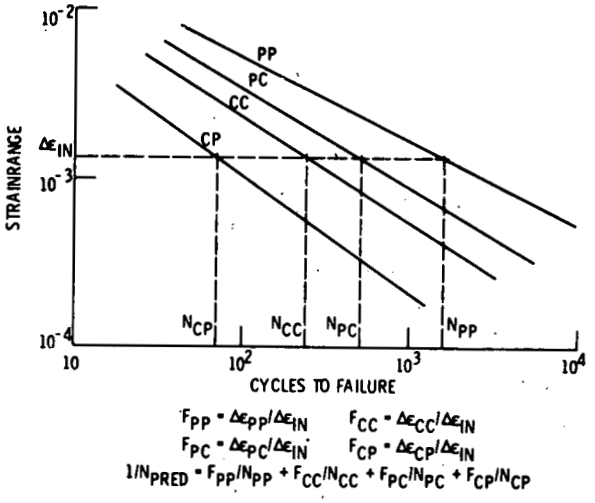

Fig. 17 - Relationships for determining life when two or more strainrange components are present. From Ref. 25.

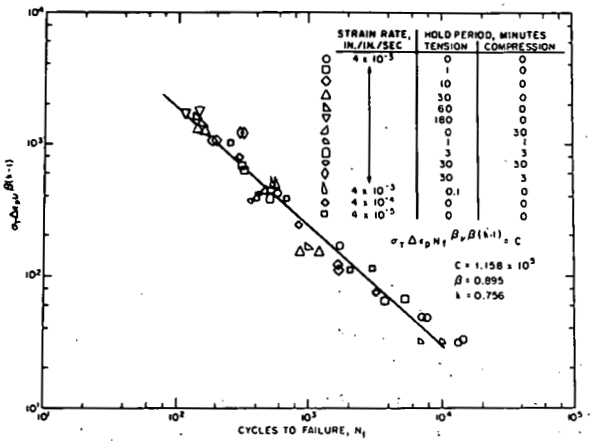

Fig. 18 - Ostergren's damage relationship for AISI 304 at 1200°F.(35)

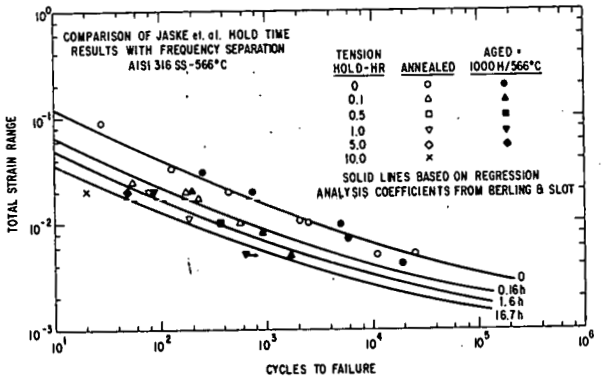

Fig. 19 - Comparison of Jaske et al. hold-time results with frequency separation (AISI 316 stainless steel, 566°C).

HIGH TEMPERATURE FRACTURE OF CERAMIC MATERIALS

S. M. Wiederhorn
National Bureau of Standards
Washington, D. C. 20234

Abstract

This report presents a review of fracture mechanisms and methods of lifetime prediction in ceramic materials. Techniques of lifetime prediction are based on the science of fracture mechanics. Application of these techniques to structural ceramics is limited by our incomplete understanding of fracture mechanisms in these materials, and by the occurrence of flaw generation in these materials at elevated temperatures. Research on flaw generation and fracture mechanisms is recommended as a way of improving the reliability of structural ceramics.

Introduction

Because of national goals for energy self-sufficiency, ceramic materials are being considered for high-temperature, structural applications. Potential uses of ceramic materials include coal conversion systems where ceramics will be used in high-temperature applications: linings of reactors, cyclones, and transfer lines; components of gas turbines; structural members in regenerative and recuperative heat exchangers; let-down valves in synthetic liquid fuel plants; and lock-hopper valves in coal gasification plants. Hence an understanding of the critical factors that determine the mechanical integrity of ceramic materials at elevated temperatures is important. At somewhat lower temperatures, an understanding of the mechanical properties of ceramics is important for safe disposal of nuclear wastes, and for the construction of reliable ceramic components for fuel cell operation and solar energy production. By improving our understanding of the mechanical behavior of ceramics it will be possible both to improve the lifetime of ceramics in current applications and to introduce ceramics into new applications that will lead to greater efficiency in energy production.

For greater efficiency, coal conversion facilities will require long-term operation between scheduled closings for maintenance and repair. Two to five year maintenance cycles, which are standard for oil refineries in the petrochemical industry, will be required as a standard of performance for the coal conversion industry. To achieve this level of reliability, techniques of lifetime prediction will be needed for ceramic materials to assure trouble free operation between maintenance periods. Even more stringent requirements are needed for nuclear waste disposal, for which projected lifetimes of safe operation are of the order of 10^3 years.

2. Lifetime Prediction Techniques

Current techniques of lifetime prediction for ceramic materials are deterministic in nature (1-3). Ceramics are believed to fail as the result of crack propagation from preexisting flaws. Consequently, techniques for lifetime prediction require information on flaw growth and on the size of the preexisting flaws. The flaws that act as nuclei for crack growth are often introduced by machining and grinding during finishing operations, and by impurities and foreign particles accidently included in powder batches during manufacturing operations. When ceramics are subjected to reactive environments at elevated temperatures, flaws can also nucleate as a consequence of chemical reactions at the surface of the ceramic. Once introduced into the ceramic, these flaws grow into cracks when a component is subjected to an applied stress of sufficient magnitude. Subcritical crack growth continues until the cracks reach a critical size, at which point failure occurs. Failure can occur a considerable period after full load has been applied, so that a time delay to failure is a typical occurrence for structural ceramics.

2.1 Initial Flaw Size

Lifetime prediction techniques for ceramic materials are based on the assumption that the engineering lifetime of a structural component can be determined from the initial size of the critical flaw and the time required for this flaw to grow to a critical size. The initial flaw size in a ceramic component can be established by three techniques: non-destructive evaluation; proof testing; and statistics. As implied by their names, each of these techniques measures the initial flaw size in a different way. Non-destructive evaluation techniques, such as x-ray radiography or ultrasonics, are used for direct measurement of flaw size. In the past, non-destructive evaluation techniques were not capable of resolving the 100 μm flaws that account for strength loss in ceramics. However recent advances in the field of ultrasonics (4) show that for dense structural ceramics, this technique is now capable of resolving flaws as small as 50 μm. Because of these advances, ultrasonics is being applied to the screening of blades for ceramic turbine engines. Substantial advances have been made recently with regard to flaw type characterization and estimation of the errors associated with the application of ultrasonics techniques (5).

Proof testing is used to estimate the largest flaw present in a structural ceramic (6,7). To be effective, the proof test load duplicates the actual load on the structural component. Once a component has been subjected to a proof test, the largest flaw in the component cannot exceed a maximum size given by the proof test level. From this estimate of the maximum size flaw, a minimum lifetime can be calculated for the structural component. Provided that the component is not damaged by subsequent treatment or by handling, proof testing provides a reliable method of lifetime assurance. A considerable amount of recent research has been conducted to clarify various aspects of the technique (such as weakening during the proof test, 2,8,9). Proof testing has been applied successfully in a number of applications: space craft windows (10, 11), optical fibers (12), vitreous grinding wheels (13) and ceramic turbine blades (14).

Statistics is probably the oldest technique of characterizing the strength of ceramic materials. Most often, designers use statistics to quantify the strength distribution so that safety factors can be established for practical application. It is only recently that strength statistics have been combined with crack growth characteristics to predict lifetimes as a function of initial flaw size probability (2,6,8,15). This method of combining statistical information on strength with flaw growth kinetics was first developed in Great Britain, (15) and is now widely used in that country as a means of improving structural reliability.

2.2 Crack Propagation Rates

The crack growth information needed for prediction of component lifetime can be obtained by three experimental techniques: crack growth techniques; stress rupture techniques; and stressing rate techniques.

Crack growth techniques are the most direct means of determining crack growth parameters (16). Fracture mechanics specimens are used to determine both the applied stress intensity factor, K_I, and the crack velocity, v, associated with K_I. For ceramic materials, the velocity is found to be a strong function of K_I, and for practical purposes, this relationship is given by a power function,

$$v = AK^n \tag{1}$$

where A and n are usually determined from a least squares fit to experimental data. Because n is usually greater than 10 for ceramic materials, other functions can also be used to describe the relation between v and K (17):

$$v = v_o \exp(bK_I) \tag{2}$$

$$v = v_o \exp(-c/K_I) \tag{3}$$

Equations 1-3 often fit experimental crack growth data with equal accuracy over the range of the data. However since lifetime predictions often require extrapolation of crack growth behavior beyond the range of the data, the accuracy of long-term lifetime predictions have recently been questioned and the need for an improved understanding of the process of crack growth has been stressed.

Data on crack velocities can also be obtained by the use of stress rupture techniques, in which a load, σ, is applied to a component, and the time to failure, t, is measured as a function of the applied load. Data obtained by this technique can be represented by the following simple equation (18):

$$t = B\, S_i^{n-2}\, \sigma^{-n} \tag{4}$$

where n is obtained from a least squares fit of experimental data. Theoretically, it can be shown that n in equations 1 and 4 is the same physical parameter, and that B is related to A of the equation 1 and to the critical stress intensity factor K_{IC} [$1/B=(n-2)AY^2K_{IC}^{n-2}/2$]. S_i is the strength of a specimen measured in an inert environment where subcritical crack growth does not precede fracture. S_i can be calculated from K_{IC} and the flaw size, a: $S_i=K_{IC}/Y\sqrt{a}$, where Y is a geometric constant for crack shape. For practical application, B can be used directly in equations for predicting lifetime (2), so that it is not necessary to evaluate A from B when stress rupture techniques are used to obtain crack growth data. As in the case of the crack growth techniques, extrapolation beyond the range of experimental data is often necessary in many practical applications for lifetime predictions, so that an understanding of the crack growth mechanism is of paramount importance for reliable prediction of lifetime. Finally, the close relationship between equations 1 and 4 should be noted. Equation 4 is, in fact, based on the assumption that v is a power function of K (equation 1). General theories of failure that relate failure time to arbitrary crack velocity equations, $v=f(K_I)$, have not been developed.

Crack velocity data can also be obtained from strength experiments in which the strength is measured as a function of stressing rate (18). Data obtained by this technique can be represented by an equation that is similar to equation 4:

$$t = (n+1)\ B\ S_i^{n-2}\ \sigma^{-n} \qquad (5)$$

where t is the time to failure in a constant stressing rate experiment, and σ is the specimen breaking stress. From the form of these two equations we see that at an equivalent breaking stress, the time-to-failure in a stressing rate experiment exceeds that for a stress rupture experiment: t(stressing rate)=(n+1) t(stress rupture) (15). The experimental constants given in equation 5 are used in much the same way as those given in equation 4. Again, extrapolation of the strength data beyond the range of experimentation is often necessary for purposes of long-term lifetime prediction. Consequently, a fundamental understanding of the failure mechanism is needed for accurate prediction of lifetime.

3.0 Mechanisms of Crack Growth

From the discussion presented above, the need for a basic understanding of mechanisms of fracture is apparent. Since the functional dependence of crack growth rate on stress intensity factor is not known with sufficient accuracy, long-term failure predictions cannot be made with confidence at the present time. By studying and understanding the mechanisms that control fracture, it may be possible to develop schemes that accurately exrapolate data so that reasonable predictions of lifetime can be made for structural ceramics. In the remainder of this report, mechanisms of fracture and their application to high temperature fracture problems will be discussed. The discussion will be organized in terms of relative complexity of the fracture process: simple materials such as glasses and single crystals will be discussed first; effects of environment and microstructure will be discussed next; then problems arising from flaw generation will be presented and discussed with regard to modern structural ceramics such as SiC and Si_3N_4.

3.1 Fracture of Homogeneous Materials: Inert Conditions

Homogeneous materials such as certain normal glasses and some single crystal ceramics are known to exhibit subcritical crack growth in vacuum. In these cases fracture is known to be temperature sensitive and crack propagation can be fitted to an activated process. For glass, the activation energy for crack growth ranges from 100 to 200 Kcal/mole, which is about the same range as that obtained for viscous flow at elevated temperatures (19). A similar activation energy is observed for single crystal Al_2O_3 (20). In contrast to the activated crack growth observed in these materials, slow crack growth does not occur in silicon (21), magnesium oxide (22), or in high silica glasses that show anomolous elastic behavior (19). The reasons for this dependence of crack growth behavior on structure are not understood.

Several mechanisms of crack growth have been suggested to explain the fracture behavior of solids in inert environments (23). These mechanisms may be divided into three broad categories: ductile fracture; diffusion; and brittle fracture. Ductile fracture involves the generation and propagation of a plastic zone from the crack tip. In line with this view, the fracture of glass has been explained by a quantitative theory that relates the hardness of glass to the crack growth rate as measured by fracture mechanics techniques (24,25,26). The theory successfully predicts the stress dependence of the crack growth rate. In contrast to these results, recent transmission electron microscopy studies of crack tips have shown that there are no slip dislocations associated with arrested cracks in brittle crystalline materials (Al_2O_3, Si, Ge, SiC) within a resolution of $\sim$1 nm, suggesting that cracks in these materials propagate without the benefit of plastic deformation (27). These results clearly indicate a need for further study of crack tip phenomenon occurring during crack propagation in inert environments.

Diffusion, as a crack growth mechanism, has been suggested to explain crack motion at elevated temperatures (28, 29). Here it is believed that material diffuses from the projected plane of the crack leaving a plane of vacancies behind that assists crack propagation. Equations derived for this mechanism have been shown to fit experimental data taken on ceramic materials at elevated temperatures. However, this mechanism probably cannot be used to explain crack motion at room temperature where the atoms of most ceramic materials are immobile. Glass containing alkali ions may be an exception to this generalization, because alkali ions are mobile at room temperature. Several authors have suggested alkali ion diffusion as a possible cause of stress-corrosion cracking of glass at room temperature (23).

With regard to brittle fracture, lattice-trapping has been recently proposed as a mechanism of crack propagation (30-32). The concept of lattice trapping takes into account the atomicity of solids to modify the Griffith Thomson theory of fracture (30-32). When this is done it can be shown that there is a critical stress intensity factor, K_I, for crack growth, and another, at a much lower value of K_I, for crack healing. The classical Griffith condition for crack proagation lies between these two limits. At stresses greater than the Griffith stress, crack growth can occur by a thermally activation process. Conversely, at stresses less than the Griffith stress, crack healing can occur by a thermally activated process. Fuller and Thomson (33) have recently devised analytical models of crack growth that predict the temperature and stress dependence of subcritical crack growth in crystalline materials.

Fruitful areas of research on the fracture of homogeneous materials in inert environments include:

o Characterization of critical aspects of the atomic structure of solids that permits subcritical crack growth.

o Comparison of crack growth and crack healing data with atomic models of lattice trapping to evaluate the validity of this fracture theory.

o Collection of crack growth data in vacuum on a variety of crystalline materials to serve as a data base for fracture theories.

o Apply high resolution transmission electron microscopy to further ascertain the structure of cracks in brittle solids.

3.2 Fracture of Homogeneous Materials: Active Environments

First observed in glass and sapphire, subcritical crack growth in ceramic materials was attributed to water vapor in the environment. Recent studies indicate that water is a stress-corrosion agent for many structural ceramics. Because subcritical crack results from a stress enhanced chemical reaction, materials that undergo stress corrosion cracking exhibit a strong dependence on temperature in the low temperature range <500°C. Chemical attack on ceramic materials is also important at elevated temperatures for other systems that interact with their environments. The fracture of nitride and carbide ceramics, for example, which oxidize at elevated temperatures, >1000°C, is known to be sensitive to oxygen in the environment (34).

When external environments are important, subcritical crack growth can be controlled by a number of important factors: composition of the ambient environment; rate of transport of the environment to the crack tip; possibilities of chemical reaction between the environment and the crack walls as the environment moves to the crack tip; and bond breaking processes such as chemical reactions or diffusion that occur at the crack tip (23). At high or low temperature, these considerations add complexity to the process of fracture that greatly increase the task of understanding the basic fracture process.

The complexity of the fracture process in the presence of a chemical environment can be illustrated for glass at room temperature (23). Glass exhibits subcritical crack growth because of water in the environment. In nitrogen gas, fracture mechanics studies suggest three distinct mechanisms that control crack growth. At low crack velocities, fracture is controlled by the rate at which the water can react with the strained silicon-oxygen bonds at the tip of the crack. At higher velocities, transport of water to the crack tip is a critical step limiting the growth of cracks, while at still higher velocities transport is so slow that fracture is controlled by an environment free process. In water, the fracture process in glass can be complicated by cavitation of the water, and by changes in the chemical composition of the water as it moves to the crack tip. At this time, the exact mechanism of bond rupture is not fully understood in glass. Because of these complexities in the fracture process, considerable additional work will be needed to fully understand the fracture of glass.

Because the base of experimental data is smaller, our understanding of fracture is less developed for ceramic materials other than glass. However, many of the same fundamental considerations that have been applied to glass will be applicable in formulating an understanding of fracture in other systems. The importance of viscous flow and cavitation of glass at grain boundaries in hot-pressed Si_3N_4 (35) has been noted. Important factors that control crack growth in Si_3N_4 include: the chemical composition of the glass at the grain boundary; the rate of transport of oxygen through the glass to the Si_3N_4 grains; and the rate of reaction between oxygen and the Si_3N_4. As in the case of stress corrosion cracking of soda-lime-silicate glass, multi-region crack growth processes have also been observed at elevated temperatures for hot-pressed silicon nitride (36). Clarification of these processes will require basic experimental studies on creep and crack propagation in ceramic materials at elevated temperatures. For greatest effect these studies should be conducted in conjunction with appropriate theoretical modeling of high temperature stress-corrosion processes, and studies of the elementary processes (diffusion, thermodynamics, chemical kinetics, etc.) that contribute to subcritical crack growth.

In the area of environmental effects on high temperature crack growth, the following area of research are pertinent to understanding the fracture process:

o Experimental data is needed on nitride and carbide ceramics in order to clarify the types of chemical reactions that are important to crack growth.

o The importance of crack tip plastic deformation and diffusion should be elucidated in order to characterize the factors that control the formation and propagation of the process zone at the crack tip.

o The effect of stress on surface chemistry should be elucidated for a fundamental understanding of stress corrosion cracking.

o Theoretical work on fluid flow in narrow channels should be conducted to establish rates of transport to crack tips, conditions for cavitation and effects of fluid viscosity on K_I.

3.3 Effects of Microstructure on Crack Growth

Our understanding of crack growth in ceramic materials is further complicated by the fact that most ceramics are not homogeneous. At room temperature, the microstructure (grain size, second phases, inclusions, porosity, etc.) of the ceramic interacts with the crack tip, forcing the crack to follow a tortuous path, so that the crack surface is no longer flat. As a consequence, the value of the fracture energy for instantaneous failure is increased by a factor of ~ 2 (37). Microcracking in front of the propagating crack increases the surface area even more, and consequently may also contribute significantly toward increasing the fracture toughness

of ceramic materials (38). Thermal expansion anisotropy may also play an important role in increasing fracture toughness, because of the development of internal stresses when ceramics are cooled from processing temperatures. Resulting from thermal expansion mismatch between adjacent grains, these internal stresses retard crack motion and hence increase the fracture energy (39). Finally, a toughening mechanism of great current interest involves phase transformations that are triggered by the advancing crack (40,41). This so called "transformation toughening" has been shown to double the critical stress intensity factor of partially stabilized zirconia.

At elevated temperature (>1000°C), the fracture of most polycrystalline ceramics is governed by increased mobility of the microstructure. Diffusion, plastic deformation, and sliding at grain boundaries cause the material in the vicinity of the crack tip undergo permament deformation. In many ceramic materials, creep cracking is a dominant mode of fracture at elevated temperatures. Crack branching as a consequence of void formation in front of the crack tip is an important fracture process (42). Crack propagation in ceramic materials at elevated temperatures is similar in many ways to that occurring in metals at lower temperatures. The recent discovery that most polycrystalline ceramic materials have a thin layer of glass at the grain boundary (43-45) suggests that grain boundary sliding is the dominant mode of deformation near the crack tip. When structural ceramics are exposed to corrosive environments at elevated temperatures, the chemical composition of the glass at the grain boundary can be modified, and deterioration (or enhancement (46)) of mechanical properties can occur. Thus, the mechanical properties of structural refractories are observed to deteriorate dramatically in the presence of low viscosity slag (47).

Areas of research that will enhance our understanding of high temperature fracture of polycrystalline ceramic materials include the following:

o Measurement of the energy required to fracture grain boundaries (grain boundary fracture is one of the elementary process in the fracture of polycrystalline ceramics, and as such, should be characterized).

o Development of models of fluid penetration along grain boundaries in ceramic materials, since intergranular glass appears to be the rule rather than the exception in ceramic materials.

o Development of relations between creep and fracture in polycrystalline materials.

o Investigate the possibility of transformation toughening as a method of improving the fracture properties of ceramic materials at elevated temperatures.

o Quantify the influence of microstructure on fracture toughness of brittle ceramics (no creep).

3.4 Effect of Flaw Generation on Fracture

As noted in section 2 of this review, crack growth from pre-existing flaws is an underlying assumption developed for ceramic materials. If the crack growth rate, and the original crack size can be quantified, the lifetime of a structural component can be predicted. Recent studies on structural nitrides and carbides, however, indicate that flaw generation at elevated temperatures may intervene to invalidate failure prediction schemes that are based on crack growth (48,49). Studies on magnesia doped, hot-pressed silicon nitride have shown the principle cause of failure in certain grades of this material to be pits that grow into the surface of the silicon nitride as a consequence of high temperature oxidation (48-51). Although it is believed that pit formation depends on local impurities in the silicon nitride, the identity of the impurities are at present uncertain. Similar results are obtained in yttria doped, hot-pressed silicon nitride, which cracks spontaneously at elevated temperatures (800 to 1000°C) as a result of precipitation at grain boundaries (52). The cause of the precipitation is not fully understood.

Structural failures of the type reported for hot-pressed silicon nitride suggest a need to deepen our understanding of the type of chemical reactions and phase transformations that occur in these materials at elevated temperatures. Thermodynamic stability of the structure relative to the environment and temperature should be established. Since similar effects may occur in other high temperature ceramic materials, general studies of this type are warrented. In this way, flaw generation as a cause of material failure can be better understood and possibly be eliminated. If flaw generation, and microstructural changes are not unavoidable, then techniques of predicting failure that take these processes into account will be necessary.

In view of the above discussion the following research is recommended to improve the high temperature mechanical behavior of ceramic materials:

o Clarify the causes for pit formation and microstructural deterioration in structural ceramics.

o Investigate the dynamics of crack healing as a way of improving structural integrity of ceramic materials.

o Develop techniques of failure prediction that can be used to establish the useful lifetime of structural ceramics when flaw generation is a problem.

4. Summary

In this report a review is presented of failure mechanisms and methods of lifetime prediction in ceramic materials. Current failure prediction techniques for ceramic materials are based on the science of

fracture mechanics. These techniques are limited by our lack of understanding of failure mechanisms in ceramic materials, and by our inability to predict failure when flaw generation is a major problem. In a review of failure mechanisms in ceramic materials a number of topics were suggested for research to enhance our understanding of fracture of ceramic materials. Theoretical modeling and experimental investigations were recommended. Areas of study include: atomic and molecular processes in homogeneous ceramics; effects of environment on fracture; influence of microstructural effects on fracture toughness; role of high temperature cavitation and creep on crack growth; and effects of flaw generation on lifetime prediction schemes. The goal of this research is the development of ceramic materials for high strength structural applications at elevated temperatures.

References

1. S. M. Wiederhorn, N. J. Tighe and A. G. Evans, "Mechanical Properties of Ceramics for High Temperature Applications," Advisory Group for Aerospace Research and Development (AGARD) Report No. 651, 1976, pp. 41-55.

2. J. E. Ritter, Jr., "Engineering Design and Fatigue Failure of Brittle Materials," in Fracture Mechanics of Ceramics, Vol. 4, R. C. Bradt, D. P. H. Hasselman and F. F. Lange, Eds. Plenum Publishing Corp., New York (1978), pp 667-686.

3. S. M. Wiederhorn and J. E. Ritter, Jr., "Application of Fracture Mechanics Concepts to Structural Ceramics," in Fracture Mechanics Applied to Brittle Materials, S. W. Freiman, ed., ASTM STP 678 (1979).

4. A. G. Evans, "Non-Destructive Failure Prediction in Ceramics," Rockwell International Science Center Report, SC5064.3FR, Sept. 1978.

5. J. M. Richerson and A. G. Evans, "Accept Reject Decisions and Failure Prediction for Structural Ceramics," J. Appl. Physics, in press.

6. A. G. Evans and S. M. Wiederhorn, "Proof Testing of Ceramic Materials -- An Analytical Basis for Failure Prediction," Int. J. Fracture 10, 379-392 (1974).

7. S. M. Wiederhorn, "Reliability, Life Prediction, and Proof Testing of Ceramics," in Ceramics for High Performance Applications, J. J. Burke, A. E. Gorum and R. N. Katz, eds., Brook Hill Publishing Co., Chestnut Hill, Mass. (1974). pp. 633-663.

8. E. R. Fuller, Jr., S. M. Wiederhorn, J. E. Ritter and P. B. Oates, "Proof-Testing of Ceramics: II. Theory,", To be published.

9. A. G. Evans and E. R. Fuller, Jr., "Proof Testing - The Effects of Slow Crack Growth," Mat. Sci. and Engr., 19 69-77 (1975).

10. S. M. Wiederhorn, A. G. Evans and D. E. Roberts, "A Fracture Mechanics Study of the Skylab Windows", in Fracture Mechanics of Ceramics, Vol. 2, R. C. Bradt, D. P. H. Hasselman and F. F. Lange, eds., Plenum Publishing Corp., New York (1974), pp 829-841.

11. S. M. Wiederhorn, A. G. Evans, E. R. Fuller, Jr. and H. Johnson, "Application of Fracture Mechanics to Space-Shuttle Windows," J. Am. Ceram. Soc. 57, 319-23 (1974).

12. B. K. Tariyal, D. Kalish and M. R. Santana, "Proof Testing of Long Length Optical Fibers for a Communications Cable," Am. Ceram. Soc. Bull., 56, 204-5, 212 (1977).

13. J. E. Ritter, Jr. and S. A. Wulf, "Evaluation of Proof Testing to Assure Against Delayed Failure," Am. Ceram. Soc. Bull., 57, 186-89, 192 (1978).

14. L. P. Wynn, D. J. Tree, T. M. Yonushonis, and R. A. Solomon, "Proof-Testing of Ceramic Components," Proc. of the 1977 DARPA/NAVSEA Ceramic Gas Turbine Demonstration Engine Program Review, J. W. Fairbanks and R. W. Rice Editors, Metals and Ceramics Information Center, Battell Columbus Laboratories, Columbus, Ohio (1978), MCIC-78-36, pp 493-516.

15. R. W. Davidge, J. R. McLaren, and G. Tappin, "Strength-Probability-Time (SPT) Relationships in Ceramics," J. Mat. Sci. 8, 1699-1705 (1973).

16. S. M. Wiederhorn, "Subcritical Crack Growth in Ceramics," in Fracture Mechanics of Ceramics, Vol. 2, R. C. Bradt, D. P. H. Hasselman, and F. F. Lange, eds., Plenum Publishing Corp., New York (1974), pp 613-646.

17. S. M. Wiederhorn, "Dependence of Lifetime Predictions on the Form of the Crack Propagation Equation," in Fracture 1977, D. M. R. Taplin, ed., Univ. of Waterloo Press, Waterloo, Canada (1977), pp 893-901.

18. J. E. Ritter, Jr. and J. A. Meisel, "Strength and Failure Predictions for Glass and Ceramics," J. Am. Ceram. Soc., 59, 478-81, (1976).

19. S. M. Wiederhorn, H. Johnson, A. M. Diness, and A. H. Heuer, "Fracture of Glass in Vacuum," J. Am. Ceram. Soc. 57, 336-41 (1974).

20. S. M. Wiederhorn, B. J. Hockey and D. E. Roberts, "Effect of Temperature on the Fracture of Sapphire," Phil. Mag. 28, 783-96 (1973).

21. C. St. John, "The Brittle-to-Ductile Transition in Pre-Cleaved Silicon Single Crystals," Phil. Mag. 32, 1193-1212 (1975).

22. D. A. Shockey and G. W. Groves, "Effect of Water on Toughness of MgO Crystals", J. Am. Ceram. Soc. 51, 299-303 (1968).

23. S. M. Wiederhorn, "Mechanisms of Subcritical Crack Growth in Glass," in Fracture Mechanics of Ceramics, Vol. 4, R. C. Bradt, D. P. H. Hasselman and F. F. Lange, Plenum Publishing Corp., New York (1978) pp 549-580.

24. D. M. Marsh, "Plastic Flow and Fracture of Glass," Proc. Phys. Soc., London, 282A, 33-43 (1964).

25. J. G. Williams and G. P. Marshall, "Environmental Crack and Craze Growth Phenomena in Polymers," Proc. Roy. Soc., London, A342, 55-77 (1975).

26. G. W. Weidmann and D. G. Holloway, "Plastic Flow-Slow Crack Propagation and Static Fatigue in Glass," Phys. Chem. Glasses, 15, 68-75 (1974).

27. B. R. Lawn, B. J. Hockey and S. M. Wiederhorn, "Atomically Sharp Cracks in Brittle Solids: An Electron Microscopy Study," submitted for publication.

28. R. N. Stevens and R. Dutton, "The Propagation of Griffith Cracks at High Temperatures by Mass Transport Processes," Mater. Sci. Engr., 8, 220-234 (1971).

29. D. P. H. Hasselman, "Proposed Theory for the Static Fatigue Behavior of Brittle Ceramics," in Ultrafine-Grain Ceramics, J. J. Burke, N. L. Reed and V. Weiss eds. Syracuse University Press, Syracuse, New York (1970) pp 297-315.

30. R. Thomson, C. Hsieh, and V. Rana, "Lattice Trapping of Fracture Cracks," J. Appl. Phys. 42, 3154-60 (1971).

31. E. R. Fuller, Jr. and R. Thomson, "Nonlinear Lattice Theory of Fracture," in Fracture 1977, D. M. R. Taplin, Editor, University of Waterloo Press, Waterloo Canada, 1977, Vol. 3, pp 387-394.

32. E. R. Fuller, Jr. and R. M. Thomson, "Lattice Theories of Fracture," in Fracture Mechanics of Ceramics, Vol. 4, R. C. Bradt, D. P. H. Hasselman and F. F. Lange, editors, Plenum Publishing Co., New YOrk, (1978), pp 507-548.

33. E. R. Fuller, Jr. and R. M. Thomson, "Theory of Chemically Assisted Fracture," Third International Conference on Mechanical Behavior of Materials, Cambridge, University August 20-24 (1979).

34. N. J. Tighe, "Microstructural Aspects of Deformation and Oxidation of Magnesia-Doped Silicon Nitride," in Nitrogen Ceramics, F. L. Riley, editor, Noordhoff, Leyden (1977) pp 441-448.

35. F. F. Lange, "Evidence for Cavitation Crack Growth in Si_3N_4," J. Am. Ceram. Soc. 62, 222-224 (1979).

36. A. G. Evans and S. M. Wiederhorn," Crack Propagation and Failure Prediction in Silicon Nitride at Elevated Temperatures," J. Mater. Sci., 9, 270-278 (1974).

37. R. Rice, "Microstructure Dependence of Mechanical Behavior of Ceramics," in Treatise on Materials Science and Technology, Vol. II, Properties and Microstructure, Academic Press, New York (1977) pp 199-381.

38. C. Cm. Wu, S. W. Freiman, R. W. Rice and J. J. Mecholsky, "Microstructural Aspects of Crack Propagation in Ceramics," J. Mat. Sci. 13, 2659-2670 (1978).

39. R. W. Rice, S. W. Freiman, R. C. Pohanka, J. J. Mecholsky, Jr., and C. Cm. Wu, "Microstructural Dependence of Fracture Mechanics Parameters in Ceramics," in Fracture Mechanics of Ceramics, Vol. 4, R. C. Bradt, D.P. H. Hasselman, and F. F. Lange, editors, Plenum Publishing Co., New York (1978) pp 849-876.

40. D. L. Porter and A. H. Heuer, "Mechanisms of Toughening Partially Stabilized Zirconia (PSZ)," J. Am. Ceram. Soc., 60, 183-4 (1977).

41. A. G. Evans and A. H. Heuer, "Transformation Toughening in Ceramics: Martinsitic Transformation in Crack Tip Stress Fields," J. Am. Ceram. Soc., to be published.

42. N. J. Tighe, "Structure of Slow Crack Interfaces in Silicon Nitride," J. Mater. Sci., 13, 1455-63 (1978).

43. D. R. Clarke and G. Thomas, "Grain Boundary Phases in a Hot-Pressed MgO Fluxed Silicon Nitride," J. Am. Ceram. Soc., 60, 491-5 (1977).

44. L. K. V. Lou, T. E. Mitchell and A. H. Heuer, "Impurity Phases in Hot-Pressed Si_3N_4," J. Am. Ceram. Soc., 61, 392-396 (1978).

45. R. Kossowsky, "Microstructure of Hot-Pressed Silicon Nitride," J. Mat. Sci. 8, 1603-15 (1973).

46. F. F. Lange, B. I. Davis and D. R. Clarke, "Compressive Creep of Si_3N_4/MgO Alloys Pt. 3: Effect of Oxidation Induced Compositional Changes," Rockwell International Science Center Report, SC 5099.2AR, January 1979.

47. N. J. Tighe and J. R. Kreglo, Jr., "Electron Microscopy of Periclase Brick," Am. Ceram. Soc. Bull. 49, 188-192 (1970).

48. S. M. Wiederhorn and N. J. Tighe, "Proof-Testing of Hot-Pressed Silicon Nitride," J. Mat. Sci. 13, 1781-93 (1978).

49. S. M. Wiederhorn and N. J. Tighe, "Effect of Flaw Generation on Proof-Testing", Proc. of the 1977 DARPA/NAVSEA Ceramic Gas Turbine Demonstration Engine Program Review, J. W. Fairbanks and R. W. Rice, eds., Metals and Ceramics Information Center, Battelle Columbus Laboratories, Columbus, Ohio (1978), MCIC-78-36, pp 689-700.

50. S. W. Freiman, A. Williams, J. J. Mecholsky, and R. W. Rice, "Fracture of Si_3N_4 and SiC," in Ceramic Microstructures '76, R. M. Fulrath and J. A. Pask, editors, Westview Press, Inc., Boulder, Colorado (1977) pp 824-834.

51. D. W. Richerson and T. M. Yonushonis, "Environmental Effects on the Strength of Silicon-Nitride Materials," in Proc. of the 1977 DARPA/NAVSEA Ceramic Gas Turbine Demonstration Engine Program Review, J. W. Fairbanks and R. W. Rice, editors, Metals and Ceramics Information Center, Battelle Columbus Laboratories, Columbus, Ohio (1978), MCIC-78-36, pp 247-272.

52. W. D. Carruthers, D. W. Richerson, and K. Benn, "Combustor Rig Durability Testing of Ceramic Materials," To be published as part of the proceedings of the Sixth AMMRC Materials Technology Conference: Ceramics for High Performance Applications - III - Reliability. July 10-13, 1979, Orcas Island, Washington.

CREEP MECHANISMS AND CONSTITUTIVE RELATIONS IN PURE METALS

W. D. Nix
Stanford University, Stanford, California 94305

The current status of our understanding of the mechanisms of creep of pure metals is briefly reviewed. The review is divided into two parts: (I) Steady state flow mechanisms, and (II) Non-steady state flow mechanisms and constitutive relations.

Creep by diffusional flow is now reasonably well understood, with theory and experiment in good agreement. The closely related phenomenon of Harper-Dorn creep can also be understood in terms of diffusion between grown-in dislocations. These diffusional creep mechanisms are briefly reviewed.

Power law creep almost surely involves the climb of edge dislocations controlled by lattice self diffusion. Theoretical treatments of this process invariably give a power law exponent of 3. This natural creep law is compared with the data for FCC and BCC metals. It is suggested that diffusion controlled climb is the controlling process in BCC metals at very high temperatures. At lower temperatures, other processes are also involved. It is also suggested that stacking fault energy effects may preclude the possibility that creep is controlled entirely by lattice self diffusion in some FCC metals. The subject of power law breakdown is presented as a natural consequence of the transition to low temperature flow phenomena. The role of core diffusion in this transition is briefly discussed.

The recent activity in the field of constitutive equations centers mainly on the development of equations to predict non-steady state flow behavior. The results of load drop and load relaxation experiments are described. The basic framework for constitutive equations in terms of structure parameters is reviewed and the particular forms suggested by Hart, Kocks and Miller are described.

INTRODUCTION

In the present paper we review the mechanisms by which pure metals creep at elevated temperatures. While most of this review deals with the mechanisms of steady state flow, some discussion is devoted to creep flow under non-steady state conditions. This latter topic is discussed in connection with the development of constitutive equations for describing plastic flow in metals.

Because of limitations of space, this review will be extremely brief. The reader is therefore encouraged to refer to the several excellent and extensive reviews of high temperature creep that have been published during the last few years. These include the review papers by Sherby and Burke [1], Mukherjee, Bird and Dorn [2], Mukherjee [3], and Takeuchi and Argon [4]. An excellent treatment of recent developments in constitutive equations can be found in the book edited by Argon [5]. The reader is also referred to the original literature on the grounds that review papers, such as the present one, can be misleading.

PART I: STEADY STATE FLOW MECHANISMS

DIFFUSIONAL CREEP

The simplest and best understood mechanism of creep flow is one developed originally by Nabarro [6] and Herring [7]. In this process, vacancies flow from grain boundaries under tension to nearby grain boundaries under compression. As a consequence, individual crystals elongate in the direction of the tensile axis as vacancies are created and destroyed at the grain boundaries. At very high temperatures, vacancies flow mainly through the crystal lattice and lattice self diffusion is the rate limiting process. The creep rate depends linearly on the applied stress and inversely on the square of the grain size.

At low temperatures or for very fine grain sizes, the diffusional flow process can occur along the grain boundaries. Coble [8] was the first to extend the diffusional creep mechanism to the case of boundary diffusion. In his analysis the rate of creep is proportional to the grain boundary self diffusion coefficient and varies inversely with the cube of grain size. While the lattice and boundary diffusional creep processes are probably not strictly additive, the overall rate of diffusional creep can be approximated by:

$$\frac{\dot{\varepsilon}_s kT}{GDb} = 10\left(\frac{b}{d}\right)^2 \frac{\sigma}{G}\left\{D_L + 2.5\left(\frac{b}{d}\right) D_{gb}\right\} . \qquad (1)$$

In this equation and throughout this paper the terms are defined as follows:

$\dot{\varepsilon}_s$ = steady state tensile creep rate

kT = usual meaning

b = Burgers vector

G = shear modulus

d = grain diameter

σ = tensile stress

D_L = lattice self diffusion coefficient

D_{gb} = grain boundary self diffusion coefficient

It should be mentioned that some grain boundary sliding (GBS) must accompany diffusional flow. If each crystal in a polycrystalline solid were permitted to change its shape by diffusional flow alone, the crystals would no longer fit together perfectly. To maintain compatibility it is necessary to slide the crystals slightly with respect to each other. Thus, one can consider diffusional flow to be accommodated by GBS. An alternate but equivalent view is that creep deformation occurs by GBS and is accommodated by diffusional flow. This interrelationship has been discussed in a number of papers [9,10].

Burton [11] has observed that polycrystalline copper containing Al_2O_3 particles at the grain boundaries creeps more slowly than the diffusional flow theory predicts. It may be that the particles inhibit the motion of grain boundary dislocations and thus limit the overall creep rate. Here the kinetics

of boundary sliding might be important and the process might not be controlled entirely by diffusion.

HARPER-DORN CREEP

About 20 years ago Harper and Dorn [12] reported that creep of aluminum becomes linearly viscous at very high temperatures and that the temperature dependence is the same as that for lattice self diffusion. The phenomenon has been observed in single crystals and cannot be explained in terms of Nabarro-Herring diffusional creep. It also has been observed in Al-Mg, Pb, Sn and Ag. It is therefore considered to be a generic creep mechanism [13]. The most plausible explanation of Harper-Dorn creep is that suggested by Mohamed et al [13]. They pointed out that Harper-Dorn creep of Al occurs when the stresses are so low that the grown-in dislocation density exceeds the dislocation density expected from the relation $\rho = (\sigma/\alpha Gb)^2$. Indeed, the Harper-Dorn creep rate can be accurately described by considering creep to occur by vacancy flow between dislocations. Later in this paper we develop a natural creep equation (see Eq. (12)) which is based in part on a stress dependent structure. For the special case of a fixed dislocation density this relation can be written as

$$\frac{\dot{\varepsilon}_s \, kT}{D_L \, Gb} = \rho_o \, b^2 \, \left(\frac{\sigma}{G}\right) \quad , \tag{2}$$

where ρ_o is the stress independent grown-in dislocation density. This relation accurately describes the Harper-Dorn creep process in Al. If this interpretation is correct, it should be possible to avoid Harper-Dorn creep by testing crystals having extremely low dislocation densities.

POWER LAW CREEP

The most important but least understood mechanism of high temperature creep is power law creep. Here the creep rate often varies as the 5th power of the applied stress. Many experiments clearly show that lattice self diffusion is the dominant process during high temperature power law creep. In particular the activation energy for creep often coincides exactly with that for lattice self diffusion even over temperature ranges where phase changes occur [14]. In addition, the true activation volume for creep corresponds with that for lattice self diffusion [15], again showing that self diffusion is surely the most important process controlling creep at high temperatures. These correlations are often described empirically with what is now known as the Dorn equation

$$\frac{\dot{\varepsilon}_s \, kT}{D_L \, Gb} = A \, \left(\frac{\sigma}{G}\right)^n \quad , \tag{3}$$

where $n = 5$ and A is about 10^7 for FCC metals.

The most widely accepted mechanism of power law creep is edge dislocation climb controlled by lattice self diffusion. However, it has not been possible to derive the Dorn equation, with its 5th power stress dependence, on the basis of diffusion controlled climb alone. As Weertman [16] has pointed out, all theoretical treatments of dislocation climb controlled by lattice self diffusion

lead to the same creep equation, which he calls the natural creep law. It is, in our notation

$$\frac{\dot{\varepsilon}_s \, kT}{D_L \, Gb} = \left(\frac{\sigma}{G}\right)^3 \quad . \tag{4}$$

Weertman has suggested that it is necessary to fudge to derive the Dorn Equation with a 5th power stress dependence. It is possible to identify a "swindle" in all treatments of creep which do not result in the natural creep law, provided they are based on diffusion controlled climb or some like process.

While there are many ways to derive the natural creep law, all are essentially equivalent. This is analogous to the situation in the theory of strain hardening where there are many apparently different ways to derive the Taylor hardening relation. One popular derivation of the natural creep law was first developed by Bailey [17] and Orowan [18] and has been used by many authors since. This treatment will be presented here not only as a derivation of the natural creep law but also to provide a basis for a discussion of constitutive equations in the last part of this paper.

The central idea of power law creep is that the creep rate at a given temperature depends on both the applied stress, σ, and the current value of at least one strength parameter, τ:

$$\dot{\varepsilon} = f(\sigma, \tau) \quad . \tag{5}$$

In the present treatment we assume that τ depends only on the dislocation density through

$$\tau = \alpha \, Gb \, \sqrt{\rho} \quad . \tag{6}$$

Under constant stress the creep rate depends on how the strength parameter changes in the course of creep. Bailey and Orowan have suggested that strain hardening and recovery serve to increase and decrease τ respectively and that at steady state the rate of increase due to strain hardening is equal to the rate of decrease due to recovery. This concept leads to the following evolutionary law for the structure (or strength parameter) during creep:

$$d\tau = \left(\frac{\partial \tau}{\partial \varepsilon}\right) d\varepsilon + \left(\frac{\partial \tau}{\partial t}\right) dt \quad . \tag{7}$$

This particular form of the theory explicitly assumes that we have only static recovery. Many experiments have indicated that recovery is typically much faster when deformation is occurring and this suggests that the present treatment should be extended to include dynamic recovery.

It is common practice to associate $\partial\tau/\partial\varepsilon$ with the rate of strain hardening during stage II hardening of FCC crystals. Thus we approximate this as

$$\frac{\partial \tau}{\partial \varepsilon} = \frac{G}{100} \quad . \tag{8}$$

In writing this we assume implicitly that no recovery occurs during Stage II hardening, a reasonable assumption in view of the temperature and strain rate independence of that process.

We assume that recovery involves the diffusion controlled climb and annihilation of oppositely signed edge dislocations. Following a treatment given by Friedel [19] this leads to

$$\frac{\partial \tau}{\partial t} = - \frac{\sqrt{2}\ D_L G^2 b}{\alpha\ kT} \left(\frac{\tau}{G}\right)^3 \quad . \tag{9}$$

At steady state the competing effects of strain hardening (dislocation multiplication) and recovery (dislocation annihilation) are expected to nullify each other, with the consequence that the dislocation density, ρ, or, equivalently, the shear strength parameter, τ, reaches a steady state value. Thus at steady state we require $d\tau = 0$ and from Eqs. (7-9), we write

$$\dot{\varepsilon}_s = - \frac{r}{h} = \frac{100\sqrt{2}}{\alpha} \frac{D_L\ Gb}{kT} \left(\frac{\tau_s}{G}\right)^3 \quad . \tag{10}$$

In this simple form of the theory, the applied shear stress must be just equal to the shear strength of the solid established by the competition between strain hardening and recovery. Thus, we write

$$\frac{\sigma}{2} = f\ \tau_s \quad , \tag{11}$$

and take $f = 1$. If f were smaller than 1 then flow could only occur by thermal activation of dislocations past each other. Indeed, allowing f to be less than unity may be a way to include the effects of thermally activated slip on creep. However, in the present treatment we restrict our attention to the case in which creep flow is controlled entirely by lattice self diffusion. In this limit, flow would not occur if f were less than 1 and τ would have to be decreased by recovery before flow could occur.

Using the above relations, the natural creep law for diffusion controlled climb is

$$\frac{\dot{\varepsilon}_s\ kT}{D_L\ Gb} = A \left(\frac{\sigma}{G}\right)^3 \quad , \tag{12}$$

where $A \approx 1$. As noted above, this same result has been derived by a number of workers in many apparently different ways. Because of its persistence it may be concluded that it does represent the creep law of diffusion controlled climb.

It is widely recognized that the natural creep law does not compare favorable with the existing body of experimental evidence. This is shown in Fig. 1 for the case of several FCC metals. It should be noted that the power law exponent for FCC metals is about 5 instead of 3. In addition, most of these FCC

metals creep more slowly than the prediction of the natural law. It is also evident from the data that Ag creeps much more slowly than Al, with Au, Cu and Ni showing intermediate creep rates. As shown first by Barrett and Sherby [20], this variation in creep rate correlates strongly with stacking fault energy, γ_{SFE}. Silver has a particularly low γ_{SFE}, especially compared to Al. A consequence is that Shockley partials in Ag are much more widely separated than in Al. It is reasonable to expect that this would inhibit the climb process and thus reduce the creep rate. Following this line of reasoning, Barrett and Sherby [20] and others have proposed that the Dorn creep equation be written as

$$\frac{\dot{\varepsilon}_s \, kT}{D_L \, Gb} = A' \left(\frac{\gamma_{SFE}}{Gb}\right)^{3.5} \left(\frac{\sigma}{G}\right)^5 \quad . \tag{13}$$

The power exponent of 3.5 is the result of the correlation between creep rate (properly normalized with respect to σ, G and D_L) and stacking fault energy.

The discrepancy between the natural creep law and the Dorn equation has been recognized for many years. In general we have assumed that the assumptions underlying the derivation of the natural creep law are either wrong or incomplete, and we have sought to modify the theory to be consistent with the empirical equation, thus far without success. It may be that we have been misled by the data correlation of Fig. 1. It is possible that power law creep is not controlled entirely by lattice self diffusion, at least for some FCC metals. Let us consider the extreme case of Ag where the creep rate falls far below the rate predicted by the natural theory. Here it is reasonable to attribute this low creep rate to the presence of widely extended dislocations which do not climb easily. However, it may be possible for the climb rate to be reduced by widely separated partials and still not controlled entirely by the transport of vacansion. If the climb process were controlled entirely by the transport of vacancies between dislocations, then the process of vacancy absorption or emmission at the dislocation might be expected to be fast by comparison. Thus, if stacking fault effects do reduce the climb rate, then they might also affect the rate controlling process. Indeed, Weertman's theory [21] of stacking fault energy effects on creep is based on the idea that flow of vacancies along the climbing dislocation becomes more difficult as the partials become more widely separated. Thus in his treatment core diffusion (as modified by the presence of stacking faults) enters the creep equation and the process is no longer controlled entirely by lattice self diffusion.

The difficulties associated with climb of extended dislocations in FCC metals suggest that the natural creep law may be more directly applicable to BCC metals where separation into partials is much less severe and where the assumption that climb is controlled entirely by vacancy transport between dislocations may be more appropriate. The natural creep law is compared with some creep data for BCC metals in Fig. 2. Here it is noted that the experimental creep rates are almost all faster than the predictions of the natural theory. The average power law exponent is again about 5 but the data for Ta suggest that at high temperatures and low stresses the stress exponent may be nearer 3. It is certainly well known that at lower temperatures and higher stresses the power law exponent becomes very much larger than 5. This so-called power law breakdown regime is not shown in this figure.

One might argue that the data for BCC metals corresponds favorably with the natural creep theory at the highest temperatures and lowest stresses. To test this idea one needs to have creep data at very high temperatures. The recent work by Stang [22] on Fe - 3% Si and Wray [23] on δ Fe provide such a test. Their data along with other data for Fe or Fe - 3% Si are shown in Fig. 3. Here one sees that the creep data are in excellent agreement with the natural creep theory at very high temperatures and low stresses. Indeed, the rest of the creep data appears as a very gradual transition from a power law exponent of 3 to the very high stress exponents associated with low temperature flow. In this description the power law exponents of 5 or 6 do not appear as fundamental exponents but merely as natural consequences of the transition from high temperature to low temperature deformation.

The remarks in the above paragraphs should be taken as speculative. The views expressed here are likely to be controversial and may be wrong. In its simplest form the suggestion is that the natural creep law is valid at least for BCC metals at very high temperatures. At lower temperatures other thermally activated processes may come into play to cause the creep rate to exceed this natural law prediction. For FCC metals the difficulties associated with climb of extended dislocations may mean that climb and creep are not controlled entirely by lattice self diffusion and that the other processes involved, once understood, will permit us to rationalize the observed creep behavior of FCC metals.

To be fair it should be noted that some FCC metals with high stacking fault energies show a constant stress exponent $n > 3$ over a wide range of stress or strain rate. In the case of Al, for example, the power law exponent is 4.5 and there is no indication of curvature in the power law plot. The viewpoint being expressed here does not provide a natural explanation of that observation.

In the above paragraphs it is suggested that when high temperature creep is controlled entirely by self diffusion the 3rd power natural creep law should be observed. Support for this concept was given by Stocker and Ashby [24] who studied the creep properties of various classes of crystalline solids and showed that the constants A and n in the Dorn equation (Eq. (3)) can be related empirically as follows

$$n = 3.0 + 0.3 \log A \ . \qquad (14)$$

Thus, when $A = 1$, $n = 3.0$, in agreement with the natural creep law. Aside from certain diffusional creep results, all of the experimental data examined by Stocker and Ashby falls in the $n \geq 3.0$ or $A \geq 1.0$ regime. This observation is consistent with the suggestion above that the natural creep law is a limiting kind of creep behavior that may only be approached in some materials.

POWER LAW BREAKDOWN

The creep data in Figs. 1-3 show the so-called power law regime of creep. At stresses of the order of $\sigma/G = 10^{-3}$ and higher, the observed creep rates become much faster than would be predicted by simple extrapolation of the power law. This deviation at high stress is usually called power law breakdown. The power law function is often replaced by exponential or hyperbolic sine functions in this regime [25]. In view of the earlier discussion in this paper it should

be made clear that power law breakdown ordinarily refers to deviations from a power law exponent of 5. As noted earlier, at least for BCC metals, a case can be made for n = 3 being the natural power law exponent, so that any deviation from that behavior might also be termed power law breakdown.

The mechanisms responsible for power law breakdown have been debated for many years. Some authors have suggested that the "faster creep rates" arise from the effects of excess vacancies produced by deformation [1,26], while others have argued that short circuit diffusion along dislocation cores is the primary cause [27]. It would appear that neither of these explanations is sufficient to explain the observations. Surely the most basic statement is that power law breakdown is simply a manifestation of a transition from high temperature to low temperature flow. It is well known that the flow stress at low temperatures is relatively insensitive to strain rate. This, of course, is another way of saying that the flow rate depends very strongly on the stress. Thus, the high stress exponents associated with power law breakdown are naturally expected.

While the idea of short circuit diffusion down dislocation cores cannot fully describe power law breakdown in metals, there is little doubt that diffusion can occur along dislocations. Thus, any model of creep based on dislocation climb should account for the fact that diffusion may occur either in the lattice or along dislocations. Spingarn, Barnett and Nix [28] have recently studied models of dislocation climb controlled by core diffusion. In their treatment the dislocations are not regarded as simple pipes for diffusion as had been done previously [29-30]. Rather, the dislocation along which diffusion occurs is allowed to act as a perfect source or sink for vacancies. In spite of this refinement the creep equation for core diffusion controlled climb is essentially the same as that found by others [29-30]. When allowance is made for both lattice and dislocation core diffusion the natural creep law becomes

$$\frac{\dot{\varepsilon}\, kT}{Gb} = \left(\frac{\sigma}{G}\right)^3 \left\{D_L + 2.5 \left(\frac{\sigma}{G}\right)^2 D_c\right\} . \qquad (15)$$

Notice that at high stresses or when $D_c \gg D_L$, the second term dominates and a 5 power creep law is naturally predicted. However, in such limits the activation energy is that for core diffusion, not lattice diffusion. If one is willing to empirically generalize Eq. (15) to coincide with 5 power lattice diffusion controlled creep, then the following relation would be expected to hold

$$\frac{\dot{\varepsilon}_s\, kT}{Gb} = A \left(\frac{\sigma}{G}\right)^5 \left\{D_L + 2.5 \left(\frac{\sigma}{G}\right)^2 D_c\right\} . \qquad (16)$$

Here we see a 7 power law can be "predicted" at low temperatures and high stresses. Generally speaking this relation permits one to rationalize the creep properties of pure metals at intermediate temperatures. The creep properties of Ni at high and intermediate temperatures can be made to coincide using this relation. However, close examination of the data for several metals including Ni shows that the predictions of the core diffusion correlation are sometimes inconsistent with experiment [28].

PART II: NON-STEADY STATE FLOW MECHANISMS AND CONSTITUTIVE EQUATIONS

In the first part of this paper our attention was focused on the physical mechanisms for steady state flow in pure metals. In this second part we address the problem of non-steady state flow and the closely related subject of constitutive equations. Non-steady state flow is important because structural materials almost never reach steady state in service. The stress continually changes in service with the result that non-steady state flow is the rule rather than the exception. Non-steady state flow phenomena are also important because they provide more stringent tests of deformation models than do steady state data alone.

A variety of different kinds of creep transients are exhibited by metals in the power law creep regime. Primary creep itself is a creep transient that is caused by changes in structure that occur during creep. Generally the creep rate decreases during primary creep as the dislocation structure develops and becomes more refined. For heavily cold worked or pre-strained metals, the dislocation structure naturally coarsens during creep and an inverted creep curve (accelerating creep) is observed.

Once steady state is achieved, a new creep transient is produced whenever the stress is changed. For a stress reduction, the creep rate falls far below the steady state rate expected for the reduced stress and then gradually increases until the new steady state is achieved. The opposite occurs when the stress is increased. Here the creep rate just after the stress change exceeds the steady state rate at the new stress level and gradually declines in the course of creep. Again the new steady state is eventually achieved.

Within the past decade a number of new experimental techniques have been developed for studying the non-steady state flow properties of metals A number of these techniques are based on the analysis of creep transients associated with stress reductions. As noted above, the creep rate just after a stress reduction is typically much smaller than the steady state creep rate at the reduced stress. Some authors report that the creep rate after a small stress drop is essentially zero [31-33], while others claim that a small but finite creep rate is observed [34,35]. One source of confusion in the interpretation of creep transients associated with stress changes arises from the difficulty of making accurate measurements of very low creep rates. Some recent work by Gibeling [36] indicates that the foreward creep rates following stress reductions in copper fall as the 17th power of the remaining stress. For moderate stress reductions this might appear as a zero creep rate. Another source of error arises from the anelastic back flow that invariably occurs in metals when stress reductions are made. In order to characterize the so-called "constant structure" creep rate it is necessary to wait for the back flow effects to dissipate before measuring the forward creep rate at the reduced stress level.

For metals such as aluminum the creep rate following a stress reduction is sufficiently large to be easily measurable and one can determine the way in which the creep rate varies with reduced stress for an ostensibly constant structure [37]. Such experiments typically show that the creep rates under constant structure conditions vary approximately as $\dot{\varepsilon} \sim \sigma_r^7$. This result clearly suggests that the isostructural stress dependence of the creep rate, σ_r^7, is quite different from the ordinary (non-isostructural) stress dependence $\sigma^{4.5}$.

This result provides an important test for creep models and it suggests a basic framework for the formulation of a constitutive equation.

Hart, Li and co-workers [38,39] have used the load relaxation test to provide information about the flow of metals under "constant structure"* conditions. Most of their experiments have been conducted at relatively low temperatures compared to the usual steady state creep regime. During load relaxation in an infinitely hard testing machine the elastic strain in the sample is exchanged for plastic strain as the stress relaxes. Thus the creep rate-stress relation can be studied over many orders of magnitude of strain rate while the sample undergoes very little plastic deformation. This relation is taken to be that for a fixed structure. The extent to which static recovery occurs in the course of the relaxation is the extent to which the structure may not remain constant during this kind of test. This error would be expected to become important at high temperatures where climb controlled static recovery is relatively fast.

The constant structure experiments above clearly indicate that the rate of creep flow of metals at a given temperature depends not only on the applied stress but also on the structure. The steady state creep laws discussed in PART I of this paper cannot be used to describe constant structure creep properties since the structure terms (like τ in Eq. (5)) have been assigned their steady state values and are thus expressed as functions of the stress, strain rate and temperature. To describe non-steady state flow behavior, it is necessary to clearly distinguish between the applied stress, σ, on the one hand and one or more structural strength parameters, τ_1, τ_2, ... This provides the following basic framework for constitutive equations

$$\dot{\varepsilon} = f\ (\sigma,\ \tau_1,\ \tau_2,\ \tau_3,\ ....) \quad . \tag{17}$$

The structure parameters τ_1, τ_2, τ_3, ... are presumed to be related to identifiable and measurable features of the dislocation substructure, such as the average dislocation density, the cell or subgrain size, or some other feature of the arrangement of dislocations (pile-ups in the simplest case).

The most universally accepted structure parameter is the average dislocation density, ρ. In PART I of this paper we assumed the dislocation density to be the structure parameter when we used $\tau = \alpha\ Gb\ \sqrt{\rho}$ to characterize the state of a deforming metal. However, in that treatment our interest was restricted to the steady state condition and it was not necessary to write an explicit equation for the creep rate as a function of both σ and τ. Such a relation would represent a general constitutive equation and would in principle be applicable to both steady state and non-steady state behavior.

In the last few years a number of different constitutive equations have been developed and used to describe non-steady state flow properties of metals. The constitutive equation proposed by Hart, Li and their co-workers [38] has received a great deal of attention. Their equation, in its simplest form, includes a single structure parameter that they call the hardness and which is denoted τ in this paper. By studying the functional form of the stress-strain rate relation for load relaxation experiments they concluded that the constitutive relation should take the following form

* The term "constant structure," as used here, refers to one which remains invariant with changes in stress.

$$\dot{\varepsilon} = \frac{\dot{\varepsilon}_o}{(\ln \tau/\sigma)^n} \quad , \tag{18}$$

where $\dot{\varepsilon}_o$ is a function of the hardness or state parameter τ through the equation

$$\dot{\varepsilon}_o = A\tau^n \quad . \tag{19}$$

The key idea of this development is that the hardness τ uniquely characterizes the current structural state of the solid. It does not change in the course of the load relaxation experiment, for example, and all samples having the same hardness would exhibit the very same stress-strain rate relation.

The hardness as conceived by Hart is a scalar state variable. In microscopic terms it is related to the average dislocation density in the usual way. Such a structure parameter does not depend on the direction of deformation and is therefore a scalar quantity. The observation of anelastic back flow on unloading clearly indicates that a single scalar structure parameter is not sufficient to describe the non-steady state flow properties. Thus, more recently Hart [39] has introduced a tensor state variable, a, to account for this kind of behavior.

We noted earlier that the constant structure creep experiment provides the basis for the establishment of constitutive laws. Kocks [40] has suggested that the form of the constitutive law should reflect the way in which dislocations surmount obstacles in their slip plane during deformation. The condition of fixed structure can be considered as a condition of fixed obstacle structure. By considering the statistical aspects of dislocation-obstacle interactions Kocks [41] has shown that the area swept out by a dislocation after being successfully activated past an obstacle is a strong function of both the applied shear stress, τ_{app}, and the shear strength parameter, τ. Following this he suggested a constitutive relation of the form

$$\dot{\varepsilon} = \frac{\dot{\varepsilon}_o}{\{1 - \exp(1 - (\tau/\tau_{app})^2)\}^n} \tag{20}$$

where again $\dot{\varepsilon}_o$ is directly related to the structure parameter τ through

$$\dot{\varepsilon}_o = A\,\tau^n \tag{21}$$

In Kocks' development τ is determined by an evolutionary law which includes both strain hardening and recovery. Research along these lines is continuing.

Perhaps the most elaborate set of constitutive equations for describing non-elastic deformation is that developed by Miller [42,43]. His treatment is one in which the basic forms of the equations are those suggested by physical mechanisms but the constants and in some cases the detailed forms are adjusted so that the equations can describe the observed deformation behavior. For pure metals, two structure parameters are defined and used in the equations: F_{DEF},

an isotropic strength parameter analogous to τ in the present paper and R, a tensor structure parameter included to model back flow effects. The basic form of the equation is

$$\dot{\varepsilon} = B\theta' \left\{ \sinh \left(\frac{\sigma / E - R}{\sqrt{F}_{DEF}} \right)^{1.5} \right\}^n \qquad (22)$$

Both F_{DEF} and R are assumed to be governed by evolutionary laws of the strain hardening/recovery type. This system of equations is called MATMOD on the basis of its use in materials modeling studies. The system of equations being developed can describe a remarkable variety of different kinds of non-steady state flow properties. While the equations and terms are adjusted to fit the experimental data, and thus are not capable of predicting totally new phenomena, the treatment does keep excellent track of the deformation state during complex loading histories. The MATMOD equations often show that seemingly unrelated deformation phenomena can have a common cause. In this way the equations, though empirical, actually lead to improvements in our understanding of the physical mechanisms involved.

ACKNOWLEDGEMENTS

The author wishes to thank his graduate student colleagues at Stanford for their help in the preparation of this manuscript. Discussions with J. C. Gibeling, G. M. Pharr, T. G. Nieh and K. P. Fuchs have been especially helpful. The contributions to this work by Dr. R. Singer and Professor B. Ilschner of the University of Erlangen are also gratefully acknowledged. The work was supported by the Division of Materials Sciences, Office of Basic Energy Sciences, United States Department of Energy.

REFERENCES

1. O. D. Sherby and P. M. Burke, Prog. Mater. Sci., 13, 325 (1968).
2. A. K. Mukherjee, J. E. Bird and J. E. Dorn, ASM Trans. Quart., 62, 155 (1969).
3. A. K. Mukherjee, Treatise on Materials Science and Technology, Ed.: R. J. Arsenault, 6, 169 (1975).
4. S. Takeuchi and A. S. Argon, J. Mat'ls. Sci., 11, 1542 (1976).
5. A. S. Argon (Ed.), Constitutive Equations in Plasticity, MIT Press (1975).
6. F. R. N. Nabarro, Rep. Conf. Strength of Solids, The Physical Society, 75 (1948).
7. C. Herring, J. Appl. Phys., 21, 437 (1950).
8. R. L. Coble, J. Appl. Phys., 34, 1679 (1963).
9. R. . Stevens, Phil. Mag., 23, 265 (1971).
10. W. R. Cannon, Phil. Mag., 25, 1489 (1972).
11. B. Burton, Met. Sci. J., 5, 11 (1971).
12. J. G. Harper and J. E. Dorn, Acta Met., 5, 654 (1957).
13. F. A. Mohamed, K. L. Murty and J. W. Morris, Jr., Met. Trans., 4, 935 (1973).
14. O. D. Sherby, Trans. AIME, 212, 708 (1958).
15. J. Weertman, ASM Trans. Quart., 61, 681 (1968).

16. J. Weertman, Rate Processes in Plastic Deformation of Materials, Eds.: J. C. M. Li and A. K. Mukherjee, ASM (1975), p. 315.
17. R. W. Bailey, J. Inst. Metals, 35, 27 (1926).
18. E. Orowan, J. West Scotland Iron and Steel Inst., 54, 54 (1946-47).
19. J. Friedel, Dislocations, Addison Wesley Inc. (1964), p. 312.
20. C. R. Barrett and O. D. Sherby, Trans. AIME, 233, 1116 (1965).
21. J. Weertman, Trans. AIME, 233, 2069 (1965).
22. R. G. Stang, W. D. Nix and C. R. Barrett, Met. Trans., 4, 1695 (1973).
23. P. J. Wray, Met. Trans., 7A, 1621 (1976).
24. R. L. Stocker and M. F. Ashby, Scripta Met., 7, 115 (1973).
25. J. J. Jonas, Acta Met., 17, 397 (1969).
26. K. Hirano, M. Cohen, B. L. Averbach and N. Ujiiye, Trans. AIME, 227, 950 (1963).
27. S. L. Robinson and O. D. Sherby, Acta Met., 17, 109 (1969).
28. J. R. Spingarn, D. M. Barnett and W. D. Nix (accepted for publication in Acta Met.).
29. E. Hart, Acta Met., 5, 597 (1957).
30. H. E. Evans and G. Knowles, Acta Met., 25, 963 (1977).
31. P. W. Davies, G. Nelmes, K. R. Williams and B. Wilshire, Met. Sci. J., 7, 87 (1973).
32. K. R. Williams and B. Wilshire, Met. Sci. J., 7, 176 (1973).
33. J. D. Parker and B. Wilshire, Met. Sci. J., 9, 248 (1975).
34. J. C. Gibeling and W. D. Nix, Met. Sci. J., 11, 453 (1977).
35. W. Blum, J. Hausselt and G. König, Acta Met., 24, 293 (1976).
36. J. C. Gibeling, Ph.D. Dissertation, Stanford University (1979).
37. C. M. Young, S. L. Robinson and O. D. Sherby, Acta Met., 23, 633 (1975).
38. E. W. Hart, C. Y. Li, H. Yamada and G. L. Wire, Constitutive Equations in Plasticity (A. S. Argon, ed.), MIT Press (1975), p. 149.
39. E. W. Hart, J. Engr. Mat'ls. and Tech., H96, 193 (1976).
40. U. F. Kocks, Constitutive Equations in Plasticity (A. S. Argon, ed.), MIT Press (1975), p. 81.
41. U. F. Kocks, Phil. Mag., 13, 541 (1966).
42. A. K. Miller, J. Engr. Mat'ls and Tech., H96, 97 (1976).
43. A. K. Miller and O. D. Sherby, Acta Met., 26, 289 (1978).

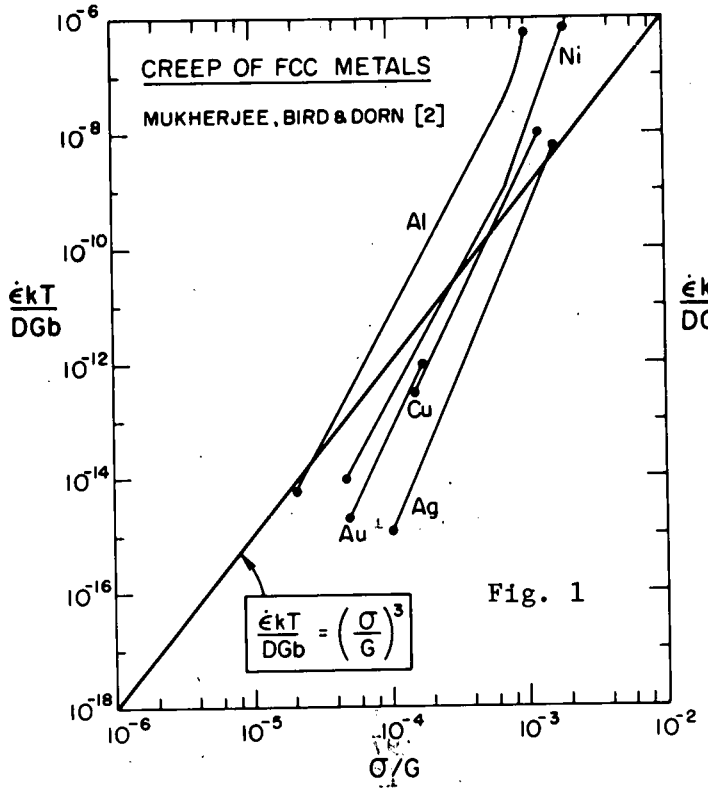

Fig. 1

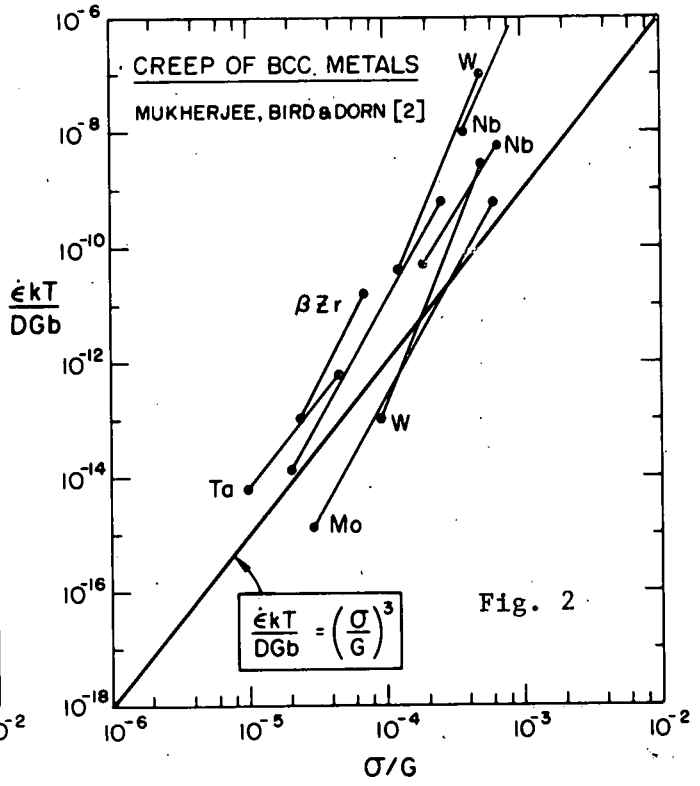

Fig. 2

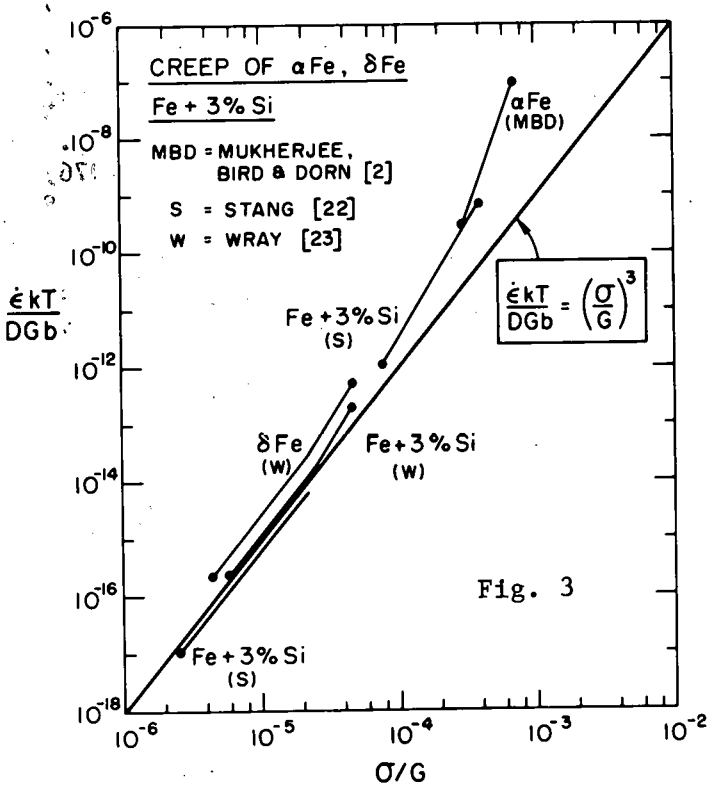

Fig. 3

Comparison of the Natural Creep Law, Eq. (12), with the Creep Properties of FCC and BCC Metals.

DEFORMATION MECHANISMS IN CYCLIC CREEP AND FATIGUE

By

Campbell Laird

Department of Materials Science and Engineering
University of Pennsylvania
Philadelphia, Pennsylvania 19104

ABSTRACT

Service conditions in which static and cyclic loading occur in conjunction are numerous. It is argued that an understanding of cyclic creep and cyclic deformation are necessary both for design and for understanding creep-fatigue fracture. Accordingly a brief, and selective, review of cyclic creep and cyclic deformation at both low and high strain amplitudes is provided. Cyclic loading in conjunction with static loading can lead to creep retardation if cyclic hardening occurs, or creep acceleration if softening occurs. Low strain amplitude cyclic deformation is understood in terms of dislocation loop patch and persistent slip band behavior, high strain deformation in terms of dislocation cell-shuttling models. While interesting advances in these fields have been made in the last few years, the deformation mechanisms are generally poorly understood.

INTRODUCTION

Service conditions in which static and cyclic loading occur in conjunction are quite widespread, so much so that Coffin, in a pioneering paper dealing with the influence of mean stress on shifts in the mechanical hysteresis loops of commercially pure aluminum (1), stated that they were too numerous to mention and refrained from doing so. However, to illustrate that the problem of creep-fatigue touches many aspects of our lives, the following examples, taken from many documented by Miller (2), are cited:

1) High speed aircraft - fluctuating thermal stresses due to speed variations superposed on regular wing loading.

2) Pressure vessels: sustained internal pressure operates in conjunction with cyclic thermal stresses associated with temperature changes in the working fluid.

3) Electrical motors: the conductors are subjected to mechanical and thermal expansive loads.

4) Pressure piping: bimetallic joints subjected to slow temperature cycling create fatigue loading in conjunction with the mean load.

5) Two-phase materials: if such a material bears a service stress, and the coefficients of thermal expansion of the two phases are different, then temperature cycling will cause creep-fatigue loading.

6) Turbine blades: centrifugal loading is combined with the fatigue effects of temperature transients.

In view of these service conditions, it is not surprising that creep-fatigue fracture processes have been the subject of intense investigation (3, 4, 5). Creep-fatigue deformation, however, is a relatively neglected field. While studies of creep deformation and cyclic deformation are numerous, very little cross fertilization has occurred. The neglect of

creep-fatigue deformation is unfortunate because it is difficult to understand many aspects of fracture without understanding the deformation which precedes it and often accompanies it. For example, our present inability to understand crack nucleation in fatigue stems largely from our ignorance (now happily diminishing) of cyclic deformation. Also, it would have been difficult to have confidence in the existence of a fatigue limit in f.c.c. and other types of metals (6), without critical developments in understanding cyclic deformation (for review, see (7)).

One reason for the neglect of creep-fatigue deformation lies in its complexity. Creep deformation operates in many different mechanistic variants, e.g., Herring-Nabarro, Coble, and creep plasticity, (3, 8-11) depending on the conditions, and when these are combined with fatigue, in itself mechanistically complicated enough, also depending on the external and microstructural variables, the sum of the two can be daunting. There is the additional complexity of deciding how the combination should (or does) occur, either in sequence, as Sidey, for example, has conducted his experiments with respect to fracture (12), or Kennedy (3) and Shetty and Meshii(13) with respect to deformation, or simultaneously, as explored by Coffin (1, 14, 15). It is unlikely that any combination would be trivially different from the individual creep and fatigue processes separately. For example, cyclic plasticity can occur at quite low stresses, and Burton has shown that transient diffusional creep by dislocation climb can be significant (16). Under an applied stress (not alternating), diffusion between dislocations acting as vacancy sources and sinks can give rise to a diffusional creep component. This component is in addition to that occurring by diffusion from grain boundary sources to grain boundary sinks. The steady state creep due to climb is usually less than that due to diffusion between boundary sources and sinks. However, since fatigue at low stresses is ideal for producing paired dislocation sources and sinks, it is quite possible that low stress creep-fatigue could lead to creep rates enhanced with respect to those resulting from static creep.

Because the problem of creep-fatigue is so large, an ad hoc approach is probably the most economical. The existing literature emphasizes cyclic creep (creep-fatigue under pulsating tension), and high temperature cyclic deformation (reversed creep plasticity). Accordingly these subjects will be briefly (and selectively) reviewed, along with recent advances in understanding cyclic deformation at room temperature, because the methods developed for them could be useful for understanding cyclic creep, and because they allow speculation about behavior at higher temperatures where creep plasticity could occur. No attempt will be made to review creep deformation (3, 8-11) or cyclic deformation (Instead, see 7, 26, or the references cited in 17).

Plastic Deformation Under Repeated Tensile Loading (CYCLIC CREEP)

In early investigations, the basic aspects of cyclic creep were explored by superimposing a vibratory stress on a static stress (18, 19), and an enhancement of the creep rate was observed when the vibratory stress was applied. Although such an enhancement might be expected if the vibratory stress raises the maximum applied stress, Kennedy et al (20, 21) and Meleka et al (22, 23) demonstrated a rather more surprising result, namely, the creep rate was enhanced when the peak stress of the creep-fatigue experiment equalled that of the static experiment (3). As Kennedy pointed out, such a cyclic creep behavior cannot be predicted from an analysis of the static creep behavior.

Typical behavior can be illustrated from more recent studies, which have served to bring out the complexity of the phenomena. As shown in Figure 1, which applies to Cadmium at 78K studied by Feltner(24), repeated loading causes an enhancement of the creep strain rate. It will be noted that this loading produces a cyclic creep curve which has a number of features common with those of regular static creep curves. Feltner concluded that, in the low temperature range, cyclic creep is cycle dependent, meaning that cylic softening can enhance the creep deformation. Consistent with this conclusion is his observation, shown in Figure 2, that increasing the percent unloading increases the cylic creep rate. The interpretation here is that the greater the unloading, the greater the strain recovery during the unloading, the wider the hysteresis loop, and thus the greater the cyclic softening. The importance of the unloading behavior can be seen from later work by Feltner and Laird (25), who conducted the experiment shown in the inset of Figure 3. Annealed copper polycrystals were strained in tension at 298K to a flow stress of 24 ksi (165.5 MPa) and then, after unloading, were stress cycled well into saturation (i.e., until no further flow stress changes could be detected) by a stress cycle in which the tensile peak was fixed at 15 ksi (103.5 MPa) and, for different specimens, the compressive peak was varied. After cycling, carefully limited so that no incipient fracture process would perturb the results, the specimen was again pulled in tension and the flow stress measured. It will be noted from Figure 3 that, up to a compressive stress of ~ 7 ksi (48 MPa), no softening occurred, but thereafter, as the amplitude of the cycle increased, the amount of cyclic softening also increased. Feltner and Laird (25) measured the plastic strain range (the width of the loop) as the compressive stress was varied. For stresses lower than that necessary to cause softening, they were unable to detect a 'width' of the loop with their apparatus, but at the lowest stress necessary to cause softening, they found that the plastic strain range was 8×10^{-5}. It is intriguing, and possibly not completely fortuitous, that this strain is close to the fatigue limit strain for f.c.c. metals (6). It would be valuable to explore further the unloading strains which occur in cyclic creep, and also the effects of compressive reversals on cyclic creep. Coffin's studies (1, 14, 15) do cover the latter, but for a limited range of stresses and materials.

The cyclic creep behavior of Cd at 300K, is shown in Figure 4. It will be noted that, in contrast to the result at 78K, the static creep rate is higher than the cyclic. Feltner (24) explained the difference by concluding that the deformation is time-dependent (i.e., not cycle dependent) at higher temperatures and he claimed that an increase in the percent unloading results in lower creep rates in the high temperature range. While the effect of the percent unloading does increase at lower temperatures (24), it is noteworthy that the creep rate nevertheless is shown to increase (Figure 2) as the percent unloading increases. Thus, while Feltner's interpretation can be regarded as containing more than a grain of truth, the situation is clearly a great deal more complicated, as still more recent studies, by Shetty and Meshii (13), show.

Typical results by these authors, in apparent conflict with those of Feltner (24), are shown in Figure 5; it appears that cyclic creep is retarded at low temperatures in this case for single crystals. It is not intended to suggest that cyclic stress retardation is characteristic of single crystals only (13), but rather that, in assessing behavior, all the experimental variables have to be considered very carefully and indeed, the behaviors of mono or polycrystalline material are qualitatively similar,

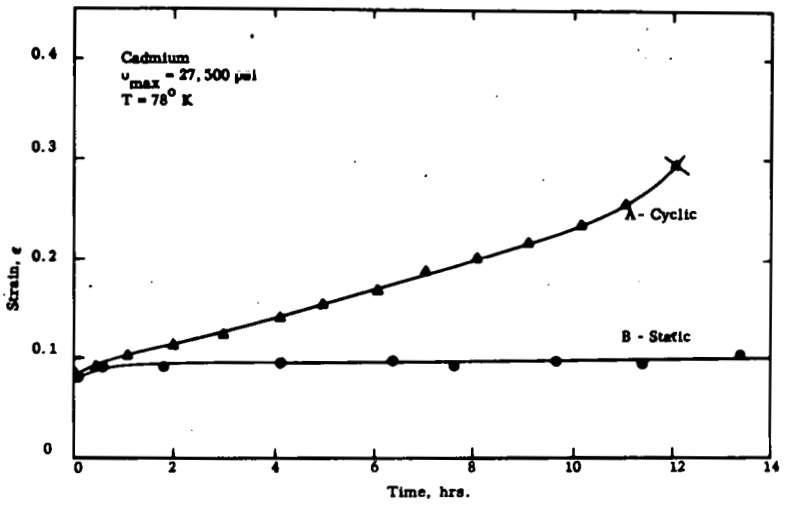

Figure 1

Comparison of the static and cyclic creep behavior of cadmium at 78K, under the same maximum stress, and 100% unloading for the cyclic experiment. Courtesy of Feltner (24).

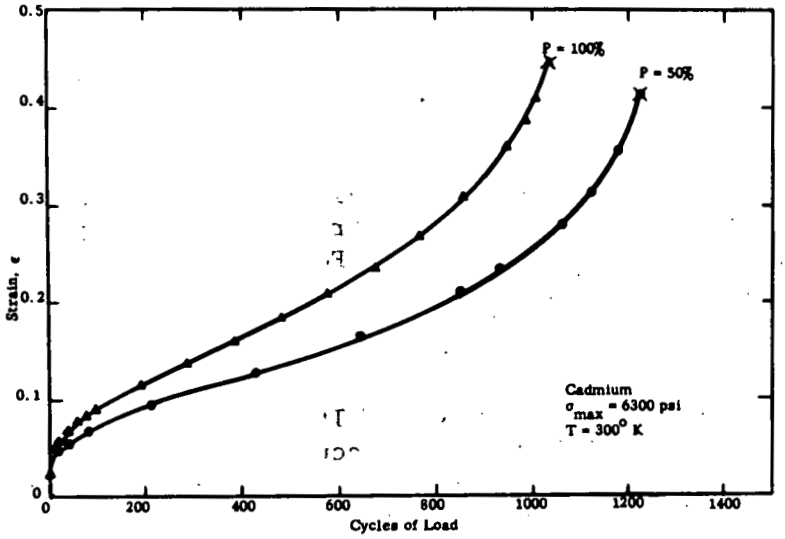

Figure 2

The effect of percent unloading, indicated by P, on the cyclic creep of cadmium at 300K. Courtesy of Feltner (24).

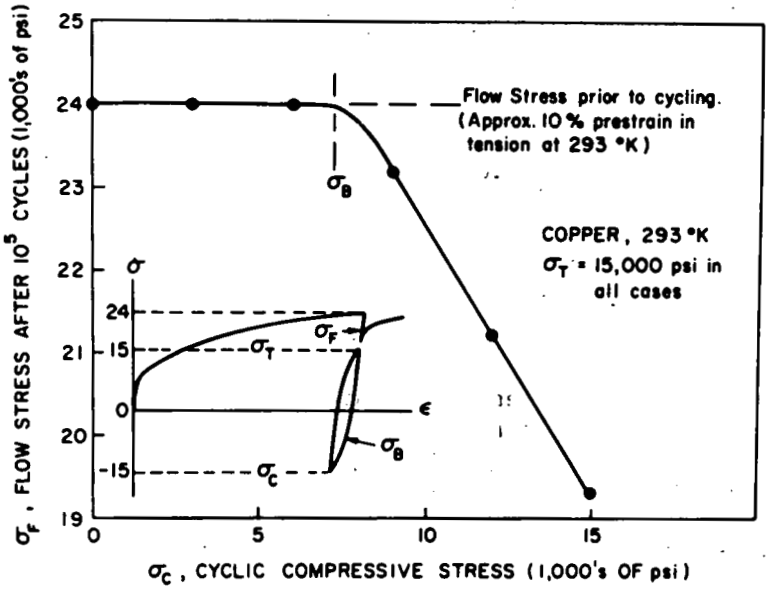

Figure 3

The effect of the magnitude of the compressive stress on the amount of cyclic softening, as measured by the flow stress observed in a tensile test following cycling. The inset shows the way the experiment was conducted, as explained in the text. Courtesy of Feltner and Laird (25), and the editor of Acta Metallurgica.

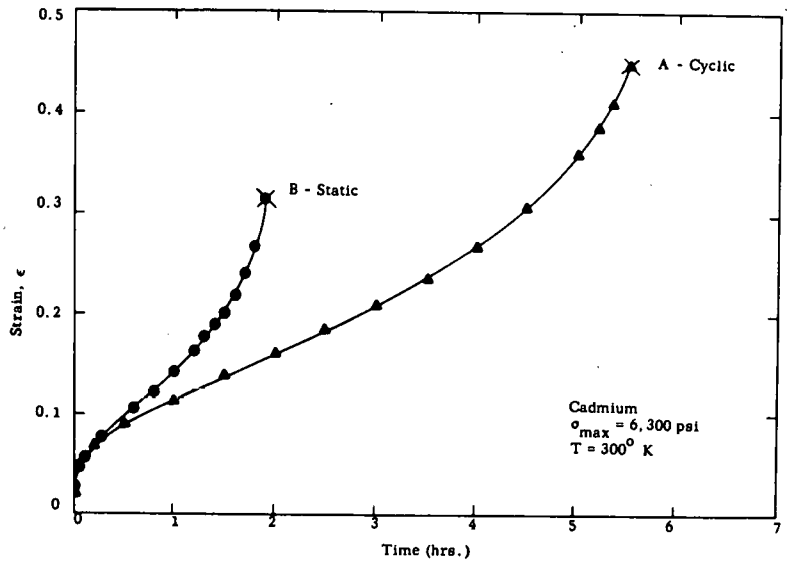

Figure 4

Comparison, similar to that of Figure 1, of the static and cyclic creep behavior of cadmium at 300K. Courtesy of Feltner (24).

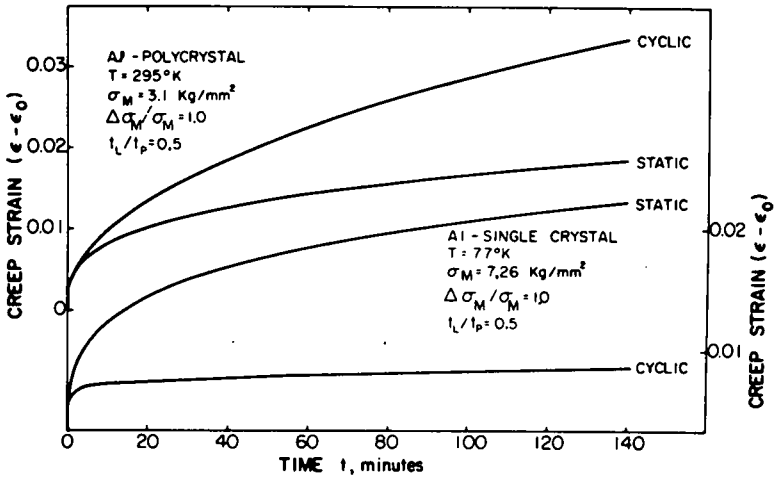

Figure 5

Comparison of the static and cyclic creep behavior of aluminum under different conditions. The pair of cyclic and static creep curves at the top of the figure were obtained for polycrystalline aluminum at 295K and show cyclic stress acceleration. The pair of curves at the bottom indicate the cylcic stress retardation behavior of single crystal aluminum at 77K. Courtesy of Shetty and Meshii (13), and the editors of Met. Trans.

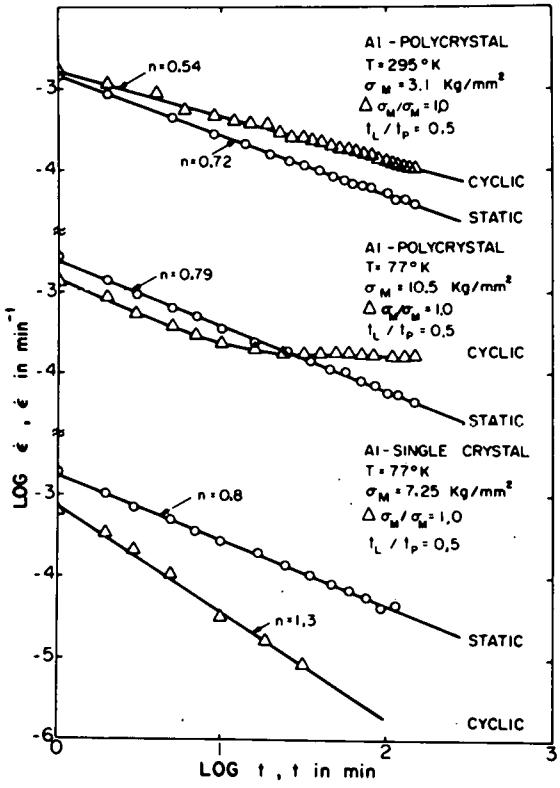

Figure 6

Cyclic and static creep rates vs time on log-log scale for aluminum under various conditions. The power time law is obeyed in all cases except the cyclic creep behavior in the intermediate case, where "cross-over" behavior is observed. Courtesy of Shetty and Meshii (13) and the editor of Met. Trans.

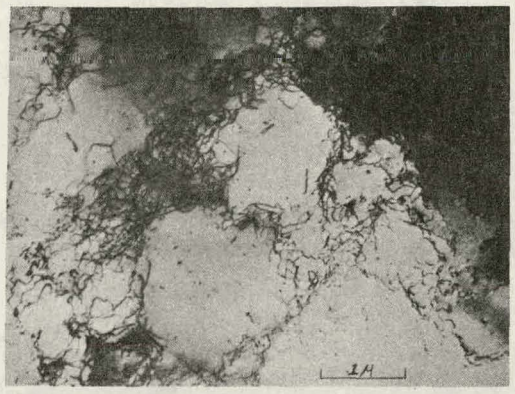

a.

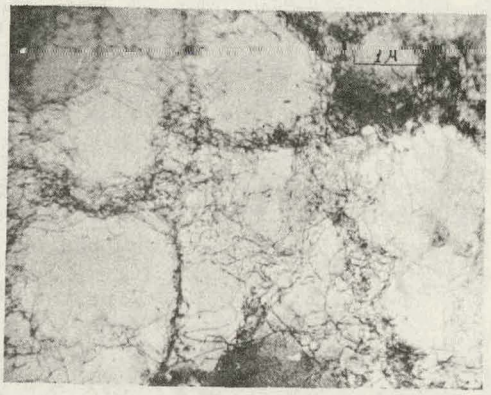

b.

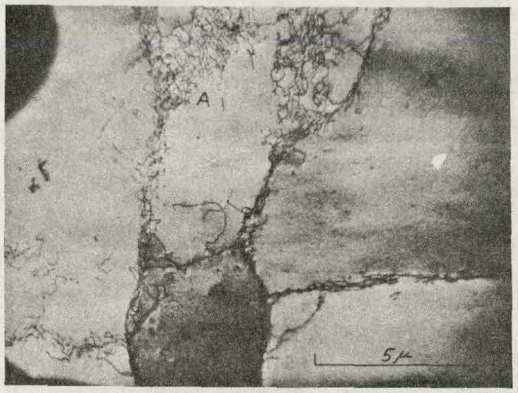

c.

Figure 7

Dislocation arrangements in aluminum after various amounts of cyclic creep: a) one cycle of load to a peak stress of 12 ksi (82.7 MPa) at 78K (10% plastic strain); b) 500 cycles of repeated tension, 12 ksi, at 78K; c) 100,000 cycles of repeated tension, 2 ksi (13.8 MPa) at 300K. Courtesy of Feltner (24).

at least in wavy slip materials (13). Figure 6, also taken from reference (13), shows three pairs of creep rate-time plots for mono and polycrystalline aluminum. It is apparent that the power time law is obeyed in most cases. The pair of plots at the top of the figure corresponds to cyclic stress acceleration while the pair at the bottom describes cyclic stress retardation. An intermediate situation with cross-over behavior is shown in the plots in the middle. Shetty and Meshii (13) interpret this complex behavior by pointing out that stress cycling during creep can cause either cyclic softening or cyclic hardening, and it is possible that their differences from Feltner can be reconciled on this basis. When cyclic softening is the predominant effect of stress cycling, the resulting cyclic creep behavior if cyclic stress acceleration. However, under other conditions, cyclic hardening is caused by stress cycling, and then the cyclic creep behavior is cyclic stress retardation.

Meshii and his co-workers have also studied the cyclic creep of a bcc metal, α-Fe, as influenced by the presence of interstitials (27, 28) but clearly, more work is needed. They have attempted (29, 30) to model cyclic creep semi-quantitatively, employing a back stress idea for explaining creep retardation, and explaining cyclic creep acceleration by homogenization of the internal stresses during cycling.

Precise interpretation of cyclic creep will require a detailed knowledge of the dislocation structures, and to date a very few investigations have been reported. Feltner's early work appears to be one of the most extensive (24). Typical results for aluminum are shown in Figure 7. Comparison of 7a and b shows that the dislocation structures are not typical of those in fatigue because the cells are larger, more misoriented and have more ragged walls than those in fatigue, nor do they appear to change significantly with cycles. Only after many thousands of cycles, 7c, do the walls become

thinner and the cells more marked. However, even these lack the regularity of cells produced by push-pull cycling and they appear more similar to those produced in pure creep deformation. However, the fact that they are 'softer' than those of pure creep has been demonstrated by Bradley et al (31). It would be interesting to correlate such observations with cylic creep retardation and acceleration so that the cyclic hardening and softening ininterpretation could be checked. Turner reports (37) results essentially similar to those of Feltner, but for stainless steel at elevated temperature.

Cyclic Deformation At Low Strains

The attempts by Meshii and his co-workers (29) to explain cyclic creep in terms of internal stress, which are still underway, provide a point of contact with recent developments in cyclic deformation, at low plastic strains. It appears the present custom is to discriminate low strain fatigue from high strain fatigue in terms of the "transition" life, defined as the life associated with a plastic strain at which the elastic strain has an equal magnitude. For strains lower than this, the life is greater than the transition life and the regime of low strain fatigue is defined. A corollary definition can be obtained from a consideration of the cyclic stress-strain curve - the plot of the saturation stress, i.e., when cyclic hardening is completed, required to enforce a given applied plastic strain, against that strain. The cyclic stress-strain curve for copper single crystals is shown in Figure 8, and it is seen to consist of three parts, namely a parabolic component at very low strains, less than 6×10^{-5}, region A, a plateau up to a strain of 7.5×10^{-3}, region B, and a more familiar hardening region C, at greater strains. Regions A & B correspond to low strain fatigue because the lives are greater than 10^5, and the crack nucleation mechanism, region B, is typical of low strain fatigue. It will be noted that data for polycrystalline copper, taken from several different workers, are also plotted in Figure 8. These data have been compared to those for single crystals by use of Taylor's orientation factor and it is extremely interesting that, at the transition life, the plot for polycrystals joins that for monocrystals (33). It is tempting to conclude (33) that the cyclic stress-strain curve for polycrystals also has a plateau and there is evidence for this (33), but the matter is still controversial and more research is needed on low strain behavior. Recent advances concerned with questions of internal stress have emphasized this region, as follows.

The TEM observations of Hancock and Grosskreutz (34) and of Basinski et al (35) make it clear that, prior to saturation, hardening occurs by the mutual trapping of edge dislocations, which gather in bundles, and yield the well known 'veins' in which screw dislocations glide to and fro in response to the strain reversals. The edge dislocation bundles show near-zero deviations in crystallographic orientation, suggesting that the dislocations are accurately paired in sign, and the bundles thus consist of dipolar loop patches. The deformation is homogeneous in these structures and the slip is largely reversible in a mechanical sense. Under these conditions the cyclic plastic strain is not damaging, and the life of the specimen could effectively be infinite (6).

Kuhlmann-Wilsdorf and Laird (36) have recently obtained measurements of the dislocation friction stress, interpreted as Peierls effects, point defect hardening, jog-dragging, etc., and the back stress, associated with these structures, by analyzing cyclic hysteresis loops through a very simple

scheme derived from the remote literature. The well-known method, little used, surprisingly, is illustrated in Figure 9. At the start of the plastic deformation in the cycle (at τ_s), the back stress, τ_β, which was generated in the preceding half-cycle, acts in the same direction as the (now reversed) stress. Therefore, in the presence of a friction stress, τ_F, acting on the dislocations, $\tau_s = \tau_F - \tau_\beta$. At the end of the forward cycle, when the back stress has again reached its maximum value - but now opposed to the deformation - the applied stress is the sum of the friction stress and the back stress: $\tau_E = \tau_F + \tau_\beta$. The friction stress and back stress calculated from these equations and measured from the hysteresis loops of three different investigators, obtained for copper, are shown in Figure 10. The most striking result is that the friction stress and back stress rise is parallel. From this and related analysis, Kuhlmann-Wilsdorf and Laird separate the friction stress into two parts, one equal in magnitude to the back stress (and presumed to have the same physical cause), the other, smaller, part with a different dependence on the number of cycles and saturating earlier than the former (36). The latter part is associated with jog-dragging by the screw dislocations in the channels between the loop patches. The interpretation of the back stress depends critically on whether the loop patches participate in the plastic strain or instead act as rigid barriers to deformation. After an exhaustive examination of this question (37), it is concluded that they undergo strain. Thus Kuhlmann-Wilsdorf treats the loop patches as a Taylor lattice (38), and relates the back stress to that required to flip rows of similarly signed edge dislocations past their dipolar mates. Up to the point of flipping, the strain is reversible and the anelastic motion of the dislocations causes an apparent reduction of the shear modulus. This reduction is shown in Figure 11 and can be seen as considerable. The observed apparent shear modulus can be used, as in Figure 11 (38), to establish the scale and geometry of the dislocation structure in the loop patches, because it is too fine and too complex to be accessible to TEM. Close packing of the dislocations is approximated. Once the dislocations in the rows have flipped past their mates, their motion becomes irreversible and thus "frictional". This explains the connection between the back stress and friction stress.

Kuhlmann-Wilsdorf's theory (38) is open to considerable application, of which an example taken from her paper is shown in Figure 12. The hysteresis loops observed by Mughrabi (17) are shown on the left, and a set of hysteresis loops constructed using her theoretical transformation, for which one experimental loop (cumulative plastic shear strain = 2) is required as a basis, on the right. For the theoretical curves only the tensile parts have been constructed, while the compression parts of the loops have been assumed to be symmetrical to the strain axis. It is well known that there is a slight difference between tensile and compressive parts of loops; nevertheless the agreement between the theoretical and experimental curves is most satisfactory. Thus the Taylor lattice approach yields an impressive constitutive equation.

If the fatigue strain is in the plateau range, the loop patch dislocation mechanisms terminate as saturation is approached, and the general fine slip gives way to the localized slip that produces the "persistent slip band" (PSB). Since this phenomenon causes crack nucleation, PSB's have long been an object of interest in fatigue (for review, see 26). The dislocation mechanism by which loop patches convert to the different dislocation structure of the PSB is still not known. Considerable TEM studies show that PSB's lie parallel to the active slip planes and consist, at ambient

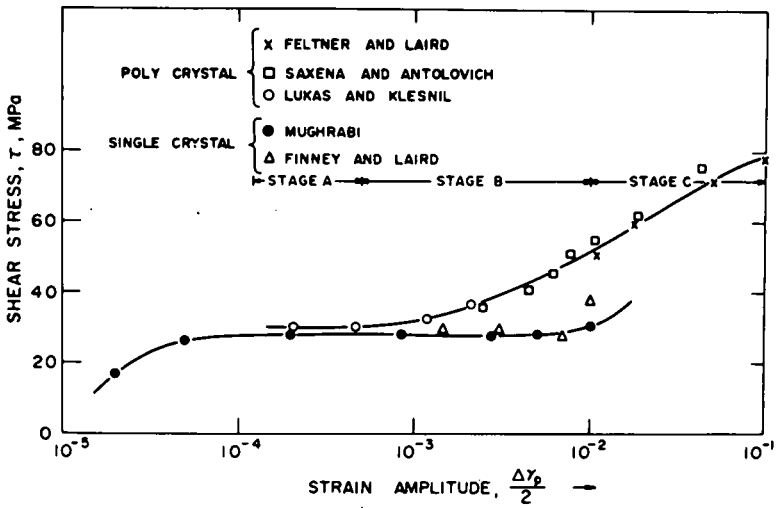

Figure 8

Cyclic stress-strain curves for single and polycrystalline copper. The single crystals show plateau behavior at low strain amplitudes and it is possible that polycrystals do as well. Data are from references 58 to 60 for polycrystals and from 17 and 39 for single crystals. Courtesy of Bhat and Laird (33) and the editors of Scripta Met.

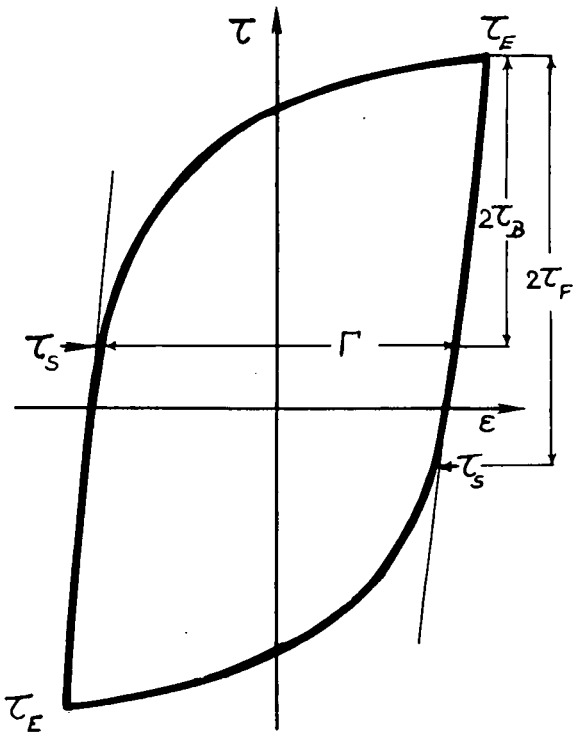

Figure 9

The connection between the yield stress, τ_s, the maximum cyclic stress, τ_E, the friction stress, τ_F, and the back stress, τ_β, derivable as explained in the text. Courtesy of Kuhlmann-Wilsdorf and Laird (36) and the editor of Mat. Sci. Eng.

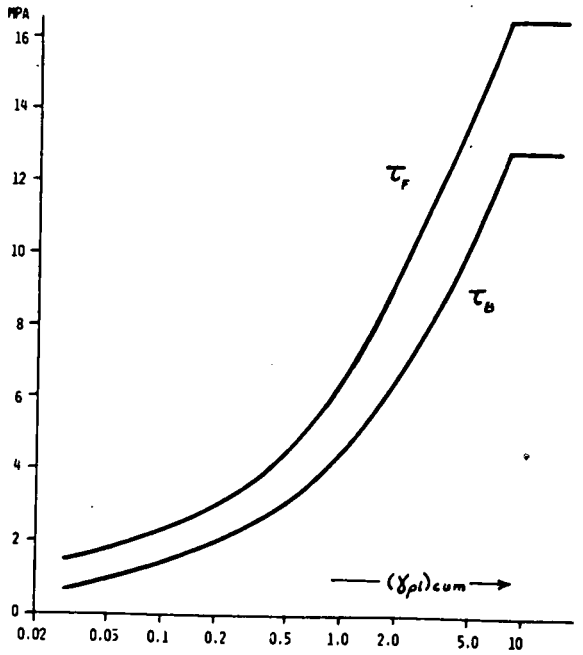

Figure 10

The values of the friction stress, τ_F, and back stress, τ_β, derived in accordance with Figure 9 for copper cycled at a strain typical of the mid-plateau region of the cyclic stress strain curve. Courtesy of Kuhlmann-Wilsdorf and Laird (36) and the editor of Mat. Sci. Eng.

temperature, of narrow hedges of densely packed dislocations, about 1.5 μm apart normal both to the primary Burgers vector and the slip plane, and separated by clear volumes containing a little debris. The hedges are believed to be, primarily, a few layers of dipolar walls, mixed with debris (40), and the strain is carried in the PSB's by screw dislocations moving to and fro with the reversed strain between hedges and coordinated between hedge-rows so as to maintain their dipolar character (40).

A really definitive investigation of time-dependency in connection with the above behavior has never been made, although the available evidence indicates an insignificant frequency effect at ambient temperature. There have been few investigations of cyclic deformation in single crystals above 0.25 of the homologous melting temperature (41), and to this author's knowledge never in a useful orientation, i.e., for single slip. It is possible, however, to speculate on the nature of high temperature behavior from studies of recovery behavior (42, 43). Segall et al (43), having observed loop patches in Cu and Ni, considered the ways in which loops can anneal out. First, if pipe diffusion is easy, the loop can change its shape by breaking up into a series of circular loops, which subsequently anneal out. The second process by which loops may anneal out is directly by self-diffusion. The ends of the loop will tend to become curved, but the radius of curvature will always be less than half the dipole height. Hence vacancies will be emitted preferentially at the curved ends and the loops anneal by becoming shorter, in agreement with the TEM hot-stage observations of Segall et al (43). In view of this, it is extremely unlikely that loop patches could long survive at temperatures much above ambient, even in nickel, especially when one considers that loop patches are neatly paired as vacancy-interstitial loops and self-diffusion sources and sinks are thus available at short distances apart. Evidence for this can be obtained from the work of Nine and Wood (44) who compared the lives of copper single crystals cycled in torsion at $\pm$ 0.003 either at ambient temperature completely, or else first at 573K for large numbers of cycles and then to failure at ambient temperature. Their results are shown in Table I, and most interestingly, pre-cycling at high temperature is shown to increase the subsequent lives at ambient temperature beyond reasonable limits of scatter. The interpretation is as follows. For the torsional strain employed by Nine and Wood, they were probably within the plateau region of the cyclic stress-strain curve at ambient temperature, and thus the strain was concentrated in relatively few PSB's. At high temperature, however, the loop patches would readily convert to cells, of a structure not radically different from that of PSB's. Thus, on subsequent cycling at ambient temperature, the applied strain could be carried by the whole gage section and thus the most damaging local strain was extenuated. This raises the intriguing possibility that, environmental effects aside, the fatigue lives of monocrystals are insensitive to temperature under strain cycling conditions. Unfortunately, this will not be true of polycrystals because strain homogenization promotes grain boundary cracking (45, 46). It is important to note that we are very ignorant of deformation behavior under stress cycling conditions, in spite of some notable contributions at ambient temperature (47-49).

Gasca-Neri and Nix (50) have studied high temperature creep by computer simulation, considering the properties of an array of positive and negative dislocations with a common slip system, and permitting the dislocations to glide and climb. It is unfortunate that this approach has not been applied to cyclic deformation in assessing high temperature properties because it appears very promising.

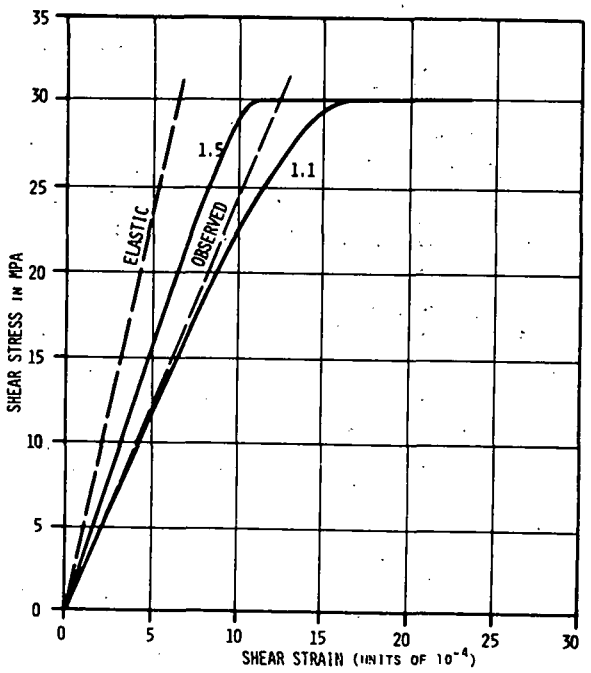

Figure 11
The theoretical shear stress/ shear strain curve for a specimen containing loop patches which occupy 50% of the volume and are surrounded by channels which have a much lower critical shear stress than the loop patches. The ratios of 1.5 and 1.1, as marked, refer to the geometry of the loop patch Taylor lattice, and are obtained from the distance between the dislocations in their rows, to the distance (at right angles) between the rows. The computation assumes the loop patches flip at the saturation stress, and the "observed" curve refers to the hysteresis loops by Finney and Laird (39) in the unloading part of the cycle. Courtesy of D. Kuhlmann-Wilsdorf (38) and the editor of Mat. Sci. Eng.

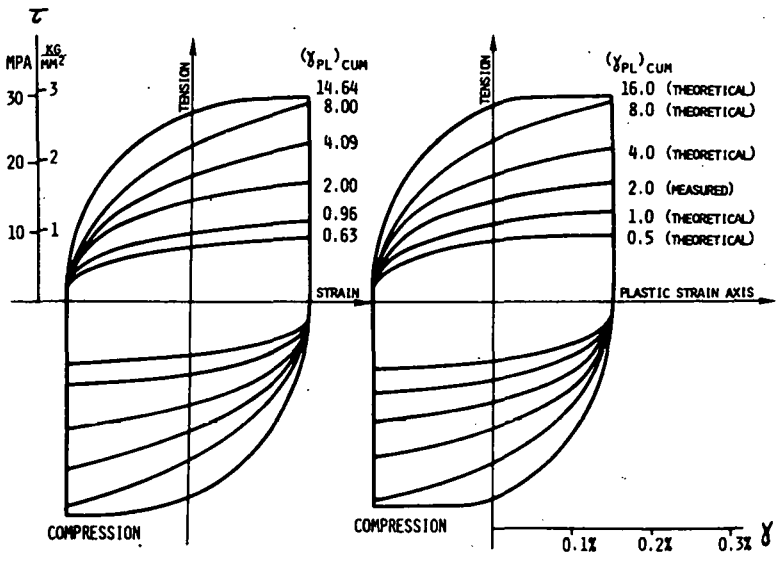

Figure 12
Comparison of Mughrabi's measured hysteresis loops (left) and Kuhlmann-Wilsdorf's theoretically-constructed loops, as explained in the text. Note that Mughrabi appears to have cycled his specimens in plastic strain control so that the loops are recorded with a correction subtracting the quasi-elastic behavior of the loop patches. Courtesy of D. Kuhlmann-Wilsdorf (38) and the editor of Mat. Sci. Eng.

TABLE I

Nine and Wood's Results on Copper Single Crystals (44)

Standing Time at 300C	Precycles at 300C	Subsequent Life at Ambient Temperature
none	none	1.2×10^6
1 hr. in N_2	none	1.2×10^6
1 hr. in Air	none	1.2×10^6
not reported	10^5 in air	6×10^6, 10×10^6
" "	10^5 in N_2	4.2×10^6, 6.8×10^6
" "	3×10^5 in air	5.5×10^6 5.8×10^6
" "	6×10^5 in air	4.5×10^6

Cyclic Deformation At High Strains

At high cyclic strains, irrespective of temperature, dislocation cells are commonly formed in saturation. Depending on the temperature and strain amplitude, rapid hardening is associated with debris formation, often in loop patches. However, most investigations have been carried out on polycrystals and the operation of many slip systems rapidly converts the initial structures into dislocation cells. Typical behavior is shown in Figure 13. Although minor substructural variations do occur for a given amount of cumulative strain, the structures are remarkably regular, and by the time saturation is attained (about 50 cycles for the stainless steel, strain amplitude and temperature illustrated in Figure 13) the cell walls have become quite thin as compared to those in tensile deformation. After saturation is attained, the cell size remains constant but the average misorientation between cells increases. Feltner and Laird (25) proposed that the stress needed to bow out the free mesh length in the wall controls the saturation stress. Nahm et al (51) associate this length with the sub-boundary misorientation network - an unnecessary restriction in this writer's opinion, and contrary to the well substantiated constancy of the saturation stress during life. Thus the strain is carried by dislocations shuttling between the walls. It is possible that dislocations can shuttle in the same manner as within PSB's, in which case the flow stress would depend on the interjog length on the dislocations. However, on this basis, it would be difficult to explain the stress dependence on the strain amplitude. Feltner and Laird (25) also proposed that some of the strain could be carried by dislocation flipping within walls and by overall motion of the walls. The observation that cells enlarge very rapidly with reduction in strain amplitude (25) and consequent cyclic softening supports the latter proposal. Careful TEM studies in single crystals of copper (52) and nickel (53) support the dislocation cell shuttling model, but Excell and Warrington (54) and Imura (55) have also shown sub-boundary migration during creep and tensile testing respectively.

The temperature dependence of the high strain cyclic deformation of fcc metals has recently been explored by Bhat and Laird (56), using nickel as a vehicle. Figure 14 shows that dependence, compared to the dependence of the monotonic deformation, expressed as the UTS, and to the behavior of DS nickel. While the temperature variation of the cyclic stress (saturation stress for plastic strain amplitude = 1%) for nickel has the same general form as the monotonic behavior, there are important differences in detail. Specifically, in cyclic deformation, an athermal region of flow is not observed, and the cyclic stress decreases linearly with increasing temperature until about 0.65 of the melting temperature, at which point it drops precipitously. No quantitative theory has been proposed for this behavior. Bhat and Laird suggest, however, that point defects produced by the cyclic plastic strain, in combination with the effects of defect clusters and jog-dragging, lead to the increased temperature dependence (as compared to monotonic behavior) at temperatures below $0.5\ T_M$ (Bhat and Laird observe rather minor variations in the dislocation structures over this range of temperature). The sharp decrease in flow stress occurring at $0.65\ T_M$ is attributed to recovery processes, and the reason for its occurrence at a higher temperature than observed for monotonic deformation is explained by the observation that dislocations agglomerate in cyclic deformation with evenly balanced signs. Of course, the temperature at which the transition to recovery-dominated behavior occurs is highly strain amplitude dependent, increasing with decrease of amplitude.

One of the more surprising observations made by Bhat and Laird (56) is the inferiority of the cyclic flow stress of DS nickel (associated with 1% strain amplitude) as compared to nickel, between about 400K and 800K. (See Figure 14). This result would have been very hard to accept were it not for Leverant and Sullivan's previous observation that the cyclic stress-strain curves for nickel and T-D nickel were similar at ambient temperature (57). In Bhat and Laird's DS nickel, the processing substructures were different from those of Leverant and Sullivan, and as shown in Figure 14, the DS nickel is stronger than nickel at ambient temperature. It also asserts its superiority, of course, at very high temperature. With increase in temperature in the range 400 - 800K, the rapid fall in the flow stress of DS nickel is extraordinary. Bhat and Laird attributed this behavior to very rapid recovery processes occurring in the dislocation tangles surrounding thoria particles due to short circuit diffusion mechanisms (56). It would be interesting to check these mechanisms by experiments using different strain rates or particle sizes, but no appropriate results have yet been obtained.

CONCLUSIONS

The phenomena of cyclic creep and cyclic deformation have been briefly, and selectively, reviewed. On the basis of this review, the following conclusions can be drawn: 1) The mechanisms of cyclic creep have not been extensively explored; some work exists for stresses giving rise to creep plasticity. The softening which occurs in cyclic creep is not understood (the same problem also applies to cyclic deformation) and there is a great dearth of substructural studies. Bcc metals and alloys are particularly neglected.

2) In the last few years some interesting advances have been made in understanding cyclic deformation, unfortunately only for quite low strains and low temperatures. The necessary fundamental experiments using single crystals are very difficult to do, especially at higher temperatures, and the emphasis on applied research and "relevant" materials during the seventies has been quite damaging for fundamental work. It is astounding that the problems of cyclic creep and fatigue, which have cost the nation and the world many billions of dollars and many lost lives, receive such modest support for fundamental research.

ACKNOWLEDGEMENTS

Helpful discussions with M. Meshii, D. P. Pope, A. P. L. Turner and V. Vitek are gratefully acknowledged. At the time of writing this review, the author received generous support from the ARO, Grant No. DAAG29-78-C-0039, the DMR of the NSF, Grant No. DMR77-13934 and from the Materials Failure thrust area of the Laboratory for Research on the Structure of Matter, University of Pennsylvania, Grant No. DMR76-80994A01.

REFERENCES

1. L. F. Coffin, Trans., A.S.M.E., J. Basic Eng., 86D, 1964, 673.
2. D. R. Miller, Trans., A.S.M.E., J. Basic Eng., 81D, 1959, 190.
3. A. J. Kennedy, "Processes of Creep and Fatigue in Metals", J. Wiley & Sons, New York, 1963.
4. A. H. Meleka, "Combined Creep and Fatigue Properties", Metallurgical Reviews, 7, 1962, 43.

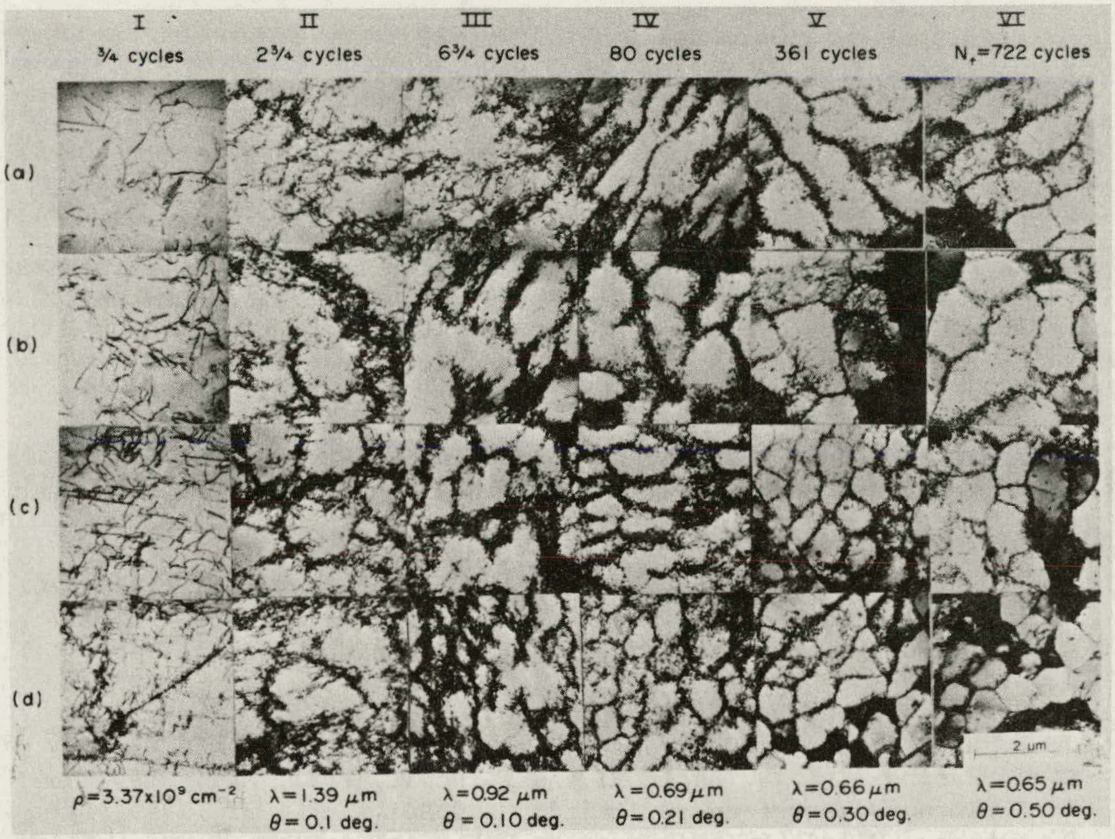

Figure 13 Low cycle fatigue (total strain range ~ 2%) in AISI 304 stainless steel at 649C, showing substructural developments during life. Each column shows the variation in substructure (a-d) that can occur within a given specimen after the indicated number of cycles. λ = sub-boundary intercept size, θ = average misorientation angle between cells. Courtesy of Nahm et al (51) and the editor of Acta Met.

5. "Time-Dependent Fatigue of Structural Alloys", ORNL-5073, Oak Ridge National Lab., Oak Ridge, Tenn., 1977.
6. C. Laird, Mat. Sci. Eng., 22, 1976, 231.
7. C. Laird, in "Work-Hardening in Tension and Fatigue", Ed., A. W. Thompson, AIME, New York, 1977, p150.
8. B. Burton, "Diffusional Creep of Polycrystalline Materials", Trans. Tech Publications, 1977.
9. O. Sherby and P. Burke, Prog. in Mat. Sci., 13, 1968, 325.
10. M. F. Ashby, Surface Sci., 31, 1972, 498.
11. F. Garofalo, "Fundamentals of Creep and Creep Rupture in Metals", MacMillan, New York, 1965.
12. D. Sidey, Mat. Sci. Eng., 33, 1978, 189.
13. D. K. Shetty and M. Meshii, Met. Trans., 6A, 1975, 349.
14. M. H. Raymond and L. F. Coffin, Trans. A.S.M.E., J. Basic Eng., 85D, 1963, 548.
15. L. F. Coffin, Trans. A.S.M.E., J. Basic Eng., 82D, 1960, 671.
16. B. Burton, Mat. Sci. Eng., 18, 1975, 245.

17. H. Mughrabi, Mat. Sci. Eng., 33, 1978, 207.
18. B. J. Lazan, Proc. A.S.T.M., 49, 1949, 757.
19. J. N. Greenwood, Proc. A.S.T.M., 49, 1949, 834.
20. A. J. Kennedy, J. Inst. Met., 87, 1958-59, 145.
21. A. J. Kennedy and N. C. McGill, Nature, 207, 1965, 1086.
22. A. H. Meleka and A. V. Evershed, J. Inst. Met., 88, 1959-60, 411.
23. A. H. Meleka and G. B. Dunn, J. Inst. Met., 88, 1959-60, 407.
24. C. E. Feltner, "Cycle Dependent Deformation Behavior of Close Packed Metals", Tech. Doc. Report, No. RTD-TDR-63-4149, T. & A.M. Dept., Univ. of Illinois, 1963.
25. C. E. Feltner and C. Laird, Acta Met., 15, 1967, 1632.
26. C. Laird, in "Fatigue and Microstructure", ASM Seminar, St. Louis, 1978, in press.
27. D. K. Shetty and M. Meshii, Mat. Sci. Eng., 32, 1977, 283.
28. A. K. Vasudevan and M. Meshii, Proceedings, 2nd Int. Conf. on Mech. Behavior of Materials (ICM-II), Boston, Mass., 1976, p518.
29. T. Mura, A. Novakovic and M. Meshii, Mat. Sci. Eng., 17, 1975, 221.
30. D. K. Shetty, T. Mura and M. Meshii, Mat. Sci. Eng., 17, 1975, 261.
31. W. L. Bradley, S. W. Nam, and D. W. Matlock, Met. Trans. 7A, 1976, 425.
32. A. P. L. Turner, Private Communication, Argonne National Lab., Illinois, 1979.
33. S. P. Bhat and C. Laird, Scripta Met., 12, 1978, 687.
34. J. R. Hancock and J. C. Grosskreutz, Acta Met., 17, 1969, 77.
35. S. J. Basinski, Z. S. Basinski and A. Howie, Phil. Mag., 19, 1969, 899.
36. D. Kuhlmann-Wilsdorf and C. Laird, Mat. Sci. Eng., 37, 1979, 111.
37. D. Kuhlmann-Wilsdorf, "Dislocation Behavior in Fatigue, Part III", Mat. Sci. Eng., in press, 1979.
38. D. Kuhlmann-Wilsdorf, "Dislocation Behavior in Fatigue, Part IV", Mat. Sci. Eng., in press, 1979.
39. J. M. Finney and C. Laird, Phil. Mag., 31, 1975, 339.
40. D. Kuhlmann-Wilsdorf and C. Laird, Mat. Sci. Eng., 21, 1977, 137.
41. C. E. Feltner, Phil. Mag., 12, 1965, 1229.
42. J. C. M. Li, in "Recrystallization, Grain Growth and Textures", ASM, 1966, 45.
43. R. L. Segall, P. G. Partridge and P. B. Hirsch, Phil. Mag., 6, 1961, 1493.
44. H. D. Nine and W. A. Wood, J. Inst. Met., 95, 1967, 252.
45. W. H. Kim and C. Laird, Acta Met., 26, 1978, 777.
46. W. H. Kim and C. Laird, Acta Met., 26, 1978, 788.
47. P. O. Kettunen, Proc. 2nd Int. Conf. on Strength of Metals and Alloys, ASM, 1970.
48. P. O. Kettunen and U. F. Kocks, Scripta Met., 1, 1967, 13.
49. P. O. Kettunen and U. F. Kocks, Acta Met., 20, 1972, 95.
50. R. Gasca-Neri and W. D. Nix, Mat. Sci. Eng., 14, 1974, 131; Acta Met., 22, 1974, 257.
51. H. Nahm, J. Moteff and D. R. Diercks, Acta Met., 25, 1977, 107.
52. H. Mughrabi, in Proc. 3rd Int. Conf. on the Strength of Metals and Alloys, Vol. 1, 1973, p407, Cambridge, UK.
53. H. Saka, K. Noda, K. Masumoto and T. Imura, Scripta Met., 10, 1976, 29.
54. S. F. Excell and D. H. Warrington, Phil. Mag., 26, 1972, 1121.
55. T. Imura, in "Electron Microscopy and Structure of Materials", Ed., G. Thomas, Univ. Calif. Press, Berkeley, 1972.
56. S. P. Bhat and C. Laird, Fatigue of Eng. Materials and Structures, 1979, in press.

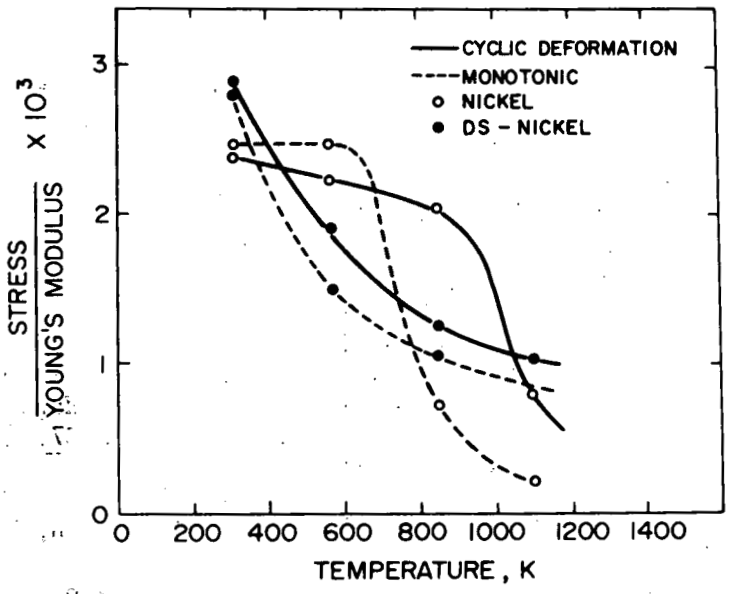

Figure 14 Comparison of the temperature dependence of the saturated cyclic flow stress (for 1% strain amplitude) and the UTS of Ni-200 and DS nickel. Courtesy of Bhat and Laird (56) and the editor of "Fatigue of Engineering Materials and Structures".

57. G. R. Leverant and C. P. Sullivan, Trans. A.I.M.E., 242, 1968, 2347.
58. C. E. Feltner and C. Laird, Acta Met., 15, 1967, 1621.
59. P. Lukáš and M. Klesnil, Mat. Sci. Eng., 11, 1973, 345.
60. A. Saxena and S. Antolovich, Met. Trans., 6A, 1975, 1809.

STRESS RUPTURE IN METALS AND CERAMICS*

Rishi Raj
Department of Materials Science and Engineering
Bard Hall
Cornell University
Ithaca, NY 14853

ABSTRACT

The mechanisms of nucleation and growth of cavities in grain boundaries in metals and ceramics are reviewed. A stress and time condition for nucleation is derived and it is suggested that the junctions of three interfaces such as those formed between inclusions and grain boundaries are the most probable sites for nucleation. Growth of cavities by diffusion also leads to a stress and time condition for failure. Both grain boundary and surface diffusion enter into the fracture equation. In metals, cavities can also grow by power law creep for which a strain and strain rate condition for fracture is obtained. In those ceramic materials, which contain a glass phase in the grain boundaries, the fracture process is dominated by the viscous flow of the glass and the formation of cavities in the glass phase. There is considerable opportunity for new micro-mechanical-modelling and experimental work in ceramic materials which could lead to the design of new ceramics with unusual properties such as superplasticity. In metals, the influence of environment, multiaxial stresses, and notches on cavitation are recommended as topics for further research.

*Report No: 4092 issued by the Materials Science Center, Cornell University.

INTRODUCTION

(a) General

Most metals and alloys suffer from a ductility minimum at about half the melting temperature.[1,2] This is quite surprising because ductile fracture at low temperature bears certain similarities to fracture at elevated temperature. In both instances fracture occurs by the initiation and growth of cavities which form at second phase particles;* the main difference being that at low temperature cavities form at all particles whereas at elevated temperature they form at only those particles which are present in the grain boundaries. Still, if the mechanisms of cavity nucleation and growth were the same one would expect the ductility to increase, not decrease, as the temperature is raised. We must therefore, consider effects which operate only at high temperature, the obvious ones being grain boundary diffusion, surface diffusion, and grain boundary sliding. The mechanisms of high temperature fracture in this report are interpreted in terms of these phenomena. Another important factor is that metal flow becomes strain rate sensitive at high temperatures; this is reflected in the ductility of metal, and hence must in some way affect the cavity growth process.

It should be mentioned that there is a vast amount of published work in this area and many different effects have been reported which will not be covered here. For example: cavitation in Mg is more profuse under high frequency cyclic loading,[3] grain boundaries migrate and assume a preferred orientation,[4] and boundaries become faceted during stress rupture.[5] The last point is quite important because it offers an opportunity to relate cavitation to the structure of the boundaries. The cavities appear to form at the tip of the asperities in the faceted boundary, and in my view, they form after the boundary has become faceted. These special effects are more commonly observed in single phase metals rather than in engineering alloys in which the grain boundaries are heavily decorated with second phase precipitates.

(b) Fracture modes: metallographic evidence

In a stress rupture test a dead weight load is applied, and the time to fracture and the creep curve are measured. The creep curve yields the secondary creep rate, $\dot{\varepsilon}_s$. A plot of $\ln(1/\dot{\varepsilon}_s)$ and $\ln(t_f)$ vs $\ln(\sigma)$ for a model copper-silica alloy is shown in Fig. 1.[6] Essentially three modes of fracture were observed. At low stresses failure occurred due to numerous cavities (Fig. 2a) which formed preferentially on those boundaries which were aligned normal to the tensile axis. At very high stresses, dynamic recrystallization (Fig. 2c) preempted cavity formation, and one hundred percent ducility was achieved. There was a transition at intermediate stresses where the failure process was distinctly different. In this instance wedge shaped "cracks" formed as shown in Fig. 2b. In the present experiments[6] the wedge cracks form predominantly near the surface but they can also form everywhere as shown in Fig. 3.

*High temperature fracture is often caused by cavity nucleation at second phase particles, but not always.

(c) "r" and "w" type cavities

The observations reported in Figs. 1 and 2 apply generally to most materials i.e. at low stresses failure occurs by the formation of cavities on grain boundaries which are aligned normal to the tensile axis ("r" type) whereas at the higher stresses wedge cracking dominates. The relative regions of strain rate and temperature in which one or the other mechanism dominates varies from material to material. But generally, in those materials which contain a small area fraction of second phase particles in the grain boundary, and in which the grain matrix is quite creep resistant (monel is a good example), wedge type of cracking is more prevalent. Normally, materials which show extensive wedge-cracking are also prone to exhibit notch sensitivity.

There is firm evidence that in r type cavitation, cavities form at second phase particles as shown in Fig. 4, although suggestions have been made that they may also form at ledges in the grain boundary.[8] In single phase materials they do appear to form at the asperities in boundaries which have become faceted during the creep process (see Fig. 5). There are suggestions in the literature that obstruction of sliding at particles and ledges contributes to the nucleation of r type cavities[9] but there is no metallographic evidence for this, and theoretical analysis does not support the idea.[10] On the other hand, there is abundant metallographic evidence that sliding is an important factor in wedge crack formation. The initiation and growth of wedge cracks is probably promoted by the stress concentration produced by sliding at triple grain junctions and by the accommodation of sliding by crack opening rather than by diffusion or power law creep. The opening of cavities at particles just ahead of the crack tip[11] may also play an important part in some materials.[12]

(c) Summary of this report

This report will deal primarily with mechanisms of nucleation and growth of r type cavities. Nucleation will be described in terms of formation of supercritical vacancy clusters at heterogenous nucleation sites. Growth will be described in terms of grain boundary and surface diffusion and power law creep coupled with diffusion. Models will be supported by experimental evidence. The details will be omitted because they are available in published literature. Wedge cracking is included as one of the "unsolved" problems since in the author's opinion a satisfactory explanation is not yet available.

NUCLEATION OF CAVITIES AT SECOND PHASE PARTICLES IN GRAIN BOUNDARIES

(a) Essential difference between low temperature and high temperature nucleation

In low temperature ductile fracture considerable plastic strain must be exerted before cavities are seen to form at second phase particles. Palmer and Smith[13] found that they needed about 10% strain in copper silica. Im and Argon[14] needed more than 20% strain in speriodised steel. In contrast, in long term creep experiments with a copper-chromium alloy, Fleck et al.[15]

determined that cavities nucleated at a stress much lower than the yield stress provided that an incubation period was allowed. In fact in their experiments cavities nucleated after such a long waiting period that the development of stress concentrations at particles due to sliding could be ruled out.[10,16] A further observation is that whereas cavities initiate at all particles in low temperature deformation, they nucleate selectively at those which are present in the grain boundaries at elevated temperature. A reasonable conclusion in view of the above information is that the mechanism of cavity nucleation is quite different at high and low temperatures.

(b) Threshold stress for nucleation

In the mechanism being proposed, vacancies condense to form a cavity of supercritical size under the influence of a tensile stress applied normal to the grain boundary.[10] By this mechanism nucleation is most probable at a site where, for a given value of the applied normal traction, σ_n, the volume of the critical cavity is the minimum. As an example the nucleation of a cavity, for a fixed value of σ_n, at four different possible sites: within the grain matrix, at two grain junctions, at a particle matrix interface, and at the triple junction where grain boundary and particle meet, is shown in Fig. 6. The radius of curvature of the surface, in each case, is the same:

$$r_c = \frac{2\gamma}{\sigma_n} \qquad (1)$$

The volume of the cavity is determined by the equilibrium between various interface tensions. The fourth case leads to the lowest volume and is therefore the most probable. The volume of the critical cavity, in this case, is defined in terms of r_c, and the interface energy angles α, β, and μ as shown in Fig. 7. If γ and γ_I are the specific surface energies for the free surface of the matrix and particle, respectively, and γ_B and γ_{IB} are the respective values for the matrix-grain boundary and particle-matrix interface, then $\cos\alpha = \gamma_B/2\gamma$, $\cos\beta = (\gamma_{IB} - \gamma_I)/\gamma$ and $\cos\mu = \gamma_B/2\gamma_{IB}$.[10]

The steady state rate of nucleation by this mechanism leads to:

$$\dot{\rho} = \frac{4\pi\gamma}{\sigma_n\Omega} \frac{\delta D_B}{\Omega^{1/3}} \rho_{max} \exp\left(-\frac{r_c^3 F_v \sigma_n}{2kT}\right) \qquad (2)$$

where ρ_{max} is the maximum density of nucleation sites, Ω is the atomic volume, δ is the boundary width and D_B the boundary diffusion coefficient, and $r_c^3 F_v$ is the volume of the critical cavity where F_v is function of α, β and μ. Eq. 2 depends very strongly on σ_n so that when ρ is plotted against σ_n, one obtains an appearance of a threshold stress, σ_{th}, which we assume is that stress at which Eq. 2 provides a nucleation rate of 1 s^{-1}. The dependence of σ_{th} with γ_{IB} is shown in Fig. 8. Note that $(\gamma_{IB} - \gamma - \gamma_B)$ is a measure of the bonding between the particle and the matrix; when it goes to zero the matrix does not wet the particle and the nucleation stress as well as the ideal strength of the interface reduce to zero. At finite bonding, however, note that nucleation by the kinetic process can occur at a stress much lower than the ideal strength of the interface.

It is difficult to compare this model with quantitative measurements of nucleation since the interface energies are usually not known, but it is significant that the site proposed by this model (Fig. 7) has almost always been the site where cavities have been observed.[15,17] The model also gives a reasonable explanation why cavities can form at very low applied stresses at elevated temperature.

(c) Incubation time for nucleation

The expression in Eq. 2 gives the steady state rate of nucleation. It is more sensitive to stress than to temperature. We expect, though, that temperature plays a critical role since if the vacancies cannot diffuse rapidly then the clusters will not grow and the steady state will not be reached in a reasonable period of time. This leads to the concept of an incubation period for the formation of clusters of critical size. There is a net growth of clusters towards the critical size with time, even though the free energy favors dissociation, simply because at any one instant the concentration of clusters which are likely to gain one vacancy is much larger than the concentration of clusters which are one vacancy larger. The result is that the higher probability of dissociation of the larger cluster is more than offset by the greater concentration of the smaller clusters. Thus, as time progresses, some clusters grow larger until the critical size is reached. The incubation time for this process is difficult to calculate but a lower bound can be calculated assuming that the probability is unity for association and zero for dissociation. This leads to the following expression for incubation time:[10]

$$t_i = \frac{r_c^3 F_v}{4\delta D_B} \qquad (3)$$

Data for comparison with the above equation is almost non-existent. A comparison with two data points with the work of Fleck et al., shows that Eq. 3 underestimates the incubation time by nearly eight orders of magnitude. This may appear unreasonable but it is not out of the question in view of the approximations made. It points toward the need for computer simulation of the atom by atom events which lead to the growth of clusters in a two dimensional interface. There is also a need for more experimental work aimed at studying nucleation specifically.

(d) Discussion

If the model described above is a valid one, then it means that a combination of stress and time is needed for cavity nucleation. When stress concentrations develop in a creeping solid, for example by the obstruction of grain boundary sliding at particle and triple grain junctions, or in the regions of crack tips, they are usually transient. Therefore, it may happen than large stress concentrations arise but do not persist for a long enough time for nucleation to be completed. Successful nucleation would depend upon the relative kinetics of nucleation and stress relief.

(a) Grain boundary diffusion controlled growth

One of the mechanisms by which cavities can grow at elevated temperature is the transport of atoms from the cavity surface to the adjacent grain boundary. The driving force for this process arises from the gradient in the normal traction at the interfaces.[18] Diffusion can occur simultaneously through the lattice and along the grain boundary, but in most problems of interest i.e. for cavity spacing of less than 10 μm and temperature in the range $0.4\text{-}0.7T_m$, grain boundary diffusion dominates. The growth of the cavities was first calculated by Hull and Rimmer and later by Speight and Harris[20] with the assumption that the cavities are of a spherical shape. In a more complete approach, shown in Fig. 9, the cavities are assumed to grow in their equilibrium, lenticular shape. First the volumetric growth rate of the cavities is calculated in terms of the diffusion, compatability and equilibrium equations. This is translated into a growth rate for grain boundary damage (area fraction of separated boundary) by assuming the cavity to have an equilibrium shape. The damage function is integrated to yield an expression for time to fracture:[21,22]

$$t_f = 0.006 \frac{\lambda^3}{\delta D_B} \frac{kT}{\sigma_\infty \Omega} \tag{4}$$

here σ_∞ is the remote tensile stress applied normal to the grain boundary and λ is the average spacing between the cavities. Provided that growth (rather than nucleation)is the rate controlling step in fracture, Eq. 4 provides a simple answer to failure prediction. In reality the situation seems more complicated, partly because the grain boundary diffusion coefficients in engineering materials are not well characterized, and partly because of hereto ununderstood problems. This is discussed later.

(b) Role of surface diffusion

When cavities are growing by grain boundary diffusion, the atoms are removed from where the cavity meets the boundary i.e. the triple junction. Surface diffusion is then responsible for restoring the cavity to its equilibrium shape; if it is not fast enough then the cavity will become elongated along the grain boundary. This would reduce the time to fracture relative to Eq. 4 because the same volume of cavity will now occupy a larger boundary area. This problem has been studied in detail by Chuang and Rice[23] et al.[24] Some of their results are summarized here. The transition from quasi-equilibrium to crack-like growth of cavities occurs when:

$$\frac{kT}{\Omega\gamma} \cdot \frac{r_B^3 v}{\delta_s D_s} > 24 \tag{5}$$

where v is the radial growth velocity of the cavity in the boundary plane, γ is the surface energy, δ_s is the width of the surface diffusion layer and D_s is the surface diffusion coefficient. In the crack like mode the time to fracture is given by:

$$t_f' = 0.015 \frac{\lambda^4 kT}{\delta_s D_s \Omega \gamma} \cdot H\left(\frac{2r_B}{\lambda}\right) \left[\frac{\delta_s D_s / \delta D_B}{(1 + C)^{1/2} - 1}\right]^3 \quad (6)$$

where

$$C = 0.4 \frac{\sigma_\infty \lambda}{\gamma \mathrm{Sin}\ \alpha/2} \frac{\delta_s D_s}{\delta D_B} \quad (7)$$

Here r_B and $\lambda = 2\ell$ are shown in Fig. 9. In Eq. 5, $H\left(\frac{2r_B}{\lambda}\right)$ is a fourth degree polynomial and will normally be of order one. There are two interesting limits to Eq. 6 and 7: a) when $C << 1$ then the equation depends only upon D_s and varies inversly as the third power of σ_∞ , and b) when $C >> 1$, then t_f depends on both D_B and D_s and varies as the 3/2 power of σ_∞. Chuang et al.[24] find that in most practical instances case (b) would apply and in this case the relative magnitudes of fracture time according to Eqs. 6, 7 and 4 is given by (assuming a nominal value of 0.25 for $2r_B/\lambda$):

$$\frac{t_f'}{t_f} = 0.5 \left(\frac{\sigma_\infty \lambda}{\gamma} \frac{\delta D_B}{\delta_s D_s}\right)^{1/2} \quad (8)$$

This factor will be only weakly temperature dependent and more strongly dependent on σ_∞. As a result it may be more important in hard materials such as nickel base superalloys and ceramics where diffusion mechanisms should dominate up to a higher value of the applied stresses.

It is interesting to study the transition at which a switch to the crack-like growth is predicted. Approximately, we assume the velocity to be equal to half the cavity spacing divided by the time to fracture for quasi-equilibrium growth (Eq. 4). We then obtain the following condition in lieu of Eq. 5:

$$\frac{\delta D_B}{\delta_s D_s} \cdot \frac{r_B^3 \sigma_\infty}{\lambda^2 \gamma} > 0.3 \quad (9)$$

The interesting point is that when the cavities are small and widely spaced (small r_B and large λ) the equilibrium growth is favored. It may be that in their entire lifetime, the cavities grow in the equilibrium shape when they are small and in the crack like mode when they are larger.

(c) Experimental evidence

In the diffusion controlled models for fracture, the time to failure is either boundary diffusion controlled or surface diffusion controlled. In the first case the stress dependence ranges from linear to a power of 1.5, while in the second it has a power of three. Provided that the diffusion coefficients are known, quantitative comparison between theory and experiment can be made. There is good experimental evidence for both cases. In the first case, experiments with bicrystals of copper in which the cavities nucleated at oxide particles yielded good quantitative agreement with Eq. 4 as shown in Figure 10.[25] When correction is made according to Eq. 8, the agreement is even better.[24] Agreement with surface diffusion controlled crack like growth of cavities (Eq. 6 case (a)) was demonstrated nicely by Goods and Nix[26] in silver in which steam bubbles had been introduced in the grain boundaries. The agreement was good even though the criterion for crack-like growth ($C \ll 1$, Eqs. 6 and 7) was not satisfied.

There is also some data in creep fracture studies in ceramics in which the linear stress dependence for time to fracture is obeyed.[32] But in most of the data on polycrystals in metals, fracture time varies with time and temperature in the same manner as the secondary creep rate. This has led to the following expression due to Monkman and Grant:[28]

$$\dot{\varepsilon}_s t_f = \text{constant} \tag{10}$$

The wide applicability of the above equation to experimental data raises the possibility that cavities grow by the same process by which the matrix creeps, that is power law creep. This will be discussed further in the next section.

(d) Diffusion controlled growth in metal polycrystals--a dilemma

There are at least three examples in the literature where the time to fracture of face-centered-cubic metal polycrystals is described by power law creep (Eq. 10) even though the diffusion equation (Eq. 4) predicts a value for t_f which is several orders of magnitude shorter. In all cases, the cavities were already present so that nucleation was not causing the delay in fracture. In one case[29] the cavities were introduced by prestraining followed by annealing, in the second[6] the cavities were seen to have formed before the onset of secondary creep, and in the third case the cavities which consisted of He bubbles were formed in Ni-8%W by neutron irradiation.[30] The comparison of the measured and the calculated fracture times for the last case is shown in Fig. 11; the discrepancy here is the least amongst all three cases. The grain boundary diffusion data for the calculation of the theoretical curve was taken from pure nickel; it is possible that in engineering materials the diffusion may be slower which causes the discrepancy but in the author's opinion this is probably not the case since the same discrepancy seems to arise in the copper silica work[6] in which the diffusion coefficients are known to within an order of magnitude from internal friction[31] and bicrystal fracture[25] experiments.

The inference is that diffusion controlled fracture operates in bicrystals[25] but not in fcc metal polycrystals[6] of the same material. Why this

is so is not clear. In my own view, it stems from the difficulty in transporting matter across the triple junction (it is necessary to do so in order to redistribute stress and achieve a steady state) because matter can be transported only by the climb of grain boundary dislocations. Thus there is a barrier to the dissociation of dislocations at the triple junctions. The strength of this barrier would vary from material to material. For example, we find that in polycrystals of Al_2O_3 there is good agreement with diffusion controlled fracture.(32,33)

If incompatability at triple junctions is the cause of the inhibition of diffusional cavity growth in fcc metal polycrystals under uniaxial stress, the problem should not arise under hydrostatic tension since then cavities can grow equally at all grain boundaries.(25) This aspect of diffusional cavity growth needs to be studied further since, if true, the diffusional mechanism may be quite important in the growth of cavities near notches and crack tips under plane strain conditions.

APPARENT CAVITY GROWTH BY POWER LAW CREEP

In a systematic study of stress rupture in copper-silica alloys in which the particle content was varied, the applicability of Monkman Grant relation (Eq. 10) was confirmed over a wide range of stress, temperature, and microstructure. A semi-empirical model for growth of an array of cavities by power law creep ($\dot{\varepsilon}_s = A\sigma^n$) was developed which incorporated the cavity spacing and the strain rate sensitivity, $m = 1/n$, as the important parameters.(6) Cavities grow in the boundary plane because they interact with their neighbors thus creating hydrostatic tension stress in the regions in between. The importance of hydrostatic stress in cavity growth has been well recognized in ductile fracture.(34,35) Theoretically, the cavities can grow and link purely by the power law creep mechanism although it is possible to conceive of mechanisms whereby diffusion can accelerate the process. For example, as strain accumulates, the cavities would tend to become elongated in the straining direction thus reducing the triaxiality. If surface diffusion continuously restores the cavities to their equilibrium lenticular shape then it would promote cavity transverse cavity growth by increasing the grain boundary area occupied by the cavity for the same cavity volume, and also by increasing the triaxial stress. Models which couple diffusion and power law creep to explain cavity growth are currently under development. In the meanwhile the semi-empirical equation of Pavinich and Raj(6) provides a reasonable estimate of Monkman Grant ductility in many engineering materials:(6)

$$\dot{\varepsilon}_s t_f = \frac{0.23\ \lambda}{d}\ e^{\frac{4m}{1-m}}$$

Here where λ is the cavity spacing (also the particle spacing), d is the grain size and m is the strain-rate-sensitivity (equal to the inverse of the power law stress exponent).

UNSOLVED PROBLEMS IN CREEP FRACTURE IN METALS UNDER MONOTONIC LOADING

Most of this report has dealt with the nucleation and growth of r type cavities which form predominantly at boundaries which are transverse to the tensile axis. Wedge cracking is another, and in the author's opinion, a distinctly different mechanism of intergranular fracture. Williams[36] has dealt with the initiation of wedge cracks using the Stroh[37] mechanism and Dimelfi and Nix[11] have dealt with the growth of wedge cracks by secondary cavitation. In both instances, the stress relaxation which must occur at and near the triple junctions have not been taken into account. In the approach of Min and Raj[38,39] a strain rate and sliding displacement criteria is considered in which it is held that the strain rate must be such that the rate of increase of stress concentration at triple junctions by sliding is faster than the rate of stress relaxation, and that a certain critical sliding displacement must accumulate before a wedge crack extends across a full grain facet. More modelling work is needed which couples sliding, diffusion and power law creep mechanisms of deformation. In order to obtain a better comparison with experiment, it may be easier to think in terms of an applied strain rate rather than an applied stress since some recent experiments on supperalloys have shown that the loading rate can have a significant effect on the stress rupture life.[40]

Many engineering materials, especially nickel base alloys are very sensitive to environment. Whether the environment affects nucleation, or growth, or both is totally unclear. One of the possibilities is that environment (e.g. oxygen) influences the trace element concentration in the grain boundaries which leads to a much faster rate of grain boundary diffusion, thereby accelerating growth and nucleation.

Evidence is accumulating that in monotonic and in cyclic loading intergranular fracture can occur by the initiation and propagation of cracks from the surface (see Fig. 2b). A good start will be to study cavity formation in the region of well defined stress concentrators such as notches. In fact it is possible to imagine two extremes: one in which grain boundary damage forms in the entire cross section before failure occurs, and the other where damage is tightly localized at a notch root or a crack tip. Conditions under which one or the other failure process dominates should be established. It is suspected that the effect of multiaxial stress field on cavitation will be significant when damage occurs near notches and cracks.

FRACTURE IN CERAMIC MATERIALS

(a) Fracture by Diffusional Mechanisms in Purely Crystalline Ceramics

What I have said about the nucleation and growth of cavities by diffusional mechanisms in metals applies equally to ceramics. The temperature at which diffusion becomes the dominating mechanism, however, is higher in

ceramics than in metals. This is because in ceramics the atom binding is either ionic or covalent, as a result the ductile-brittle transition occurs at 0.4- 0.7 of the melting temperature (as compared to 0.1- 0.3 in b.c.c. metals). The other difference is that even at high temperatures, ceramics can cleave at the higher stresses because the stress required for dislocation-slip at barriers such as grain boundaries is often comparable to the stress required to form cracks. In softer materials, however, such as magnesium oxide and alkali halides, ductile hole growth has in fact been observed. The fracture behavior of M_gO and Al_2O_3 is contrasted in the fracture maps for the two materials shown in Figures 12 and 13. In these maps cleavage-one refers to completely brittle fracture, cleavage-two to crystallographic fracture with some ductility, brittle-intergranular-fracture to fracture without cavitation, ductile creep fracture to fracture by plastic hole growth, and intergranular creep fracture to fracture by the growth of cavities in the grain boundary. Note that ductile creep fracture is not observed in polycrystalline alumina. Brittle intergranular fracture is essentially cleavage which depends on the size of the pre-existing cracks; in "perfect" material the cracks are produced by slip and are effectively as large as the grain size. This mode of fracture effectively prescribes an upper limit to the stress that can be imposed on the material during service; also fracture in this mode is not time dependent.

The principal mode of time dependent fracture in strong, creep resistant ceramic materials such as alumina, silicon nitride and silicon carbide, is the nucleation and growth cavities in grain boundaries by diffusional mechanisms. Since ceramics are often sintered and hence contain some residual porosity,* the nucleation of cavities should not be the limiting factor in fracture and in the simplest case, Eq. (4) should provide good prediction of fracture behavior. Unfortunately, stress rupture data in which the stress, the cavity spacing and the diffusion coefficients are well specified, are extremely scarce. We have found one case, in alumina, where we can compare theory and experiment,[32] which is shown in Fig. 14. For theory a modified version of Eq. (4) was used since lattice diffusion of the cation rather than grain boundary diffusion is expected to be the rate controlling process in Al_2O_3.[33] The agreement is very encouraging. The transition to a higher slope in Fig. 14 is probably associated with the development of wedge cracks in the grain boundaries.

Despite the importance of diffusional mechanisms in high temperature fracture in ceramic materials, and the fact that the theory of diffusional fracture is quite well developed, experimental studies of stress rupture in ceramics have received little attention. There is clearly a need for experiments, preferably in pure tension, in which parameters such as cavity spacing and diffusion coefficients are well known. It should be kept in mind that in ceramics, the environment can influence the defect concentration and, therefore, the diffusivity making it necessary to carry out the experiments under specified environmental conditions.

---

*Even if the material is 99.999% dense it means that the average cavity spacing will be less than a 0.2 μm if we assume the cavities to be 10 nm in diameter, which is about the size of a critical nucleus from Eq. (1), and the grain size to be 1 μm .

(b) Fracture in the Presence of a Glass Phase in the Grain Boundaries

When ceramics are sintered or hot-pressed in the presence of a liquid phase, high densities are achieved but a residual glass phase is left behind in the grain boundaries. The glass is segregated mostly to the triple grain junctions but if the diahedral angle is equal to zero the glass also penetrates the two grain junctions, as in the case in hot-pressed silicon nitride[42,43] as shown in Fig. 15. The glass phase has a profound influence on the high temperature mechanical behavior. As the temperature is raised the glass in the two grain junctions facilitates grain boundary sliding, while at the triple grain junctions large tensile hydrostatic stresses can be produced due to the concentration of sliding displacement. It is conceivable that this results in the nucleation and growth of cavities in the glass pockets at triple grain junctions.

The simplest mechanisms for time dependent failure in such a microstructure is shown in Figs. 16 (a & b) due to Lange[44] and Raj and Dang.[45] Cavities grow in the same manner as penny shaped bubbles will grow in an adhesive layer sandwiched between two plates when the plates are pulled apart. The time to fracture by this mechanism can be rigorously calculated and is given by:

$$t_f = \frac{1.25\ \lambda^2\ \mu}{h_o^2\ \sigma_\infty} I \qquad (11)$$

where λ is the average spacing of the cavities, h_o is the thickness of the glass layer, μ is the viscosity, σ_∞ is the stress normal to the grain boundary. I is a numerical integration factor which is equal to 0.18 if the cavities are already present or 46.5 if the cavities have to be nucleated by means of the applied stress. At least in hot-pressed silicon nitride, in which extensive transmission microscopy has been carried out there is no evidence of any cavities in the virgin material. We must assume, therefore, that nucleation is necessary. This leads to a threshold stress given by:

$$\sigma_{th} = \frac{4\gamma_g}{h_o} \qquad (12)$$

where γ_g is the surface energy of the glass phase. When Eqs. (11) and (12) are applied to fracture in hot-pressed silicon nitride then the curve shown in Fig. 17 is obtained (λ = 1 μm, $\mu_{SiO_2} = 10^{10}$ P, h_o = 2 mm, and γ_g = 0.5 Jm^{-2}; the viscosity was derived at 1300°C assuming the glass to be pure silica[46]). Since fracture in HP-Si_3N_4 occurs in a time period which is several orders of magnitude shorter than what we calculate, we assume that this is not the rate controlling mechanism of failure in this material.

The other mechanism of failure which has been proposed by us is shown schematically in Fig. 18. The idea is that sliding at boundary AB produces a stress concentration at the triple junction. A cavity is formed in the glass pocket in the triple junction which grows and produces a wedge crack BC just

ahead of the primary crack. Several such cracks may form a "damage zone" of many microcracks in the crack tip region. When the damage zone gets large enough that the stress at the tip of the primary crack exceeds the fracture stress of the interface, then the crack advances by a distance of one grain length. This mechanism leads to subcritical crack growth.[47] The approximate rate of crack growth by this process would then be given by

$$\dot{a} = \frac{d}{\tau} \tag{13}$$

where d is the grain diameter and τ is the time required for the formation of a wedge crack. Several rate processes act sequentially in producing a wedge crack. The slowest one of them determines the value for τ in Eq. (13). First the boundary slides to produce a stress concentration at the triple junction; second, the cavity nucleated in the triple junction grows just as a bubble grows in a viscous medium; and third the bubble grows and impinges on the two grain junction and propagates a wedge crack. We have measured the rate of grain boundary sliding from internal friction experiments in HP-Si_3N_4 and find that the substitution of this time constant into Eq. 13 gives a crack propagation rate of nearly 1 ms^{-1} at a temperature of 1300°C which is nearly six orders of magnitude faster than the measured value.[47] We then calculated the time required for the growth of the bubble in the triple grain junction:

$$\tau_g = \frac{4\mu}{P} \tag{14}$$

where P is the hydrostatic tension produced in the triple grain junction by grain boundary sliding, and μ is the viscosity of the glass at the given temperature. We do not have knowledge of the viscosity of the glass but if we assume that the glass is pure silica then the maximum possible value of the viscosity and hence the slowest possible crack growth rate is obtained. Using this we calculate the crack growth rates to be about 10^{-7} ms^{-1} which is one to two orders of magnitude lower than the measured value. On this basis we conclude that the growth of the cavity in the glass pocket at triple junctions rather than grain boundary sliding is the rate controlling step in time dependent fracture of HP-Si_3N_4. This has some interesting implications. For example, according to Eqs. (13) and (14), the viscosity of the glass will directly affect the crack growth rate. The presence of alkaline impurities will, therefore, lower the viscosity and hence accelerate fracture. The model also suggests that grain boundary sliding, although necessary for fracture, is not the rate controlling step. Changing the grain boundary microstructure so as to impede sliding, for example by introducing inclusions, is not likely to affect the fracture kinetics.

There is one important aspect of the above model. We have considered only those processes which produce stress concentration and fracture. At high temperature the stress concentration can also be relieved by creep, specifically by dissolution/precipitation of the ceramic from the glass phase at the triple junction. The driving force for this would be a finite difference in the partial molar volume of the ceramic in the glass phase and its molar volume in the crystalline phase. If the kinetics of the stress relaxation process is faster than the kinetics of bubble growth then cavities

will not form and the material will be ductile. Since HP-Si_3N_4 has a fine grained structure, it is quite likely that it would exhibit superplastic deformation if the nucleation and growth of cavities can be suppressed.

(c) Correlation between Processing Variables and Fracture Behavior

The fundamental parameters which are so important in the fracture of ceramics, such as diffusion, viscosity of the glass, and interaction between the ceramic and the glass phase, are equally important in the processing and preparation of ceramic materials. This is because ceramics are often prepared by sintering which involves diffusion, or by hot-pressing which involves dissolution/precipitation through a liquid phase. In both fracture and in processing, control of the chemistry and the vapor pressures of the various components in the environment is vital since it has a very significant effect on the diffusion and the properties of the liquid phase. In my opinion, systematic studies of thermodynamics and kinetics, micromechanical modelling, and mechanical testing will lead to some very exciting science and may well lead to a breakthrough in the technology of making ceramic materials with the desired high temperature mechanical properties through a well thought out and calculated control of the processing variables.

ACKNOWLEDGMENTS

The majority of the work on metals was supported by a grant from the Air Force Office of Scientific Research AFOSR-76-2930, while the work on ceramics was supported by a grant from the Department of Energy, EG-77-S-020 4386. Support was also received from the National Science Foundation through use of the facilities of Materials Science Center at Cornell University. Several helpful discussions with Dr. C. Gandhi are gratefully acknowledged. The ceramics work reported here was carried out by R. L. Tsai toward partial fulfillment of the Ph.D. degree.

REFERENCES

1. G. D. Bengough, J. Inst. Metals, 1912, vol. 7, p. 123.
2. F. N. Rhines and P. J. Wray, Trans. ASM, 1961, vol. 54, p. 117.
3. R. P. Skelton, Phil. Mag., 1966, vol. 14, p. 563.
4. V. Singh, P. Rama Rao, G. J. Cocks and D. M. R. Taplin, J. Mat. Sci., 1977, vol. 12, p. 373.
5. N. J. Grant, Fracture Vol. III, Ed. H. Liebowitz, Academic Press, 1971, p. 519.
6. W. Pavinich and R. Raj, Met. Trans. A, 1977, vol. 8A, p. 1917.
7. J. O. Steigler and J. R. Weir, Jr., Ductility, ASM, 1968, p. 311.
8. R. C. Gifkins, Acta Met., 1956, vol. 4, p. 98.
9. J. E. Harris, Trans. AIME, 1965, vol. 233, p. 1509.
10. R. Raj, Acta Met., 1978, vol. 26, p. 995.
11. W. D. Nix, D. K. Matlock and R. J. Dimelfi, Acta Met., 1977, vol. 25, p. 495.
12. D. A. Miller and R. Pilkington, Met. Trans A, 1978, vol. 9A, p. 489.
13. I. G. Palmer and G. C. Smith, Oxide Dispersion Strengthening, ed. G. S. Ansell, Gordon and Breach, 1968, p. 253.
14. A. S. Argon and J. Im, Met. Trans. A, 1975, vol. 6A, p. 814.
15. R. G. Fleck, D. M. R. Raplin and C. J. Beevers, Acta Met., 1975, vol. 23, p. 415.
16. C. J. Beevers, private communication.
17. J. Weertman, Scripta Met., 1978, vol. 12, p. 187.
18. C. Herring, J. Appl. Phys., 1950, vol. 21, p. 437.
19. D. Hull and D. E. Rimmer, Phil. Mag., 1959, vol. 4, p. 673.
20. M. V. Speight and J. E. Harris, Met. Sci. J., 1967, vol. 1, p. 83.
21. R. Raj and M. F. Ashby, Acta Met., 1975, vol. 23, p. 653.
22. R. Raj, H. M. Shih and H. H. Johnson, Scripta Met., 1977, vol. 11, p. 839.
23. T.-j. Chuang and J. R. Rice, Acta Met., 1973, vol. 21, p. 1625.
24. T.-j. Chuang, K. I. Kagawa, J. R. Rice and L. B. Sills, "Non-equilibrium models for diffusive cavitation of grain interfaces," Brown University Report, June 1978.
25. R. Raj, Acta Met., 1978, vol. 26, p. 341.
26. S. H. Goods and W. D. Nix, Acta Met., 1978, vol. 26, p. 739.
28. F. C. Monkman and N. J. Grant, Proc. ASTM, 1956, vol. 56, p. 593.
29. B. F. Dyson and M. J. Rodgers, Metal Sci. J., 1974, vol. 8 , p. 261.
30. D. K. Matlock and W. D. Nix, J. Nucl. Mater., 1975, vol. 56, p. 145.
31. D. R. Mosher and R. Raj, Acta Met., 1974, vol. 22, p. 1469.
32. C. K. L. Davies and S. K. Sinha Ray, Brit. Cer. Res. Assoc., vol. 5, ed. P. Popper, 1972, p. 193.
33. S. Panchanadeeswaran and R. Raj, to be published.
34. F. A. McClintock, J. Appl. Mech., 1968, vol. 35, p. 363.
35. J. R. Rice and D. M. Tracey, J. Mech. Phys., 1969, vol. 17, p. 201.
36. J. A. Williams, Phil. Mag., 1969, vol. 20, p. 635.
37. A. N. Stroh, Adv. in Phys., 1957, vol. 6, p. 418.
38. B. K. Min and R. Raj, "A Mechanism of Intergranular Failure in High Temperature Fatigue," ASTM, Fatigue Mechanisms, 1979 (in press).
39. B. K. Min and R. Raj, "The Importance of Wedge Cracking in Creep Fatigue," Can. Met. Quart., June 1979, in press.
40. C. C. Law, private communication.

41. C. Gandhi and M. F. Ashby, "Development of Fracture Mechanism Maps for Ceramics," Cambridge University Engineering Department Report, 1978, Cambridge, England.
42. D. R. Clarke and G. Thomas, J. Amer. Cer. Soc., 1977, vol. 60, pp. 491-95.
43. L. K. V. Lou, T. E. Mitchell and A. H. Heuer, J. Amer. Cer. Soc., 1978, pp. 392-396.
44. F. F. Lange, Deformation of Ceramic Materials, Eds. R. C. Bradt and R. E. Tressler, Plenum Press, 1975, pp. 361-381.
45. R. Raj and C. H. Dang, Phil. Mag., 1975, vol. 32, pp. 909-921.
46. G. Hetherington, K. H. Jack and J. C. Kennedy, Phy. Chem. Glasses, 1964, vol. 5, p. 130.
47. A. G. Evans and S. M. Wiederhorn, J. Mat. Sci., 1974, vol. 9, p. 270.
48. T. B. Sweeting and J. A. Pask, J. Amer. Cer. Soc., 1976, vol. 59, p. 226.
49. J. M. Birch, P. J. King and B. Wilshire, J. Mat. Sci., 1975, vol. 10, p. 175.
50. A. G. Evans, D. Gilling and R. W. Davidge, J. Mat. Sci., 1970, vol. 5, p. 187.
51. R. B. Day and R. J. Stokes, J. Amer. Cer. Soc., 1966, vol. 49, p. 72. Also ibid., p. 345.
52. S. M. Copley and J. A. Pask, J. Amer. Cer. Soc., 1965, vol. 48, p. 636.
53. T. Vasilos, J. B. Mitchell and R. L. Spriggs, J. Amer. Cer. Soc., 1964, vol. 47, p. 606.
54. C. O. Hulse, S. M. Copley and J. A. Pask, J. Amer. Cer. Soc., 1963, vol. 46, p. 317.
55. P. T. B. Shaffer, High Temperature Materials: No. 1 Materials Index, Plenum Press, New York, 1964.
56. J. Lankford, J. Mat. Sci., 1978, vol. 13, p. 351.
57. S. K. Teh, Ph.D. Thesis, Materials Department, Queens Mary College, University of London, 1976, p. 234.
58. C. K. L. Davies, Physical Metallurgy of Reactor Fuel Elements, Eds. J. Harris and T. Sykes, Metals Society, 1975, p. 19.
59. L. A. Simpson and G. J. Merrett, J. Mat. Sci., 1974, vol. 9, p. 685.
60. A. Crosby and P. E. Evans, J. Mat. Sci., 1973, vol. 8, p. 1573.
61. K. F. A. Walles, Proc. Brit. Cer. Soc., 1970, vol. 15, p. 157.
62. E. Passmore, A. Moschetti and T. Vasilos, Phil. Mag., 1966, vol. 13, p. 1157.
63. R. M. Spriggs, J. B. Mitchell and T. Vasilos, J. Amer. Cer. Soc., 1964, vol. 47, p. 323.
64. R. J. Charles, "Studies of the Brittle Behavior of Ceramic Materials," 1963, ASD-TR-61-628, General Electric Co., R & D Center, Schenectady, N.Y.
65. J. A. Stavrolakis and F. H. Norton, J. Amer. Cer. Soc., 1950, vol. 33, p. 263.

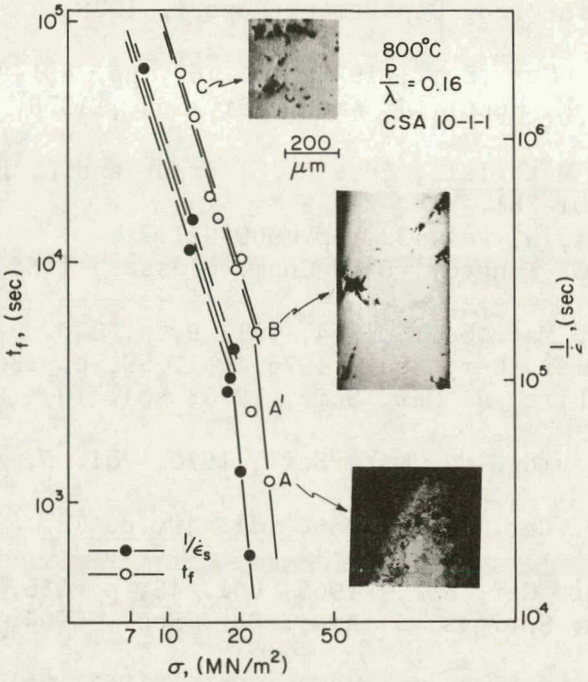

1. A break in the $\ell n(t_f)$ vs $\ell n(\sigma)$ curve is accompanied by a change in the mode of fracture from 'r' type cavitation to wedge type cavitation to dynamic recrystallization at very high stresses.(6) Note that in 'r' cavitation $1/\dot{\varepsilon}_s$ and t_f curves are parallel to each other.

(a)

(b)

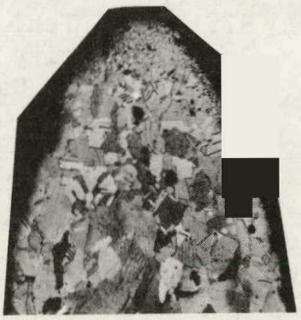

(c)

2. An enlargement of the three failure mechanisms described in Fig. 1. (a) 'r' type, (b) 'w' type, and (c) dynamic recrystallization.(6)

3. Wedge type cracking in irradiated stainless steel.[7]

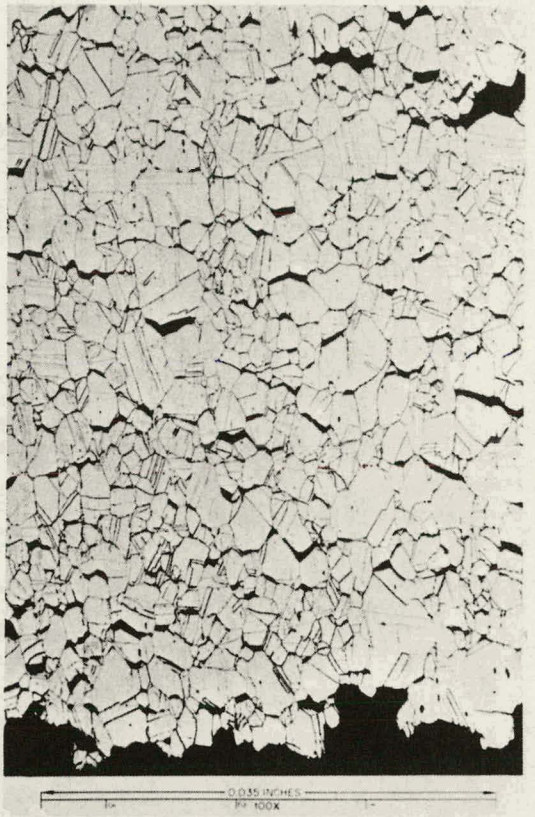

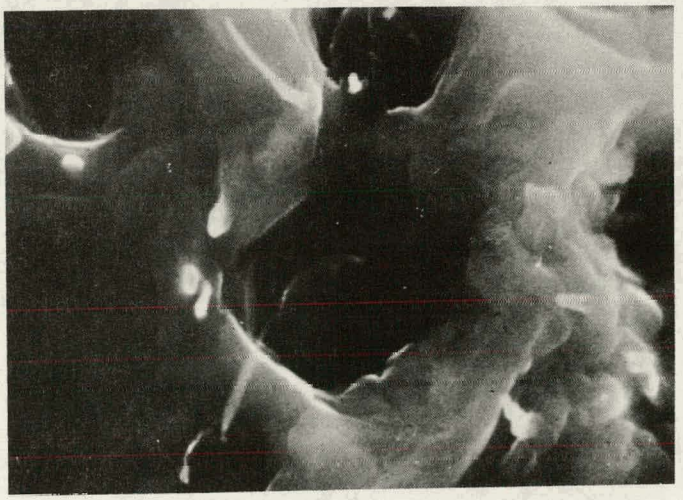

4. A scanning micrograph of a grain boundary fracture surface.

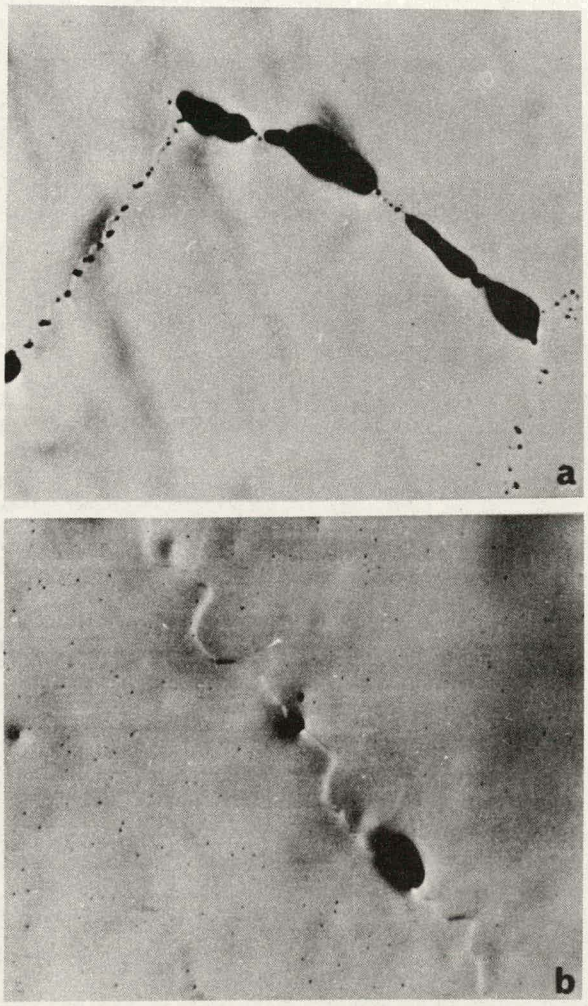

5. Cavity formation at asperities in a faceted boundary.[5]

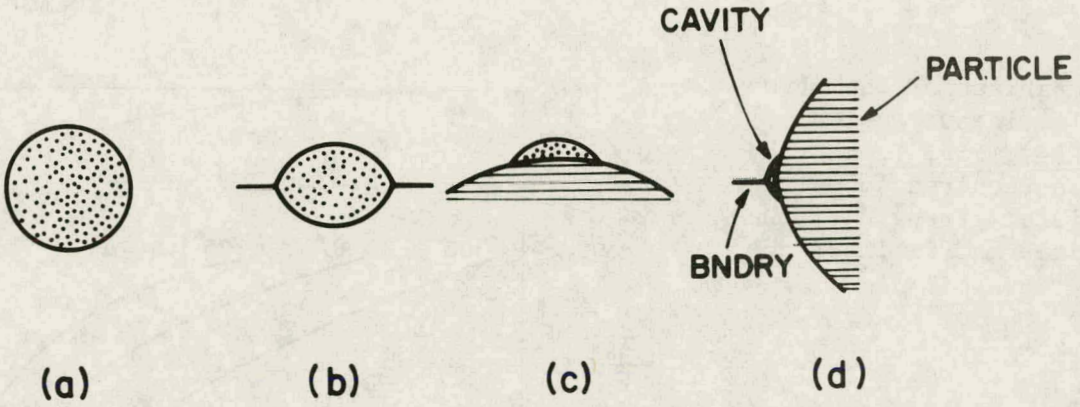

6. The volume of a cavity of a critical size at a fixed value of applied stress at various nucleation sites. Case (d) is the most probable site.

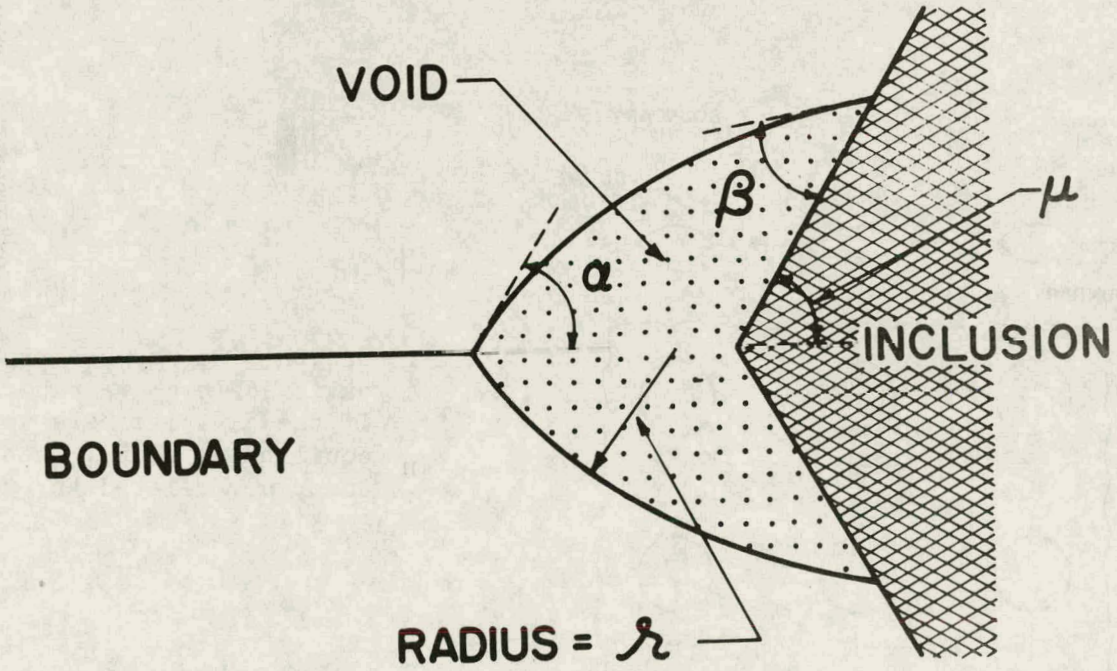

7. The details of the cavity morphology for case (d) in Fig. 6.

8. A comparison of the stress of kinetic nucleation at side (d), Fig. 7, and the stress required to overcome the ideal strength of the particle matrix interface.

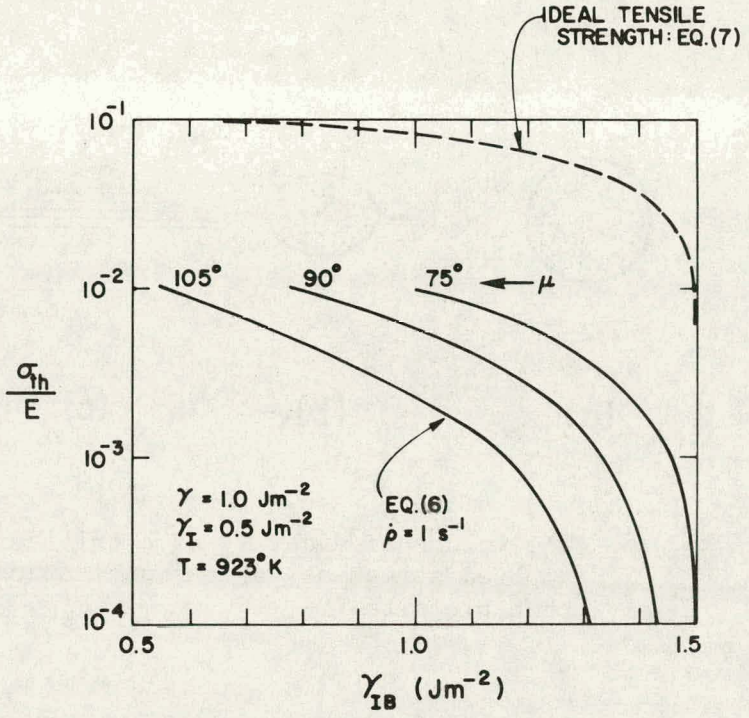

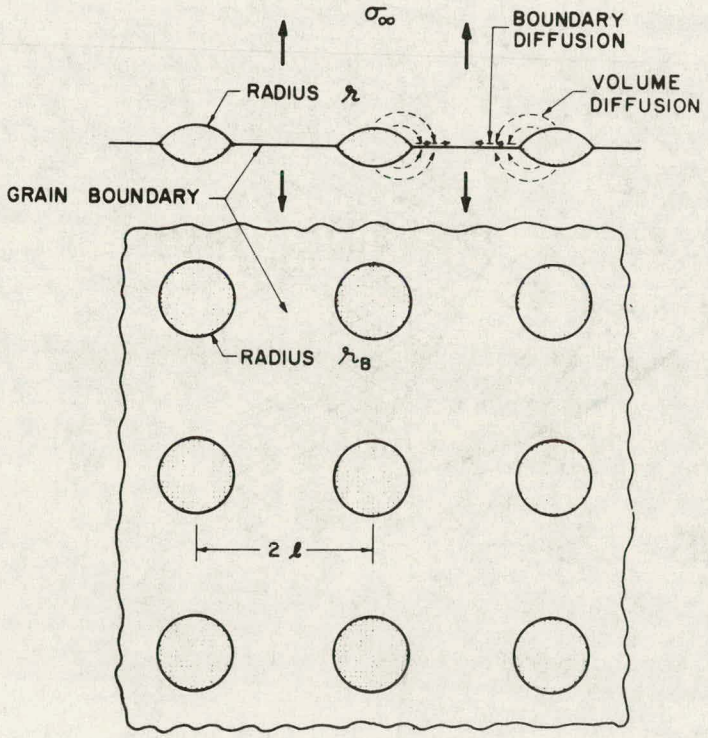

9. Growth of a square array of cavities in a grain boundary. If the cavities have an equilibrium shape, then r_B and r are related through α.

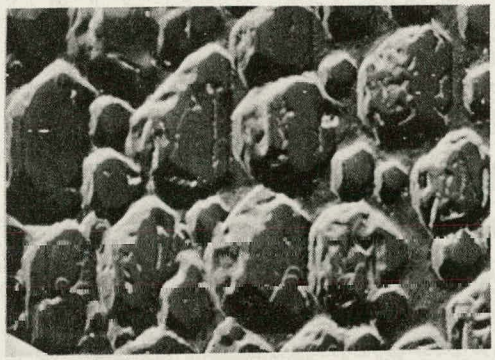

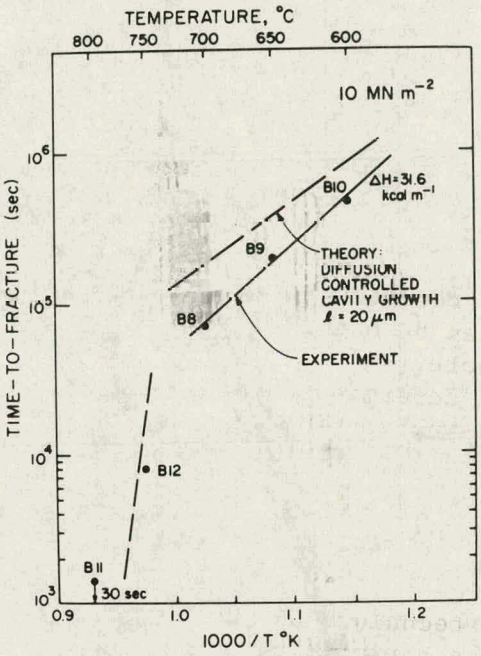

10. A comparison of experimental data with theory for grain boundary diffusion controlled growth of cavities. The picture on the left is the fracture surface. Experiments were performed on bicrystals.(25)

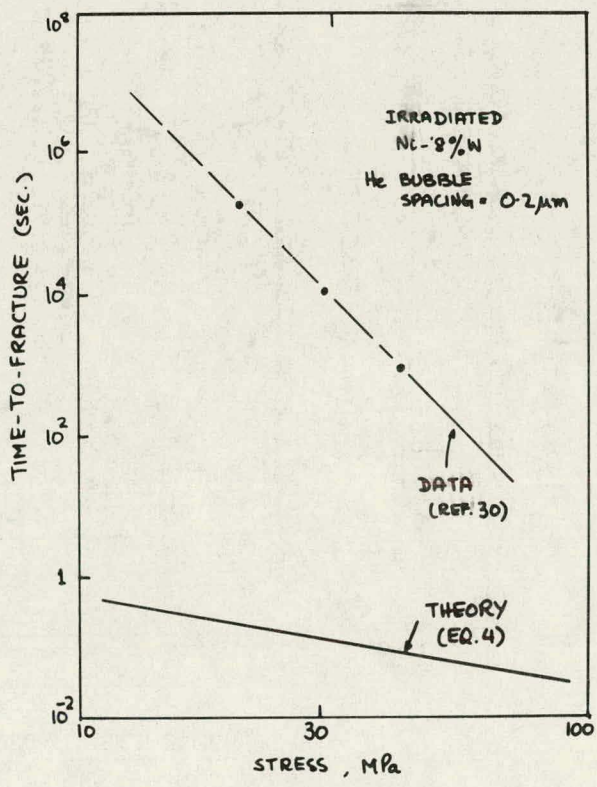

11. A comparison of fracture time of polycrystals containing He bubbles (of spacing ∿0.2μm)(30) with theoretical estimate (Eq. 4).

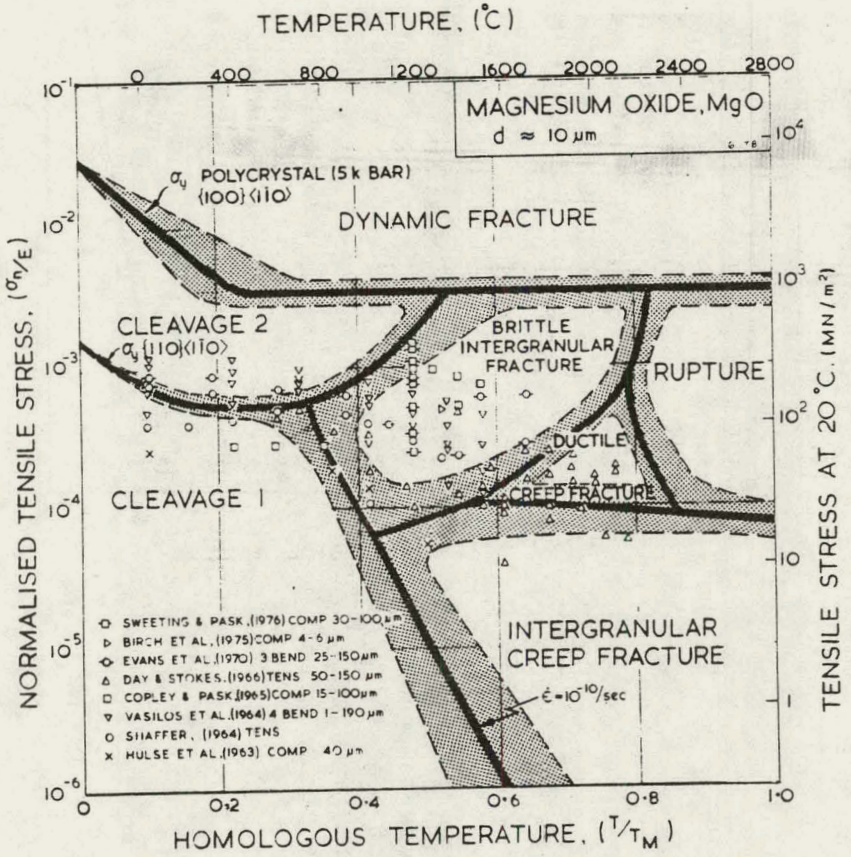

Figure 12

Fracture Map due to Gandhi and Ashby[41]. Time dependent fracture mechanisms are ductile creep fracture and intergranular creep fracture. Data from references 48-55.

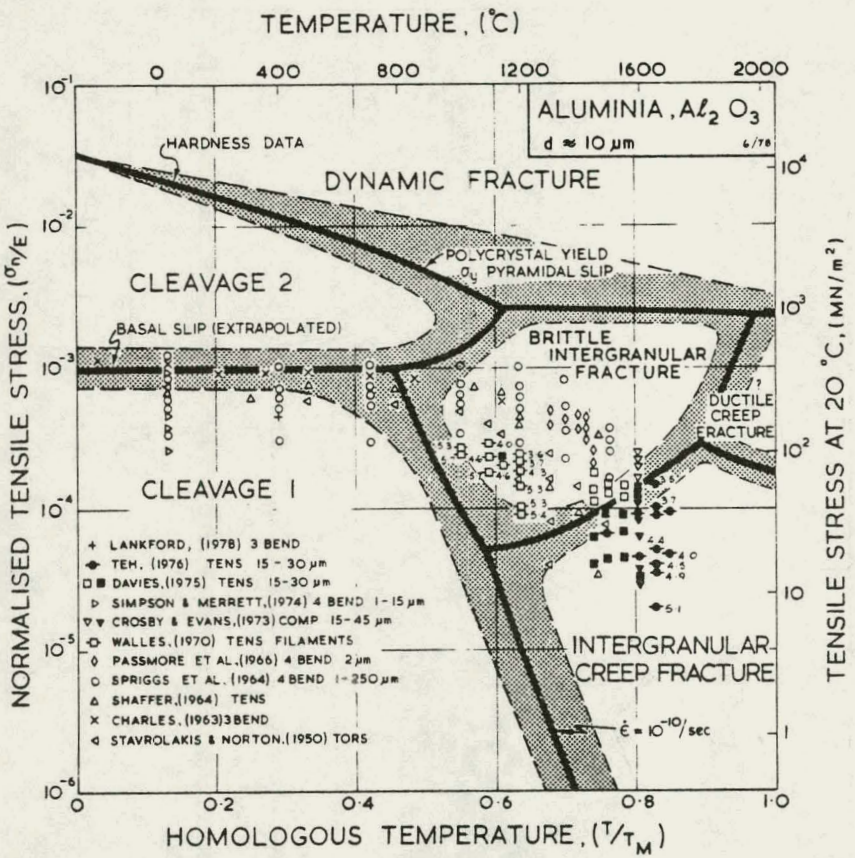

Figure 13

Fracture map due to Gandhi and Ashby[42]. Note that brittle and cleavage fracture occurs upto $0.7T_m$. Data from references: 55-65.

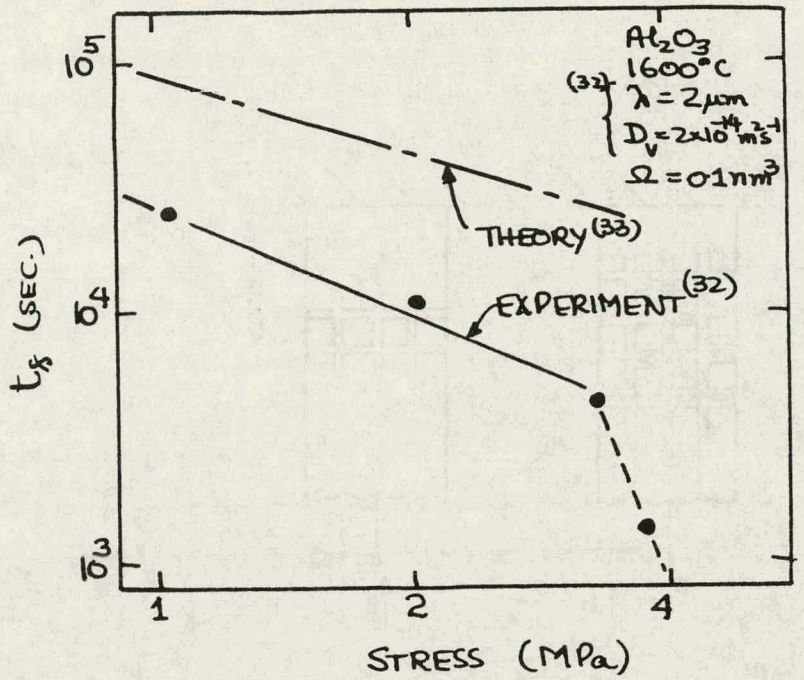

Figure 14

Fracture in Al_2O_3 by dif usion controlled cavity growth.

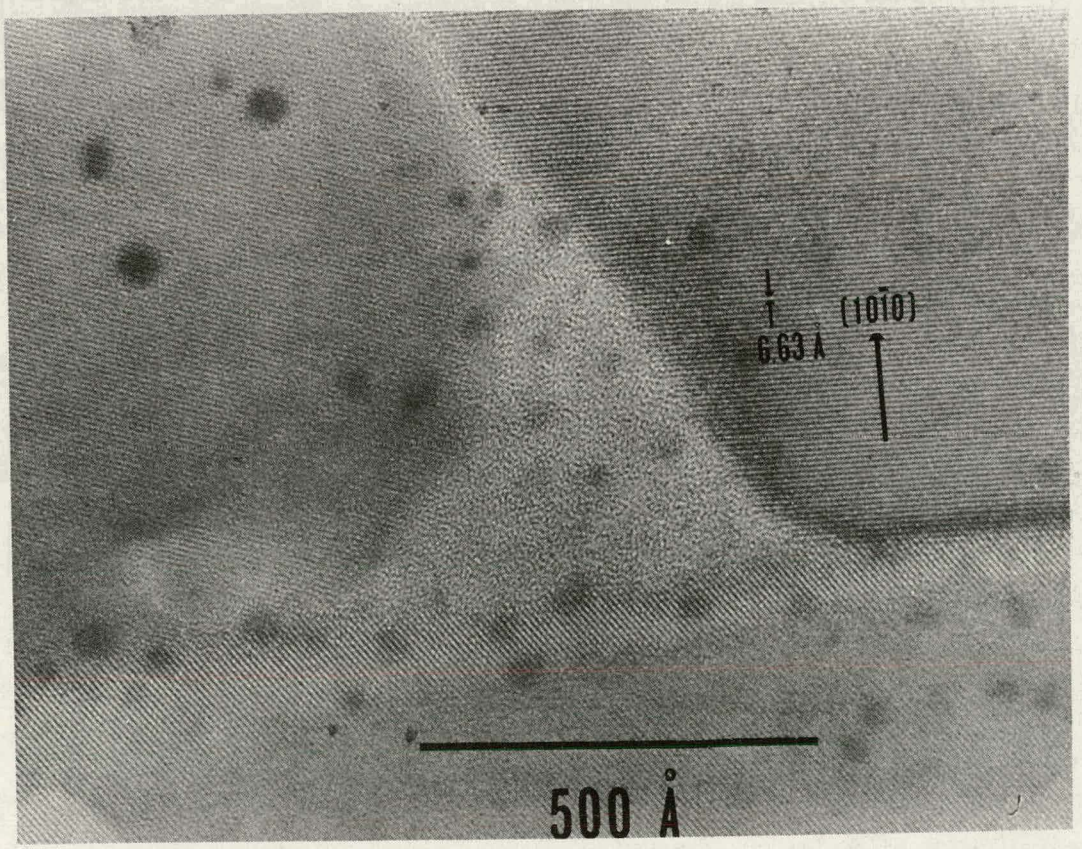

Figure 15

A glass pocket at a triple grain junction in HP-Si_3N_4 (picture by R. L. Tsai).

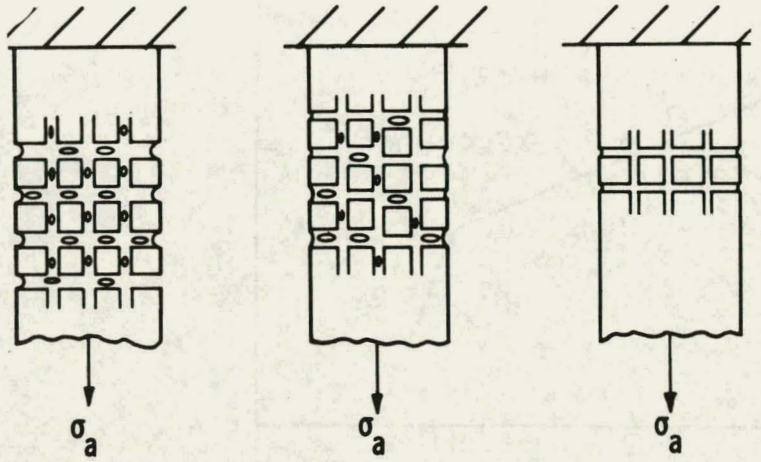

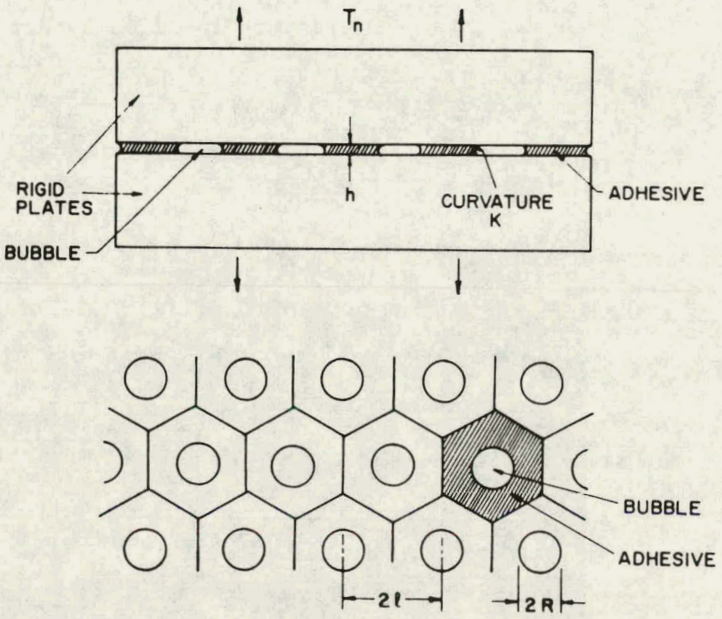

Figure 16

Schematics of fracture by the growth of penny shaped bubbles in a glass layer due to Lange[44] and Raj and Dang[45] (right).

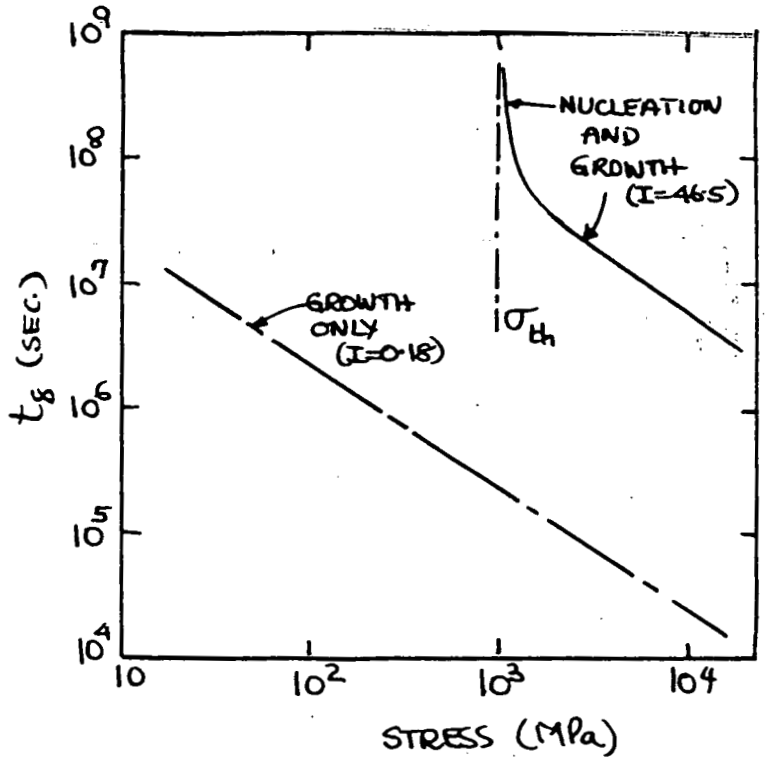

Figure 17

Theoretical prediction of fracture in HP-Si_3N_4 by the growth of penny shaped bubbles in the glass layer contained between two grain junctions.

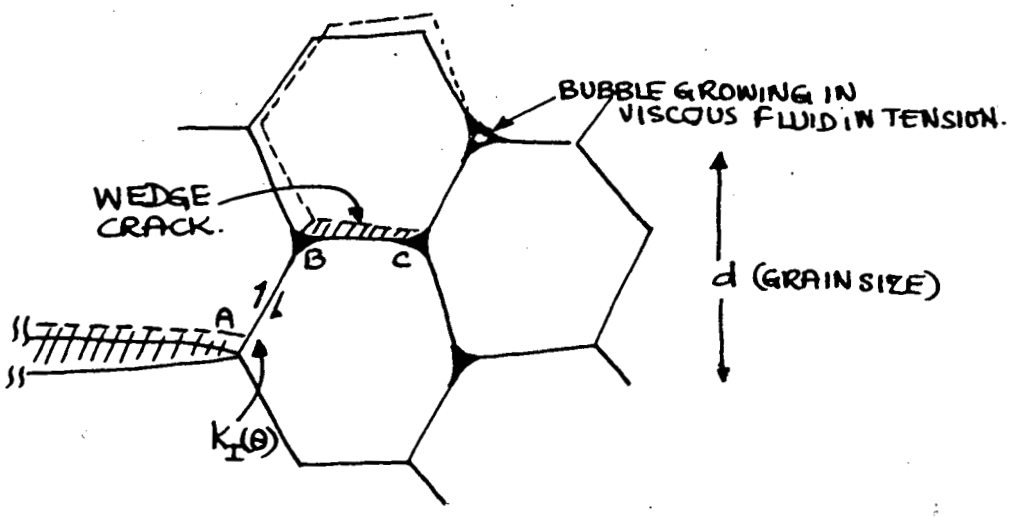

Figure 18

Slow crack growth by the formation of wedge cracks.

Presentation at Department of Energy Workshop on Time-Dependent Fracture of Materials at Elevated Temperature, Germantown, Md., 15-16 February 1979:

PLASTIC CREEP FLOW PROCESSES IN FRACTURE AT ELEVATED TEMPERATURES

James R. Rice
Division of Engineering, Brown University, Providence, R.I.

February 1979

Summary

This paper discusses recent theoretical developments on fracture at elevated temperature in the presence of overall plastic (dislocation) creep.

Two topics are considered:

1. Stress fields at tips of macroscopic cracks in creeping solids: Here consideration is given to the transient development of an effectively steady state of creep in a cracked body, following sudden load application for which the short-time material response is elastic. At long times (steady creep state) the severity of the near-crack-tip deformation rate field can be characterized in terms of a path-independent integral C^*, which is a generalization for non-linearly viscous materials of the J integral for rate-independent materials. Based on recent work by Riedel and Rice, it is shown that the short time transient field of creep flow has the same functional form at the crack tip, but that its amplitude parameter C^* is replaced, approximately, by $G/(1+n)t$, where t is time since load application, n is the exponent in a power-law creep relation $\dot{\varepsilon} \propto \sigma^n$, and G is Irwin's elastic energy release rate (calculated in terms of the stress intensity K_I as if the body were elastic). Hence $G/(1+n)C^*$ can be identified as a characteristic time for stress redistribution in attaining the steady creep state. Macroscopic creep crack growth is discussed in terms of these concepts and associated analyses.

2. Diffusive growth of microscopic grain boundary cavities in creeping solids: Previous analyses of this problem are based on an assumption that grains adjoining the cavitating boundary separate in an effectively rigid manner. However, important interactions between cavitation, by surface and grain boundary diffusion, and plastic creep processes are observed to occur when a state of overall dislocation creep prevails. These arise from two

effects. First, even in the absence of matter transport along the grain boundary (D_b very small), the presence of overall creep causes an increase in volume of the cavity and tends to cause a change in shape. The latter would, generally, tend to decrease rather than increase the cavity radius, but in the presence of sufficiently rapid surface diffusion the spherical-caps shape of the cavity is retained and the creep-flow-induced volumetric opening rate of the cavity causes a continuous enlargement of cavity radius. Second, when grain boundary diffusion is considered, the deformability of the adjoining grains means that matter diffusion from the cavity surfaces can be accommodated by highly localized relative separation velocities across the grain boundary. Hence the diffusion path length is not set by cavity spacing (as in the rigid-grain Hull-Rimmer model), but can be much shorter, resulting in a far more rapid removal of material from the cavity walls. A precise analysis of the problem has not yet been developed, but a variational principle governing simultaneous dislocation creep and grain boundary diffusion has been established, and this should lead to effective finite-element solution procedures. Also, an approximate model of the process suggests that for pure metals in the range of 0.5 to 0.8 Tm , and at stress levels of $10^{-3}\mu$ (μ = shear modulus) and $10^{-4}\mu$, respectively, the resulting cavity growth rate may exceed predictions of the rigid grain model by as much as factors of 10 to 100.

Stress fields at tips of macroscopic cracks in creeping solids:

This section is based on recent work of Riedel and Rice [1] on tensile (Mode I) cracks in elastic-creeping solids and on earlier work by Riedel [2] on anti-plane (Mode III) shear cracks. The materials considered are assumed to follow the stress strain relation

$$\dot{\varepsilon} = \dot{\sigma}/E + B\sigma^n \qquad (1)$$

in uniaxial tension. The exponent n is typically in the range 4 to 6, sometimes higher, for dislocation creep processes.

A body containing a crack is supposed to be loaded in tension. If the load is applied suddenly, the instantaneous stress field developed in the material is elastic. The stress concentration at the crack tip causes a zone of rapid creep straining to develop there, effectively to alleviate the elastic $r^{-\frac{1}{2}}$ stress singularity. The early stages of this process may be described in analogy to analyses for rate-independent plastic materials. Accordingly, this (short-time) field, in which elastic strains are much greater than creep strains everywhere except within a small region at the crack tip, is referred to as "small scale yielding." The near tip solution in this regime is complicated, but the parameter which governs it is the (far field) elastic stress intensity factor K_I.

On the other hand, at long times after load application there is complete redistribution of stresses and subsequent response of the material under fixed load takes place as if the material were purely viscous, $\dot{\varepsilon} = B\sigma^n$. In such cases, referred to as "extensive yielding," the near tip stress and creep rate fields have an intensity characterized by C^*, where C^* is a path-independent integral [3].

In both the "small scale" and "extensive" yielding limits, and for intermediate cases, the r,θ form of the near tip field is controlled (for $n>1$) by the non-linear term in (1). Accordingly, the near-tip fields of stress and strain rate are of the same form as the fields of stress and strain in a rate-independent material with $\varepsilon \propto \sigma^n$. Such fields are given in [4,5], and referred to as "HRR" fields.

For example, in the case of extensive yielding the near tip stress field (in plane strain or in plane stress) is given by an expression of the form

$$\sigma_{ij} \to \left(\frac{C^*}{Br}\right)^{1/(1+n)} f_{ij}(\theta) \qquad \text{as } r \to 0 \qquad (2)$$

where the f_{ij} are dimensionless and appropriately normalized functions of θ, dependent also on n.

By dimensional considerations, and by the requirement that the loading be characterized only by K_I, the short time, or small scale yielding, solution has the form

$$\sigma_{ij} = (EBt)^{-1/(n-1)} g_{ij}\left[r/K_I^2(EBt)^{2/(n-1)}, \theta\right] \qquad (3)$$

at time t after load application. Here g_{ij} is dimensionless, dependent also on n and ν (Poisson ratio), and $g_{ij}[\rho,\theta]$ decays as $\rho^{-\frac{1}{2}}$ for large ρ. This stress field involves a near tip singularity in the same form as (2) except that C^* is replaced by a factor proportional to K_I^2/Et. Indeed, Riedel and Rice [1] give an approximate argument showing that, for small scale yielding,

$$C^* \text{ should be replaced by } G/(1+n)t \qquad (4)$$

in (2), where G ($=(1-\nu^2)K_I^2/E$ for plane strain) is Irwin's energy release rate. Their comparisons with exact numerical results [2] for the field analogous to (3) in Mode III suggest that the approximation of (4) is accurate to ±10% for $n \geq 4$.

On the basis of (3) and the stress-strain relationship, it is possible to define a "creep zone," somewhat arbitrarily, as the region where creep strains exceed elastic strains, both reduced to equivalent tensile strains. This zone has a size which increases in proportion to the parameter

$$K_I^2 (EBt)^{2/(n-1)} ,$$

and small scale yielding conditions may be assumed to prevail whenever the creep zone is small compared to characteristic lengths of the cracked body (e.g., crack length, uncracked ligament width). By (4), a transition time t_1 between the short-time, small scale yielding and long-time, extensive yielding cases may be defined by

$$t_1 = G/(1+n)C^* . \qquad (5)$$

For example, consider a short plane stress crack of length a in a large body under stress σ_∞, with associated creep strain rate $\dot{\varepsilon}_\infty^{cr}$. For this geometry, $G = \pi\sigma_\infty^2 a/E$ is well known, and we write it as

$$\int_0^a G\, da = (\sigma_\infty^2/2E)[(\pi/2)(\sqrt{2}\, a)^2] , \qquad (6)$$

which can be interpreted as the loss of strain energy, $\sigma_\infty^2/2E$, on crack introduction, from an "affected" area consisting of a semi-circle of radius $\sqrt{2}\,a$. A similar interpretation gives, approximately

$$\int_0^a C^* da \approx \left[\frac{n}{n+1}\,\sigma_\infty \dot{\varepsilon}_\infty^{cr}\right]\left[\frac{\pi}{2}\left(\sqrt{2}\,a\right)^2\right] , \text{ or } C^* \approx \frac{2n}{n+1}\,\sigma_\infty \dot{\varepsilon}_\infty^{cr} \pi a \quad . \tag{7}$$

Thus the characteristic time t_1 , for transition from small scale to extensive yielding is, approximately,

$$t_1 \approx \frac{1}{2n}\,\frac{\sigma_\infty}{E\dot{\varepsilon}_\infty^{cr}} = \frac{1}{2nEB}\,\sigma_\infty^{-(n-1)} , \tag{8}$$

and is shorter at high stress levels than at low.

Correlation of creep crack growth by K_I seems appropriate when advance takes place over a time scale much less than t_1 , and by C^* for a time scale much greater than t_1 . The analyses just discussed are for a stationary crack; it is known [6] that there must be a different type of singularity at a growing crack tip than that described by (2), or by its short-time version based on (4). In analogy with growing crack solutions for rate-independent plastic materials [7], however, it is expected that this different singularity, for which elastic and creep strains are of the same order, will be important only in a small inner core of the heavily crept zone near the crack tip, for the more ductile of materials. The point needs further elaboration.

Diffusive growth of microscopic grain boundary cavities in creeping solids:

The well known Hull-Rimmer [8] model for diffusive void growth along a grain interface is illustrated in fig. 1. First, surface diffusion is presumed to be rapid enough so that the void retains a quasi-equilibrium spherical-caps shape (see Chuang et al. [9] for a detailed analysis of conditions under which this assumption is valid, and solutions to a more general version of the Hull-Rimmer model in cases for which it is not). Second, the grains are assumed to be effectively rigid, so that the only way in which the voids can grow (e.g., by grain boundary diffusion, which is typically the most rapid matter-transport process) is by diffusion along the whole grain interface between voids, since the grains must separate uniformly. This diffusion is driven by the difference between the potential, per unit volume, $-\sigma_n$ (σ_n = normal stress) on the interface and $-2\gamma_s\kappa$ (κ = surface curvature) on the void, which is negative whenever the net stress on the unvoided portion of interface exceeds the sintering limit of $2\gamma_s \sin\psi/a$.

But at applied stresses of the order $10^{-3}\mu$ (μ = shear modulus) at $0.5\ T_m$ or, for example, $10^{-4}\mu$ at $0.8\ T_m$, plastic creep flow of the grains is generally rapid enough, according to the data summarized by Ashby in [10], that the grains can hardly be considered rigid. Besides, it is known on empirical grounds (Monkman-Grant correlation) that the product of rupture time t_r and steady state creep strain rate $\dot{\varepsilon}_{ss}$ is not strongly variable over variations of stress and temperature that cause changes by several powers of 10 in $\dot{\varepsilon}_{ss}$. This suggests a strong coupling between plastic creep flow and creep rupture, even though diffusive processes as envisioned in the Hull-Rimmer model seem to be active.

There are two major ways in which plastic creep flow can interact with diffusive matter transport processes, and the net effect seems typically to be a significant increase of the void growth rate over what is predicted for the rigid grains model. The first way is illustrated in fig. 2a where, for simplicity, it is assumed that there is negligible matter transport along the grain boundary. Since the grains flow in creep, the material points immediately adjacent to the void surface take on a distribution of velocities which tend to make the void increase in volume and, in general under uniaxial tension and for widely spaced voids (so that plastic flow is not concentrated in a voided layer adjoining the grain boundary), to make

the void radius, a, decrease. This change in size and shape is indicated schematically by the dashed curve in fig. 2a. But when surface diffusion is rapid, local matter transport along the void surface retains the spherical caps shape (dash-dot-dash curve in fig. 2a) so that the net effect is to increase the void radius. Hence, if $\dot{V}_{cr}$ is the rate of void volume enlargment due to creep flow on the adjoining grains, the contribution to the growth rate is

$$\frac{d}{dt}\left[\frac{4\pi}{3}a^3 h(\psi)\right] = \dot{V}_{cr} \quad , \quad \text{or} \quad h(\psi)\dot{a} = \dot{V}_{cr}/4\pi a^2 \ . \tag{9}$$

Here the bracketed term is the void volume; $h(90°) = 1$, $h(70°) = 0.61$ ($70°$ is a typical angle ψ for metals). $\dot{V}_{cr}$ may be evaluated from classical creeping flow solutions for widely spaced spherical voids in a linear viscous material under uniaxial tension; it is not very different for a penny shaped crack, suggesting only a mild dependence on ψ . The result is

$$h(\psi)\dot{a} = \frac{1}{2\sqrt{3}}\dot{\varepsilon}_\infty a \ . \tag{10}$$

For comparison, the rigid-grains model predicts a result which, for $b/a \geq 5$, reduces to approximately [8,9]

$$h(\psi)\dot{a} \approx \frac{\mathcal{D}(\sigma_\infty - 2\gamma_s \sin\psi/a)}{2a^2 \ell n(b/2.1a)} \quad , \quad \text{where} \quad \mathcal{D} = \frac{D_b \delta_b \Omega}{kT} \tag{11}$$

and the notation is standard. In fact the ratio $\dot{a}$ from (10) to that from (11) is typically of the order a^3/L^3 where L is a stress level and temperature dependent length defined by

$$L = (\mathcal{D}\sigma_\infty/\dot{\varepsilon}_\infty)^{1/3} \ . \tag{12}$$

This length will appear subsequently and some numerical values will be given.

The second process by which plastic creep flow interacts with diffusion is illustrated in fig. 2b. Now matter transport along the grain boundary, with matter deposition on the adjoining grains, is considered. One the left is shown the void at one instant and two straight lines have been inscribed on the grains parallel to the grain boundary. On the right the void and inscribed lines are shown after some amount of growth. Obviously, in the rigid grain model the lines remain straight and matter must be transported

along the entire grain boundary. But, as remarked first by Beere and Speight [11], with plastic creep flow of the grains the matter can be accommodated locally, resulting in the strongly non-uniform motion of the inscribed lines as shown. This means that the diffusive path length can be much shorter than in the rigid-grains model, depending on how deformable the grains actually are, and this is expected to result in a more rapid removal of matter from the cavity walls (i.e., higher $\dot{a}$) than for the rigid grains model.

The process has not yet been modelled in a convincing way. Beere and Speight [11] assume that the grains separate in an effectively rigid way under low stress in some shell of material adjoining the void, with plastic creep flow taking place outside of this shell. However, the picture of the inscribed lines in fig. 2b suggests, instead, severe creep distortions near the cavity boundary. Such problems of combined plastic creep flow and diffusion are amenable to finite element analysis, and are being studied currently [12].

The finite element method is formulated according to a variational principle which leads to the system of equations shown in fig. 3. Here an axisymmetric problem of a spherical caps void of radius $r=a$, in a cylinder or radius $r=b$ ($\approx$ void half-spacing) is shown. The principle is written in dimensionless form with $R=r/a$, $B=b/a$, $H=h/a$, $Z=z/a$, $V_i = v_i/\dot{\varepsilon}_\infty a$, and is $\delta F=0$ (F=min.) where F is the following functional of dimensionless velocities V_i and associated dimensionless strain rates $\dot{E}_{ij} = \dot{\varepsilon}_{ij}/\dot{\varepsilon}_\infty$:

$$F = \int_0^H \int_{R_o(Z)}^B \frac{n}{1+n} \left(\sqrt{\frac{2}{3} \dot{E}_{ij} \dot{E}_{ij}} \right)^{(1+n)/n} R\,dR\,dZ$$

$$- \int_0^B (V_Z)_{Z=H}\, R\,dR$$

$$+ \left(\frac{a}{L}\right)^3 \int_1^B \left[\int_R^B R (V_Z)_{Z=0}\, dR \right]^2 \frac{dR}{R}$$

$$+ \frac{2\gamma_s \sin\psi}{a\sigma_\infty} \int_1^B R (V_Z)_{Z=0}\, dR \quad , \qquad (13)$$

where it is understood that $(V_R)_{R=B} = -\frac{1}{2} B$.

The first two terms of (13) are those which appear in a classical variational principle for creeping solids; the last two refer to g.b. (grain boundary) diffusion. When $L >> a$ and b, only the last three terms differ sensibly from zero in the solution field (i.e., the behavior is rigid in this limit) and the classical Hull-Rimmer result, summarized in (11), is recovered. On the other hand, when $L << a$, only the first two terms can differ sensibly from zero, grain boundary diffusion is unimportant, and the prediction of the growth rate reduces to that of (9), or of (10) for a linearly viscous material. At intermediate values of L, e.g., a/L of order unity, the coupling between g.b. diffusion and plastic creep flow is important.

To estimate L one may write

$$\mathcal{D} = \frac{D_{bo}\delta_b\Omega}{kT}\exp\left(-\frac{Q_b}{RT}\right) \tag{14}$$

and, following Ashby [10] for dislocation creep,

$$\dot{\varepsilon} = A\frac{D_{vo}\mu b}{kT}\left(\frac{\sigma}{\mu}\right)^n \exp\left(-\frac{Q_v}{RT}\right) \tag{15}$$

where, in the last expression A is a constant, μ the shear modulus, the dislocation slip step and D_{vo}, Q_v refer to bulk diffusion. Accordingly, with some rearrangement one may write

$$L \equiv (\mathcal{D}\sigma/\dot{\varepsilon})^{1/3} = L_o \exp\left(\frac{\kappa T_m}{T}\right)\left(\frac{10^{-3}\mu}{\sigma}\right)^{(n-1)/3} \tag{16}$$

where T_m is the melting temperature. Using data for all material parameters in (14,15) from the Ashby tabulation [10], values of n, κ, and L_o are shown for several metals in Table 1. Also shown are values of L at stress level of $10^{-3}\mu$ at $0.5\ T_m$ and $0.8\ T_m$. A tenfold decrease in stress, to $10^{-4}\mu$ would increase the values of L shown by about a factor of 20.

What emerges, then, is that a, typically growing through a range of from 1 to 10 μm, will generally be of a size comparable to L at stress levels of order $10^{-3}\mu$ at $0.5\ T_m$ and $10^{-4}\mu$ at $0.8\ T_m$. In such cases coupling between creep flow and g.b. diffusion must be considered. At significantly lower stress levels, L is much larger than a and b, and rigid grains behavior applies, eq. (11). At significantly higher stress levels, L is much smaller than a, and growth is described by eq. (9)

which, it may be recalled, predicts a result of order $(a/L)^3$ times that of eq. (11).

A highly approximate model in which the continuum of fig. 3 has been replaced by a "shear plate" has been studied by the writer in unpublished work. The variational functional F analogous to (13), but now reduced to a one-dimensional functional, has been minimized on the class of grain boundary velocity fields

$$(V_Z)_{Z=0} = H \exp\left(\frac{R-1}{\eta}\right)$$

(i.e., H and η chosen to minimize F), where ηa is the decay distance and the outer radius b is taken as infinite.

Some results of this very approximate analysis are quoted here, in lieu of accurate finite-element results, unavailable at present. Consider the case where σ_∞ is large compared to the sintering level, $2\gamma_s \sin\psi/a$, and take $n=5$. In this case the predicted growth rate, $\dot{a}$, in presence of simultaneous creep and g.b. diffusion, is about equal to that predicted by the rigid grains model (with $b/a = 10$) when $a/L \approx 0.03$. The growth rate is 3 times higher than the rigid grains prediction when $a/L \approx 0.3$, 20 times when $a/L \approx 1$, 70 times when $a/L \approx 3$, and 500 times for $a/L \approx 10$. Thus, whenever a/L exceeds, say 0.1, the rigid grains model must be considered too conservative. When a/L is larger than about 10, eqs. (9) or (10) can be used with reasonable accuracy. As is seen from Table 1, the intermediate range, $0.1 < a/L < 10$, will be encountered in many practical cases.

Additional Note: A related study by Edward and Ashby ["Intergranular Fracture during Power Law Creep," Acta Met, in press] comes to similar conclusions on the importance of plastic creep flow on diffusive cavitation.

Acknowledgement: This research was supported by DOE under Contract EY-76-S-02-3084 with Brown University.

References

1. H. Riedel and J. R. Rice, "Tensile cracks in creeping solids," to be presented at May 1979 ASTM Annual Symposium on Fracture Mechanics, Washington Univ., St. Louis.

2. H. Riedel, Z. Metallkinde 69, 1978, 755-760.

3. J. D. Landes and J. A. Begley, in Mechanics of Crack Growth, ASTM STP 590, 1976, 128-148.

4. J. R. Rice and G. F. Rosengren, J. Mech. Phys. Solids 16, 1968, 1-12.

5. J. W. Hutchinson, ibid., 13-31.

6. H. Riedel and H. Hui, research in progress at Brown and Harvard Universities.

7. J. R. Rice and E. P. Sorensen, J. Mech. Phys. Solids 26, 1978, 163-186.

8. D. Hull and D. E. Rimmer, Phil. Mag. 4, 1959, 673.

9. T-j. Chuang, K. I. Kagawa, J. R. Rice and L. Sills, Acta Met., in press, 1979.

10. M. F. Ashby, Acta Met. 20, 1972, 887-897.

11. W. Beere and M. V. Speight, Met. Sci., 1978, 172-176.

12. J. R. Rice and A. Needleman, research in progress at Brown University.

Figure Captions

Fig. 1 Hull-Rimmer model for grain boundary cavitation by surface and grain-boundary diffusion. The adjoining grains are assumed to separate as rigid bodies in this model.

Fig. 2 (a) Cavity growth by combination of plastic creep flow (which, if considered alone, generally tends to decrease cavity radius, dashed curve) and rapid surface diffusion.

(b) Local accommodation of matter diffused into grain boundary, by deformation of grains. Note that the inscribed (dashed) lines do not remain straight, as assumed in the rigid-grains model, and thus the diffusion path length necessary to accommodate a given amount of matter is shorter.

Fig. 3 Summary of field equations and boundary conditions for axi-symmetric problem of combined plastic creep flow and grain boundary diffusion. Outer radius b of cylinder represents half-spacing between adjacent voids.

Table 1

Values of $L \equiv (\mathcal{D}\sigma/\dot{\varepsilon})^{1/3} = L_o e^{\kappa T_m/T}\left(\frac{\mu}{10^3\sigma}\right)^{(n-1)/3}$

Material	n	κ	L_o (μm)	L (μm) at 0.5 T_m	L (μm) at 0.8 T_m
Ag	5.3	3.08	2.87×10^{-2}	13.6	1.35
Cu	4.8	3.05	1.09×10^{-2}	4.85	.493
Ni	4.6	3.92	$.511 \times 10^{-2}$	13.0	.686
Al	4.4	2.57	$.762 \times 10^{-2}$	1.30	.189
γFe	5.75	2.44	$.955 \times 10^{-2}$	1.26	.202
Zn	6.1	1.79	2.02×10^{-2}	.724	.189
αFe	6.9	2.20	$.213 \times 10^{-2}$	.174	.0332
Mo	4.3	1.70	$.396 \times 10^{-2}$	1.18	.330

values are for $\sigma = 10^{-3}\mu$; would be approximately 20 times larger for $\sigma = 10^{-4}\mu$, if n=5 .

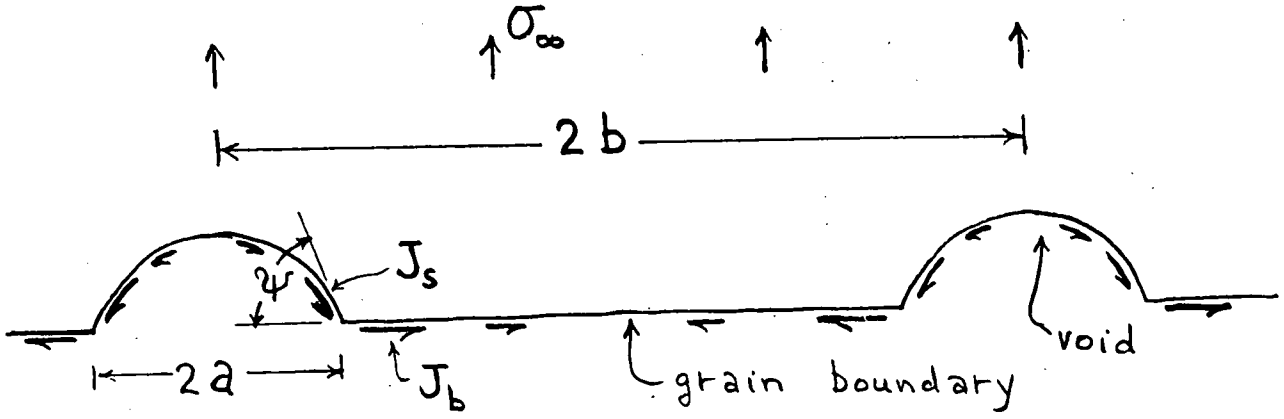

Fig. 1

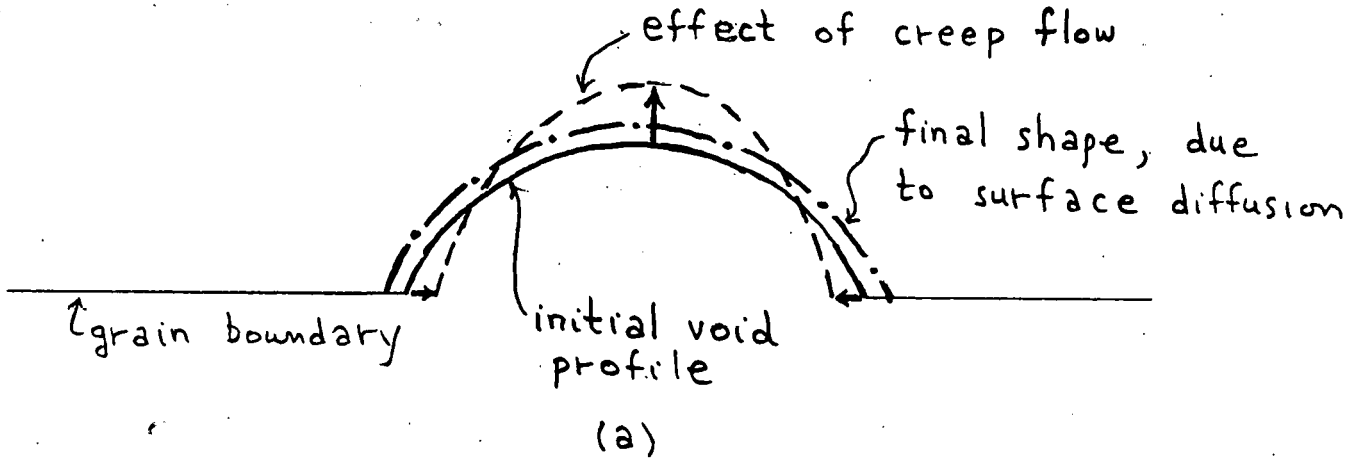
effect of creep flow
final shape, due to surface diffusion
grain boundary
initial void profile

(a)

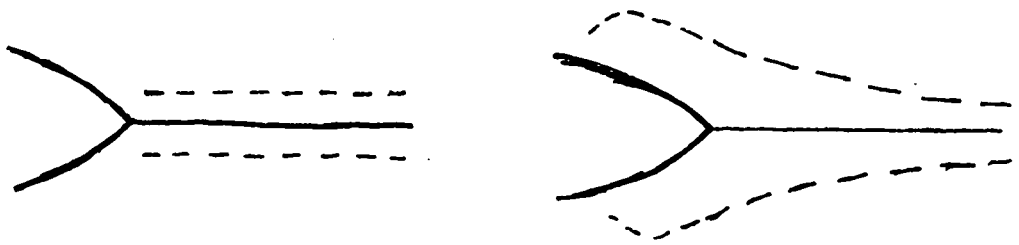

(b)

Fig. 2

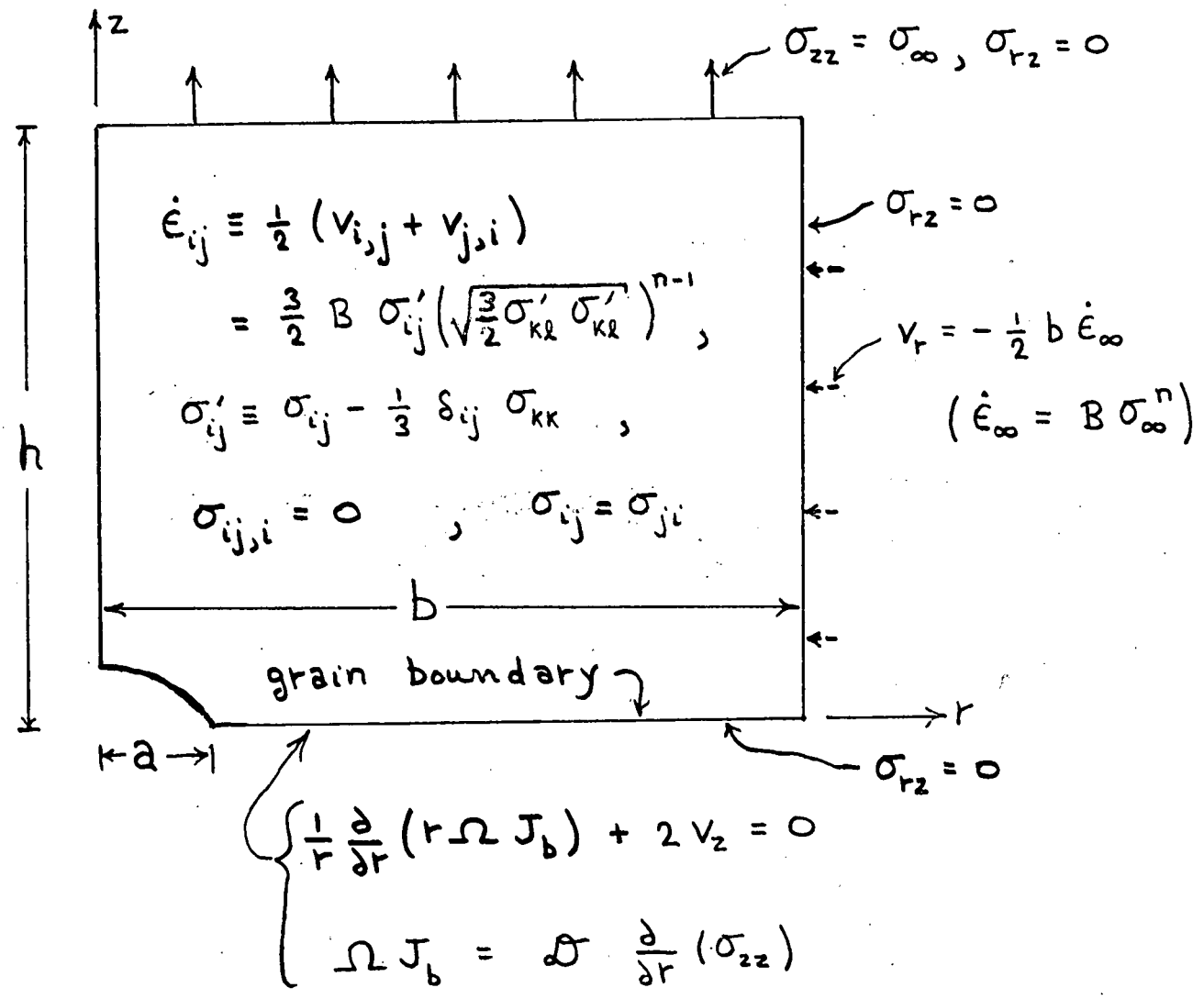
z
$\sigma_{zz} = \sigma_\infty$, $\sigma_{rz} = 0$
$\dot{\epsilon}_{ij} \equiv \frac{1}{2}(v_{i,j} + v_{j,i})$
$= \frac{3}{2} B \sigma'_{ij} \left(\sqrt{\frac{3}{2}\sigma'_{kl}\sigma'_{kl}}\right)^{n-1}$,
$\sigma'_{ij} \equiv \sigma_{ij} - \frac{1}{3}\delta_{ij}\sigma_{kk}$,
$\sigma_{ij,i} = 0$, $\sigma_{ij} = \sigma_{ji}$
$\sigma_{rz} = 0$
$v_r = -\frac{1}{2} b \dot{\epsilon}_\infty$
$(\dot{\epsilon}_\infty = B \sigma_\infty^n)$
h
b
grain boundary
r
a
$\sigma_{rz} = 0$
$\frac{1}{r}\frac{\partial}{\partial r}(r \Omega J_b) + 2 v_z = 0$
$\Omega J_b = D \frac{\partial}{\partial r}(\sigma_{zz})$

Fig. 3

GRAIN BOUNDARY STRUCTURE AND PROPERTIES

R. W. Balluffi

Department of Materials Science and Engineering
Massachusetts Institute of Technology, Cambridge, MA 02139

ABSTRACT

An attempt is made to distinguish those fundamental aspects of grain boundaries which should be relevant to the problem of the time dependent fracture of high temperature structural materials. These include the basic phenomena which are thought to be associated with cavitation and cracking at grain boundaries during service and with the more general microstructural changes which occur during both processing and service. A very brief discussion of the current state of our knowledge of these fundamentals is given. Included are the following:

1. STRUCTURE OF IDEAL PERFECT BOUNDARIES
   - 1.1 Detailed Atomic Structure
   - 1.2 Special Boundaries and Boundary Energy
   - 1.3 Secondary Relaxations (Collective Relaxations)
   - 1.4 Facet and Ledge Structures
2. DEFECT STRUCTURE OF GRAIN BOUNDARIES
   - 2.1 Point Defects (Vacancies and Interstitials)
   - 2.2 Line Defects (Grain Boundary Dislocations)
   - 2.3 Solute Atoms
3. DIFFUSION AT GRAIN BOUNDARIES
4. GRAIN BOUNDARIES AS SOURCES/SINKS FOR POINT DEFECTS
5. GRAIN BOUNDARY MIGRATION
6. DISLOCATION PHENOMENA AT GRAIN BOUNDARIES
   - 6.1 Grain Boundaries as Lattice Dislocation Sinks
   - 6.2 Grain Boundaries as Lattice Dislocation Sources
   - 6.3 Grain Boundary Sliding
7. ATOMIC BONDING AND COHESION AT GRAIN BOUNDARIES
8. NON-EQUILIBRIUM PROPERTIES OF GRAIN BOUNDARIES
9. TECHNIQUES FOR STUDYING GRAIN BOUNDARIES.

1. STRUCTURE OF IDEAL PERFECT BOUNDARIES

Since many of the properties of grain boundaries which are important to the problem of time dependent fracture depend intimately upon the boundary structure and the existence of point, line and planar defects in this structure, we begin by considering the ideal intrinsic structure of perfect boundaries. (A number of reviews of this topic are available in [1-7].)

It is helpful to visualize the construction of such a boundary by the following process. Place the two misoriented crystals (which will adjoin the boundary) together along the desired grain boundary plane rigidly in a standard reference position (as in Fig. 1) and then let the entire ensemble relax. In this process the atoms in the boundary region will relax their positions to minimize the total energy and at the same time Crystal 2 will find a minimum energy position relative to Crystal 1 by a rigid body translation without rotation, i.e., $\vec{R}$ in Fig. 1.

In general, eight macroscopic parameters are then required in order to give a complete macroscopic specification of a given boundary. These include the following:

3 parameters to describe the crystal misorientation;

2 parameters to describe the orientation of the boundary plane;

3 parameters to describe the rigid body translation of Crystal 2 with respect to Crystal 1.

We note that the rigid body translation must be defined in order to avoid ambiguities which arise due to structural degeneracy when the boundary possesses certain symmetry elements [8,9].

On the other hand, the microscopic structure of the grain boundary can only be specified by describing the positions of all the atoms in the ensemble, which of course also serve to specify $\vec{R}$. Of particular interest is the positions of the atoms in the "bad material" in the grain boundary core region (Fig. 1).

It is apparent from the above that grain boundaries are highly complicated many-bodied crystal defects which may exist with a wide variety of structures and properties depending upon the eight parameters listed previously. In general, no such thing as a "typical grain boundary" exists. In any consideration of grain boundary structure and properties it is therefore necessary to include a wide variety of boundaries each of which is itself highly complex. This fact, unfortunately, greatly complicates the entire situation!

1.1 Detailed Atomic Structure

So far, essentially all of our information about the detailed structure of the core has come from computer simulation studies. Only limited information has been obtained from more direct experimental observations. For example, field ion microscopy [10] has shown that the core region is relatively narrow (at least in metals) and is at most only a few atomic distances wide. However, it is not possible to obtain exact atomic positions in the core by this method. Direct lattice imaging [11] has been restricted to revealing the projected structure of

a few simple tilt boundaries along low index directions.

In the computer simulation work the procedure has been to calculate the total energy as a sum of the interaction energies between the individual atoms. The interaction energies, in turn, are derived from a suitable interatomic potential function.

The many-bodied system is then adjusted (relaxed) until a minimum energy configuration is found. In a number of cases, efforts have been made to compare calculated results characteristic of the boundary, i.e., energy, relative crystal displacement $\vec{R}$ [8,12], X-ray structure factor [13], etc., with experimentally measured results for certain selected boundaries. Reasonable agreement has usually been obtained lending credence to the computer simulation method.

So far, the results have verified the conclusion that the given boundary core is relatively narrow. The work [12,14,15] has also revealed the existence of a limited number of basic structural units in a wide range of boundaries. These correspond to compact polyhedra of atoms (see Fig. 2) which are similar in many respects to the close packed polyhedra found in Bernal's [16] model of a liquid. However, the compact polyhedra are not generally completely close packed but consist of compact clusters arranged so that an additional atom cannot be inserted into them. The simulation results have also aided our understanding of the "crystallography of grain boundaries" and the significance of such concepts as the density of coincidence sites (see Section 1.2 below) and the possible degeneracy of grain boundary structures [8,9].

Despite the very substantial and important contributions which have been made by computer simulation, a number of problems have persisted. These include the following:

(i) simplified 2-body central force approximations are generally used;

(ii) interatomic potentials are often used which are strictly empirical and which lack a sound theoretical base;

(iii) difficulties have arisen in avoiding metastable states and finding true equilibrium configurations;

(iv) the calculations have usually been made with static models which neglect the effects of lattice vibrations and entropy;

(v) the calculations have all been made on special grain boundaries with structures of short wave length periodicity (see Section 1.2 below) in order to avoid large ensembles.

1.2 Special Boundaries and Boundary Energy

Both experimental work and computer simulation show that many particular boundaries exist which possess relatively low energy. These low energy boundaries often, but not always, possess ordered atomic structures (with short wave length periodicities) due to relatively good atomic matching (i.e., periodic coincidence) of the lattices across the boundary. Boundaries with significant periodic structure have usually been called "special" boundaries and can be described locally by

ordered arrays of the compact polyhedra mentioned in Section 1.1. These boundaries have also been classified further [17] according to the type of periodic matching which is present, i.e.,

(i) CSL (Coincidence Site Lattice) matching: in this case the two adjoining crystals exhibit matching in three dimensions, and a fraction of their atoms falls on a 3-dimensional coincidence site lattice [18].

(ii) NCSL (Near Coincidence Site Lattice) matching: in this case 2-dimensional lattice matching is achieved across the boundary plane when suitable atomic nets exist on the crystal faces adjoining the boundary which almost match in size and shape. Exact coincidence is then obtained by applying stresses which can then be canceled by a network of suitable grain boundary dislocations (GBDs).

(iii) PM (Plane Matching): in this case 1-dimensional matching is obtained when stacks of identical and relatively low {hkl} planes in each of the two crystals adjoining the boundary intersect the boundary in sets of traces which match in spacing and direction. Any mismatch is forced into narrow lines (GBDs) which bear a close relationship to the Moiré pattern produced by the unrelaxed planar traces.

As pointed out above, short wave length periodicity is not a reliable criterion for low boundary energy [17,19], and other particular boundaries in addition to many special boundaries possess relatively low energy. Evidently, other factors such as the electronic energy and further aspects of the atomic arrangement must frequently be important. In general, at the present time we have no simple and universal structural rules for predicting low energy boundaries.

1.3 Secondary Relaxations (Collective Relaxations)

Many boundaries with crystal misorientations near misorientations corresponding to those of special boundaries of relatively low energy relax into "fit/misfit" structures consisting of patches of the special boundary plus arrays of GBDs [2,3,5-7]. The GBD array therefore compensates for the deviation from the low energy orientation in much the same way as a low angle grain boundary dislocation network compensates for the small crystal misorientation of such a boundary. These boundaries therefore tend to exist near the curves of $E = E(\theta)$ curves where E = grain boundary energy and θ = misorientation angle. A major problem at present is the fact that criteria for the existence of these structures are not well established and that we have little reliable information about the range of conditions over which these fit/misfit structures are stable [7].

1.4 Facet and Ledge Structures

In many cases the energy of the boundary depends upon the orientation of the boundary plane, and there is a tendency for the boundary to break up into a structure containing facets or ledges. This phenomenon is not understood quantitatively at present, since well established criteria are not available for predicting the boundary energy as a function of the orientation of the grain boundary plane [19].

2. DEFECT STRUCTURE OF GRAIN BOUNDARIES

2.1 Point Defects (Vacancies and Interstitials)

No reliable calculations have been made of the structure and energies of point defects (vacancies or interstitials) in grain boundaries. It is not known whether such defects remain localized when they are formed in the boundary or whether they dissociate over a relatively larger volume (particularly in non-special boundaries).

The binding energy of such defects to the grain boundary is therefore unknown, as is the rate at which they might diffuse (extended or not). The binding energies of point defects in grain boundaries of ceramic materials is of unusual importance and complexity as these defects control the boundary electrical charge which influences solute segregation, migration and possible other phenomena.

2.2 Line Defects (Grain Boundary Dislocations [GBDs])

GBDs are known to exist in a wide range of special boundaries [2, 3, 5, 6, 7]. A schematic diagram of such a GBD is shown in Figure 3. Grain boundary ledges are often associated with such dislocations [20] as may be seen in Fig. 3. These defects may be either intrinsic (i.e., part of the equilibrium boundary structure, Section 1.3) or extrinsic (i.e., excess nonequilibrium defects).

The Burgers vectors of such GBDs tend to decrease in magnitude as the boundary becomes less special (i.e., less ordered and of longer periodicity). At some point, as boundaries become less special, the Burgers vectors become sufficiently small so that the corresponding dislocations become physically insignificant, and the concept of GBDs is then lost.

It has also been postulated that the GBD core width increases as the boundary becomes less special, and the Burgers vector decreases. However, this point is controversial at present, and is an important unresolved question. In any case, it is known that GBDs become less well defined as the boundary becomes less special and that they cannot be detected (by electron microscropy, for example) in nonspecial boundaries.

2.3 Solute Atoms

From the standpoint of solute atom segregation, grain boundaries are highly complex defects which possess widely varying structures and a wide variety of sites which may be attractive to solute atoms.

In a recent review of segregation at grain boundaries, Balluffi [7] reached the following conclusions:

(i) a wide range of segregation behavior may be expected ranging from relatively simple situations where the segregating atoms adopt the basic structure of the host boundary to complex situations where the segregation produces a new structure in the boundary core; the latter situation is most likely in the case of non-special

boundaries in the presence of a high concentration of strongly interacting solute atoms;

(ii) measurements of the extent of grain boundary segregation confirm the existence of a wide range of behavior as suggested above; situations range from highly dilute segregates to the formation of multi-layered segregates and possible 2-dimensional ordered compounds;

(iii) a number of different types of observations indicate that the degree of segregation often varies between boundaries and therefore depends upon the boundary structure. There is experimental evidence that the degree of segregation to special boundaries tends to be lower than to non-special boundaries;

(iv) ambiguous results exist regarding the magnitudes of the variations in the degree of segregation which may occur at different boundaries in typical polycrystalline materials;

(v) no really adequate systematic and quantitative studies have been made of the relationship between grain boundary structure and segregation over a range of thermodynamic conditions; also, no detailed determinations of the atomic structure of grain boundary segregates have been made.

3. DIFFUSION AT GRAIN BOUNDARIES

It is well established that atomic diffusion and mass transport are relatively rapid along grain boundaries and that they generally act as diffusion "short circuits". The diffusivity spectrum for metals [22] is shown in Fig. 4 using a reduced reciprocal temperature scale. The results show rather clearly that

$$D_S > D_{GB} > D_L$$

where D_S = surface diffusivity, D_{GB} = grain boundary diffusivity, and D_L = lattice diffusivity.

However, measurements of grain boundary diffusivities are generally of relatively low accuracy as seen, for example, from the large scatter of the data for metals [23] in Fig. 5 where a reduced reciprocal temperature scale has again been used.

Satisfactory measurements of the "chemical diffusivities" of solute atoms are particularly lacking. The results are usually not corrected for segregation effects, and little information is available regarding the diffusion rates of the individual species involved, i.e., the "intrinsic" chemical diffusivities, and the compositional dependence of the diffusion.

Only a few measurements of diffusivity versus type of boundary have been made [24]. No satisfactory general rules relating the diffusion rate to the boundary type have been established. Negligible information is available regarding the possible anisotropy of diffusion in boundaries.

The atomic mechanism of grain boundary diffusion is not established. The important relationship between mass transport along grain boundaries (motivated, say, by stress) and measurements of tracer self-diffusion rates is not clearly established.

Grain boundary diffusion rates in a number of important systems have not yet been measured. For example, the important question of whether small interstitial atoms (such as carbon atoms in iron) diffuse faster, or slower, in grain boundaries or the lattice is not yet answered.

Finally, we remark that grain boundary diffusion rates may be strongly influenced by the presence of impurities and other solute atoms. Recent evidence [25] indicates that diffusive transport is often enhanced by orders of magnitude by additions of second elements which form low melting eutectics. The evidence is unclear whether this results from solute enhancement of the grain boundary diffusivity by several orders of magnitude or from solid "carrier" phases along the boundaries which have high diffusivities.

4. GRAIN BOUNDARIES AS SOURCES/SINKS FOR POINT DEFECTS

Grain boundaries as sources/sinks for point defects have been discussed recently by Balluffi [26] and Gleiter [27].

Non-special boundaries in pure metals appear to act as good vacancy sources/sinks at point defect chemical potentials as low as 10^{-3} - 10^{-5} ev. There are indications [28] that boundaries in many ceramic materials may not be comparably efficient and that the efficiency may be relatively low at defect potentials as high as 10^{-3} ev.

The sink efficiencies of special boundaries in metals appear to be lower than those of non-special boundaries particularly at low point defect chemical potentials.

Special boundaries act as point defect sources/sinks by a mechanism involving the climb of GBDs in the boundary plane.

The mechanism by which non-special boundaries act as highly efficient sources/sinks is not well understood at present, nor are the differences which make boundaries in ceramics less efficient. It seems possible that point defects dissociate in non-special boundaries, and that a vacancy entering such a boundary is eliminated by a general collapse process spread over an appreciable volume [26]. This process is similar to the dissociation and collapse of a vacancy in amorphous bulk material which has been demonstrated recently [29, 30].

Fine dispersions of hard particles appear to lower the source/sink efficiency of boundaries and hence inhibit the rate of diffusional creep [31]. Although this behavior has been interpreted in terms of particle inhibition of GBD climb detailed understanding is lacking.

5. GRAIN BOUNDARY MIGRATION

There is extensive evidence [32] that the rate of grain boundary migration is often controlled by the rate at which solute atoms, bound to the core, are able to migrate along with the boundary. The rate of grain boundary migration in many materials is therefore expected to be a complex function of a number of variables such as solute atom concentration, solute atom diffusivity, intrinsic boundary mobility, temperature and driving force. An example of the effect of solute content on the grain boundary mobility is shown in Fig. 6 [33].

In a few cases, migration has been studied in ultra pure materials in the absence of strong impurity effects [32]. Even in this case the mechanism for migration is not yet determined. A popular atomistic model [34] has involved the loss of atoms from the shrinking crystal to the boundary and the diffusion of these atoms in the boundary to points where they join the growing crystal. Evidence has been claimed [34] for the widespread existence of dissolution/growth GBD spirals as the points where atoms are removed from the shrinking crystal or added to the growing crystal. This would seem possible for special boundaries but unrealistic for non-special boundaries which, as pointed out above in Section 2.2, cannot support physically significant GBDs. As usual, our lack of information about the structure (and defect structure) of non-special boundaries makes it difficult to model and understand a complex phenomenon such as grain boundary migration.

In general, it has been particularly difficult to measure grain boundary mobilities for specified boundaries under known driving forces. There is some evidence [32] that the mobilities of special boundaries are greater than those of non-special boundaries, and it has been suggested that this may be due to the fact that special boundaries have a smaller interaction with impurities than non-special boundaries. However, this point of view is controversial [35]. It has also been found [35] that boundaries formed by a 41-42° rotation around [111] have an unusually high mobility in aluminum. This boundary has no obvious special structural features, and the cause of this high mobility therefore remains unknown.

6. DISLOCATION PHENOMENA AT GRAIN BOUNDARIES

6.1 Grain Boundaries as Lattice Dislocation Sinks

When lattice dislocations impinge on grain boundaries they generally tend to dissociate into GBDs possessing smaller Burgers vectors [36, 37]. When the boundary is a special boundary the product GBDs have sufficiently large Burgers vectors to remain as physically distinguishable GBDs. However,

when the boundary becomes less special the Burgers vectors become smaller and the product GBDs become less well defined. In the limit of vanishingly small Burgers vectors, the formal model of dissociation into indistinguishable GBDs becomes formally equivalent to a uniform core-spreading model, since a uniform spreading can be well represented by a distribution consisting of an infinite number of GBDs possessing infinitesimal Burgers vectors.

The rate of the dissociation depends upon whether the product GBDs are glissile or sessile in the boundary plane. When the GBDs are all glissile the dissociation occurs rapidly without thermal activation. When climb is required thermal activation is required, and the process becomes much slower. No quantitative studies of the kinetics of this process have yet been reported.

6.2 Grain Boundaries as Lattice Dislocation Sources

It has been pointed out that grain boundaries may act as sources of lattice dislocations under certain circumstances [38, 39]. Rather casual observation has shown that lattice dislocations are often emitted at regions of high stress concentration such as at ledges. However, systematic studies of this phenomenon have not yet been carried out.

6.3 Grain Boundary Sliding

It has often been proposed that the important phenomenon of grain boundary sliding occurs as a result of the movement of GBDs. Models based on the movement of either intrinsic GBDs or extrinsic GBDs have been suggested [40].

It has also been proposed that sliding occurs by a mechanism in which lattice dislocations from the grain interiors are held up at the boundary and cause sliding by a combination of climb and glide in the boundary plane [41].

Models based on GBD movement appear to be realistic for special boundaries where GBDs are well defined entities. However, such models become poorly defined for non-special boundaries because of our inadequate understanding of the structure of conceivable line defects in such boundaries (see Section 6.1).

In general, we may conclude that present models for sliding are inadequate, particularly for non-special boundaries.

7. ATOMIC BONDING AND COHESION AT GRAIN BOUNDARIES

It is well known experimentally that preferential brittle fracture often occurs along grain boundaries. However, very little is known at the basic level about the atomistic nature of bonding and cohesion at grain boundaries, and of the brittle versus ductile behavior of sharp cracks [42] at boundaries. The problem of dealing with the separation of the two grains at the grain boundary should be intimately connected with the grain boundary structure and energy. Apparently, no fundamental treatments of this problem exist.

It is also well known that solute atom segregation can play an important role in this phenomenon. Of special importance, therefore, would be experi-

mental and theoretical information about the effect of grain boundary segregation on intergranular cohesion. A theoretical approach to this problem may be feasible using the grain boundary model consisting of compact polyhedral groups of atoms (see Section 1.1) in conjunction with self-consistent-field cluster molecular-orbital model techniques in current use [43]. In this approach an impurity atom can be inserted in the grain boundary polyhedral group (i.e., cluster) and a full quantum mechanical calculation of the electronic states can then be made.

8. NON-EQUILIBRIUM PROPERTIES OF GRAIN BOUNDARIES

It is known that large increases in the density of extrinsic GBDs occur in special grain boundaries during plastic deformation at low and intermediate temperatures. There is also evidence that this defect structure anneals out rather abruptly at more elevated temperatures by a process which might be called "grain boundary recrystallization" by analogy with the well known phenomenon of lattice recrystallization [44]. It seems conceivable that an extrinsic defect structure of some sort may also build up and anneal out in plastically deformed and annealed non-special boundaries. No systematic studies have been made of the energetics or kinetics of such recovery processes.

It has been suggested by at least several workers that non-equilibrated boundaries may have physical properties which differ appreciably from corresponding properties characteristic of the equilibrated state. Presumably such effects would be due to the presence of an extrinsic defect structure. Specifically, evidence has been claimed that diffusion rates along migrating boundaries can be orders-of-magnitude greater than along corresponding stationary boundaries in a more equilibrated state [45, 46]. It has also been proposed that boundaries which have absorbed excess vacancies or lattice dislocations behave differently than well equilibrated boundaries [47]. In a number of these experiments questions of interpretation remain, and further more conclusive investigations regarding possible non-equilibrium effects would be desirable.

9. TECHNIQUES FOR STUDYING GRAIN BOUNDARIES

The relatively recent development of powerful high resolution electron optical microscopic and micro-analytical techniques has produced a renaissance in the field of grain boundary research. It is now becoming possible to study details of the atomic structure and local chemistry which were unobservable previously. Techniques of value include, for example:

(i) high resolution electron microscopy;

(ii) scanning transmission electron microscopy;

(iii) scanning Auger spectroscopy.

It has recently been demonstrated that electron and X-ray diffraction patterns can be obtained from the relatively small number of atoms in the grain boundary core [48]. It therefore seems feasible to carry out grain boundary structural determinations using standard diffraction methods. The use of high intensity synchrotron radiation for this purpose in the near future could lead to rapid progress.

Modern developments in atom probe—field ion microscopy have produced instruments [49] which should make possible detailed studies during field evaporation of the distribution of segregated atoms at grain boundaries. So far, this technique has not been seriously applied to the problem although it seems to be a promising possibility.

Large scale computer simulation studies of greater reliability are becoming increasingly feasible as computer capability becomes cheaper and more convenient.

The use of these techniques, in conjunction with properly designed experiments, should lead to continued progress in the field.

ACKNOWLEDGMENTS

The writer would like to thank the various members of the Subgroup on Grain Boundary Structure and Properties for a number of helpful suggestions which were useful in preparing the final version of the present, necessarily brief review. Members of this group include R.M. Cannon, D.R. Clarke, A.H. Heuer, P.S. Ho, B.H. Kear, V. Vitek, J.R. Weertman, and C.L. White. This work was supported by the United States Department of Energy under Contract No. ER-78-S-02-5002.A000.

REFERENCES

(1) H. Gleiter and B. Chalmers, High Angle Grain Boundaries (Pergamon Press, New York, 1972).

(2) P. Chaudhari and J.W. Matthews (eds.), Grain Boundaries and Interfaces (North-Holland, Amsterdam, 1972).

(3) H. Hu (ed.), The Nature and Behavior of Grain Boundaries (Plenum Press, New York, 1972).

(4) Papers collected in Canad. Met. Quarterly 13 No. 1 (1974).

(5) Papers collected in J. de Physique, Supple. to 36, Colloque No. 4 (1975).

(6) G.A. Chadwick and D.A. Smith (eds.), Grain Boundary Structure and Properties (Academic Press, New York, 1976).

(7) R.W. Balluffi, in Interfacial Segregation, ed. by W.C. Johnson and J.M. Blakely (American Society for Metals, Metals Park, Ohio, 1979).

(8) R.C. Pond and V. Vitek, Proc. Roy. Soc. London A 357, 453 (1977).

(9) R.C. Pond, Proc. Roy. Soc. London A 357, 471 (1977).

(10) S. Ranganathan, in Field Ion Microscopy, ed. by J.J. Hren and S. Ranganathan (Plenum Press, New York, 1968) p. 137.

(11) O.L. Krivanek, S. Isoda & K. Kobayaski, Phil. Mag. 36, 931 (1977).

(12) D.A. Smith, V. Vitek and R.C. Pond, Acta Met. 25, 475 (1977).

(13) P.D. Bristowe and S.L. Sass, work in progress, private communication.

(14) M.F. Ashby, F. Spaepen and S. Williams, Acta Met. 26, 1647 (1978).

(15) R.C. Pond, D.A. Smith and V. Vitek, Acta Met. 27, 235 (1979).

(16) J.D. Bernal, Proc. Roy. Soc. A 280, 299 (1964).

(17) See, for example, R.W. Balluffi, P.J. Goodhew, T.Y. Tan and W.R. Wagner, J. de Physique, Supple. to 36, Colloque C4, C4-17 (1975).

(18) W. Bollmann, Crystal Defects and Crystalline Interfaces (Springer-Verlag, New York, 1970).

(19) P.J. Goodhew, T.Y. Tan and R.W. Balluffi, Acta Met. 26, 557 (1978).

(20) J.P. Hirth and R.W. Balluffi, Acta Met. 21, 929 (1973).

(21) H. Gleiter, Phil Mag. 36, 1109 (1977).

(22) N.A. Gjostein, in Diffusion (American Society for Metals, Metals Park, Ohio, 1973) p. 241.

(23) J.C.M. Hwang and R.W. Balluffi, Scripta Met. 12, 709 (1978).

(24) G. Martin and B. Perraillon, J. de Physique, Supple. to 36, Colloque C4, C4-165 (1975).

(25) R.L. Coble and R.M. Cannon, in Processing of Crystalline Ceramics, ed. by H. Palmour III, R.F. Davis and T.M. Hare (Plenum Publ. Corp., 1978) p. 151.

(26) R.W. Balluffi, Proc. of the Conference on Fundamental Aspects of Radiation Damage in Metals (National Technical Info. Service, U.S. Dept. of Commerce, Springfield, VA 22161, 1975) p. 852.

(27) H. Gleiter, Acta Met. 27, 187 (1979).

(28) R.M. Cannon, W. H. Rhodes and A. H. Heuer, in press, J Amer. Ceramic Soc: B. Burton and G.L. Reynolds, Acta Met. 21, 1073 (1973); 21, 1641 (1973).

(29) F. Spaepen, Technical Report No. 4, Office of Naval Research Contract N00014-77-C-0002 NR-039-136, Harvard University, May 1978.

(30) C.H. Bennett, P. Chaudhari and V. Moruzzi, to be published.

(31) B. Burton, in Vacancies '76, ed. by R.E. Smallman and J.E. Harris (The Metals Society, London, 1977) p. 156.

(32) C.J. Simpson, W.C. Winegard and K.T. Aust, in Grain Boundary Structure and Properties, ed. by G.A. Chadwick and D.A. Smith (Academic Press, New York, 1976) p. 201.

(33) J.P. Drolet and A. Galibois, Met. Trans. 2, 53 (1971).

(34) H. Gleiter, Acta Met. 17, 565 (1969): 17, 853 (1969).

(35) K. Lucke, Canad. Met. Quarterly 13, No. 1, 261 (1974).

(36) R.C. Pond and D.A. Smith, Phil Mag. 36, 353 (1977).

(37) T.P. Darby, R. Schindler and R.W. Balluffi, Phil. Mag. A 37, 245 (1978).

(38) J.P. Hirth, Met. Trans. 3, 3047 (1972).

(39) T. Malis and K. Tangri, Acta Met. 27, 25 (1979).

(40) See, for example, R.C. Pond, D.A. Smith and P.W.J. Southerden, Phil. Mag. A 37, 27 (1978).

(41) See, for example, T. Wanatabe and P.W. Davies, Phil. Mag. A 37, 649 (1978).

(42) J.R. Rice and R. Thomson, Phil, Mag. 29, 73 (1974).

(43) J.C. Slater and K.H. Johnson, Phys. Rev. B5, 844 (1972): K.H. Johnson and F.C. Smith, Jr., Phys. Rev. B5, 831 (1972): J.C. Slater and K.H. Johnson, Physics Today 27, 34 (1974).

(44) A.R. Jones, P.R. Howell and B. Ralph, Phil Mag. 35, 603 (1977).

(45) M. Hillert and G.R. Purdy, Acta Met. 26, 333 (1978)

(46) K. Smidoda, W. Gottschalk and H. Gleiter, Acta Met. 26, 1833 (1978).

(47) P.H. Pumphrey and H. Gleiter, Phil. Mag. 32, 881 (1975).

(48) S.L. Sass, Electron Microscopy 1976, Proc. of the Sixth European Congress on Electron Microscopy, Vol. 1, ed. by D.G. Brandon (Tal International Publ. Co., Israel, 1976) p. 221.

(49) T.M. Hall, A. Wagner and D.N. Seidman, J. of Phys. E 10, 884 (1977).

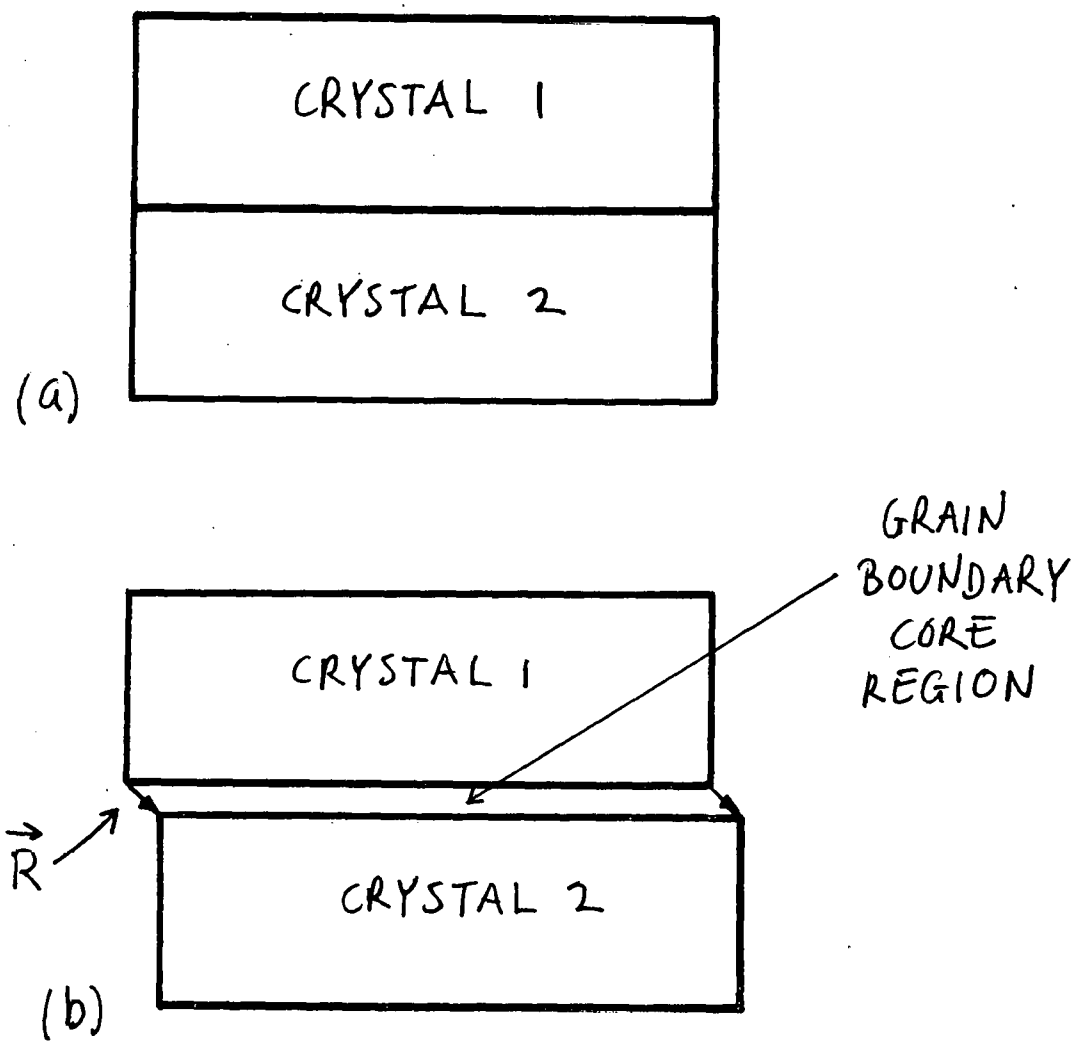

Fig. 1 Construction of grain boundary. (a) Crystals placed rigidly together in standard reference position. (b) Bicrystal after relaxation of configuration in (a).

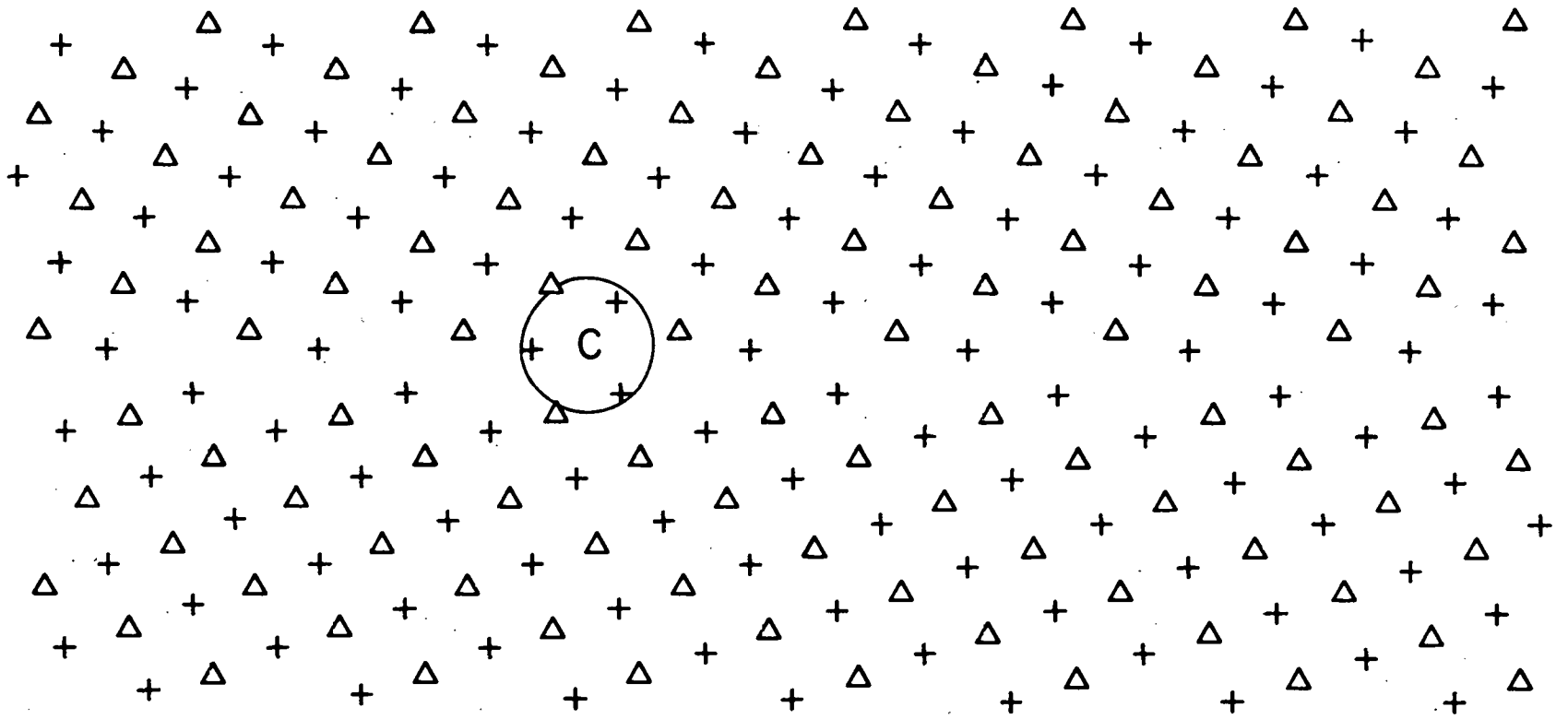

Fig. 2 Computer simulated structure of [001] tilt boundary in aluminum. Tilt angle = 36.9°. Compact polyhedron at C. (from Ref. 12)

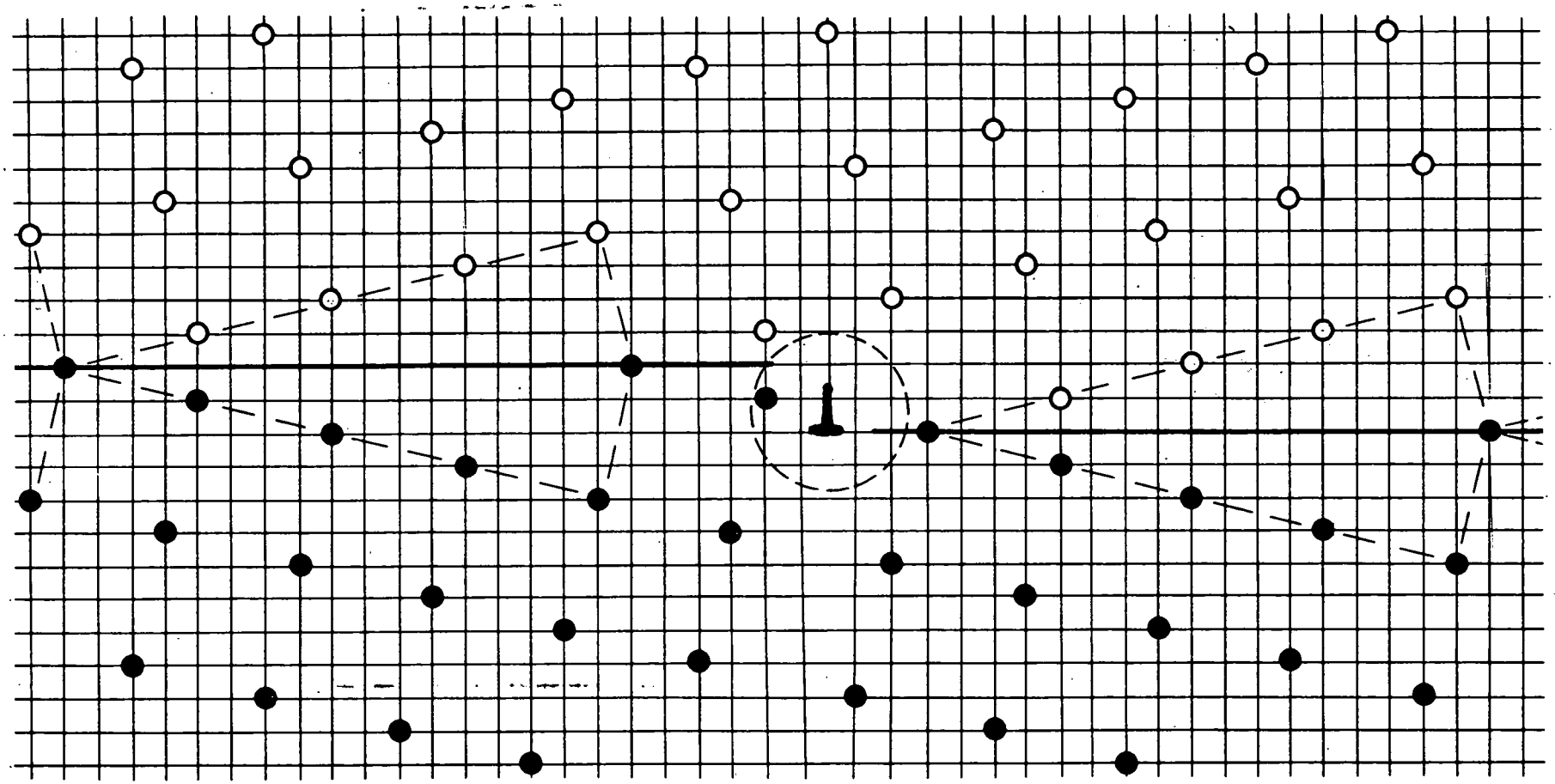

Fig. 3 Grain boundary edge dislocation in tilt boundary formed by rotating cubic crystals with respect to one another around [001] by 28.1°. Dislocation core encircled.

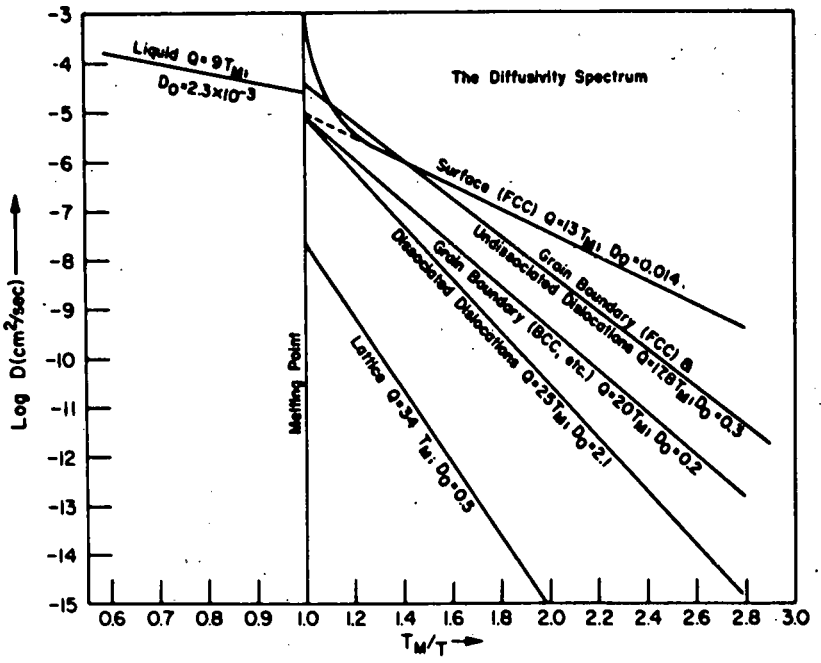

Fig. 4 Diffusivity spectrum for metallic solids and liquids. T_M = melting temperature (K). Curves represent average data. (from Ref. 22)

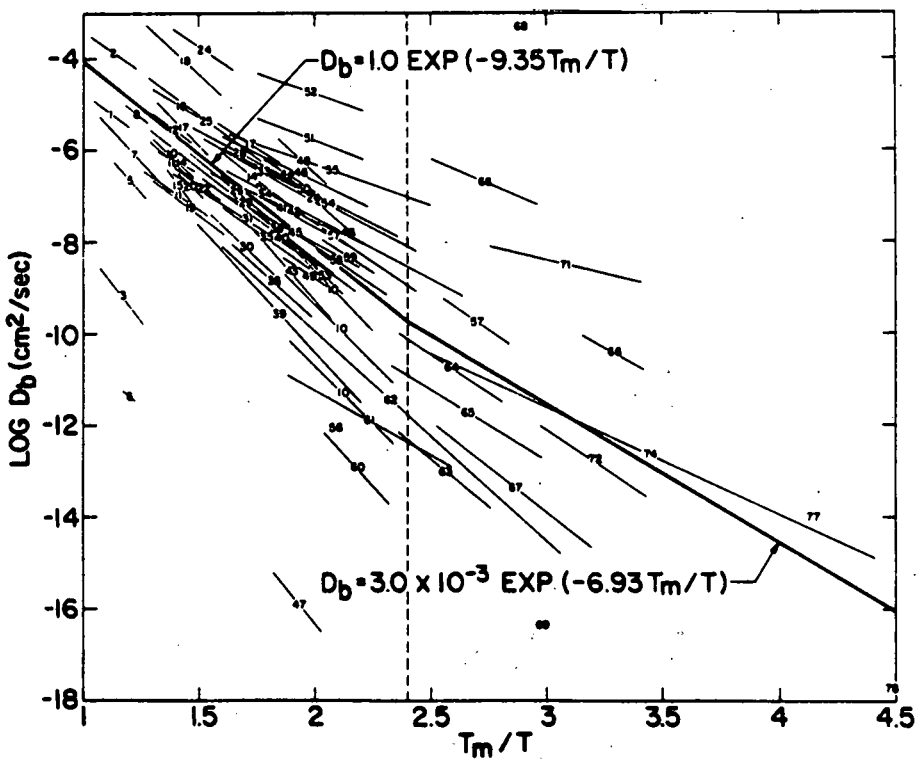

Fig. 5 Arrhenius plot of all presently available grain boundary diffusivities in polycrystalline metals. Numbers indicate the references listin [23]. (from Ref. 23.)

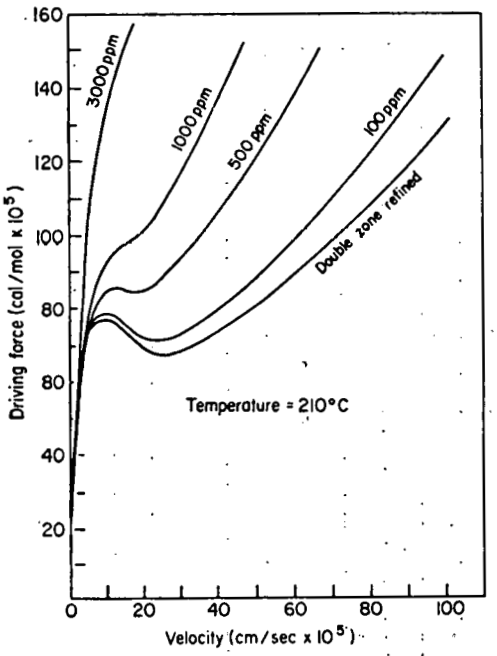

Fig. 6 Driving force versus grain growth velocity for zone-refined lead containing various tin additions. (from Ref. 33.)

DEFORMATION ASPECTS OF TIME DEPENDENT FRACTURE

*Che-Yu Li** - Dept. of Materials Science and Engineering, Cornell University, Ithaca, NY 14853
*A. P. L. Turner*** - Materials Science Division, Argonne National Laboratory, Argonne, IL 60439
Dwight R. Diercks - Dept. of Materials Sciences, Southwest Research Inst., 6220 Culebra Road, San Antonio, TX 78284
Campbell Laird - Dept. of Metallurgy and Materials Science, University of Pennsylvania, Philadelphia, PA 19104
Terence G. Langdon - Dept. of Materials Science, University of Southern California, University Park, Los Angeles, CA 90007
William D. Nix - Department of Materials Science and Engineering, Stanford University, Stanford, CA 94305
Robert Swindeman - Metals and Ceramics Division, Oak Ridge National Laboratory, Oak Ridge, TN 37830
W. G. Wolfer - Department of Nuclear Engineering, University of Wisconsin, Madison, WI 53211
David A. Woodford - Corporate R&D Center, General Electric Company, Box 8, Schenectady, NY 12301

1. INTRODUCTION

For all metallic materials, particularly at elevated temperatures, deformation plays an important role in fracture. On the macro-continuum level, the inelastic deformation behavior of the material determines how stress is distributed in the body and thus determines the driving force for fracture. At the micro-continuum level, inelastic deformation alters the elastic stress singularity at the crack tip and so determines the local environment in which crack advance takes place. At the microscopic and mechanistic level, there are many possibilities for the mechanisms of deformation to be related to those for crack initiation and growth.

At elevated temperatures, inelastic deformation in metallic systems is time dependent so that the distribution of stress in a body will vary with time, affecting conditions for crack initiation and propagation. Creep deformation can reduce the tendency for fracture by relaxing the stresses at geometric stress concentrations. It can also, under suitable constraints, cause a concentration of stresses at specific loading points as a result of relaxation elsewhere in the body. A combination of deformation and unequal heating, as in welding, can generate large residual stress which cannot be predicted from the external loads on the body. On the other hand, acceleration of deformation by raising the temperature can be an effective way to relieve such residual stresses, for example, by a post-weld heat treatment. The effectiveness of such treatments depends in part on a knowledge of the temperature dependence of deformation rates. In a nonconstant temperature environment, deformation accompanying temperature changes can aggravate thermal stresses and set up cyclic stresses to produce thermal fatigue.

---

*Subgroup Chairperson
**Subgroup Cochairperson

Since any analysis of fracture in a part must involve a knowledge of the stresses acting to cause the fracture, an inelastic stress analysis of the part will always be required. This analysis can only give reliable results to the extent that deformation behavior of the material can be accurately described in the temperature range of interest.

On the microscopic continuum level, on a size scale comparable to the crack tip stress field, deformation plays a similar role. Plastic and time dependent creep deformation, localized in the crack tip region, cause a redistribution of the crack tip stresses. In general as the inelastic strains increase, the peak stresses are reduced, but the influence of the crack tip is extended to larger distances. Any attempts to establish the local stress or strain criteria for crack advance will require that the time dependent stress and strain distributions around the crack tip be established. In many cases of interest, the rate of crack growth may be comparable to that for stress relaxation by creep. In such a case, the inelastic analysis required to determine the local stress and strain distributions is complicated by the fact that the boundary of the body does not remain fixed. An additional complication arises if voids are growing in the crack tip stress field ahead of the crack. Clearly this most general problem is very formidable, but such a problem must eventually be analyzed if correlations of time dependent fracture, with quantities such as the stress intensity factor, K_I, or the J integral are to be justified. Similarly an accurate description of local crack tip conditions is required before one can determine whether the criterion for crack advance is more closely related to the crack tip stress or the crack opening displacement.

At the microscopic and mechanistic level of understanding of fracture, there are a number of possible connections between deformation and fracture. Inhomogeneous modes of deformation such as grain boundary sliding or concentration of slip into shear bands are often cited as mechanisms for producing high local stresses as for example, around grain boundary precipitates or at the intersection of shear bands with grain boundaries. The high local stresses are in turn assumed to be responsible for the nucleation of voids eventually leading to fracture. It has been suggested that absorption of slip dislocations by grain boundaries creates a boundary structure which can nucleate voids without requiring boundary precipitates or a structure which is a more efficient source of the vacancies required for cavity growth by diffusion. Generation of excess vacancies within the grains by moving jogged dislocations has also been suggested as a source of vacancies for cavity growth, particularly when cyclic deformation is involved. Creation of new surface by localized shear at the crack tip is certainly one mechanism of crack growth in fatigue and may be important in static time dependent fracture. Creation of fresh reactive surfaces and disruption of oxide coatings by slip bands emerging from surfaces at a crack tip are mechanisms of crack propagation which are often mentioned for cases where an aggressive environment is present. Understanding interactions between deformation and fracture at this microscopic level will require that the microscopic mechanisms of deformation are also understood. Such an understanding requires knowledge of deformation on an entirely different scale than that required for continuum calculations where only averages over many grains are important.

Based on the above general considerations, the following four research areas in deformation are identified as particularly important for basic research and will be discussed separately. They are:

Deformation Properties
Nature of Damage
Constitutive Equations
Crack Tip Problems

2. DEFORMATION PROPERTIES

Research on deformation properties is required to provide a mechanistic basis for the development of constitutive equations for the calculation of the distribution of stress at the continuum level. It is also required to provide an understanding of the nucleation and growth of cracks and cavities at the microscopic level. The following research topics are considered to be high priority items.

2.1 Heterogeneous Modes of Deformation

In terms of its importance to high temperature fracture processes, grain boundary sliding is the most important heterogeneous mode of deformation and deserves special attention. Grain boundary sliding is known to play a key role in the nucleation and growth of grain boundary cavities and cracks. Some theoretical progress has been made in recent years on defining the mechanisms of grain boundary sliding.[1,2] Accurate experimental data are needed to test the validity of these theoretical concepts and to provide the basis for extending and improving the theories. Careful experiments are needed in a number of areas. The basic mechanisms of grain boundary sliding should be investigated in pure polycrystals. The role of grain boundary particles must be investigated in a carefully controlled way in order to provide a basis for the understanding of the behavior of engineering materials. For example, it is still undetermined whether grain boundary particles are advantageous because they hinder sliding, or are deleterious because they cause stress concentrations and nucleate cavities. The importance of particle coherency, and of segregation of impurities to grain boundaries and particle interfaces also remains to be determined.

The nature of the stress and strain concentrations that result from heterogeneous modes of deformation and their role in fracture processes are important areas that should be emphasized. For example, the build up and relaxation of stresses at triple points is important not only for crack and cavity nucleation, but also in controlling growth rates. A clearer understanding of the distribution and strength of the stress and strain concentrations that result from deformation at elevated temperature is essential to reaching an understanding of the basic mechanisms of cavitation and fracture.

In spite of the fact that cavitation at grain boundaries has been recognized as an important mechanism of high temperature rupture for many years, a theory for nucleation of these cavities which agrees with experiment

does not exist. Theories for nucleation at particles are often found to be in error by several orders of magnitude. A possible explanation for these discrepancies is that local stresses were not properly accounted for. Progress in this area can probably be achieved by experiments on materials with well characterized deformation behavior and under conditions where stress concentrations can be properly taken into account.

Other heterogeneous modes of deformation including shear localization, anelasticity, and various modes of discontinuous flow also require further investigation. A quantitative description of the role of shear localization in crack nucleation at the surface and at grain boundaries is presently lacking. Similar situations exist in theoretical modeling of various modes of discontinuous flow.

2.2 Mechanisms of High- and Low-temperature Deformation

Although a mechanistic understanding exists of certain modes of deformation that operate in some temperature regimes, a unified description of high- and low-temperature deformation is not available and is urgently needed. In the homologous temperature range 0.3-0.5 T_m (T_m = absolute melting temperature) where many engineering materials are used, a number of mechanisms may contribute to deformation. These processes include grain boundary sliding and both dislocation glide and dislocation climb controlled processes. It is known also that the extent of the mix of these processes will vary with stress or strain rate and temperature. Present knowledge does not, however, allow a quantitative measure of the contribution of various deformation processes and how they change as a function of temperature and strain rate. The lack of a unified description of these deformation processes will hinder the development of accurate constitutive equations, especially for conditions where experimental data are not easily available.

A major need in both theoretical and experimental efforts is the identification and independent measurement of the various components of the total inelastic strain. For example, it is not presently possible to determine what portion of the strain in a creep test results from grain boundary sliding and what portion is from matrix deformation. It is not possible with present experimental methods to separate true plastic strain from recoverable anelastic strain. The lack of such information makes comparison of experiment with theory difficult and makes it very difficult to extrapolate experimental results to different temperatures or strain rates where the relative contributions of various mechanisms may be different.

The importance of understanding transient and cyclic effects in deformation should be emphasized. In most service conditions, even when stresses and temperatures are steady, the limitations on allowable strain require that the material always be in the transient creep regime. Furthermore, engineering materials are nearly always subjected to changes in stress and temperature which can introduce repeated transients. These changes can be monotonic or cyclic, and stress changes and temperature changes frequently occur in a coordinated way. In spite of their obvious importance, transient

effects on deformation have not been carefully studied. In spite of the widespread occurrence of creep-fatigue failure in service, fundamental studies of deformation phenomena in such situations are quite rare compared to studies on the fracture aspects. Most of the reported transient deformation is concerned with primary creep, cyclic creep (repeated tension loading at low homologous temperatures) and fatigue deformation (tension-compression loading at both low and high homologous temperatures). Material behavior under stress reversals where tensile ratcheting is occurring, where compressive excursions happen during creep in tension, etc. are rarely studied over the whole temperature range. Therefore, many of the constitutive equations existing today are not adequate under conditions where various combinations of temperature and stress transients occur.

2.3 Irradiation Effects

According to present understanding, irradiation creep is not simply an enhanced thermal creep mechanism. Therefore, it deserves special attention as a new deformation mechanism of fundamental and practical importance.

A few results reported in the literature[3] indicate that irradiation creep enhances the creep rupture life of materials. This effect counteracts the adverse effects of radiation hardening and embrittlement on post-irradiation ductility and post-irradiation creep rupture. Apart from the practical implications of this effect in fission and fusion reactors, irradiation creep offers an added dimension to investigate the interplay between bulk deformation in the grain, and grain boundary sliding and cavitation as processes involved in high-temperature failure.

Several mechanisms for irradiation creep have been proposed in the past. They can be categorized into

a) Climb-only mechanisms [stress induced preferential absorption (SIPA) on faulted loops and SIPA on dislocations].

b) Climb-controlled glide (climb may be either radiation- or stress-induced or both).

c) Glide-only mechanisms (Cottrell yielding, unfaulting of loops).

Virtually no work in the basic materials sciences has been done in the experimental area to identify or verify any of these proposed mechanisms. Theoretical modeling of microstructural evolution indicates that the dominant irradiation creep mechanism depends on the material, the irradiation temperature, and the fluence. In fact, it appears that there is a transition from a glide to a SIPA process as a function of fluence.

Three areas of research are deemed to be particularly worthy of further investigation:

1) Identification and verification of irradiation creep mechanisms by experimental methods in conjunction with theoretical support.

2) Investigations on the effect of irradiation creep and irradiation induced segregation and phase changes on grain boundary sliding and cavitation.

3) Investigations on the effect of irradiation creep on flow localization and plastic instability.

Among these three areas, the first two rank the highest. The third area, although no less important, requires that progress in the understanding of flow localization be made first or in parallel with research on irradiation creep.

2.4 Multiaxial Effects

Deformation under multiaxial loading has not been investigated extensively in the past in materials science, even though an engineering material is likely to experience this type of loading during service. Deformation phenomena which are observed only under multiaxial loading have been reported in the literature. For example, it has been shown experimentally that a thin wall tube will be elongated in the axial direction when it is deformed in the nonelastic range under torsion.[4] Extensive experimental effort is required to characterize those phenomena which are known and to discover new phenomena under conditions which have not been explored.

Some constitutive relations that have already been proposed may account for some unusual multiaxial behavior. At present, however, there has been insufficient experimentation or analytical application of the constitutive equations to such cases. It is clear that considerable experimental work is required for multiaxial loading. This is especially true for the rate dependent high temperature range.

At present most constitutive theory for multiaxial behavior is based on the J_2 isotropic plasticity theory of the von Mises type. Such theory is unable to describe the anisotropy associated with multiaxial straining. It may be that some of the mechanistic ideas from materials science may provide clues for developing more realistic constitutive equations, perhaps through the concept of internal stress.

3. NATURE OF DAMAGE

Damage in a material accumulated during service can be measured, for example, in terms of the number and size of grain boundary cavities and cracks. From a broader viewpoint, changes in the composition and microstructure of a material resulting from thermal and mechanical history with or without the presence of environmental effects can also be viewed as a form of damage because these changes can lead to the deterioration of the properties of a material. For both scientific and engineering interests it would be desirable if the extent and the rate of damage accumulation can be

correlated with deformation parameters such as stress, strain rate, temperature, etc., which characterize the service history of a material. This type of correlation will provide a useful basis for formulating the failure criteria in order to predict the useful life of a material. In the following the need of characterizing the various forms of damage from the above viewpoint will be discussed.

3.1 Nucleation and Growth of Cracks and Grain Boundary Cavities

It should be recognized that, in addition to grain boundary cavities and cracks, the nucleation and growth of surface cracks in the temperature range near 0.3 T_m and below are of technological interest. At these temperatures, linear fracture mechanics is not expected to be applicable because of the increased influence of nonelastic deformation at the crack tip while the structural component itself operates essentially in the elastic range. The growth of cracks in the pressure vessel of low alloy steels of a light water reactor under thermal stress cycles, the nucleation and growth of cracks in the heat-affected zone near a weld in the stainless steel pipes of a boiling water reactor, and the expected crack growth in the first wall of a tokamak type fusion reactor are examples of this type of time dependent fracture. It should be recognized also that under static loading and in a simulated boiling water reactor environment, laboratory tests have shown that the crack growth in an austenitic stainless will proceed in a discontinuous mode.

Since deformation at the crack tip is expected to play an important role in crack growth in the temperature range near 0.3 T_m and below, one would expect that the crack growth rate will be strongly dependent on the deformation parameters both at the macro-continuum level and the micro-continuum level at the crack tip.

It has been established that depending on the extent of incompatibility between grain boundary sliding and grain matrix deformation one can expect damage in the form of wedge type of grain boundary cracks at higher strain rates and damage in the form of grain boundary cavities at lower strain rates. Once the cavities and cracks are nucleated, their growth rate will depend on the magnitude of the local stress at the grain boundary and at the triple point. The incompatibility between grain boundary sliding and grain matrix deformation and the related stress concentration and relaxation in turn are controlled by the relative contribution of grain boundary sliding and grain matrix deformation to deformation which varies depending on the level of applied stress and temperature. Thus one is interested again in the deformation parameters at the macro-continuum level and at the micro-continuum level, for example, at the triple point, in order to establish a correlation between the rate of nucleation and growth of grain boundary cracks and cavities and the service condition of an engineering material.

3.2 Changes in Composition and Microstructure Due to Thermal and Mechanical Effects

Changes in composition and microstructure involve the grain boundary as well as the grain matrix. A great deal of different phenomena can occur in different systems:

a) In some, virtually no change occurs; TD nickel is an example of this, and there are others containing intermetallics which are not greatly affected.
b) Overaging frequently occurs, sometimes involving coarsening, sometimes the replacement of one metastable precipitate by another; in some cases, hardening can actually occur, in others, more usually, softening occurs.
c) Precipitate changes in association with localized shear is a particularly damaging problem in systems containing ordered precipitates. These can be disordered in cyclic conditions, or in association with tensile ratcheting, can be sheared off and weakened by cutting.
d) Dissolution is also a problem, especially in ferrous systems generally.
e) The combined effect of deformation and thermal aging can be important, for example, prior cold work will enhance precipitation during thermal aging both in the grain boundary and in the bulk in solution treated austenitic stainless steels.
f) Changes can be concentrated at the grain boundary, for example, the sensitization phenomena in austentic stainless steels and temper embrittlement phenomena in ferritic steels.

Many of the phenomena mentioned above are time dependent and are dependent also on the particular thermal and mechanical history of interest. They will in general, influence the deformation properties of a material. A quantitative description of the kinetics of many of these phenomena and their effects on deformation properties remains to be developed.

3.3 Changes in Composition and Microstructure Due to Environmental Effects

Chemical and irradiation environments are expected to be able to change significantly the composition and microstructure of a material. In a typical environment of a coal conversion plant, both decarburization and the formation of methane bubbles at the grain boundary will occur in a low alloy steel. The latter phenomena coupled with the influence of an applied stress can accelerate grain boundary damage. In a liquid metal environment, the decarburization of ferrous alloys and the oxidation of refractory metals have been reported extensively in the literature. In an irradiation environment, in addition to the well known microstructure changes produced by displacement damage, one should consider also the effects of irradiation induced segregation and precipitation at the grain boundary, the formation of helium bubbles at the grain boundary, as well as the effects of transmutation products which can be appreciable in fusion reactor environments.

The kinetics of some of the phenomena mentioned above have been reported in the literature. In general, they have not been studied in detail for the interests of deformation properties and time dependent fracture. It should be noted that research on the correlation between changes in microstructure and in mechanical properties are usually time consuming and costly. Attention should be given to the development of approaches which will improve the efficiency of the research and will allow the establishment of the limits of the effect of a given phenomenon for the interest of engineering design.

4. CONSTITUTIVE EQUATIONS

Constitutive equations are required to calculate the stress distribution and deformation, for example, at the macro-continuum level, in a structural component and at the micro-continuum level, at the crack tip and at grain boundary triple points. The various complexities of the deformation processes discussed previously suggest that it may be difficult to develop a unified set of constitutive equations that are applicable to a variety of materials for a wide range of deformation conditions and histories (temperature, stress, etc.). In the development of the required constitutive equations, one should keep in mind that the task will be easier and more effective if it is aimed at describing the deformation properties of a specific class of material and a specific range of application. Since these constitutive equations will be used in numerical calculations, it is essential that the form of the equations be such that they can be integrated efficiently.

An important part of the work on constitutive equations is the development of associated materials testing methods to provide the specific information needed in the constitutive laws. Some of the traditional approaches such as the creep test and low strain rate tensile test are time consuming. These traditional tests may not always be capable of providing all of the information necessary to characterize the material. For characterizing deformation properties for heat-to-heat variations and for alloy selection and development, it will be desirable if more efficient approaches are developed. Once the constitutive equations are developed and the materials parameters are measured, some meaningful benchmark tests should be devised to test their validity in the range of application of interest. Because the accuracy of the constitutive equations and their ability in data extrapolation depend strongly on their mechanistic and scientific basis, it is envisaged that improvement of the constitutive equations will be made on a continuous basis as improvements in our understanding of fundamental deformation processes occur.

5. CRACK TIP PROBLEMS

One of the most critical areas for future research is dealing with the processes which take place only in the high stress and strain concentrations that are found at the crack tip. It is well recognized that local deformation plays a crucial role in determining the conditions that prevail in the microscopic region at the tip of a crack. Therefore, an improved ability to deal with the crack tip region in a quantitative fashion will have substantial impact on increasing our understanding of fracture processes.

One area where substantial progress can be made is in improved calculations of the stress and strain fields of a crack in various materials. A great deal of effort has been spent in recent years in improving numerical methods used to solve problems associated with the crack tip singularity in nonelastic media. However, very few attempts have been made at applying the most advanced of the improved constitutive relations in crack tip problems. This is particularly true of the application of time dependent constitutive relations. Such calculations should allow improved estimates of local crack tip deformation, local stresses, and the energy dissipated during crack advance. These improvements should lead to a better understanding of the relationships between the driving force for crack extension and the rate of crack growth.

Most theoretical treatments of fracture treat the material as a homogeneous continuum. Therefore, they ignore any effects which are caused by the heterogeneous nature of the material microstructure. The evaluation of the importance of specific microstructural features such as surface films, voids, dispersed phases, etc., on the progress of fracture is an important area of materials science that needs investigation. This type of information is necessary in order to improve our understanding of fracture at a mechanistic level. It should improve our ability to handle fracture problems in situations outside the realm of applicability of continuum fracture mechanics.

A crucial step in improving our understanding of fracture processes on a microscopic and mechanistic level is a better characterization of the deformation environment at a crack tip. No matter how accurate continuum level constitutive equations become in describing bulk material behavior, they will not be able to deal with strain localization, and stress and strain distributions on a scale that is small compared to important microstructural size scales. Dealing with such problems will require understanding of deformation processes on a microscopic scale where continuum averaging is meaningless. As microscopic theories of deformation processes are developed, they should be applied along with improved constitutive relations for modeling of crack tip behavior.

6. SUMMARY

We have identified a number of areas in the field of deformation where basic research can have an impact on our understanding of time dependent fracture.

In the area of deformation properties, the role of heterogeneous deformation in nucleating cracks and voids appears to be of primary importance. Of the various modes of heterogeneous deformation, grain boundary sliding has the most direct effect on high temperature fracture. However, stress and strain concentrations that arise from all modes of nonuniform deformation are important in time dependent fracture.

Other areas where understanding is lacking and where basic research should have an impact are the unification of our understanding of deformation over the entire temperature scale, irradiation effects on deformation, and deformation under multiaxial states of stress. The lack of a unified description of deformation forces us to deal with a number of different modes of deformation separately, and limits our ability to predict behavior outside of the regime where experimental data exists. We are particularly limited in our ability to handle transient deformation. Irradiation introduces new modes of deformation that we are only beginning to understand. Because of the limited knowledge in the area of irradiation effects on deformation, basic research should have a considerable impact.

The area of multiaxial effects is largely unexplored. Because of its practical importance, the need to accumulate experimental data on multiaxial behavior in order to begin to identify the scope of multiaxial effects is recognized. On the other hand, it is also felt that an understanding of multiaxial behavior at the mechanistic level can only follow an improvement of our understanding of the basic mechanisms of uniaxial deformation.

In the area of deformation damage which leads to fracture, the most important need is to identify the various types of damage and to find ways of quantifying them. In characterizing damage, we feel that there is a need to recognize a number of changes in a material as "damage." Important changes that can lead to material degradation are the formation of cracks and cavities, changes in composition and microstructure resulting from thermal and mechanical effects, and changes in composition and microstructure resulting from environmental effects. The aim of research in this area should be to determine what types of damage are important in various materials and under what service conditions, and to quantitatively relate the accumulation of the damage to the service history of the material.

A continued improvement of constitutive equations for material behavior should be a goal of deformation research. Of primary importance in this area should be improvement of the mechanistic basis for constitutive laws so that their range of applicability can be clearly defined, and so that they can be used with confidence within this range.

Of direct importance to an understanding of fracture processes will be improved modeling of the crack tip region. The more realistic is the treatment of the deformation behavior in this critical region, the more likely we are to understand the basic mechanisms involved. More realistic treatments of crack tip problems can be achieved by using more accurate constitutive relations, by recognizing that materials have a heterogeneous microstructure, and by including the heterogeneous nature of deformation into crack tip models.

7. REFERENCES

1. E.W. Hart, Acta Met. 15, 1545 (1967).

2. F.W. Crossman and M.F. Ashby, Acta Met. 23, 425 (1975).

3. E.E. Bloom and W.G. Wolfer, "In-Reactor Deformation and Fracture of Austenetic Stainless Steels", ORNL/TM-6296, June 1978.

4. J.A. Bailey, S.L. Haas and K.C. Nawab, J. Basic Eng., Trans. ASME(D), 94, 231 (1972).

REPORT OF SUBGROUP ON HIGH TEMPERATURE FRACTURE

A. S. Argon, Massachusetts Institute of Technology (Chairman)

A. G. Evans, University of California, Berkeley

F. F. Lange, Science Center, Rockwell International

S. Majumdar, Argonne National Laboratory

R. Raj, Cornell University (Co-Chairman)

J. R. Rice, Brown University

D.M.R. Taplin, University of Houston

S. Wiederhorn, National Bureau of Standards

G. Wire, Hanford Engineering Development Laboratory, Westinghouse.

I. INTRODUCTION AND SUMMARY

This subgroup report outlines specific areas where research is needed in order to establish a fundamental understanding of the mechanism by which polycrystalline materials fracture at elevated temperature. A distinction is drawn between steady loading and loading varying in time. The report is classified into six topics based upon a mechanism inspired engineering perspective. These topics are: 1) materials and microstructure, 2) fracture under steady and 3) under cyclic loading, 4) irradiation effects, 5) life prediction, and finally 6) deformation instabilities. The subclassification in each topic is based upon the specific microstructural observations of the phenomena that lead up to fracture. In most cases, these observations are quite qualitative but this reflects the lack of sophistication of the present understanding of the fundamental mechanisms of fracture at elevated temperatures. The specific phenomena are briefly outlined and recommendations for the type of research most appropriate for their elucidation are made.

Before proceeding to outline the specific topics and recommendations, we wish to enunciate the more general concerns of the committee pertaining to the approach in basic research on high temperature fracture:

a) The basic understanding of the mechanisms of fracture at high temperature is vitally important in life prediction, accelerated testing, and the development of new engineering materials. This is because high temperature fracture combines a number of highly complex phenomena which involve several mechanisms, any one of which can be rate controlling depending upon the microstructure, impurity content and segregation, environment, and the stress history. Empirical characterization of fracture behavior leads to too many parameters which renders it of little practical value. This is now widely appreciated.

b) In order for basic research to produce maximum technological impact, we recommend that experimental work be carried out on material systems that are representative of the microstructures in engineering alloys. It is recognized, however, that it may sometimes be necessary to conduct experiments on idealized model materials to establish the validity of a specific mechanism of a fracture process.

c) The experimental research should generally be designed to test the validity of specific models and mechanisms rather than providing simple characterization of the fracture behavior of a material or merely to collect data. In most cases, this will mean that fracture should be studied "microstructurally" from its inception to final separation. Whenever theoretical models are not available to guide experiments, the latter should be carried out based on the best available mechanistic models and reporting as fully as possible ranges of the characterizing parameters that might guide later theoretical modeling.

d) Modern analytical and high resolution techniques should be used to study the development of the early stages of fracture.

e) In this report we do not often distinguish between metallic and ceramic materials. However, when the mechanism of fracture in ceramics is uniquely different from that in metals, because of a radical difference in microstructure or atomic binding, then specific recommendations are made, applicable to ceramics.

f) Quantitative study of fracture is possible only if the fundamental material parameters are well known. There is a special need for data on measurements of: interface energy in all types of single phase and multiphase alloys; interface cohesive strength; self-diffusion and impurity diffusion constants along grain boundaries.

The question of priorities among the recommendations was considered at some length by the subgroup as well as in the general discussion. A clear set of priorities could not be identified for every area of research. In our view, this caution reflects the lack of fundamental understanding of the micromechanisms of high temperature fracture rather than a division of opinion. Research in this area has only recently been emphasized. Considerable and flexible support is necessary in the future if the basic understanding is to reach a level of maturity where it can contribute toward rapid advancement of high temperature technology. Nevertheless, we offer the following general priorities:

We are of the opinion that in metallic alloys, research on fracture under time dependent loading involving cyclic and transient histories should receive a higher priority than fracture under purely steady loading, on the argument that these represent more realistic service histories, the effects of which must be better understood. In ceramic materials, on the other hand, linear viscous and diffusional processes appear to play the major role in elevated temperature fracture, making it adequate to emphasize research under steady and monotonic loading for the time being.

We have listed materials in order of their technological importance and suggest that research support might follow the same order of emphasis.

II. RECOMMENDATIONS

A. *Materials and Microstructures*

Fracture of engineering materials at elevated temperatures is extremely sensitive to microstructure. Basic research, however, should seek to identify the mechanisms of fracture which are common to most materials, recognizing that the regime of temperature and stress in which a particular mechanism dominates, differs from one material to another. Research is needed to study the basic mechanisms and to establish how the microstructure shifts the transitions from one fracture mode to another.

We have classified the materials in order of their engineering importance and according to their distinguishing microstructures. It is hoped that the basic research will take into account the essential microstructural differences in each of these classes.

1. Metallic Alloys

a. Solid solution and precipitate strengthened alloys with a small volume fraction of second phase particles. Special consideration should be given to the particles in the grain boundary since the low ductility at elevated temperature results from separation at the grain boundaries that is initiated from interfaces of particles. Examples of such alloys include low and high alloy steels and refractory metals. They have a medium yield strength and good ductility.

b. Solid solution and precipitate strengthened alloys which contain a very large volume fraction of a second phase such as the nickel base superalloys. The matrix second phase is often coherent and is usually different from the grain boundary second phase which consists mostly of metallic carbides. Whereas the creep properties of the material are controlled primarily by the matrix phase, the fracture behavior is strongly influenced by the second phase present in the boundaries.

c. Dispersion strengthened alloys with or without additional cold work such as TD nickel. These alloys may be different from those in (a) and (b) in the sense that the particles may not be very strongly adhered to the matrix since they are introduced into the material often by mechanical mixing rather than by precipitation.

d. Graphite, directionally solidified multiphase composite alloys, rapidly quenched and hot isostatically compacted alloys.

Initial emphasis should be put on microstructure classes (a) and (b). Basic understanding of fracture in these alloys will provide a significant advance in more reliable high temperature energy systems.

2. Ceramic Materials

a. Single phase oxides, silicon nitrides, silicon carbides.

b. Polyphase alloys, glass ceramics and refractories. Ceramics in categories (a) and (b) make up the bulk of the promising structural materials. They incorporate differences in bonding and may contain additional glassy grain boundary phases.

c. Nuclear fuels (oxides, carbides and nitrides). Their fracture behavior is important since the volume change in the fuel due to fracture and fragmentation strains the cladding of fuel elements.

d. Silicate glasses incorporating nuclear waste.

B. *Fracture under Quasi-Stationary Loading.*

The majority of low ductility fractures occurring at elevated temperature under steady loading are intergranular. The process consists of nucleation of cavities in grain boundaries and in their growth and linkage until the boundary separates. Eventual fracture may be a result of either extensive and quasi-homogeneous intergranular cavitation or a more rapid localization of cavitation into several cracks, one of which may then propagate to separation without much additional homogeneous cavitation. Selection of one or the other of these

paths will depend on microstructural variability, specific weakening of boundaries and the aggressiveness of the environment. The exact mechanistic balance of these phenomena is, however, inadequately understood.

1. Cavity Nucleation

Observations of cavitation in grain boundaries suggest that cavities form at second phase particles in the boundary, at triple grain junctions, and at intersections of matrix slip bands and the grain boundary. Stress concentrations which develop due to non-uniform slip and due to grain boundary sliding are expected to be important in the lower homologous temperature range, ($\sim$0.4 T_m), while some evidence exists that cavities form under relaxed stress conditions over long periods of time at the high homologous temperature range (>0.6 T_m). The cavities may initiate either by overcoming the local cohesive strength of the interface (or by particle fracturing), or by the formation of vacancy clusters of supercritical size on stressed interfaces. Modeling of nucleation by vacancy clustering under a given local stress is fairly complete. Other possible nucleation models applicable to the low end of the high homologous temperature range ($\sim$0.4 T_m) should be investigated. Further theoretical work is needed to develop the time dependency of the local stress concentrations due to boundary sliding and shear localization in the matrix. Deformation processes which build up the stress concentrations may be more (sliding of boundaries with particles for example) or less (matrix shear localization) time dependent, while the relaxation of the stress concentrations will depend upon the creep mechanism that acts to relieve these local stresses. It is also expected that the magnitude of the stress concentrations that develop will depend upon whether the external loading is steady, cyclic, or mixed.

NEEDS: Theoretical work on nucleation involving local stress concentrations by grain boundary sliding and slip bands needs to be developed. Fundamental nucleation models other than the vacancy clustering model should be investigated. There is a strong need for careful experiments to measure nucleation rates of cavities at high temperatures. Simple density change measurements do not provide this data since they do not distinguish between the volume increase from a single or from several cavities. New high resolution techniques should be utilized to measure nucleation rates. Special note should be taken of grain shape and grain boundary orientation in relation to principal stress directions.
All models of nucleation need information about the interface energies and the cohesive strength of the interfaces. The kinetic nucleation models involve the grain boundary diffusion coefficients. There is a pressing need particularly for this information. Since grain boundary sliding is one of the important mechanisms by which stress concentrations are produced, and since boundaries in engineering materials always contain second phase particles (which are often semicoherent), experiments are needed to determine the effect of particles on the rate of

The nucleation of cavities and intergranular cracks in ceramics usually involves stress concentrations produced by anisotropic slip, or by grain boundary sliding, especially at high strain-rates. Since ductile to brittle transitions characterize much of the behavior of ceramics, research should be supported to study the effect of microstructure on ductile-brittle transition in ceramic alloys.

2. Growth and Linking of Cavities in Grain Boundaries in Quasi-Homogeneous Stress Fields.

The existing models have considered cavity growth by diffusional transport,

when the cavities are of an equilibrium shape or when they deviate slightly from their equilibrium shape. These models may be considered fairly complete. There are models under development which consider the growth and linkage of cavities by power law creep and by a combination of diffusion and power law creep. However, considerable new effort is needed to establish the role of grain boundary sliding in growth and linkage of cavities.

NEEDS: There is need for the development of theoretical models which incorporate the importance of grain boundary sliding into cavity growth and linkage. This appears to be an important mechanism in the high stress and intermediate temperature regime of fracture in metals, and of even more general importance in ceramics.

Experiments are needed to ascertain the extent of the regimes in which growth is dominated by diffusional flow, or by power law creep, or by the combination of both. The study of the effect of multiaxial stress state on hole growth can be fruitful in separating the roles of diffusional flow and power law creep. The sequence of phenomena involving the growth of cavities from a scale much smaller than the grain size into micro-cracks, and the growth of these into macro-cracks should be studied in some detail and should be associated with statistical models of such processes to understand geometrical and strength variability in the microstructure.

In ceramic materials which contain a glassy phase in the grain boundary regions, viscous hole growth in such thin films should be considered; in ceramics which do not contain a glassy boundary phase, the diffusional growth processes should be applicable; this can be a fruitful area where experiments could be designed to test theoretical models.

In metals, the study of cavity nucleation and growth in quasi-homogeneous stress fields should be extended to cavitation in strong gradient fields of stress and strain rate in front of a notch or a crack. Such theoretical modeling should be backed up by experimental measurements in the relevant range of loading and temperature. Environmental effects will be of great importance at such crack tip fracture processes and must be considered. Models supported by experimental work are needed which incorporate the environment as a parameter in the cavity nucleation and growth process at crack tips, as the growth of creep cracks are likely to have a strong stress-corrosion cracking aspect.

3. Time Dependent Growth of Macro-Cracks

In metals, creep crack growth has been observed in a limited region of stress and temperature in nickel base alloys. Such behavior is usually very environment sensitive. There is definite evidence that ceramics which contain a glassy grain boundary phase exhibit slow crack growth at elevated temperature under steady state loading.

NEEDS: Damage tolerant design of high temperature systems requires understanding of processes of growth of macro cracks in creeping alloys. There is a need to ascertain the range of stress and temperature under which creep cracks grow. In ceramics, this is a critical area of research since it is an important mechanism of fracture in engineering applications. Research should be supported to establish a quantitative understanding of the mechanism of the process from a theoretical and experimental standpoint. Studies should incorporate the statistical aspects of microstructural crack extension processes and their environmental aspects in high strength structural ceramics, e.g. silicon-nitride exposed to oxidizing environments.

C. *Mixtures of Steady Loading, Cyclic Loading and Transient Loading*

This should be a high priority area for research in metals. It is of critical engineering importance since structures in energy systems are always subjected to mixed stresses. Linear damage rules combining stress rupture and fatigue are often grossly inadequate in predicting life. There are very significant effects of the microstructure, the environment, and the shape of the stress cycle. Representative microstructures are those of the low and high alloy steels and nickel base alloys.

Intergranular cavitation as well as intergranular environmental attack are important considerations. Whether crack initiation or crack propagation dominates the life is still controversial. Nevertheless, there is some agreement that crack growth is dominant for lives shorter than the transition fatigue life, and that crack initiation dominates for lives longer than the transition fatigue life. Different microstructures then may only govern the magnitude of the transition fatigue life. Whether or not these simple rules apply to alloys with complex microstructure as well as to solid solution alloys remains to be established.

The fracture mode can be transgranular, intergranular, or mixed, in both initiation and in growth. Lowering the frequency, using unsymmetrical stress cycles (either in strain rate or in hold time), increasing the temperature and presence of aggressive environments, all promote intergranular fracture. The environment is important not only in the intergranular but also in the transgranular mode of fracture. Although the underlying mechanism of these behavior patterns are not yet fully understood, some simple extrapolations can be made from the present limited understanding of fracture under steady loading. Difficulties arise because the magnitude of the local stress concentrations is different in steady loading and in mixed loading, but the actual nucleation event which produces a cavity or a crack may be the same. It follows that the stress concentrations produced by time dependent processes, such as grain boundary sliding, should be coupled to the shape of the time dependent stressing cycle. Here additional micromechanical modeling will be required.

In ceramic materials, there is no data on the effect of cyclic loading on fracture at elevated temperature. Exploratory experimental investigations of the influence of cyclic loads on fracture need to be carried out in order to establish the existence or absence of genuine cyclic effects. In comparison to the problem of subcritical crack growth under steady loading, crack growth under cyclic and mixed loading is considered to be of a lower priority for ceramics. More important than cyclic stressing, however, is fracture resulting from thermal shock in polyphase ceramics.

1. Initiation and Early Growth of Cracks

It is expected that environment, grain boundary sliding and intergranular grooving are important in crack initiation. Cracks may also initiate transgranularly along crystallographic directions particularly in multi-phase alloys by a process which is similar to the strain localization by persistent slip bands. In most instances the early growth of cracks will be by shear for which little information and understanding exists.

NEEDS: The intergranular mechanisms of crack initiation should be emphasized rather than the transgranular mechanisms. In the former, the role of grain boundary sliding in both surface grooving and nucleation of cavities and their growth should be investigated. The local stress con-

centrations which will be cycle shape and microstructure dependent can be expected to play a critical role. Research on mechanisms by which the environment influences crack initiation is needed. The crack initiation process should be described in terms of the proper scaling parameters such as pre-existing flaws (from machining, for example), grain size and grain boundary sliding displacement. In many instances, it will be desirable to study the early growth of cracks in shear (Stage I crack growth). The role of the cycle shape such as unsymmetrical cycles and mixtures of steady and cyclic loading should be an important component of these investigations. The influence of grain boundary particles on fracture needs to be emphasized.

2. Crack Propagation

Engineering components can be designed either by criteria for crack initiation or crack propagation. Initiation is usually more time consuming in high cycle fatigue while propagation is important in high and low cycle fatigue. The relative importance of initiation versus propagation depends on the microstructure and the stress level. Usually, drastic increases in crack propagation rates result only when the mode of fracture is intergranular. Again environment, cycle shape, and microstructure are important.

NEEDS: Mechanistic studies are needed to investigate the acceleration of the nucleation and growth of grain boundary cavities under cyclic loading at moderate strain rates. The role of grain boundary sliding must be investigated. The distribution of second phase particles in the boundary will be important from two viewpoints: they affect the rate of grain boundary sliding and also provide sites for the formation of cavities. Both must be investigated. Cavitation in the crack tip region under cyclic loading needs to be investigated by theory and experiment. Due attention should be given to wave shape and environment effects.

Crack propagation in ceramic materials under transient loading produced by thermal shock needs to be investigated theoretically as well as experimentally.

D. *Phenomena Peculiar to Irradiation Environments*

Radiation damages alloys and produces a whole host of microstructural damage that includes formation of point defect clusters, sessile dislocations, and voids. In some instances, transmutation results in substantial production and accumulation of helium that precipitates into bubbles. When such damage congregates along grain boundaries, rapid embrittlement can result. These problems will be important in all kinds of reactors ranging from simple converter units to breeder reactors. They are expected to be most acute in first wall applications in fusion reactors.

NEEDS: Intergranular embrittlement due to precipitation of voids or helium bubbles on grain boundaries, their kinetics of formation and their effects on the fracture and fatigue behavior in characteristic reactor alloys need to be studied in detail. Surface fatigue under combined irradiation, strain cycling, and flux interruptions must be studied, particularly in candidate first wall materials.

E. *Service Life Predictions*

Most present end-of-life predictions are empirical or intuitive. They

must be based on mechanistic understanding. Accounting for expired life, predicting remaining service life, based on continuously monitored service parameters and utilizing mechanistic models making use of research in the areas discussed above are greatly needed.

Combinations of non-specific statistical models with mechanistic model components to improve predictive capability may prove of use.

NEEDS: Use of specific mechanisms of microstructural damage based on better understanding of phenomena discussed above to formulate incremental life models are needed. These must be coupled with experiments to assess validity of models and ascertain importance of transients that are usually excluded.

F. *Deformation Instabilities and Localization*

Localization of shear deformation as a source of localization of cavitational processing, analogous to low temperature ductile fracture void sheets can occur at elevated temperature and may rapidly lead to terminal fracture. Localization due to unstable microstructures is of great importance and requires both experimental study and mechanistic modeling.

NEEDS: Experiments should be carried out on specific microstructures to map out the phenomena and to determine their extent. Such phenomena should then be mechanistically modeled with the purpose of stating criteria for premature failure with a goal of final incorporation into life prediction codes.

SUBGROUP REPORT ON
GRAIN BOUNDARY AND INTERPHASE BOUNDARY
STRUCTURE AND PROPERTIES

R. W. Balluffi, Massachusetts Institute of Technology (Chairperson)

R. M. Cannon, Massachusetts Institute of Technology

D. R. Clarke, Rockwell International

A. H. Heuer, Case Western Reserve University

P. S. Ho, International Business Machine Corp.

B. H. Kear, United Technologies Research Corp.

V. Vitek, University of Pennsylvania

J. R. Weertman, Northwestern University (Co-Chairperson)

C. L. White, Oak Ridge National Laboratory

INTRODUCTION

In many high temperature structural applications, the performance characteristics of a materials system are largely controlled by the properties of its grain and interphase boundaries. For example, failure in creep and fatigue frequently occurs by cavitation, or cracking along grain boundaries, particularly boundaries oriented transversely or obliquely to the applied stress. In a few special cases, this failure problem has been overcome by directional alignment of grain and interphase boundaries by various types of metallurgical processing such as directional solidification and directional recrystallization. A good example is to be found in the application of directionally aligned structures in high performance gas-turbine airfoils. More generally, however, where fine, equiaxed grain structures are desirable, other methods of controlling grain boundary properties have been developed. Important amongst these has been the introduction of improvements in primary melting practices, which are designed to control important impurities. This is of decisive importance because even traces of certain impurity elements present in grain boundaries in high temperature materials can seriously affect properties. In many cases impurities are deleterious and need to be removed. However, in certain cases (e.g., creep fracture) controlled impurity additions can be beneficial and result in improved properties.

Another development of great significance has been the effective control of environmental interactions by the application of protective coatings. The future development of advanced alloy systems now appears to hinge on the ability to design coatings that are completely compatible with the workpiece. Coatings that are of special significance are those that are integrally bonded to the workpiece, i.e., so-called "overlay coatings". Furthermore, additional protection by thin ceramic layers, or thermal barrier coatings also appears to be mandatory in certain extreme environments, e.g., where fine particulate erosion is combined with oxidation and hot corrosion at extremely high temperatures. Thus, it seems clear that a deeper understanding of boundary phenomena, both intergranular and interphase, will be necessary to satisfy the materials requirements for advanced energy conversion

systems.

The high temperature mechanical properties of structural ceramics are also crucially dependent on the presence and properties of grain boundaries. In a numb of the most promising structural ceramics, such as the silicon nitride alloys, there exists an intergranular glassy phase rather than usual crystalline-crystalline boundaries. These glassy phases have been demonstrated to control the creep rates, oxidation resistance, sub-critical crack growth and strengths of such alloys at elevated temperatures. Elimination of the boundary phase or its controlled crystallization by both appropriate processing and control of the interface structures will enable such structural ceramics to exhibit far superior high temperature mechanical properties. In those structural ceramics in which there is no intergranular phase, a better understanding of the structure and impurity segregation to grain boundaries will undoubtedly lead to the possibility of the control of the high temperature fracture behavior. It is important to emphasize that because of a lack of both experimental data and basic understanding, the development and processing of structural ceramics lags far behind that of metals.

To summarize the foregoing it may be concluded that the characteristics of many materials systems are largely controlled by the properties of both grain boundaries and interphase boundaries. Furthermore, the properties of these interfaces are often of importance in both the processing of the material prior to its use and in the performance of the material during its service. For these reasons the Subgroup attempted to deal with proposed basic research on those aspects of

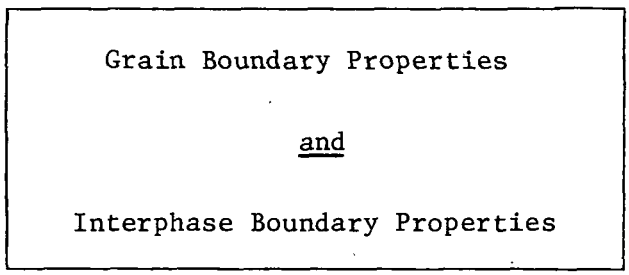

which were thought to be of fundamental importance in both the

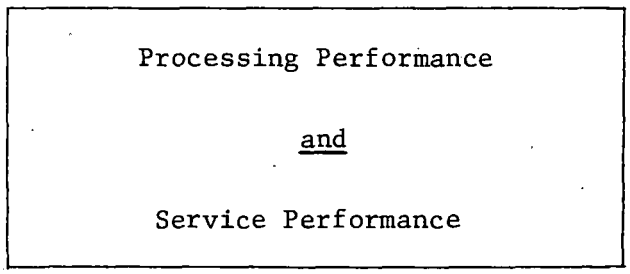

of materials subject to time dependent fracture at temperatures where thermally activated mechanisms play an important role.

The array of topics considered to be of importance was found to be essentially the same as that presented by Balluffi [1] in his review of present knowledge of grain boundaries given earlier in the present workshop report. These topics

include the following:

1. Structure of Ideal Perfect Boundaries
2. Defect Structure of Boundaries
3. Diffusion at Boundaries
4. Boundaries as Sources/Sinks for Point Defects
5. Boundary Migration
6. Dislocation and Sliding Phenomena at Boundaries
7. Atomic Bonding and Cohesion at Boundaries
8. Non-Equilibrium Properties of Boundaries
9. Techniques for Studying Boundaries.

We discuss proposed research in each of these specific areas in turn in the following. Further comments relevant to these topics may be found in [1]. Finally, we conclude with a series of summarizing remarks.

1. STRUCTURE OF IDEAL PERFECT BOUNDARIES

Knowledge of the detailed atomic structure of ideal perfect grain and interphase boundaries and the defects which may exist in these boundaries is essential in developing an understanding of their properties. Research in this area is therefore of central importance.

So far, all of the computer simulation work aimed at this problem has involved special boundaries of relatively short periods in simple metals where models possessing relatively small numbers of atoms can be employed. In general, no detailed and quantitative studies of the atomic structures of non-special grain boundaries and interphase boundaries have been carried out. There is, therefore, a strong need for work on the computer simulation of non-special grain boundaries and also interphase boundaries. It is important to note at the same time that a good deal of essential work on special boundaries is still unfinished. A logical way to proceed would therefore involve continued work on special boundaries accompanied by efforts to extend the calculations to more complex non-special boundaries as the computing methods become more realistic and powerful. The recent identification of compact polyhedral units in the cores of special grain boundaries has been a significant development, and it would be of great interest to see whether they play an important role in non-special boundaries. It is also essential to understand more about the nature and characteristics of secondary relaxations in boundaries as they become less special. What are the core widths of intrinsic grain boundary dislocations, etc.?

Continued efforts should be made to improve the computer simulation techniques themselves. Specifically, we need:

(i) construction of more realistic interatomic potentials based on a more fundamental understanding of the basic physics involved. A fundamental question which must be answered is -- to what extent can the interatomic potential approach (whether semi-empirical, or otherwise) take account of "electronic effects", particularly in

metals?

(ii) incorporation of lattice vibrations and entropy effects into more calculations. Such molecular dynamical calculations will be of importance in answering questions about possible order → disorder phase changes which are conceivable in boundaries as the temperature is raised.

Essentially no effort has gone into the quantitative modeling of any of the grain boundaries or interphase boundaries which may exist in more complex materials such as ionic solids, covalent solids or in materials such as sintered silicon nitride where a layer of amorphous material of finite thickness exists at the grain boundaries. Efforts should be made to model and understand the structure of these boundaries.

The computer simulation work mentioned above must be accompanied by experimental work which will yield data which can be compared quantitatively with calculated results derived from the computer modeling. Experimental work which appears promising in this respect includes, for example:

(i) measurement of the energy of well characterized boundaries. Of particular interest here would be a search for a possible correlation between energy and characteristic structural features of the boundaries;

(ii) measurement of the lattice displacement $\vec{R}$ (see Fig. 1 in [1]) across a boundary;

(iii) measurement of electron and x-ray diffraction effects from the grain boundary core structure;

(iv) direct observation of details of the core structure by high resolution lattice imaging in the transmission electron microscope;

(v) quantitative observation of the diffraction contrast produced in transmission electron microscope images by intrinsic grain boundary dislocation structures;

(vi) observation of boundary faceting and the appearance of low energy boundary segments in microstructures.

2. DEFECT STRUCTURE OF BOUNDARIES

Computer simulation and possibly other calculations of the structure of point defects such as vacancies and interstitials should be made in a wide variety of grain and interphase boundaries. Of particular interest is the question of whether these "point" defects remain localized or dissociate widely, particularly in non-special boundaries. The answer to this question is essential to the development of our understanding of diffusion processes in boundaries as discussed further below. Also of interest is the behavior of various clusters and the possible ways in which voids may nucleate at boundaries. This information is of critical importance in dealing with the problem of intergranular cavitation.

Computer simulation studies of the structure of grain boundary dislocations should be made on a wide variety of grain and interphase boundaries. Of particular interest is the question of whether these "line" defects dissociate widely particularly in non-special boundaries and to what extent do dislocation or "dislocation-like" defects, exist in non-special boundaries? The answer to this question is essential to the development of our understanding of many of the important grain boundary phenomena discussed below.

Our understanding of the important phenomenon of solute atom segregation at grain boundaries is presently in a primitive state. There are only a very few cases where we know quantitatively the extent of segregation as a function of bulk concentration and temperature. We do not understand the relation between the structure of the boundary and segregation, changes in the boundary structure and properties caused by segregation and, also, no information is available concerning the structure of the segregate. There is, therefore, a critical need for quantitative studies of the extent of segregation, of the structure of the boundaries with segregated solutes and of the structure of the segregate at and near the boundaries under well controlled conditions in well characterized boundaries. Various powerful experimental techniques are being developed at present [1] which should be of use in such studies. These include electron and x-ray diffraction from the core region, electron microscope lattice imaging, atom probe-field ion microscopy, scanning transmission electron microscopy, EXAFS, and others. A number of these techniques possess the important advantage that the segregation can be studied in situ without the necessity of first inducing intragranular fracture to expose the boundary. Computer simulation of boundaries with segregated solutes can also significantly contribute to an understanding of segregation phenomena, particularly the structural aspects. Practically no study of this type has been made so far, and the initiation of atomistic studies in this direction is desirable. This will also require new developments in the description of complex interatomic interactions.

The fundamental theory of segregation is also in an undeveloped state. Certain empirical rules predicting the degree of segregation and empirically based thermodynamic treatments have been developed, but a satisfactory basic theory is still lacking. It appears that progress in this direction will require the increased attention of solid state theorists.

Finally, the effects of segregation on all of the important phenomena at grain boundaries which concern us should be studied. These include, for example, cohesion, and migration. It is known that trace amounts of solute atoms can exert large effects on such phenomena and can be responsible for significant heat-to-heat variations in behavior.

3. DIFFUSION AT BOUNDARIES

Attention should be paid to the gathering of more reliable and extensive grain and interphase boundary diffusion data. As pointed out in [1], present grain boundary diffusion data are generally unsatisfactory. Unfortunately, the data base for interphase boundary diffusion is in an even poorer state. The establishment of a better data base for boundary diffusion would be of considerable assistance in the understanding of a number of important kinetic processes at boundaries.

At present we have little understanding of the way in which the boundary diffusivity varies with boundary type or with the diffusion direction in a grain boundary. Furthermore, the basic mechanism of boundary diffusion itself is unknow Coupled computer simulation studies and appropriate boundary diffusivity measurements would be helpful in clarifying this area of ignorance.

A particularly difficult but important area has been the study of seemingly "anomalous" diffusion rates along impurity contaminated boundaries in practical ceramic materials. Studies of this type should be continued in order to build up a practical data base for materials of this type and to gain some insight into the effects of boundary segregation on diffusion rates.

4. BOUNDARIES AS SOURCES/SINKS FOR POINT DEFECTS

Progress in our understanding of the mechanism of the point defect source/sink action of non-special boundaries must await progress in understanding the structure of point defects in these boundaries (see section 2).

Very few experiments aimed at the direct determination of the source/sink efficiency of grain boundaries, and especially interphase boundaries, have been carried out. Experiments of this type should be encouraged since the source/sink character of boundaries is undoubtedly intimately connected with other important boundary phenomena such as chemical diffusion in boundaries and boundary migration (see below).

Work is needed on furthering our understanding of how small second phase particles affect the source/sink action of boundaries. There is considerable evidence that such particles slow down the source/sink action. However, the mechanisms by which this occurs are undetermined. Progress in this direction could have an important effect on alloy design.

5. BOUNDARY MIGRATION

As pointed out in [1] our present knowledge of grain boundary migration mechanisms and mobilities is unsatisfactory. The same conclusion may be stated even more emphatically for interphase boundaries.

Further progress will depend upon:

(i) the performance of more extensive and well controlled mobility experiments to aid in the establishment of both the quantitative and qualitative aspects of grain and interphase boundary migration;

(ii) the performance of additional critical experiments to distinguish migration mechanisms; and

(iii) the establishment of reliable structural models for non-special boundaries and their defects.

6. DISLOCATION AND SLIDING PHENOMENA AT BOUNDARIES

Quantitative measurements should be made of the rate at which lattice dislocations dissociate in boundaries.

The generation of lattice dislocations at boundaries should be studied systematically, preferably by direct observation with, for example, high voltage electron microscopy.

Progress in understanding the basic mechanism by which boundary sliding occurs in non-special boundaries must await further progress in our understanding of the nature of grain boundary dislocations (see Section 2 above) and shear mechanisms in such boundaries. However, since grain boundary sliding plays an exceedingly important role in grain boundary failure mechanisms, efforts should be made to understand as many of the overall aspects of sliding as possible.

7. ATOMIC BONDING AND COHESION AT BOUNDARIES

Methods should be developed to measure for the first time grain and interphase boundary cohesion. Of particular interest would be experimental determinations of the effects of solute atom segregation on cohesion.

Efforts should be made to calculate boundary cohesion on a fundamental basis perhaps by the cluster method cited in Section 7 of [1].

8. NON-EQUILIBRIUM PROPERTIES OF BOUNDARIES

There is a need for more critical and more decisive experiments to decide the question of whether important non-equilibrium effects of the types cited in Section 8 of [1] exist. Such effects are not well-established at present. If they indeed do exist they would obviously play an important role in the behavior of boundaries under time dependent fracture conditions.

9. TECHNIQUES FOR STUDYING BOUNDARIES

The field of boundary studies is in a rapid and exciting stage of development. The recent development of a variety of powerful techniques allows detailed studies of the boundary structure and chemistry at essentially the atomic scale which were impossible just a few years ago. Techniques of particular interest include, for example:

(i) study of boundary diffraction contrast images by high resolution electron microscopy;

(ii) study of boundary structure by lattice imaging methods via high resolution electron microscopy;

(iii) scanning transmission electron microscopy;

(iv) high resolution scanning Auger spectroscopy;

(v) synchrotron x-ray diffraction from the core regions of boundaries;

(vi) atom probe-field ion microscopy;

(vii) EXAFS studies of atomic environments in grain boundaries.

Progress in the area of boundary studies and the successful completion of much of the research recommended above will depend in a critical way on the availability and application of the above techniques. In fact, it must be recognized that the study of boundaries is particularly dependent upon these techniques. We therefore recommend that special attention be given to the availability of such techniques in future boundary research.

SUMMARIZING REMARKS

(1) Time-dependent fracture in its various forms is, often, directly dependent upon an almost bewildering array of both grain boundary and interphase boundary phenomena. These include, for example, rapid boundary diffusion, point defect source/sink action, boundary migration, dislocation creation and annihilation and boundary cohesion. Many of these phenomena also play important roles in the processing of materials for high temperature structural applications.

(2) These boundary phenomena are related directly to the atomic structure of the boundaries and the point and line defects which may exist there (including solute atoms). Increased understanding of boundary structure is therefore central to progress in the field as a whole.

(3) Fortunately, research on the structure of grain and interphase boundaries is in a rapid and exciting stage of development. For the first time, powerful high resolution methods are available for probing the detailed structure and chemistry of boundaries. Also, increasingly powerful computer simulation techniques have been developed for constructing atomic models. Full use of these techniques should therefore be made in future work to determine and understand boundary structure. Of particular interest are the structures of non-special grain and interphase boundaries, boundaries with defects and solute atoms, and boundaries in complex materials such as ionic solids.

Special efforts should be made to ensure the availability of these techniques to the relevant research community. Increased equipment funding for individual research groups, and the establishment and support of large central facilities would be beneficial.

(4) There is a widespread need for more extensive and better defined experiments carried out in conjunction with realistic modeling in all of the subfields cited in the present report. Specific research which is likely to be particularly rewarding at the present time include:

(i) the gathering of more extensive and reliable boundary diffusivity and boundary energy data bases;

(ii) the development of techniques to measure boundary cohesion;

(iii) experimental studies under carefully characterized and controlled

conditions of the effect of solute atoms and boundary "chemistry" on many of the critical boundary phenomena cited in the present report, especially diffusion, migration, sliding, and cohesion.

REFERENCE

[1] Balluffi, R. W., earlier paper in present workshop report.

SUMMARY REPORT - SUBGROUP ON ENGINEERING NEEDS

Gopal D. Gupta, Foster Wheeler Development Corporation, Chairman
Joseph Blass, Oak Ridge National Laboratory
L. F. Coffin, General Electric Company
Bruce A. Cramer, McDonell Douglas Astronautics East
Edward W. Hart, Cornell University
Frank A. McClintock, Massachusetts Institute of Technology
David M. Moon, Westinghouse Electric Corporation
David Richerson, Airesearch Manufacturing Company of Arizona

INTRODUCTION

The objective of this summary report is to present the various key discussion areas, noting both majority and minority opinions, of the subgroup's views on designer needs in time-dependent fracture and the contribution of materials science to these. Six of the eight subgroup members had participated in the short presentations earlier in the workshop. Some of their individual recommendations are made in the written version of their presentations included elsewhere in these proceedings.

SUBGROUP DISCUSSION

There was general agreement in the subgroup regarding the need to bridge the gap between academic knowledge and industrial application. To achieve this, the discipline barriers must be broken down. More interdisciplinary interaction must be encouraged. One of the members mentioned that, in the pursuit of academic research, much of the material data generated are at unrealistic stress/temperature conditions when compared with realistic design considerations. Clearly, there is a need for greater interaction between those people generating data and those who would be using these data. This would be promoted by interactive programs among universities, research institutions, and industry. The subgroup recommends that such programs be considered and initiated. Another opinion was expressed that generalized pictures should be developed showing the

relationship of various discipline areas to design problems. This would help develop multidisciplinary interactive programs of the type indicated above. An example is shown in the figure on the next page.

There was considerable discussion about whether the subgroup should base its recommendations on currently operating energy systems or on advanced energy systems. Subgroup members were divided on this issue. One faction argued that system availabilities are likely to be improved considerably if the subgroup recommendations were concentrated on the current systems and their studies pursued. The counter argument was that system availability frequently depends on factors such as proper maintenance, operation, quality control, etc., and, in many cases, is not likely to be affected significantly by merely a better material understanding. Therefore, the attention of the subgroup should be focused on advanced energy systems in which system behavior is not well understood because of the lack of experience. It was finally decided that the subgroup should mainly emphasize the advanced energy systems but also should include any specific problem areas that are relevant to currently operating systems.

All the subgroup members agreed that much of the research and development work should be performed on service conditions and structural materials that are relevant. This led, naturally, to a number of questions. What are the relevant service conditions? What are the relevant structural materials? What are the various systems of interest? One subgroup member felt strongly that the subgroup should develop answers to these questions. However, other members felt that the subgroup could not possibly generate these answers to the extent of detail that is warranted. Therefore, the following recommendation was made:

> The relevant conditions for components in specified designs should be generated including materials, temperature ranges, environments, strain and stress limits, strain or stress rates, loading paths/histories, etc. Descriptions of systems of interest should be prepared and made available to researchers generating the relevant conditions listed above. An example of a typical condition of interest is the stress levels for steady-state creep on the order of 10^{-4}E to 10^{-3}E, giving strains typically 1 percent overall to 5 percent locally.

Oak Ridge National Laboratory Report No. ORNL-5073* was mentioned as an important reference on time-dependent material considerations. The section on specific recommendations is directly relevant to the objectives of this subgroup and is appended to this report.

RECOMMENDATIONS FOR RESEARCH

Five specific areas were identified by the subgroup as important broad categories in which future work needs to be performed. All these areas refer

*L. F. Coffin, et al., "Time-Dependent Fatigue of Structural Alloys - A General Assessment (1975)," Oak Ridge National Laboratory Report No. ORNL-5073, January 1977.

CYCLIC STRESS STRAIN BEHAVIOR
FATIGUE CRACK INITIATION MECHANISMS
TIME DEPENDENT DAMAGE PROCESSES
WAVE SHAPE EFFECTS
FREQUENCY AND STRAIN RATE EFFECTS
METALLURGICAL INSTABILITIES
DISLOCATION SUBSTRUCTURE
PERSISTENT SLIP BANDS
GRAIN BOUNDARY DAMAGE

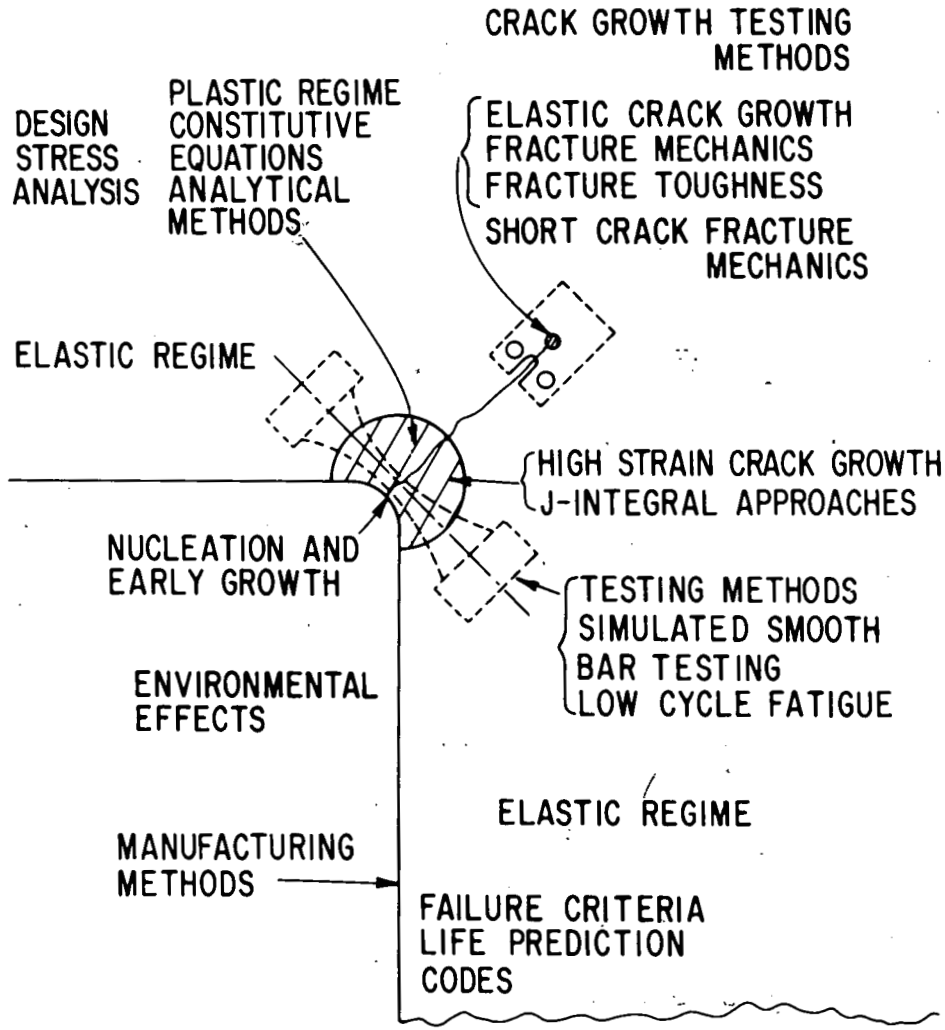

SCHEMATIC VIEW OF HIGH-TEMPERATURE FATIGUE PROBLEM SHOWING PHYSICAL STAGES IN FAILURE PROCESS AND RELEVANT DISCIPLINES.

to metallic as well as ceramic materials, including coatings. A few major subcategories were identified under each major area. They are listed in the order of priority that was assigned to each category by the subgroup members.

Cumulative Damage Concepts for Crack Initiation

- Grain boundary fracture and deformation
- Metallurgical and structural changes
- Interaction with environment
- Mechanical and thermal histories, including multiaxial and nonproportional effects
- Specific materials and service conditions.

From the designer's viewpoint, the final objective is to be able to predict the service life of relevant structures with a reasonable degree of confidence. Therefore, the most important area for future study is identified as the development of cumulative damage concepts. Such concepts require:

- Understanding of the basic nature of the creep-fatigue-environmental damage mechanisms
- Method of counting the damage as a function of the accrued history of loading.

These concepts should be developed for both crack initiation and crack growth.

The subcategories listed above are self-explanatory and need no further clarification.

Environmental Studies

- Systematic characterization
- Underlying mechanisms
- Liquid metals, water/steam, air, molten salts, combustion products including coal-derived fuels, irradiation.

Environmental studies were considered to be very important by the subgroup. It was felt that the environmental effects must be systematically characterized. An example was cited to further clarify this. Some materials show a large decrease in fatigue strength with only small traces of an oxygen environment; however, a further increase in oxygen concentration leads to an increase in fatigue strength. Such effects can be determined only by systematic environmental studies. A number of typical environments relevant to energy systems were identified.

Constitutive Equations

- More realistic approaches

- Cyclic and complex loading paths/histories, including multiaxial and non-proportional loading effects
- Bench-mark problems
- Computational methods.

A definite need to develop more realistic constitutive equations was identified. It was indicated that the present approaches do not satisfactorily treat the thermal transient and cyclic problems. There was unanimous agreement on the importance of bench-mark problems* in the development of constitutive equations. These problems should be simple yet significant enough for practical application and should serve as significant tests of theories and procedures for predicting the response of structural components. Furthermore, adequate computational methods must also be developed so that the constitutive equations can be utilized to solve practical problems both inexpensively and accurately.

Design Methodology

- Statistical approaches
- Probabilistic evaluation of nondestructive testing and examination approaches
- Accelerated testing
- Defect-tolerant design.

This category includes application problems related to the fundamental work identified in the last three categories. Presently, ASME pressure vessel and piping codes are used in the design of fossil and nuclear power plant components. The ASME codes are based on deterministic design methodology. Thus, it is difficult to assess the degree of conservatism involved in the designs. The need to develop probabilistic design methodology was identified by the subgroup members. The ASME codes are further limited by the use of crack initiation as the characterization of failure. There is a need to develop design methodology based on both crack initiation and crack growth. Because of time and economic limitations, most of the material data in the ASME codes are based on accelerated short-time tests. There is a need to relate the validity of these accelerated tests to the long-time material behavior that is expected in practice.

Processing

- Welding
- Casting
- Forging

*J. M. Corum, et al., "Interim Guidelines for Detailed Inelastic Analysis of High-Temperature Reactor System Components," Oak Ridge National Laboratory Report No. ORNL-5014, December 1974, pp. 109-118.

- Machining
- Forming (including explosive forming)
- Coatings
- Powder sintering.

All the problem areas listed in the first four categories need to be explored not only for structural materials in final form but also for special areas such as weldments and for structural materials during processing. For example, large variations in mechanical properties exist within the weld and the adjacent heat-affected zone because of the complex thermal and mechanical history experienced during the welding process. The service conditions (e.g., stress and strain limits, temperatures, etc.) involved during processing are usually entirely different from those in operating systems. Therefore, there is a need to identify these in a separate category.

APPENDIX

Recommendations from L. F. Coffin, Jr., et al., "Time-Dependent Fatigue of Structural Alloys - A General Assessment (1975)," Oak Ridge National Laboratory Report No. ORNL-5073, January 1977, are quoted below:

1. The further development of design technology for treating time-dependent fatigue. Both crack-initiation and FCG methods are to be addressed. Emphasis is to be given to proper treatment of cumulative damage, effects of multiaxial stress, and other important factors as described in this report.

2. The conduct of long-time tests that will provide conclusive answers to the effect of time on the creep-fatigue-environment interaction problem. The test program must be carefully chosen to definitively answer questions such as that concerning the existence of fatigue life saturatuion and should be designed to provide desired data of general utility. The program should involve large as well as small strains, constant and varying temperatures, and other parameters expected in service.

3. The development of criteria for characterization should include constitutive relations under cyclic and time-dependent loading and information on the influence of one mode of loading on the properties of material in another mode. For example, the effect of creep strain on plastic ductility, or fatigue loading, and vice versa should be investigated. Both uniaxial and multiaxial studies are to be included.

4. The conduct of a series of tests in several environments of special interest (e.g., vacuum, liquid sodium, and inert gases). These tests should be designed not only to provide basic information, but also to resolve numerous questions raised in this report relative to environment when the analysis is made according to the major frameworks developed in this report.

5. The development of cumulative damage concepts. Such concepts first require that we understand the basic nature of the creep-fatigue-environmental damage mechanism(s) and second that we learn how to count the damage as a function of

the accrued history of loading. It will be important to separate the crack-initiation phase from the crack-propagation phase in order to treat such damage accumulation properly.

6. The study of crack growth in the high-temperature range. Of special importance are cases involving very small cracks (in their incipient stages) and large inelastic strains (especially creep-strains).

7. The development of information on the effects of multiaxial stress. In this case, general characteristics of cyclic behavior and the mechanisms of damage are to be studied. Again, it will be important to separate crack-initiation and crack-propagation phases because of the special differences in response of materials to these two phases of damage accumulation under multiaxial conditions.

8. Special treatment of wave shapes. Since the major frameworks developed in this report are specially designed to treat complex variations of stress, strain, strain rate, and temperature, special tests should be devised to test their capability of predicting the fatigue life under typical thermomechanical cycles involving such variations. These are especially pertinent in advanced power-generation applications.

9. Extension of the time-dependent fatigue data base. From the current design point of view, emphasis should be given to materials other than type 304 stainless steel [e.g., type 316 stainless steel (both annealed and cold worked) at temperatures ranging from 1000 to 1500°F]. Data are needed on parent and weld material and on weldments.

10. Extension of the data base to include tests on notched elements in order to examine material behavior under realistic structural conditions and to evaluate various procedures developed for analyzing structural components.

*U.S. GOVERNMENT PRINTING OFFICE : 1979 0-281-704/61